

Thesis  
3995

# Soil Erosion on Buried Archaeological Sites in Arable Areas: A Modelling Approach.

By

Jonathan Paul Bowes

Submitted to:

The Faculty of Natural Sciences,  
University of Stirling,

for the degree of

Doctor of Philosophy.

This research was carried out in the Department of Environmental Science,  
University of Stirling, Stirling, UK.

1103

ProQuest Number: 13917116

All rights reserved

INFORMATION TO ALL USERS

The quality of this reproduction is dependent upon the quality of the copy submitted.

In the unlikely event that the author did not send a complete manuscript and there are missing pages, these will be noted. Also, if material had to be removed, a note will indicate the deletion.



ProQuest 13917116

Published by ProQuest LLC (2019). Copyright of the Dissertation is held by the Author.

All rights reserved.

This work is protected against unauthorized copying under Title 17, United States Code  
Microform Edition © ProQuest LLC.

ProQuest LLC.  
789 East Eisenhower Parkway  
P.O. Box 1346  
Ann Arbor, MI 48106 – 1346

## Abstract

The Monuments at risk Survey (MARS) of England (Darvill and Fulton, 1998) concluded that the dominant agent of damage to archaeological sites is intensive agriculture. No such equivalent or similar study exists for Scotland. This study aimed to assess the threat of soil erosion posed to archaeological cropmark sites across an 80 x 60 km study area by quantitatively modelling soil erosion rates. Archaeological sites are widely distributed across lowland mid-Scotland and are clustered on arable land. Focus was placed on cropmark features since very little is known about them and damage rate is difficult to ascertain without excavation. 2849 registered (NMRS) archaeological sites are present in the study area, 1707 of which are cropmarks.

To meet the aim, the total erosion budget was modelled in its component parts: water and tillage translocation. Firstly, water erosion and deposition were modelled using Desmet and Govers's (1995) simple model accounting for field boundary structure and multiple flow directions. Secondly, tillage translocation was modelled using ARCTILL. The  $^{137}\text{Cs}$  tracer technique was applied at four field sites containing cropmark archaeological features. Transect based sampling was applied using 25 m x 25 m cells to coincide exactly with the GIS grid system. Derived erosion/deposition rates were then used to optimise the water and tillage models at each field site, from which a general optimised net model was defined and applied at the regional scale.

The effect of field boundaries on patterns and magnitudes of potential overland flow and subsequent erosion/deposition was found to be significant and worthy of further research.

The archaeological features at Loanleven (NO 058 252) and Littlelour (NO 479 444) were found to be under serious threat from erosion caused by ploughing practices up to  $-1.34 \text{ kg m}^{-2} \text{ yr}^{-1}$  ( $-1.14 \text{ mm yr}^{-1}$ ) and  $-2.14 \text{ kg m}^{-2} \text{ yr}^{-1}$  ( $-1.34 \text{ mm yr}^{-1}$ ) respectively. Tillage erosion on average has contributed 75% and 69% at the Loanleven and Blairhall (NO 116 280) sites respectively clearly demonstrating the significance of the process. The highest erosion rates were located on strongly

convex slope sections, yet statistically were related only weakly. These loci were strongly correlated with topsoil depths.

For the whole study area, the general optimised net model predicted 65% of all archaeological sites (2849 in total) as being on land experiencing net erosion. Of some 1707 cropmark sites, 63% were predicted as being on land experiencing net erosion. 547 cropmark sites (32% of cropmarks) and 1053 (37% of total) of all archaeological sites present within the study area exceeded the soil loss tolerance threshold ( $0.13 \text{ kg m}^{-2} \text{ yr}^{-1}$ ).

This research underlines intensive agriculture as being the main damaging agent of buried archaeology across the study area.

## Statement of originality

I hereby confirm that the work contained within is original and written by the undersigned, and that all research material has been duly referenced and cited.

I have worked in the fast pace of the engineering world. Mick Whelan's leadership and Department guided me through many interesting projects and challenges. I have gained a lot of experience and knowledge. I am grateful for the opportunity to work with Mick.

A big salute to the staff who worked on the project. I was part of it for the purchase of a new system. The staff who worked on it were very helpful and provided the best support. The staff are so big like they would like to come highly recommend for any IT job. I was very happy to work with them and they did a great job. I was very happy to produce good products and I was very happy to produce a lot of work. Captions, titles, reference, styles, TOC, master documents - all look so without which the world would have been dark, frustrating, and worst of all repetitive.

Thanks to LRI for producing the best of all solution. ARC (the) is the foundation for the project.

## Acknowledgements

Firstly the biggest thanks have to go to my three internal supervisors, Donald Davidson, Ian Grieve, Andrew Tyler and one external supervisor Gordon Barclay (Historic Scotland). They developed the project before I appeared and secured excellent NERC funding as well as extra CASE support from Historic Scotland. Both NERC and Historic Scotland have looked after me financially very well. In particular, a special thanks to Gordon Barclay and Historic Scotland for providing me with massive amounts of OS data which has been the key to the project. Donald, Ian and Andrew were brilliant in their support, encouragement and time spent with me. They also did well to tolerate (just) my pigeon written and spoken English.

Although now in the rat race of the corporate world, Mick Whelan during his time in the Department guided me through many frightening Kirkby papers. His advice has been golden on many modelling issues and quite frankly things could have been tricky without him. Thanks Mick.

A big salute to John McArthur for his general IT help, but most of all for wangling the purchase of a non-HIGH GRADE PC for my use. That PC very rarely let me down in its 2-year service. SCAN provided the PC hardware so a big thumbs up to them and they come highly recommend for any IT kit.

You may hate them and slag 'em off, but Microsoft produce quality office products and Office 2K has allowed me to produce a fine looking thesis. Captions, cross-reference, styles, TOC, master documents - all tools in WORD 2K without which life would have been dark, frustrating, and worst of all manual and repetitive.

Thanks to ESRI for producing the benchmark GIS solution. ARC/INFO provided a rock steady foundation for the project.

Thanks to Alan Lilly at MLURI for the collaboration and comments on my ideas and work.

A huge thanks to David Tarboton for providing and helping with his  $D_{\infty}$  flow routing algorithm.

A big 'nice one' to the Departmental cartographers Bill and David. Without their earth shattering idea on how to digitally fill-in the SEPA PDF job application form, I'm sure I'd be still trawling unemployed-loser.com for the position of Big Issue sales consultant. I'll never forget that first interview question. You're the men.

Na zdraví to Dr. Nicholas Bowes for advice on general PhD matters and to avoid the human geography postgrads at the Sept. 2001 conference in Sheffield. Golden advice. Mum and Dad also deserve thanks for supporting me throughout the 3-year mission. They never fail to point me in the right direction when needed. Thanks a million. Alan, cheers for being best mate, partner in crime on nights out and hangin' out sessions, karting, piste carving, and being my D&B and XBOX sidekick. Dude ...you're *the* man.

Na zdraví also to my old and present office colleagues, in particular, Burkie, Kempy, Big Man, Griff, Chief Sadiq and Chief Sam for Departmental boisterous behaviour, banter and gossip.

Finally I am indebted to my gorgeous wife Pavla for tolerating my lifestyle over the last three years. She sacrificed a lot for me to embark on this PhD mission and it put us through rough times whilst living apart for the first year. Jseš nejlepší holka vůbec, vůbec, vůbec.

## Table of contents

<b>1. Introduction and rationale</b> .....	<b>10</b>
1.1 Background.....	10
1.2 The conflict between archaeology and agriculture.....	12
1.3 Evidence of soil erosion throughout the study area .....	19
1.4 Research aims .....	31
1.5 The study area .....	33
1.6 The field sites .....	38
1.6.1 Loanleven Farm, Almondbank, near Perth. ....	38
1.6.2 Blairhall Plantation, Mansfield Estates, Scone Palace, Perth. ....	43
1.6.3 Leadketty Holdings, Dunning. ....	47
1.6.4 Littlelour, Kirkbuddo.....	50
1.7 Field site summary .....	52
1.8 Summary .....	52
<b>2. Modelling water-based soil erosion</b> .....	<b>54</b>
2.1 Literature review .....	56
2.1.1 Factors influencing erosion .....	56
2.1.2 The basis for modelling erosion and deposition in a GIS environment.....	74
2.1.3 The selected erosion model .....	76
2.2 Pilot runs of the model .....	88
2.2.1 Water erosion model outputs.....	90
2.2.2 Sensitivity analysis .....	90
2.2.3 Modelling the effect of field boundaries.....	101
2.2.4 Results and discussion .....	102
2.3 Conclusions .....	123
2.4 Comparison of the water erosion model outputs with the MLURI erosion risk model (Lilly et al., 2002).....	126
<b>3. Modelling Tillage translocation.</b> .....	<b>134</b>
3.1 Literature review .....	134
3.1.1 The translocation process.....	137
3.1.2 Modelling tillage erosion .....	143



3.2	Development of a tillage translocation model .....	147
3.2.1	The Excel pilot model .....	147
3.2.2	Development of the tillage translocation model .....	151
<b>4.</b>	<b>Quantification of soil loss using the <sup>137</sup>Cs technique and its use as a modelling optimisation tool.....</b>	<b>165</b>
4.1	Literature review .....	165
4.1.1	Evolution of the <sup>137</sup> Cs tracer technique .....	168
4.1.2	Methodology of the <sup>137</sup> Cs tracer technique .....	170
4.1.3	Uncertainty and error.....	173
4.1.4	Applications .....	175
4.2	Sampling methodology.....	177
4.3	Baseline <sup>137</sup> Cs activity at reference sites .....	180
4.3.1	Loanleven.....	180
4.3.2	Blairhall.....	182
4.3.3	Leadketty.....	185
4.3.4	Littlelour.....	186
4.3.5	Summary.....	188
4.4	Estimation of soil erosion/deposition (calibration).....	189
4.4.1	Discussion of erosion/deposition rates .....	196
4.4.2	Error.....	198
4.5	Evaluation of the model outputs.....	200
4.5.1	The optimisation routine.....	202
4.6	Optimisation of the models. ....	203
4.6.1	Loanleven.....	203
4.6.2	Blairhall.....	223
4.6.3	Leadketty.....	237
4.6.4	Littlelour.....	252
4.7	Selection of a final optimum parameter set .....	264
4.8	Modelling discussion.....	269
<b>5.</b>	<b>Evaluating the erosion threat in an archaeological context.....</b>	<b>274</b>
5.1	Loanleven .....	274
5.2	Blairhall.....	277

5.3	Leadketty .....	279
5.4	Littlelour .....	281
5.5	Summary and discussion .....	283
5.5.1	Field site evaluation .....	283
5.5.2	Regional evaluation .....	284
6.	Summary of main results and conclusions.....	287
6.1	Principal results.....	287
6.2	Other results.....	288
6.3	Concluding discussion.....	290
Appendix A.	.....	297
Appendix B.	.....	302
7.	References.....	305

...likely to be lost or seriously damaged at intervals from one to five years ...  
...is necessary to predict what a researcher (questions such as: ...  
...what rate is damage occurring? need to be answered before projects ...  
...can be formulated.

The MARS project (Smith and Patten, 1985) identified 13 areas of ...  
...of which agriculture is listed first. This project requires ...  
...and the ways by which it modifies the landscape and can ...  
...soil erosion. Soil erosion may be broken down into ...  
...and wind and a cultivated component.

# Chapter 1

## 1. Introduction and rationale

### 1.1 Background

Archaeological remains take on many forms: ruins of former buildings, historic buildings, earthworks, finds and scatters of objects, and buried deposits. They represent the inheritance from previous communities, about which historical records may not exist. Archaeological evidence is also invaluable in supporting and complementing existing archives of historical maps and documents. The Monuments at Risk Survey (MARS) of England (Darvill and Fulton, 1998) provided a comprehensive up-to-date census of the archaeological resource in England. More importantly, projections on the future survival of a wide variety of monuments were proposed. The MARS concluded that 16% of monuments were destroyed prior to 1995, 8% within the last 50 years. The main causes of damage were identified as agriculture, urbanization and development, mineral extraction, demolition and building works and road construction. Due to this threat, some 2% of monuments in England were assessed as being at high risk and likely to be lost or seriously damaged in the next three to five years.

Is it therefore necessary to protect such a resource? Questions such as how much is there?, where is it?, what condition is it in? what are the causes of damage? at what rate is damage occurring? need to be answered before protection policy can be formulated.

The MARS project (Darvill and Fulton, 1998) identified 5 agents of archaeological damage, of which agriculture is listed first. This project focuses solely on agriculture and the ways by which it modifies the landscape and consequently influences soil erosion. Soil erosion may be broken down into a natural component due to water and wind and a cultivation component. Agriculture affects both of these components as direct and indirect effects on erosion. The direct effect is due to ploughing translocation, i.e. physical movement of soil.

The indirect effect on erosion is cultivation/management practice leading to changes in soil erodibility. The overarching aim of this study is to ascertain the magnitude of risk posed by the two components of erosion. Other causes of archaeological damage are not considered.

The context for this study has been well defined by a core of European scientists. First and foremost, the rate of soil profile truncation due to runoff and tillage translocation from archaeological cropmark sites in Perth and Kinross-shire has been quantified through the application of the  $^{137}\text{Cs}$  technique (Tyler et al., 1995; 1998; 2001). Buried archaeological features were found to be at risk due to redistribution of soil depending on the slope position. Similar field scale research using  $^{137}\text{Cs}$  in Britain and Belgium have highlighted the importance of ploughing activity on the geomorphological development of fields (Walling and Quine, 1990; Quine and Walling, 1991; 1993; Quine, 1995; 1999a; 1999b). Such work highlighted the opportunity offered by  $^{137}\text{Cs}$  to validate empirical spatial models such as those developed by Lindstrom et al., (1990) and Lindstrom et al., (1992) and provided a platform from which to investigate conditions specific to lowland central Scotland.

This first chapter presents data, arguments and anecdotal evidence to introduce the status of archaeological sites in the study area and then attempts to justify the need for detailed investigation. The chapter concludes with an outline of the research structure, aims and objectives.

## 1.2 The conflict between archaeology and agriculture.

To date very little has been done to recognize and act upon erosion damage to archaeological sites in Scotland (Barclay and Maxwell, 1998) even though it has been evident for many years. Government funds were made available to sites threatened only by commercial encroachment and coastal erosion, yet much of the archaeology around the arable lowlands of Scotland, particularly on the east coast to the Borders has been severely damaged by ploughing and other agricultural action. Saunders stated "There can be few, if any, archaeologists who are not aware that arable farming and forestry are the agencies of the greatest destruction of the material evidence for the understanding of our past..."(Hinchliffe and Schadler-Hall, 1980). Barclay (pers. Comm., 2002) described archaeology as being threatened by insidious erosion through normal agricultural operations. Many farming activities such as hedge removal, boulder clearance, and insertion/extraction of field drainage systems will have a negative impact on field archaeology but these are localized and infrequent events. Parallel to this is the continual background process of erosion and these sites are consequently subject to degradation at varying rates.

Two continuous processes threaten such archaeological remains.

1. Natural erosion, on managed and non-managed lands
2. Accelerated erosion resulting from management practices, in particular cultivation.

Exposure to natural or background erosion results in the buried archaeological evidence being brought progressively closer to the surface due to profile truncation, potentially resulting in complete exposure. Under accelerated erosion conditions, i.e. ploughing and poor vegetation management, the soil profile is gradually thinned as a result of surface water erosion. More importantly, ploughing will damage sub-surface features in the plough layer as the soil above them thins. Sites are consequently at risk of being exposed or

potentially destroyed prior to exposure by plough damage (Barclay, 1999:pers. comm.), which if confirmed may significantly shift the emphasis away from water as the agent of damage.

Cultivation is probably the most important factor in escalating the threat to archaeological remains. It results in damage through the following 5 mechanisms:

1. Abrasion and attrition damages the underlying deposits due to implement dragging.
2. Medium to long-term ploughing may result in net loss of overlying soil leading to potential site exposure.
3. Exposure at the surface leads to an increase in weathering rates.
4. Physical displacement of soil and artefacts from original locations due to plough throw. Loss of stratified archaeological information.
5. Large high performance machinery is more destructive than previous lighter machinery.

Ploughing has been regarded by archaeologists as the main destructive culprit long before geomorphologists and erosion modellers discovered it as being an important factor in erosion. Ploughing has been used in Scotland for some 6000 years. The methods of cultivation and ways by which they disturb soil and buried archaeology have been well documented by Nicholson (1980), Spoor (1980), and Lambrick (1980) in "The Past Under the Plough". The primary cultivation implement in the UK is the mouldboard plough, which turns the soil profile to a depth of up to 30cm through approximately 140° to mix organic residue into the soil. The mouldboard plough is particularly effective in damaging archaeology, both directly through the physical disturbance of the remains and indirectly through eventual truncation of the soil profile. Depending on the local topography being ploughed, the mouldboard plough will result in the lateral shift of soil both in the direction of travel and aspect and therefore has wider degradation implications. Numerous reports of archaeological damage due to the mouldboard plough in England are quoted in a recent study (Oxford Archaeological Unit (forthcoming)) on behalf of DEFRA. Other implements such

as harrows and discs also contribute to the damage, however mainly indirectly. Possibly as important, the subsoiler is used primarily to increase drainage. Usually applied to depths between 30 cm and 80 cm, it exacerbates soil loss through the break-up of the soil material, increasing susceptibility, and may directly disturb any remains in its path. Examples of damage are again reported in the DEFRA report.

Lambrick (1977) claimed that the significance and effect of the 'complicated interaction of variables' surrounding plough damage remained unestablished. This has changed, magnitudes and extents are now becoming clearer. Erosion rates have been estimated on a cropmark site at Littleour, Perth and Kinross (Davidson et al., 1998). On the cropmark a  $0.5\text{mm yr}^{-1}$  erosion rate was estimated using the in-situ  $^{137}\text{Cs}$  technique, yet within close proximity to the site rates increased to as much as  $1\text{mm yr}^{-1}$  on convex slope shoulders. Upon examining the data, topography and hydrological conditions around the site, it became clear that given the slope position such erosion rates could not be caused by runoff alone rather by ploughing. The authors concluded that rates of soil loss at this magnitude are likely across large lowland areas of fluvio-glacial sands and gravels and if maintained, will result in the loss of parts of the archaeological record.

Water based erosion also plays a role in contributing to the total threat. There is little reference made of the threat of water erosion to archaeology. Presently, extensive work is being completed in England by the Oxford Archaeological Unit on behalf of DEFRA regarding the management of archaeological sites. Preliminary work from this study reviews water erosion as being a significant factor. Water erosion is in no doubt very important as an erosive agent of the soil resource, yet in an archaeological context must be viewed differently. Water erosion is spatially very variable and is strongly controlled by topographic shape. Water erosion is commonly evident in topographic hollows where flow concentrates and negligible on sharply convex areas. Therefore topographic locus of the archaeological feature needs addressing before assumptions are made whether or not water is a significant threat to archaeology.

A comprehensive desk-based investigation of site damage has been carried out by Burke (in preparation, 1999-2002) in a slightly larger study area of 4800km<sup>2</sup> across mid-Scotland. Using the National Monument Record of Scotland (NMRS), interim results from Burke's work identify that between 1850 and 1999 some 10% of the sites were recorded as damaged in general and 6% as destroyed. The main causes of damage or loss of these sites are quoted as being archaeological excavation (16%), agriculture (18%; not necessarily solely ploughing), development (roads, buildings etc) 13%, and forestry (8%). Burke (pers. comm., 2002) also quoted that 35% of these damaged or destroyed sites are caused by unknown factors. In addition the majority of the sites having damage recorded but cause unrecorded (35%) have been noted to occur in arable or improved pasture land classes. As a result, the 18% figure attributable to agriculture will almost certainly be higher.

Scotland has had no such nationwide assessment of archaeological sites similar to the MARS. This study in close association with a project by Burke (1999-2002; in preparation) constitutes the first attempt to assess the status of a selection of sites in Scotland. This project is set at the regional scale and deals with only a small 80 km x 60 km study area (Figure 1.1. and Figure 1.2). A total of 4250 archaeological sites are located within the study area and the National Monument Record database defines 1830 of these as being cropmark sites. 2849 or 69% of all sites are located on arable land classifications (LSC, 1988) and clustering is clearly evident from Figure 1.2. 1707 or 60% of all sites on arable land sites are cropmarked.

This project concentrates on cropmark sites since very little is known about them in general. They are easily identified from aerial photographs. Initially many cropmark sites were upstanding or positive features and have since been gradually ploughed away leaving only negative features for identification. They are visible due to differences in the growth vigour of vegetation resulting from the archaeological remains under the soil surface. Both positive and negative crop-marks are visible. Cropmarks are caused by archaeological features that have been cut into the subsoil such as drainage ditches, postholes, cellars, wells and cesspits.



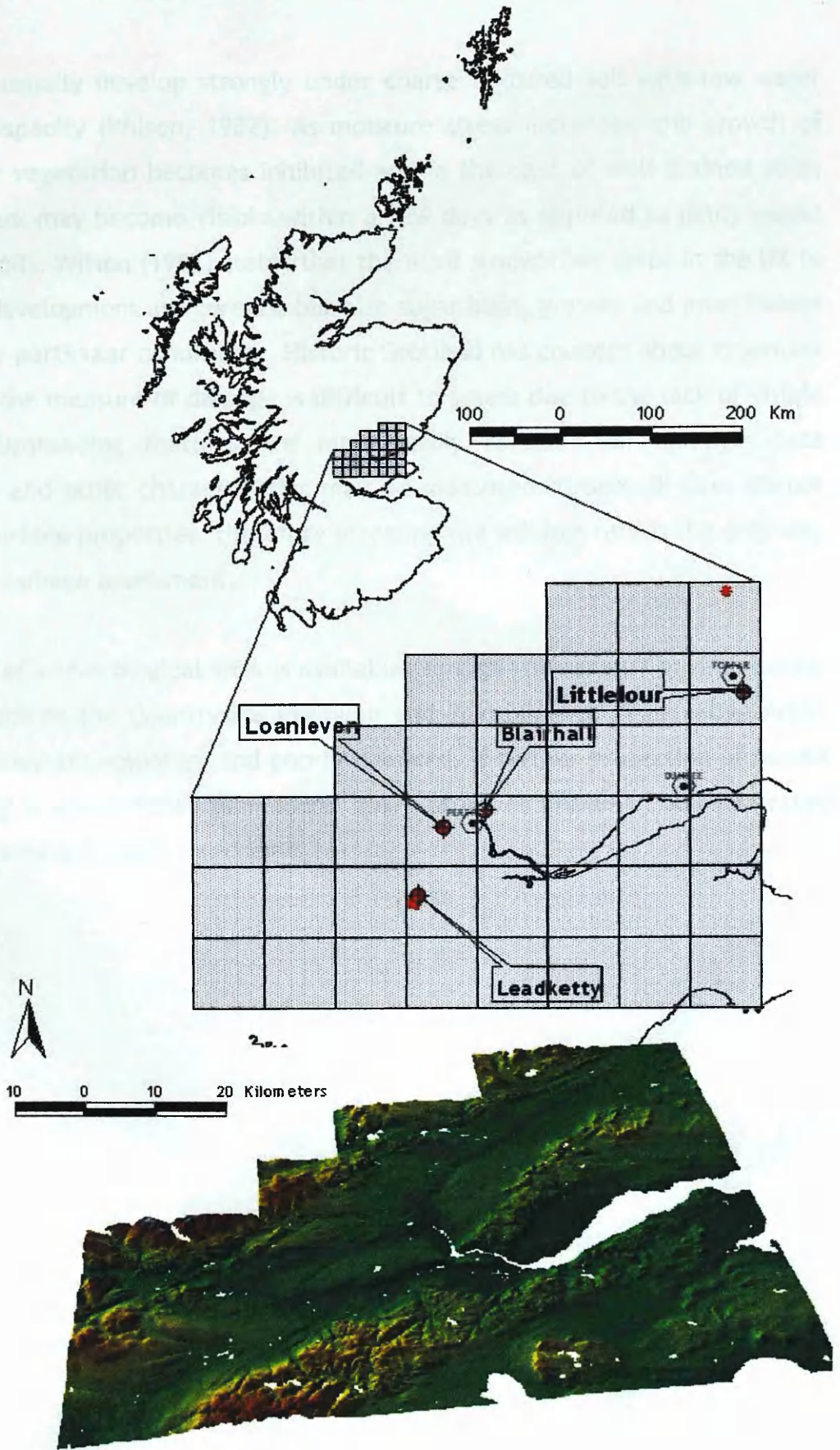


Figure 1.1. Geographical extents and 3D topography of the study area.

Cropmarks usually develop strongly under coarse textured soil with low water retention capacity (Wilson, 1982). As moisture stress increases, the growth of the crop or vegetation becomes inhibited and in the case of well-drained soils, the cropmark may become visible within a few days as opposed to many weeks on clayey soils. Wilson (1982) states that the most susceptible crops in the UK to cropmark development are cereals, but also sugar beet, grasses and most fodder crops under particular conditions. Historic Scotland has concern about cropmark sites since the measure of damage is difficult to assess due to the lack of visible features. Upstanding features are more easily assessed for damage since dimensions and other characteristics may be measured. Cropmark sites do not offer measurable properties, therefore assessing the soil loss rate is the only way forward in damage assessment.

Protection of archaeological sites is available through various agri-environmental schemes such as the Countryside Premium and Environmentally Sensitive Areas schemes. They are voluntary and poorly financed. If further protection of buried archaeology is appropriate, then sound quantitative estimates of soil loss rates and timescales are vitally important.

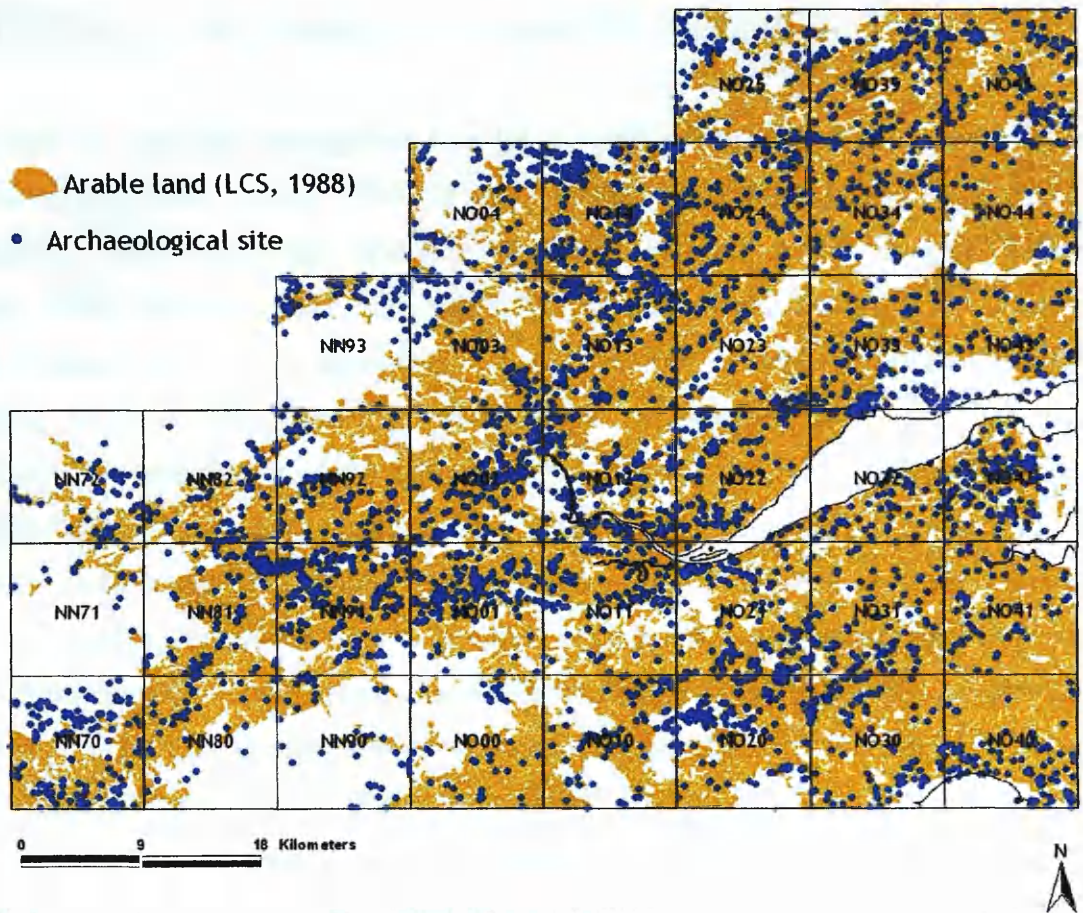


Figure 1.2. Distribution of archaeological sites across the study area.

### 1.3 Evidence of soil erosion throughout the study area

Evaluation of soil loss throughout the UK is well documented (Boardman and Favis-Mortlock, 1993; Evans, 1990a; Evans, 1990b; Frost and Speirs, 1984; Frost and Speirs, 1987; Kirkbridge and Reeves, 1993; Morgan, 1980; Morgan, 1985; Morgan, 1990; Speirs, 1987). The majority of such work, however, has been within England and Wales leaving a lack of detailed erosion investigations for Scotland. Despite this, there is evidence for accelerated soil loss. Extreme events are documented in south-east Scotland (Frost and Speirs, 1984) where an estimated  $60\text{ t ha}^{-1}$  was lost resulting from a 24 hour 28 mm rainfall event and in a parallel field some 800 t of soil was removed from 10 ha after 12.7mm of rain. In Roxburghshire, an estimate of 1000 t plus of material was washed away from a turnip field during a single event. Such events are rare and extremely localised, yet lower magnitude events appear to be similarly erosive. Duck and McManus (1987) claim to have offered the first detailed quantified account of erosion in the Dundee-Arbroath area. A weekend medium intensity event provided 65mm of rainfall and removed an estimated 88 t of topsoil equivalent to some  $14\text{ t ha}^{-1}$  for the field. More recently Kirkbride and Reeves (1993) report a similar weekend-duration event whereby 58 % of 195 fields surveyed were eroded and 30% suffered rill damage. Their estimates of  $1.17\text{--}2.22\text{ t ha}^{-1}$  appear to be in excess of loss tolerances for the region. During an 18-day period in January 1993, Davidson and Harrison (1993) mapped 208 fields across the Strath Earn district of the Perth area. They recorded 76 fields as containing erosional features, mostly as ephemeral gullies and rills. Snowmelt assisted erosion close to the town of Cupar in Fife in 1993 and 1996 was reported by Wade and Kirkbride (1998). Rapid snowpack thaw along with heavy rainfall removed some  $127\text{ m}^3$  of material from one field during January 1993. All fields were sown with winter cereals and ploughed in an up-down slope manner. Wade and Kirkbride (1998) suggest that snowmelt-generated erosion had been observed to be widespread across Fife during January of 1993. They warned further that the overlapping of certain meteorological conditions with a frozen soil profile and winter cereal sowing can result in disproportionately large volume of runoff being generated than the precipitation record would have alone predicted.

In this study a substantial amount of photographic evidence has been collected for the Perth area from December 1998 to the December 2001. A selection of it is presented here with the aim of displaying the range of features commonly witnessed. The vast majority of erosion damage has developed during the winter months and almost exclusively on finely tilled soils before the crop has become sufficiently established. Rill and gully features have by far been dominant and have been strongly influenced by the presence of linear features within the field such as wheel tracks and plough-induced microtopography or drainage/boundary features forming the field mosaics. Extensive sheetwash has been either absent or present at unnoticeably low magnitude levels. Figure 1.3 shows the locations of the following erosion evidence.

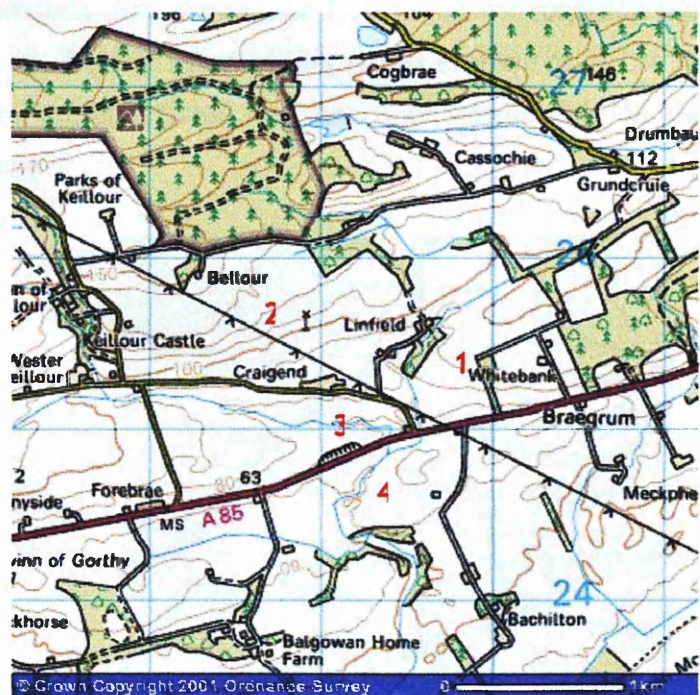


Figure 1.3. Map showing location of photographic evidence (NN996250: map centre). *Reproduced from Ordnance Survey map data by permission of Ordnance Survey, ©Crown copyright.*

Figure 1.5 shows a particularly good example of the effect of runon<sup>1</sup> from an immediately adjacent upslope field. This phenomenon has been seen many times throughout the region. Behind the fenceline at the top of the field, the slope gradient reduces close to zero. Low slope angles generally have high drainage areas and this appeared to be the case here as an incised channel (c. 20 cm deep) was present along the whole length of the upslope field boundary. This channel delivered its discharge into the photographed field via an open gate. Flow was then forced along a wheel track, which eventually reached the headland wheeltrack then changed direction almost 90°. Some flow also ‘jumped’ the junction of the two wheel tracks and was subsequently forced along the boundary edge (Figure 1.5b). Flow from the headland wheeltrack, minor rills and the adjacent upslope wheeltrack converged at point c causing the channel to widen. Approximately 20m downslope from point c deposition began and continued for 30m or so. Further minor rilling noted elsewhere in the field suggested that runon from upslope fields had not been responsible in these cases, rather due to intra-field drainage area runoff.



Figure 1.4. Map showing location of gully 5 in Figure 1.9. *Reproduced from Ordnance Survey map data by permission of Ordnance Survey, ©Crown copyright.*

<sup>1</sup> Runon: surface flow delivered from an adjacent upslope field

Figure 1.6 illustrates a particularly large and long gully that generated 500m further west (presumably) from the same event responsible for the features in Figure 1.5. Substantially larger volumes of discharge would have been necessary for such a feature to develop, however once again the same process of runoff delivery from upslope field units was the cause. There was no incised channel operating as the delivery mechanism this time upslope of the photographed field. The upslope field was covered with grass and from the 1:25,000 OS map the contours indicate a subtle topographic swale almost 300m long. There have also been a number of field boundaries removed that are present on the OS map. The source of the drainage area was woodland. The gully length was estimated at 250m from initial point of incision to the start of the deposition zone. Despite wheel tracks being present within the path, they played little part in diverting flow. The deepest channel section was 45 cm. Figure 1.6c shows a significant area of crop was lost due to the gully in addition to the large volume of sediment dumped in Figure 1.6c. Here the ground has been raised due to the accumulation of sediment. The farmer openly talked of his desperation with the feature re-occurring year after year. His latest attempt to solve the problem consisted of infilling with stone chippings and rubble. Needless to say the parts of the infill remnants are still visible in Figure 1.6c.

In the southerly bordering field to Figure 1.6 every wheeltrack had been rilled, some more than others. The two shown in Figure 1.7 were incised to depths of 20cm and had produced rill networks outside the ploughed zone, which were delivering sediment into Keillour Burn. Material had been deposited here and the same farmer talked of having to dredge periodically.

Figure 1.8 located at position 4 in Figure 1.4 was a result of agricultural runoff being contributed to by urban runoff (A85 road). The picture was taken from the A85 looking south at the point where runoff entered the field via a weakness or discontinuity on the boundary. No wheeltracks were present, however plough induced topography was and is visible in the photograph. It is difficult to assess whether flow has been controlled in any way.

Gully 5 shown in Figure 1.9 and located in Figure 1.4 is located in an area very

susceptible to water erosion due to the steep topography and up-down slope ploughing. It appeared in February 2000 and was a particularly striking feature since it strongly highlighted the importance of a number of processes. Firstly, the presence or lack of wheeltracks has been crucial as to whether or not concentrated flow erosion is triggered. There were no other signs of rilling/gullying within the field unit, only wash within other wheeltracks. Secondly, it is noticeable how the change in topography can swing erosion into deposition and vice-versa over very short distances. Incision of the wheel-track only occurred where the volume and velocity of the discharge reached a certain threshold i.e. where slope length has been sufficiently long. The farmer after summer harvest was forced to refill the gully with material from the alluvial fan. Figure 1.4 shows the whole of the north bank of the river Earn to be a complex of long convex-concave slopes and farming such zones has major potential water quality implications. Anecdotal evidence from a local fisherman who has fished this exact stretch of the Earn for twenty years spoke how he has noticed over the last ten years more and more soil is being lost from cultivated fields bordering the river Earn.

In Scotland, however, there is a distinct lack of medium to long-term monitoring of soil loss as opposed to the above anecdotal documentation of extreme events. To assess the real threat posed to archaeological sites within the next decades, an indication of areas prone to landscape modification due to erosion and deposition must be determined. Quoting isolated extreme events is insufficient since the factors influencing erosion are so spatially variable that extrapolation is just not possible as well as being non-representative.

The risk posed to the cropmark sites of lowland Scotland is determined solely by the rate at which the covering soil is being removed. From collating the available evidence it is clear that the previous low-importance rating of Scottish lowland erosion requires re-evaluation. Not only is the rate of soil removal of paramount importance, it must be placed into perspective alongside loss tolerance thresholds derived from rates of soil formation and alongside the sensitivity/importance of individual features in terms of soil loss. Kirkby and Morgan (Kirkby and Morgan, 1980) quote acceptable rates of erosion of  $2-10 \text{ t a}^{-1}$



yr<sup>-1</sup>, equivalent to 0.2-1 mm yr<sup>-1</sup> reduction of the surface. Without a base level with which to compare the erosion statement this becomes meaningless. If policy decisions are to be considered based on these results, then clear declarations on either present, historical or predictive rates of soil have to be presented in relation to soil loss tolerance values.



Figure 1.5. Rill damaged winter cereal field (location 1 Figure 1.3) located on the A85 looking north approximately 10km west of Perth (NN996250). A) concentrated runoff received from upslope adjacent field. As slope increases flow diverged and was forced by wheeltracks. B) Convergence of wheeltrack flow at headland, 90 degree change of direction and deepening of channel evident. Some flow also 'jumped' the wheeltrack and routed along boundary edge furrow. C) Further convergence of flow and deepening of channel. circa 20m downslope of C deposition begun.



Figure 1.6. Large gully (location 2 Figure 1.3) located at Craigend (NN986254)(500m west of Figure 1.5); a) 120 m tail-end section b) deposition fan c) close-up of gully channel.





Figure 1.7. Extensive evidence of wheeltrack rilling (location 3 Figure 1.3) throughout the adjacent field to Figure 1.6 previous (NN990251).



Figure 1.8. Two gullies (location 4 Figure 1.3) generated as a result of runoff from the adjacent A85 to Crieff (NN991247) and upslope fields. 28

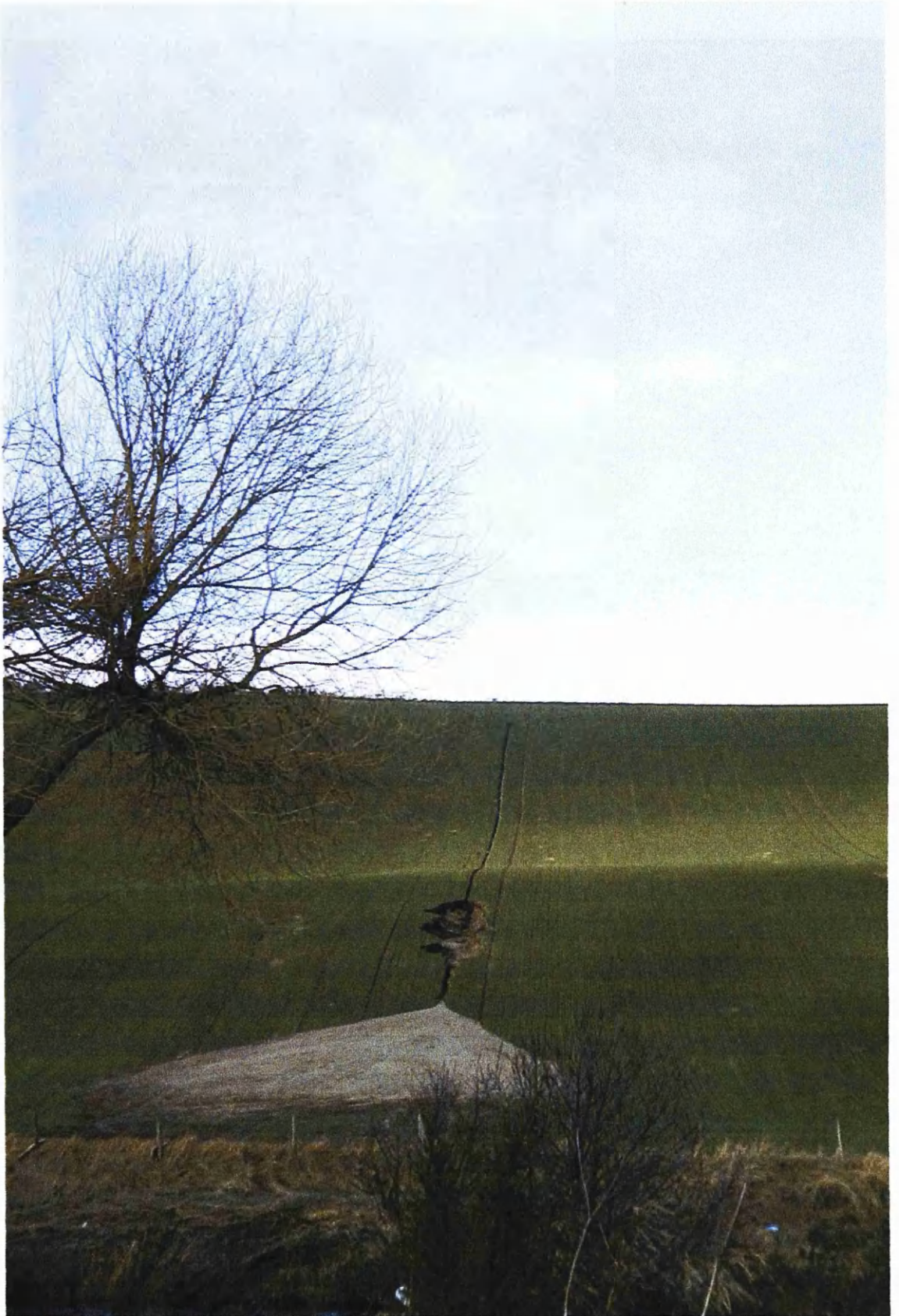


Figure 1.9. Large gully (location 5 Figure 1.4) incised in a wheel track located close to Forteviot Bridge (NO038183) resulting from winter rainfall (February 2001).



Figure 1.10. Attempts to infill a gully noted on Gask Estates (NN996180) in January 1999.

Archaeological sites across lowland Scotland are preferentially located within intensively cultivated arable land (Figure 1.10). The critical issue is therefore the effect intensive agriculture is having on the valuable cultural resource. This research aims to ascertain just whether or not the concerns of archaeologists and environmentalists can be justified and if the claims have any substance.

## 1.4 Research aims

The project overall aims to:

To assess the threat of erosion posed to archaeological cropmark sites by quantitatively modelling soil erosion rates across arable lands of lowland mid-Scotland.

There are two steps towards achieving the overall aim:

- a) Quantification of medium-term rates of soil erosion at four selected field sites using the  $^{137}\text{Cs}$  tracer technique.
- b) Development, testing and optimisation of erosion models using data collected from field sites prior to application both at the field and regional scales.

The phases of the project ran in parallel most of the time and development and testing of the erosion models within GIS was conducted mainly when fieldwork became impossible due to weather. The structural layout of the project can be seen as a flow diagram in Figure 1.11.



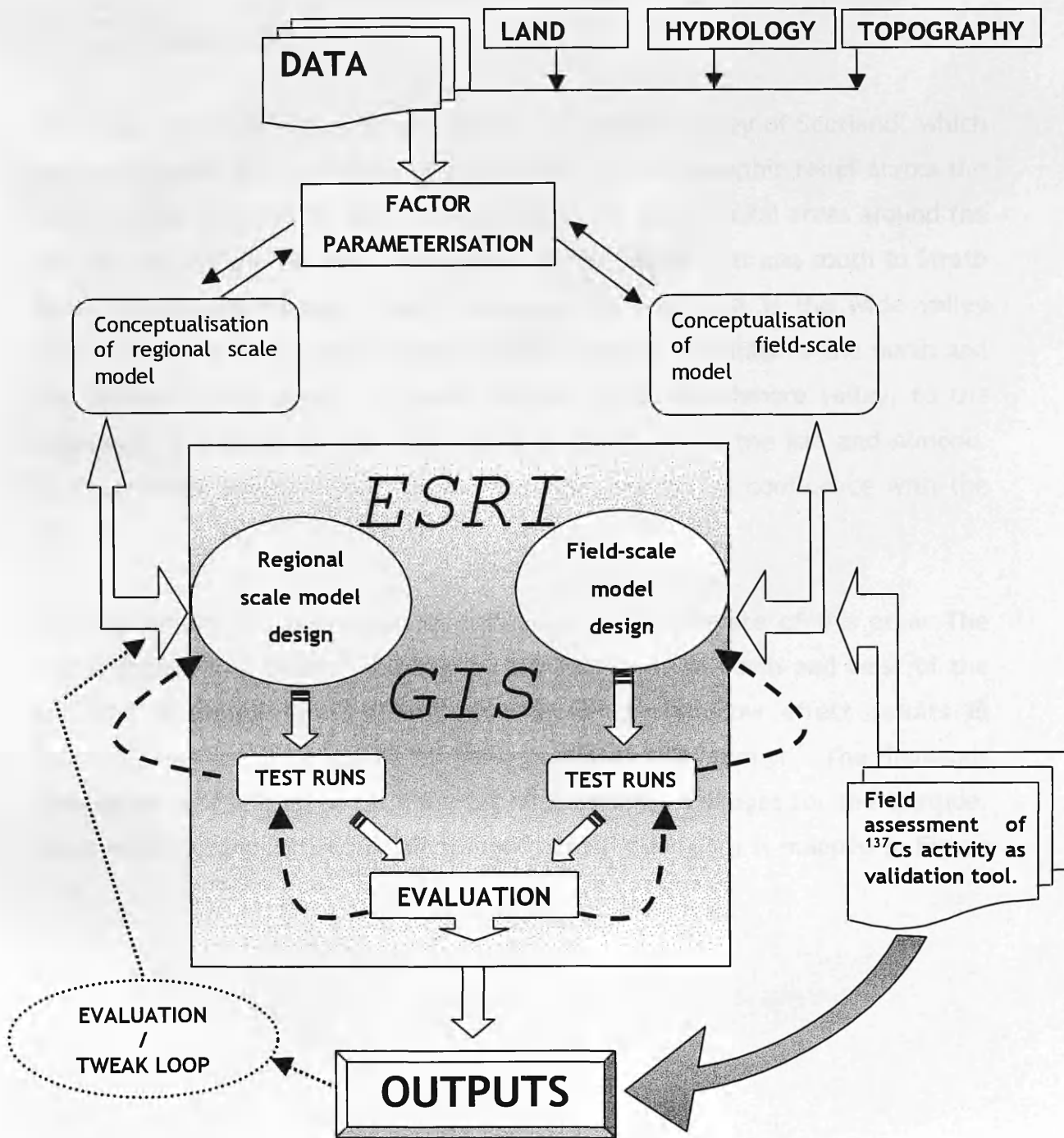


Figure 1.11. Conceptual flow diagram of the project structure.

## 1.5 The study area

The study area lies almost totally within the midland valley of Scotland, which divides naturally into a number of sub-regions. The topographic relief across the study area is 870m. In the east, the generally low lying coastal areas around the Tay estuary rise sharply both to the north as the Sidlaw Hills and south to Strath Eden. In contrast running roughly southwest to northeast is the wide valley region of Strathmore, which separates the Grampian Foothills to the north and the Sidlaws to the south. The main portion of the Strathmore valley, to the northeast, is drained by the river Tay and its tributaries the Isla and Almond. South of Perth the river Earn drains from the west to its confluence with the Tay.

The topography has a pronounced influence on the climate of this area. The whole region is in effect sheltered by the Highlands to north and west of the Highland Boundary fault. A well-pronounced rain shadow effect results in relatively low annual precipitation between 600 and 700 mm yr<sup>-1</sup>. The Highlands also cause cloud break-up allowing for high sunshine averages for the latitude. Mean winter precipitation for all stations across the region is mapped in Figure 1.12.

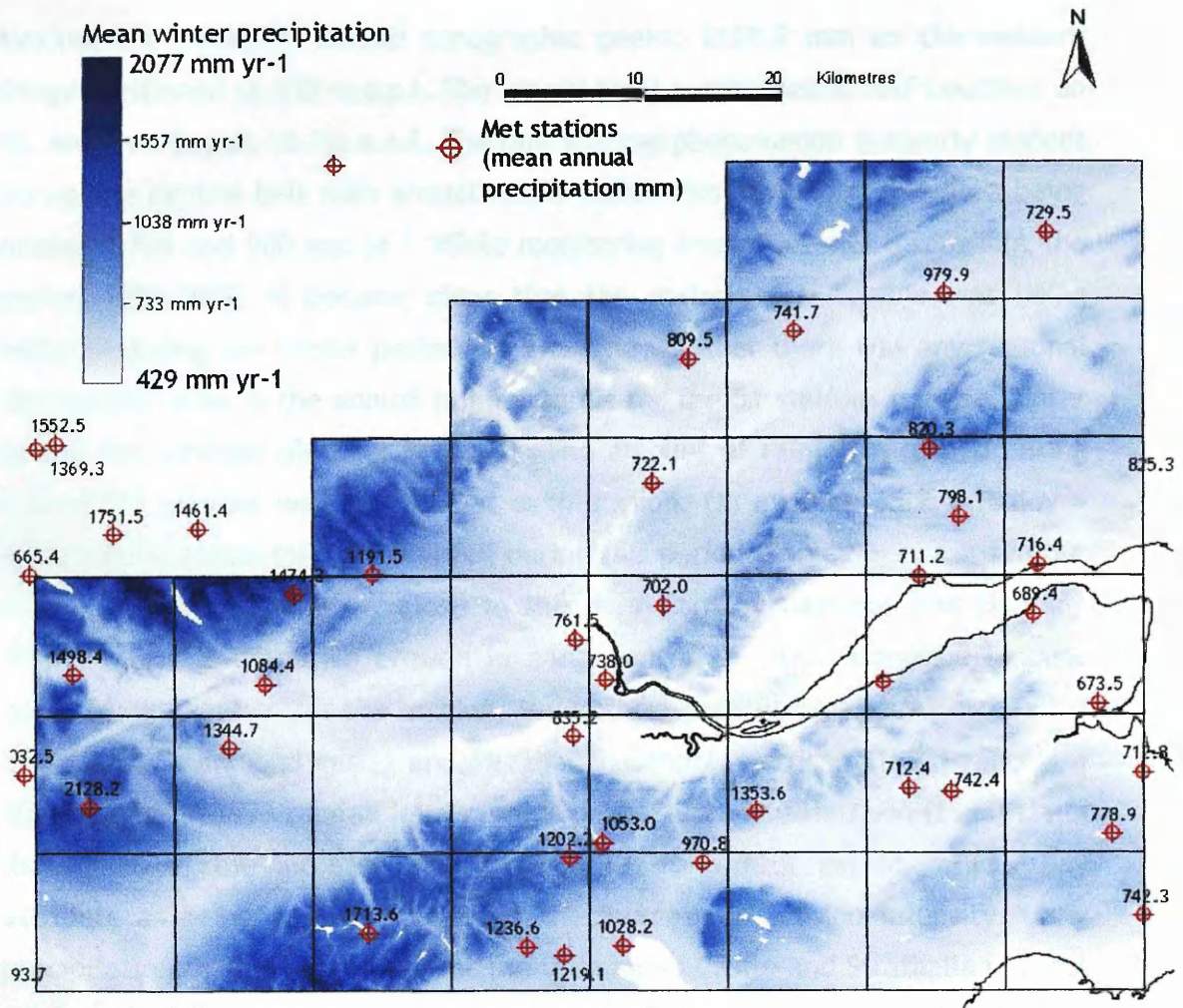


Figure 1.12. Distribution of mean winter precipitation from study area meteorological stations. Basemap is a regression model of winter precipitation, elevation, and easting ( $r^2=0.76$ ,  $p=0.000$ ,  $n = 51$ ).

Maxima are clustered around topographic peaks; 2121.2 mm on the western fringe positioned at 330 m a.s.l. The lowest total is recorded at RAF Leuchars on St. Andrews Bay at 10.1m a.s.l. The rain shadow phenomenon is clearly evident across the central belt with annual totals within this lowland arable area being between 700 and 900 mm yr<sup>-1</sup>. While monitoring erosion events throughout the period 1999-2002, it became clear that the majority of damage was being inflicted during the winter period. To examine whether there was any seasonal distribution skew in the annual rainfall totals for the 51 stations used, a winter period was defined (October to April). The amount of rainfall recorded during this winter window was analysed at each station. On average 65.2 % (stdev = 4.7%) of the annual rainfall total fell during this period. Survey work carried out in the area of Forgandenny close to the river Earn by Davidson and Harrison (1995) reported extensive erosion in early winter of 1993. Alongside landuse issues as explanation for the erosion, the authors present precipitation data for 2 stations, Drummond castle and Strathallan School. Harrison (1993) reports a 40% increase in 1973 rainfall levels for 1990. Davidson and Harrison (1995) claim that much of the increase has occurred in the winter period, which they attribute as being a prime cause for the increase in erosion intensity. Daily precipitation data was analysed for the Drummond Castle and Strathallan School stations for the periods 1977-1999 and 1978-1998 respectively to confirm whether or not an increasing trend in winter rainfall existed.

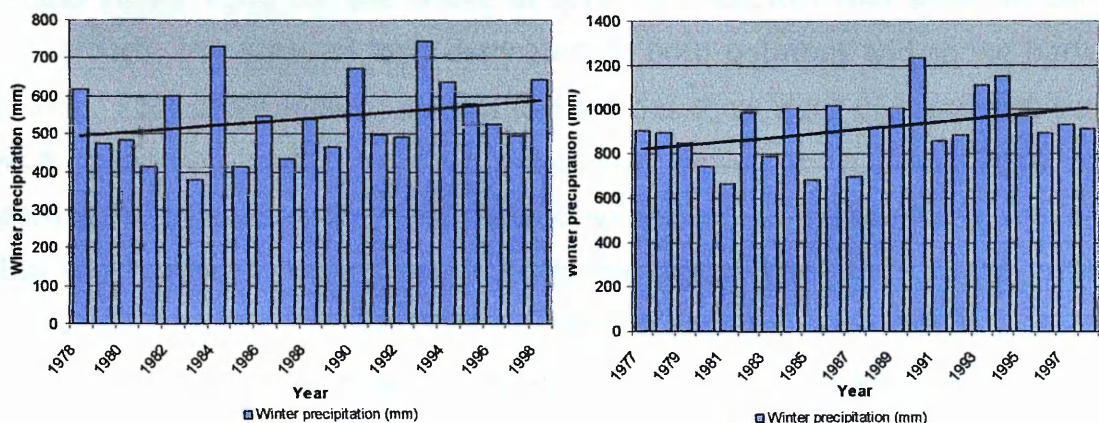


Figure 1.13. Trends in winter precipitation at a) Strathallan, School b) Drummond Castle.

Winter rainfall in 1990 was 673mm (70%) and 1234mm (78%) for Strathallan School and Drummond Castle respectively. Since 1992 when Davidson and Harrison's (1995) climate records finished percentage winter precipitation has oscillated between 61% and 79% for Strathallan School and between 63% and 80% at Drummond Castle. Figure 1.13 illustrates over the whole run of data a consistent increasing trend in winter rainfall at both stations and although not presented here data from RAF Leuchars, Faskally, Forfar, St. Andrews, and Mylnefield all display similar rising trends towards higher winter rainfall.

Parent material throughout the Midland Valley is dominated by a succession of Old Red Sandstone and Carboniferous sediments. Folded in between these are zones of volcanic lavas and tuffs as well as igneous intrusions. The Strathmore valley sits on Old red Sandstone folded into an asymmetrical syncline parallel to the Highland Boundary Fault. The Sidlaw and Ochil anticline consists of hard volcanic lava outcrops, which make up the steep slopes on the north and south sides of the Tay estuary. The influence of the underlying rock is evident in the sandiness of soils throughout the whole region. Details of soils at each site are given later in this chapter.

The soil and climate of the study area is particularly suitable for arable crop production, in particular potatoes and cereals. Data provided by SEERAD (Figure 1.14 and Figure 1.15) for the whole of Scotland indicates that after an early 1990's trough, the areas of land dedicated to both potatoes and spring barley increased. Root crops such as carrots and swedes show signs of consistent slow growth. Increasing trends quoted for the South Downs (Boardman, 1990) and eastern Scotland (Speirs, 1987) for planted winter cereals in the 1980's and 90's within the erosion literature certainly do not agree with those found across Scotland and in the study area today. Possibly an important emergence, however is the relatively rapid increase in rape both winter and spring planted. Despite being on the decrease in 1999, rape is becoming more widespread across the lowlands of the study area.

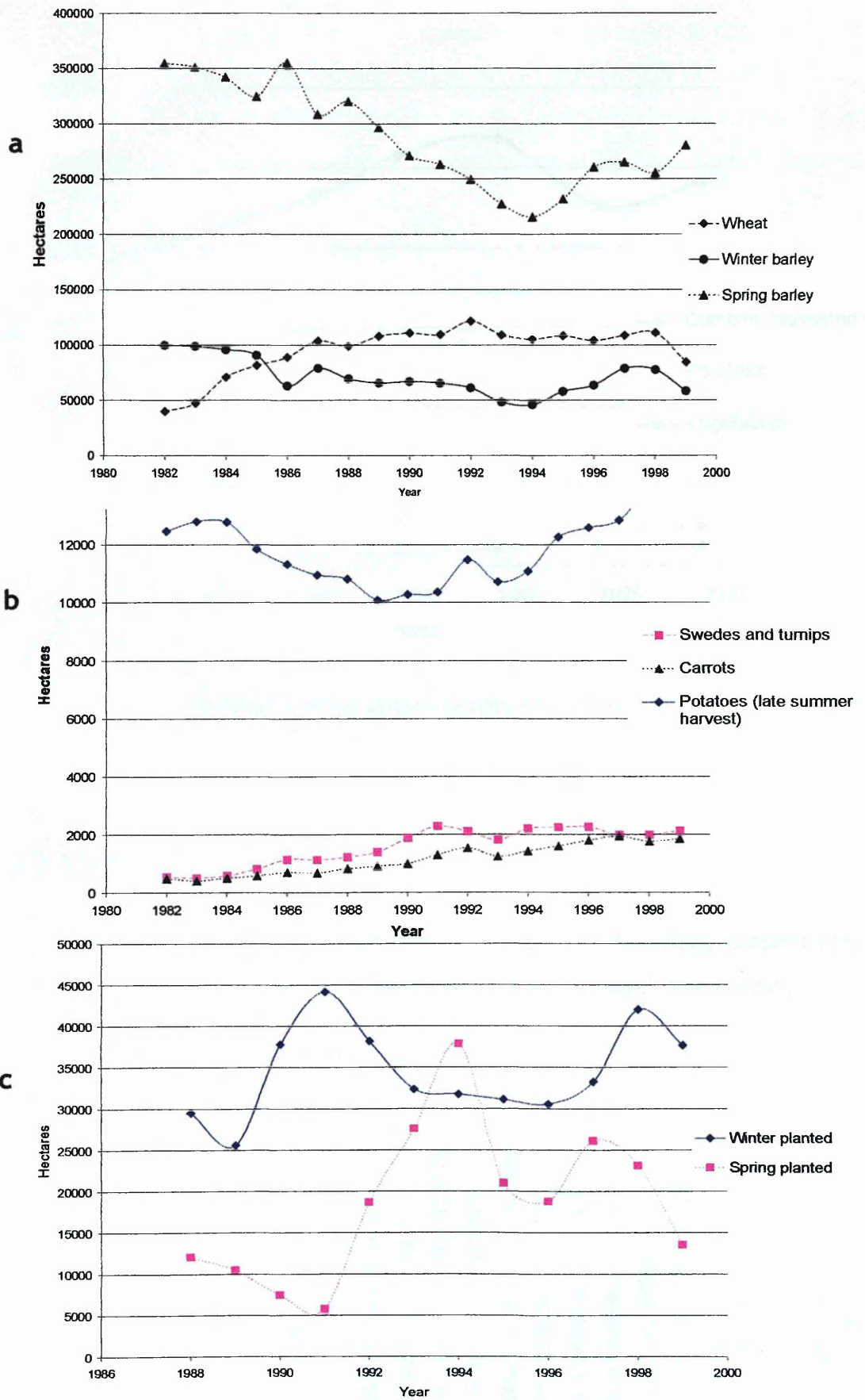


Figure 1.14. Trends in particular crops across Scotland; a) cereals b) vegetables c) rane seed oil

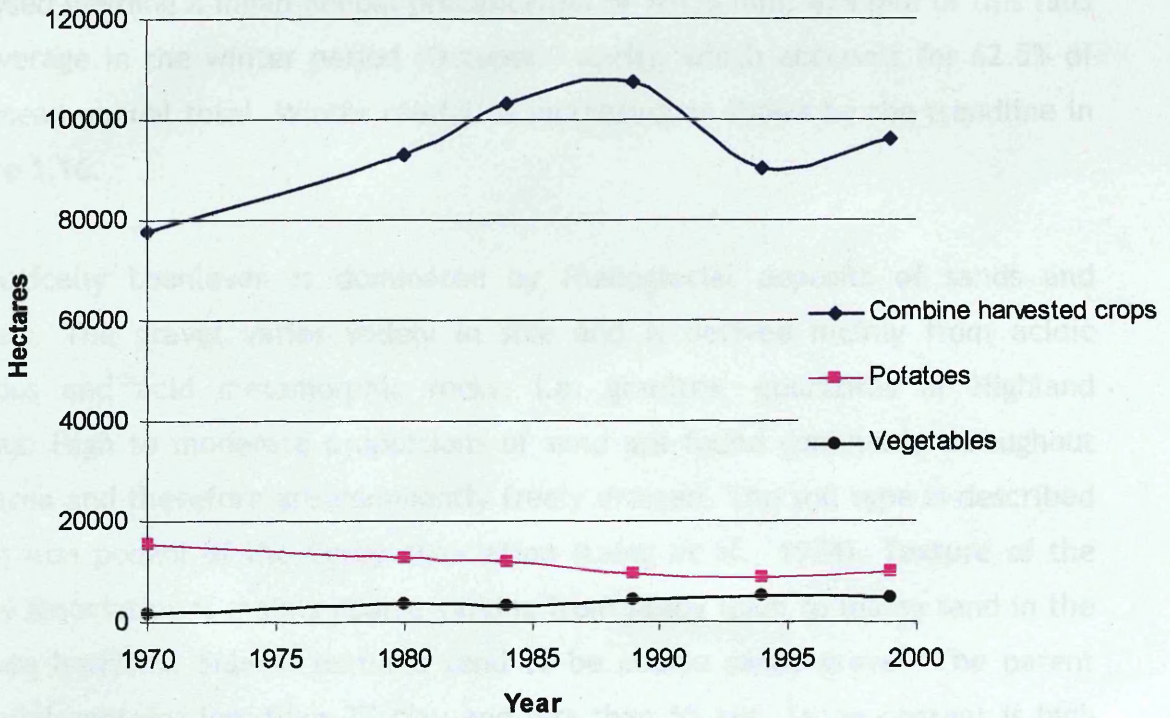


Figure 1.15. Trends in crops grown across the study area

## 1.6 The field sites

Four field sites were selected primarily on the basis of archaeology present and intensive agricultural use of the land. Brief descriptions of each site follow.

### 1.6.1 Loanleven Farm, Almondbank, near Perth.

Map reference: NO 058

252

Elevation: 40m a.s.l.

Parish: Methven

Council: Perth and

Kinross

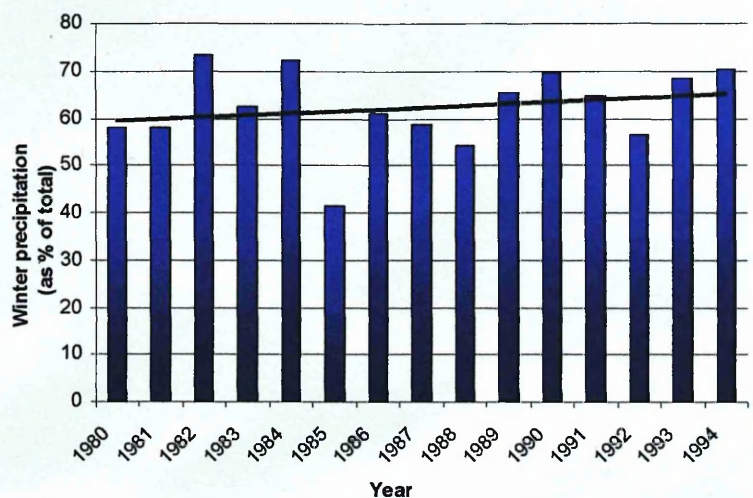


Figure 1.16. Trend in winter precipitation for Perth crematorium.

The closest rain gauge is located at Perth crematorium. 14 years of records were analysed yielding a mean annual precipitation of 761.5 mm. 474 mm of this falls on average in the winter period (October - April), which accounts for 62.5% of the mean annual total. Winter rainfall is increasing as shown by the trendline in Figure 1.16.

Geologically Loanleven is dominated by fluvioglacial deposits of sands and gravels. The gravel varies widely in size and is derived mainly from acidic igneous and acid metamorphic rocks, i.e. granites, quartzites or Highland schists. High to moderate proportions of sand are found commonly throughout the area and therefore are dominantly freely drained. The soil type is described as an iron podzol of the Corby association (Laing et al., 1974). Texture of the Corby association is mainly coarse varying from sandy loam to loamy sand in the surface horizons. Subsoil textures tend to be coarse sandy gravel. The parent material contains less than 2% clay and less than 5% silt. Stone content is high and is generally of smooth rounded types of varying sizes.

The memoirs of the Soil Survey of Great Britain defines Loanleven as being land capability - class 3. This class includes moderately severe limitations which restrict the choice of crops or that require special cultivation practices.



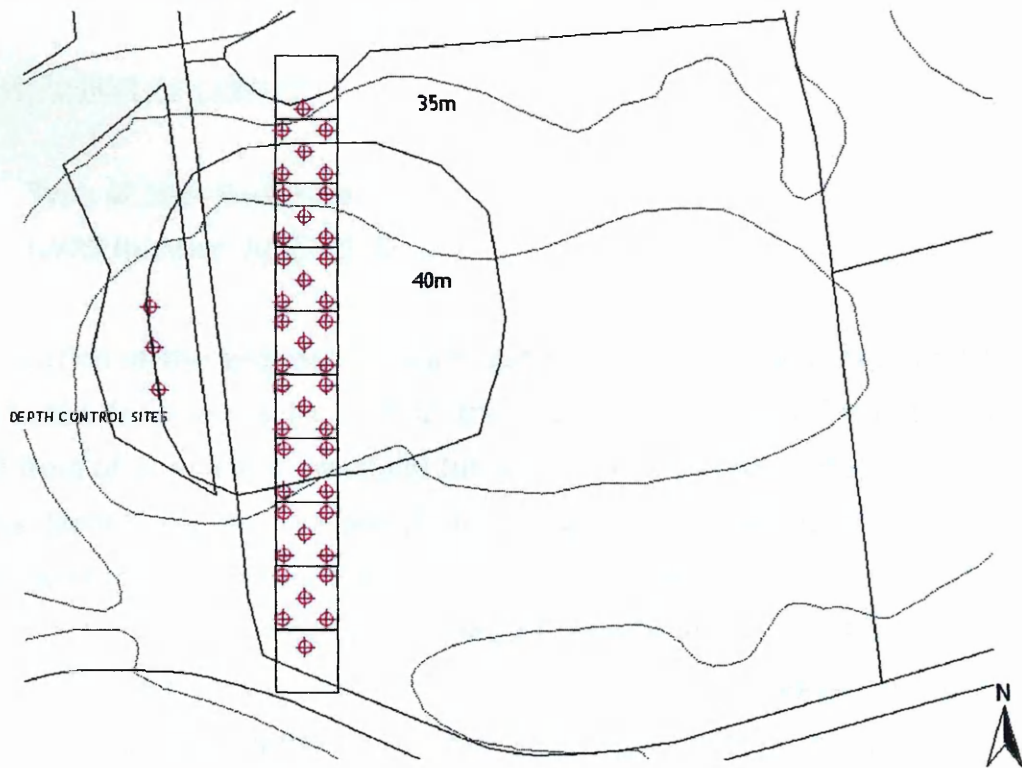
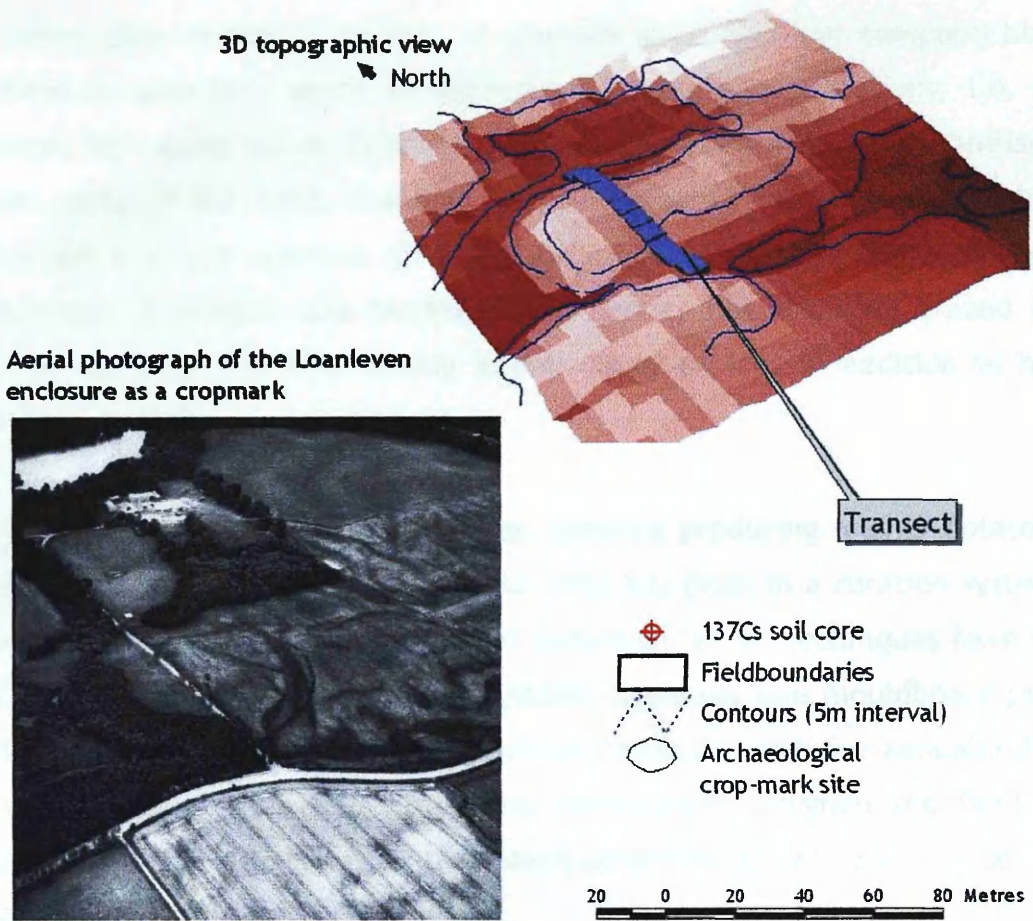


Figure 1.17. Topographic and archaeological layout of the Loanleven field site.

The survey also reports of an area of alluvium (peat-alluvium complex) bisects the field in question, which is defined as having wet limitations, i.e. poor drainage, high water table. Drainage problems have certainly been witnessed in certain parts of the field, however are likely due to topography. The highly stoney soil has poor nutrient holding capacity and therefore demands regular applications of manure and fertilizer. The farmer has regularly grazed large herds of cattle in this field during intercropping periods in addition to heavy manure spreading.

The 6.5 ha field is part of a large farm complex producing mainly potato and cereal crops. During the last 3 years the field has been in a rotation system of winter and spring cereals. Conventional individual tillage techniques have been used here as opposed to a one-pass system. Generally one mouldboard plough application, discing plus seedbed preparation has occurred twice annually during the project's lifecycle. The farmer has consistently ploughed the field in a north-north-westerly to south-south-easterly direction, effectively in an up-down slope manner.

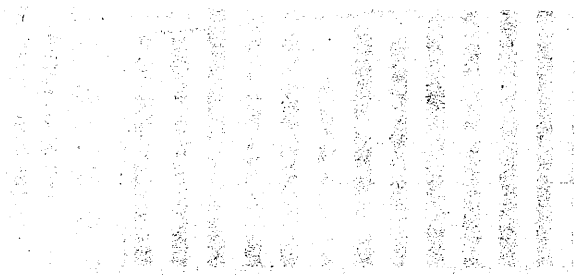
### Archaeological description

Type of Site: Enclosure

NMRS Number: NO02NE 32

The location of the enclosure is such that the farm approach road from the A85 bisects the feature leaving half in the cultivated research field and half in a small field of permanent grassland (used for <sup>137</sup>Cs reference site). The feature is clearly identifiable as a cropmark in periods of moisture stress as seen in the aerial photograph (Figure 1.17). At present the site is scheduled. The study focuses only on the portion of the feature under cultivation. The topography of the field is slight with the enclosure appearing to be positioned on the plateau-type rise, centrally positioned in the field (Figure 1.17). To the north of the feature the short slope breaks quite steeply to the field boundary. This slope continues to the eastern fence boundary and accumulated runoff has been noted standing at the base of this slope. To the south of the feature the backslope is

less steep yet longer with a significant concavity at the base. Surface runoff also appears to accumulate and stand here. In summary the field although quite small, has a varied and complex topography, therefore offered a good opportunity to observe water and tillage based erosion processes.



The field is a small, irregularly shaped plot of land, approximately 10m by 15m. It is situated on a slight slope, with the highest point on the left side and a significant concavity at the base. The soil is dark and appears to be a heavy clay or loam. The field is currently in a fallow state, with some sparse vegetation and a few small trees scattered around the perimeter. The topography is quite varied, with several small mounds and depressions. The field is bounded on the left by a fence and on the right by a road. The overall appearance is that of a well-maintained but somewhat neglected agricultural plot.

The field is a small, irregularly shaped plot of land, approximately 10m by 15m. It is situated on a slight slope, with the highest point on the left side and a significant concavity at the base. The soil is dark and appears to be a heavy clay or loam. The field is currently in a fallow state, with some sparse vegetation and a few small trees scattered around the perimeter. The topography is quite varied, with several small mounds and depressions. The field is bounded on the left by a fence and on the right by a road. The overall appearance is that of a well-maintained but somewhat neglected agricultural plot.

The field is a small, irregularly shaped plot of land, approximately 10m by 15m. It is situated on a slight slope, with the highest point on the left side and a significant concavity at the base. The soil is dark and appears to be a heavy clay or loam. The field is currently in a fallow state, with some sparse vegetation and a few small trees scattered around the perimeter. The topography is quite varied, with several small mounds and depressions. The field is bounded on the left by a fence and on the right by a road. The overall appearance is that of a well-maintained but somewhat neglected agricultural plot.

## 1.6.2 Blairhall Plantation, Mansfield Estates, Scone Palace, Perth.

Details of the site are illustrated in Figure 1.19

Map reference: NO 116 280

Elevation: 26m a.s.l.

Parish: Scone

Council: Perth And

Kinross

Mean annual precipitation is approximately 716 mm (Perth aerodrome), 63% falling on average during the winter. The field is owned and farmed by Mansfield Estates and has been planted with cereals both winter and spring since January 1999.

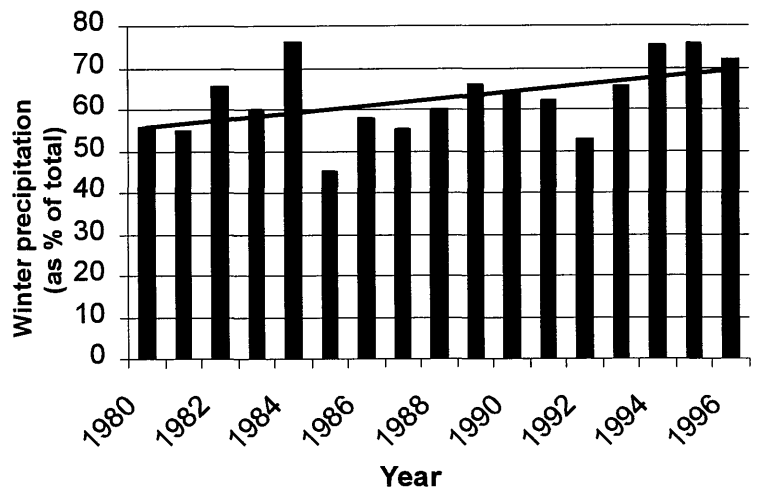


Figure 1.18. Trend in winter precipitation for Perth Aerodrome

### Archaeological description

Type of Site: Cursus; Ring-Ditches; Linear Cropmarks; Pits  
NMRS Number: NO12NW 43

The suspected closed cursus was confirmed by aerial photography and a number of new ring-ditches were also identified by pilots at Perth Aerodrome. Two additional ring-ditches were recorded in line with a row of three already identified, all lying parallel to the cursus and associated with linear cropmarks approximately halfway between the cursus and Gelly Brae Wood.

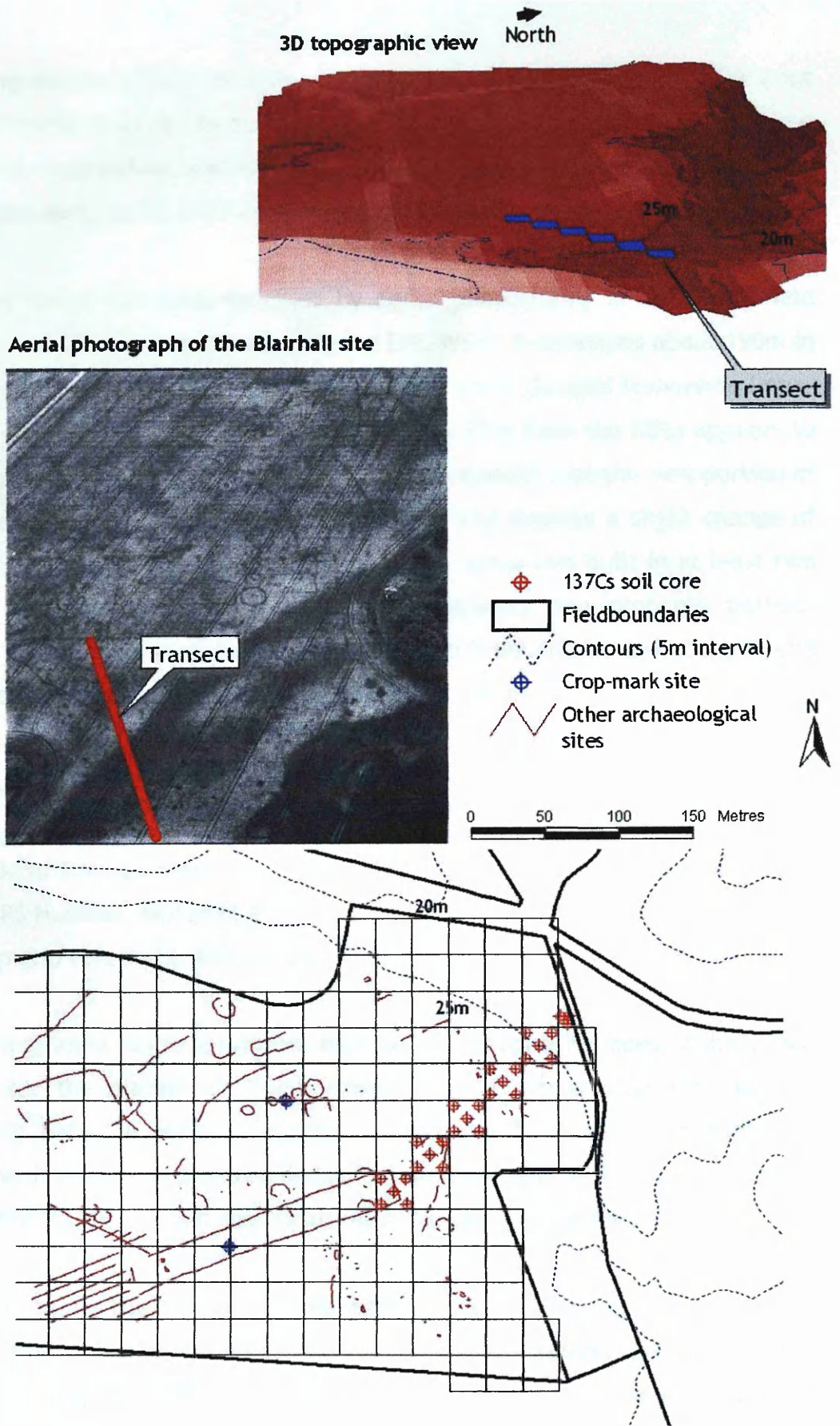


Figure 1.19. Topographic and archaeological layout of the Blairhall field site

All five ring-ditches appear to have central burials and may be the ploughed out remains of burial mounds. Two similar ring-ditches intersecting the cursus at the eastern end were noted, and two new ring-ditches were identified outside the cursus to the east, at NO 1175 2805 and NO 1175 2810.

A probable cursus has been revealed by aerial photography in an arable field 360m south of Blairhall farmhouse. Aligned ENE-WSW, it measures about 190m in length by up to 24m in breadth within a narrow ditch. Several transverse linear marks cut across it, at least one of which (about 75m from the ENE) appears to be an original internal division. However, it is noticeable that the east portion of this division is appreciably wider than the rest, and displays a slight change of alignment. It is, therefore, conceivable that the cursus was built in at least two separate stages. On the ENE, the cursus intersects two probable barrows (NO12NW 32) although their temporal relationship is uncertain, and at the W end of the interior there are traces of a probable ring-ditch.

#### Archaeological description

Type of Site: Barrows

NMRS Number: NO12NW 32

Map grid reference: NO 116 281

Aerial photography has revealed two barrows set on opposite sides of the cursus NO12NW 43; the ditches of the barrows and the cursus intersect, but the relationship between them is uncertain. Several other possible ring-ditches, together with numerous pits and linear features, are visible in the field, one of the ring-ditches lying within the cursus (RCAHMS (JRS) 14 December 1992).

In comparison to the other selected sites the collection of features within Tileworks field is probably under less of a threat from erosion primarily due to minimal topography. In the northeast corner of the field the slope breaks and forms both a zone of concave and convex slope lengths. Archaeological sites are located close to this potentially higher risk area so the transect was set along the slope as seen in Figure 1.19. The field has been regularly ploughed in an

east-west direction yet as the slope breaks in the northeast corner the farmer has always ploughed on the contour right up to the field boundary. This area also has suffered quite badly from standing water. There has been evidence of sheetwash taking place and concentrated flow erosion along wheel tracks, albeit of low intensity.

The soil type is described as a podzol of the Corby association (Laing et al., 1974). Texture of the Corby association here is mainly loamy sand to fine loamy sand in the surface horizons and are freely drained with A horizons of between 25-40cm thick. The parent material contains less than 2% clay and less than 5% silt and compared with the Loanleven site stone content is considerably lower at this location.

*[Faint, illegible text, likely bleed-through from the reverse side of the page]*

1.6.3 Leadketty Holdings,  
Dunning.

Map reference: NO 020 162

Elevation: 42m a.s.l.

Parish: Dunning

Council: Perth And Kinross

Details of the site are illustrated in Figure 1.21.

Mean annual precipitation is approximately 835 mm

(Strathallan School) of which 64% falls on average during the defined winter period.

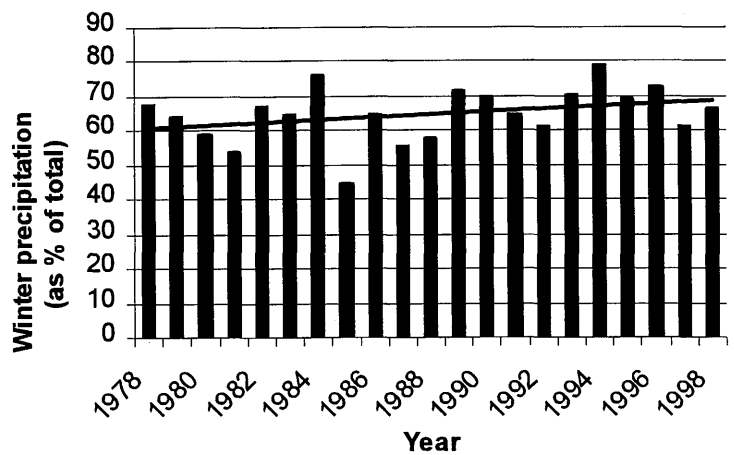


Figure 1.20. Trend in winter precipitation for Strathallan School.

Archaeological description

The cropmarks of a square barrow have been recorded from aerial photographs (RCAHMSAP 1994) situated some 250m west of Dunning Burn and slightly NW of an enclosure (NO01NW 22) recorded at NO 0216 1621. Other square barrows have also been recorded in the same approximate area (NO01NW 21; NO01NW 66).

- Type of Site: Barrow: Square  
NMRS Number: NO01NW 142
- Type of Site: Cropmarks; Pits  
NMRS Number: NO01NW 134  
Map grid reference: NO 021 16
- Type of Site: Barrow (Possible)  
NMRS Number: NO01NW 143  
Map grid reference: NO 018 159

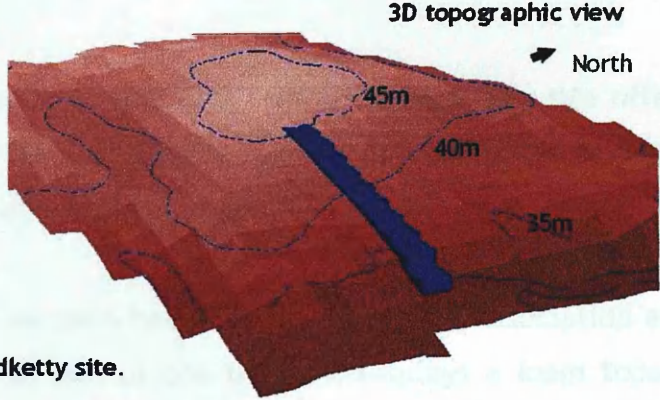


- Type of Site: Ring-Ditch (Possible); Cropmarks  
NMRS Number: NO01NW 56  
Map grid reference: NO 021 160
- Type of Site: Barrow: Square; Pits  
NMRS Number: NO01NW 66  
Map grid reference: NO 022 160
- Type of Site: Enclosure; Pit-Circle (Possible); Settlement; Unenclosed;  
Pottery; Barrow: Square (Possible)  
NMRS Number: NO01NW 21  
Map grid reference: NO 020 161

(Location cited as NO 021 161). Fieldwalking organised by Perth Museum and Art Gallery and Dunning Parish Historical Society on the site of this large oval cropmark enclosure resulted in the find of a small sherd of Late Neolithic or Early Bronze Age pottery from within the enclosure. The sherd shows a clean break suggesting that that it was the result of recent damage by the plough. Flint and fieldwalking archive held by Perth Museum and Art Gallery (Acc. No: 1993.1094).

Aerial photographs (RCAHMS, 1994) have recorded the cropmarks of the discontinuous ditch of a circular enclosure, situated some 250m west of Dunning Burn. At the approximate centre, a possible square barrow has been identified at NO 0207 1616, and some 150m northwest another recorded square barrow (NO01NW 66). Slightly to the southeast of the enclosure lies a group of pits, and to the northeast a second smaller enclosure has also been identified (NO01NW 22). Further cropmarks related to settlement activity are also visible in the area.

Leadketty has been cultivated with winter and spring wheat since the beginning of 1999. Topography is slight on the west side although towards the eastern edge where the features are located the slope increases steadily before levelling out at Dunning Burn. Significant erosion damage has been noted in adjacent fields



Aerial photograph of the Leadketty site.  
Cropmarks visible.

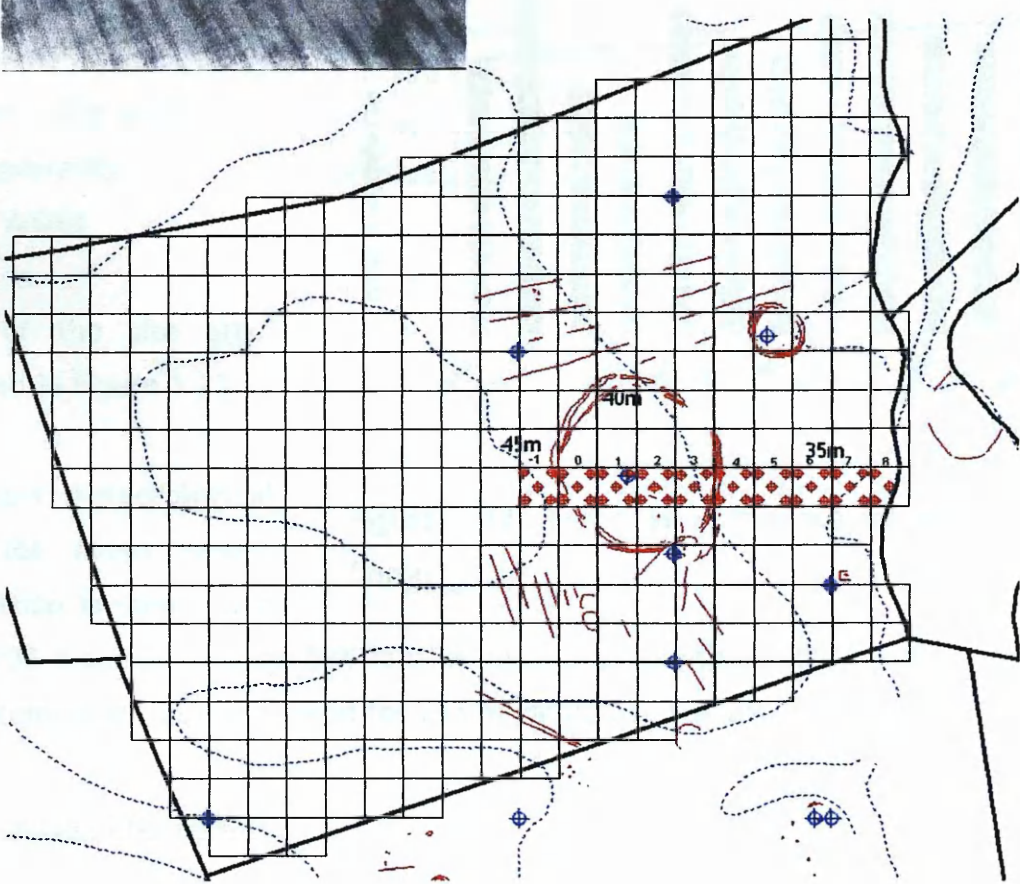
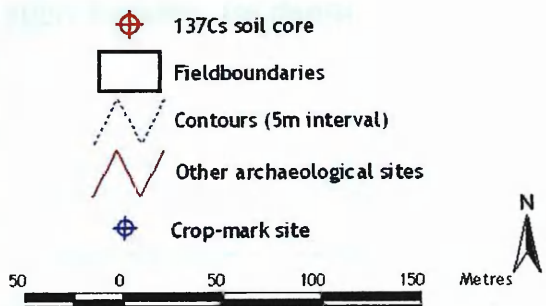
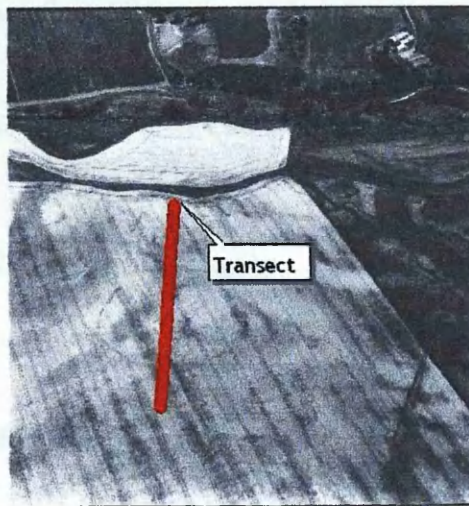


Figure 1.21. Topographic and archaeological layout of the Leadketty field site.

Baldinnies Farm, which are also cultivated with winter cereals. The site offers good potential for study given the topography, agricultural practices and the high density of archaeologically significant features.

Leadketty is located in a transition zone between the Balrownie association and an alluvial soil. Towards the west end of the transect displays a loam topsoil overlaying a sandy loam or loam subsoil. Towards the lower eastern end of the transect there is a marked shift towards a stone-free loam of the alluvial soil association. The subsoil becomes gravelly at approximately 1m depth.

#### 1.6.4 Littlelour, Kirkbuddo.

Map grid reference: NO

479 444

Elevation: 147m a.s.l.

Parish: Inverarity

Council: Angus

Details of the site are illustrated in Figure 1.23

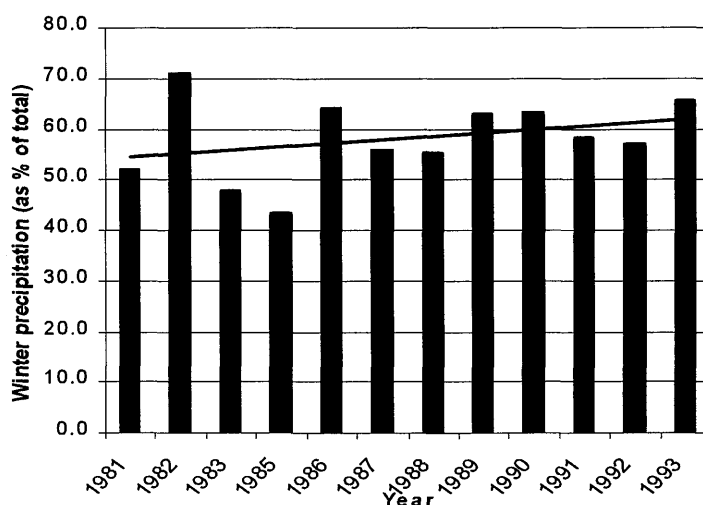


Figure 1.22. Trend in winter precipitation for Forfar.

The closest meteorological record for mean annual precipitation is taken from

Forfar (730 mm). On average 58% falls in the winter months. Despite the records being incomplete there is a trend for winter rainfall to steadily increase.

#### Archaeological description

Type of Site: Barrow

NMRS Number: NO44SE 1

NO44SE 14791 4449

3D topographic view

North

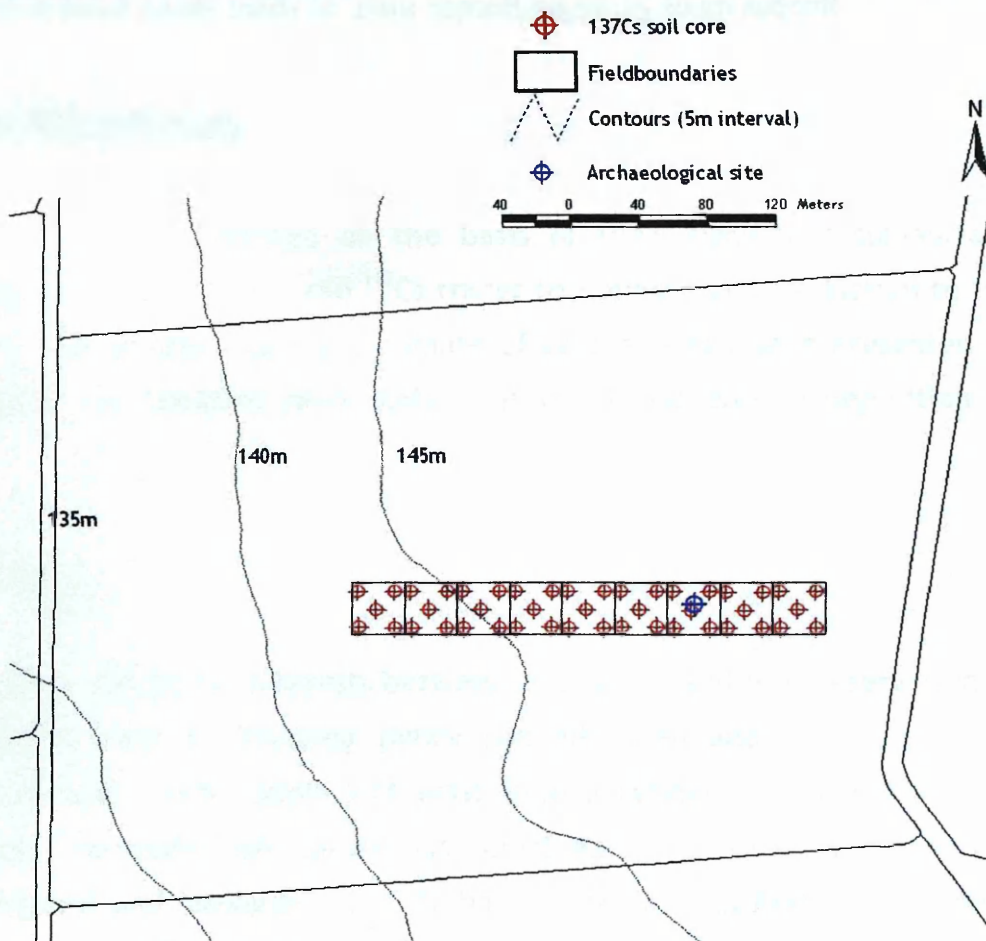
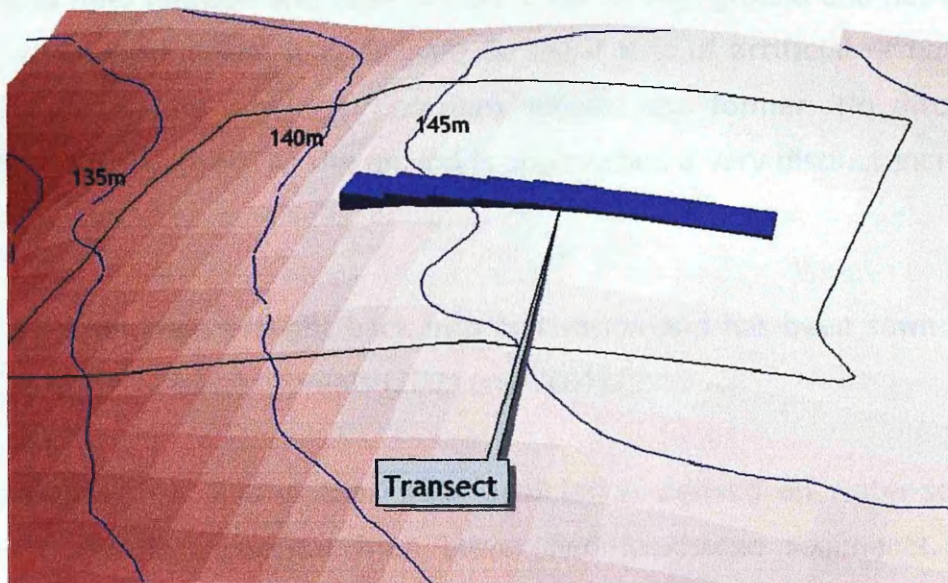


Figure 1.23. Topographic layout of the Littlelour field site.

This earthen mound is circular, 21.0m in diameter and 1.2m high. It is situated in a cultivated field (cereals and rape) on the crest of high ground and has been considerably ploughed down. It is difficult to say if it is of artificial or natural construction, though its regular proportions suggest the former. No ditch or surrounding kerb was noted. As the mound is approached a very distinct increase in stoniness is noted.

The field has since been brought back into cultivation and has been sown with rape (Sept, 1999) and winter cereals (2000 and 2001).

The site is located on soils of the Forfar association derived on water-sorted drifts and on colluvial material from Lower Red Sandstone sediments. The dominant soil has a sandy loam or loam topsoil on sandy loam subsoil.

## 1.7 Field site summary

Four field sites were selected on the basis of their significant sub-surface archaeology on which to apply the  $^{137}\text{Cs}$  tracer technique. An introduction to the topography, archaeology, soils and climate of each site has been presented to set the scene for detailed field scale analysis of soil erosion/deposition in chapter 4.

## 1.8 Summary

There is a clear conflict of interests between agriculture and the preservation of archaeology in general. Planning policy has advanced and the situation is improving (Barclay, pers. comm.) at least from a residential and commercial development viewpoint. Agriculture has remained a neglected area, yet the MARS of England and Management of Archaeological Sites in Arable Landscapes projects are significant steps towards greater awareness and policy development.

Soil erosion has been well documented in Scotland despite being previously neglected as being unimportant. Furthermore, a solid body of evidence of high

magnitude water erosion events has been presented from the study area. Tillage has become accepted as a major contributor to erosion so when combined together with the water erosion in the study area the overall threat to archaeological cropmarks may be considerable.

The thesis is structured around the following themes. Chapter 2 deals with modelling of soil erosion due to water taking into account the effects of linear features on erosion/deposition patterns and magnitudes. Soil erosion caused by tillage processes is covered in chapter 3, including pilot modelling exercises and development of a 2D spatial model. In chapter 4, details the application of the  $^{137}\text{Cs}$  tracer technique, derivation of erosion/deposition estimates, and comprehensive procedures to optimise the erosion models. The results are finally collated and placed within an archaeological context in chapter 5 to evaluate the threat posed by erosion. Final conclusions are offered in chapter 6 to complete the study.

# Chapter 2.

## 2. Modelling water-based soil erosion

The focus of this section aims to spatially and quantitatively model soil erosion/deposition patterns in the agricultural landscape. The erosion/deposition budget is viewed as being the result of tillage and water erosion.

There has been a slightly illogical order to the way in which this chapter has been executed with regard to chapter 4. Much of the preliminary development and testing of the proposed water erosion model was performed using parameter sets taken from the literature long before  $^{137}\text{Cs}$  data were available for optimisation. The final water erosion model is however presented here using a general best-fit parameter set derived from validation and optimisation work in chapter 4.

Soil erosion models if properly validated and parameterised, provide at best an estimation in prediction and understanding of future events. Of particular interest in the last 10-15 years have been models transferable into a GIS environment to represent more realistically the multitude of parameters involved and the issue of spatial distribution.

A model is in essence

*that which strikingly resembles something else; an approximate copy or image* (Webster, 1998).

Before modelling a system, it is of utmost importance to stipulate clearly the purpose of the model. This project has been developed with strong end-user requirements in mind since there is a clearly defined goal to provide policy and management tools. Emphasis here is not on explaining the physical processes of erosion and deposition. The aim is to provide quantitative statements on erosion

allowing results to be used in the decision-making processes of archaeological management/conservation.

The overall aim is to model the process of sediment transport so as to explain observed patterns of erosion and deposition. This project demanded developing a methodology to predict soil erosion risk with a view to assisting policy development in a regional-scale study area. GIS offers huge potential as a primary spatial database management tool, graphic display unit and modelling medium but natural resource information is particularly complex since it requires three descriptors - *what*, *where*, *how much*. Until the 1970's the link between them has been the traditional yet tedious manual drafting of maps. McHarg (1969) in his classic text 'Design with Nature' on landscape architecture introduced and popularised the manual innovative overlay of maps to address various impacts on urban environments.

This system is now replaced by the vast array of current GIS systems. The roots of GIS merely substituted the above procedure in a fully automated way, however, since the birth of GIS the descriptive foundation of *where*, *what*, and *how much* has drastically been overtaken with *so what* as a prescript for decision-making. Therefore, the function of physical landscape description has changed to a more quantitative analytical toolbox. GIS today is capable of enormously complex spatial statistics and modelling of any spatially distributed data in up to 4 dimensions. This research has been based upon the ESRI GIS suite of products.



## 2.1 Literature review

This section avoids an extensive review of the literature on soil erosion but rather outlines vital concepts and methodologies relevant when finalising an erosion/deposition modelling approach.

### 2.1.1 Factors influencing erosion

The following factors are the most influential in driving the erosion/deposition system:

- Topography \*
- Climate
- Land use (vegetation and agricultural practices) \*
- Soil
- Structure of landscape features (boundaries, ditches, roads etc) \*

\* = included in model.

A brief review of the importance of these factors is presented with discussion on ideas and techniques for integration into the final model.

#### 2.1.1.1 Topography

The term topography includes primary derivatives such as slope and aspect, and the secondary derivative curvature (profile and plan). Topography describes the spatial variability in acceleration due to gravity and is widely recognized as an important factor in determining the streamflow response of catchments. It has been shown to affect the path runoff takes across the landscape before reaching the stream network (Wolock et al., 1990) and the spatial distribution of soil moisture within catchments (Burt and Butcher, 1985).

#### 2.1.1.1.1 Slope

Slope has been classified as being one of the most critical factors controlling soil erosion (Bryan and Poesen, 1989). Slope provides the energy to the erosion system and when combined with contributing drainage areas may generate sufficient surface runoff conducive to erosion. Djorovic (1980) presented a whole array of relationships and suggestions from his work in Serbia, most significant of all being the very strong influence of slope angle on soil loss levels. Through examining various types of vegetated slopes with slope angle, the relationship was found to be true. Warrington et al., (1989) noted a seven-fold increase in erosion when slope angle was raised from 5 to 25%. They also quote evidence of a 10% slope threshold above which overland flow exceeds some critical value where rills and gullies formed. Below this threshold, overland flow acts as a transporting agent only for splash detached material. Soil loss was also found to decrease markedly above slope angles of 25%.

The effect of slope angle on interrill erosion rates has been commonly investigated using plot-scale studies (Chaplot and LeBissonnais, 2000; Fox and Bryan, 1999). Increasing the slope gradient directly influences runoff velocity and it has been concluded that soil loss is in fact best correlated with runoff velocity (Fox and Bryan, 1999). Soil loss was reported by the same authors to increase roughly with the square root of slope gradient. In addition Chaplot and Le Bissonnais (2000) suggested that slope length in their analysis of slope controlled soil loss was also significant (Chaplot and LeBissonnais, 2000). They also confirmed the sharp increase in runoff velocity with increasing slope but they highlighted the fact that sediment concentration only increased with slope in larger 10m<sup>2</sup> plots rather than in 1m<sup>2</sup> plots.

Poesen (in Parsons and Abrahams, 1992) pointed out that for sandy and loamy soils, which are very susceptible to sealing, the probability of rill formation increases with slope. The authors attribute this to the decrease in topsoil shear strength. This emphasizes the fact that slope is not a clear-cut variable as a direct controller of erosion and is rather a variable having a knock-on effect upon other soil properties which themselves create the erosion susceptibility of

soil. For example, sealing intensity is inversely proportional to slope steepness, i.e., the steeper the slope, the lower intensity of sealing and the higher the rate of final infiltration. This supports the findings of Agassi et al. (1989). Topsoil shear strength also decreases with slope steepness, which in combination with other soil conditions will accelerate erosion rates. Chaplot and Le Bissonnais (2000) however found infiltration rates to decrease with increasing slope gradient and claimed the trend is due to the lack of rill formation.

Slope length as a further factor has been researched in the laboratory by Bryan and Poesen (1989). The relationship between slope length and overland-flow volume per unit area appears as a clear exponential decrease with increase in slope length for loamy soils. It is suggested that longer slopes offer a greater time period with which to absorb flow than on shorter slopes. As slope lengthened, microrills across the seal became more abundant and the occurrence of deep rills and head-cut incision, which break the seal formation, became particularly widespread. Rill intensity was also found to be clearly linked to slope length (Agassi and Ben-Hur, 1991). In their study of topographic effects on soil erosion, they discovered a very significant relationship between slope length and erosion. Larger plots presented some 6.4 times the amount of material lost compared with smaller plots. The increased velocity of runoff explains the difference. Aspect was also reported to be a significant influence. Little evidence of work carried out on slopes longer than 100m was found which is of particular importance to this project. Only the reference made by Poesen and Bryan (1989) touches on this subject. They suggested that if the rates of increase were to be extrapolated, then 100% rill coverage would be expected on a slope of 185m.

Slope length today is rarely used in catchment-scale modelling and is substituted with contributing area per unit length/width of contour (Kirkby and Chorley, 1967). It represents in essence the size of mini-drainage catchments within catchments, i.e. each point in the landscape has a contributing area defined by upslope topography and this is one of the key factor in determining soil erosion (Moore et al., 1993; Rustomji and Prosser, 2001). Overland flow and soil loss do not depend on distance from the catchment divide, i.e. slope length, rather on

how flow converges and diverges to a point (Desmet and Govers, 1996).

#### 2.1.1.1.2 Climate

Climate is the driving force of erosion. It supplies energy to the earth's surface resulting in detachment, compaction and transport of surface material. Climate, however, is a composite of many elements and Douglas (1976) examined 7 climatic variables linked with the spatial explanation and a further 8 variables to temporal variations in soil erosion. Of the many climatic variables, rainfall intensity is considered to be the most important characteristic of climate (Fournier, 1972; Morgan, 1993). Intensity based approaches such as  $KE > 25$  (Hudson, 1981a),  $EI_{30}$  and its variants (Arnoldus, 1980; Bolline et al., 1980; Lal, 1976; Renard and Freimund, 1994; Sinzot et al., 1989; Wischmeier and Smith, 1958) can be questioned in terms of their relevance to the UK climate. Low intensity and long duration precipitation events have been reported as being equally important when dealing with temperate humid climates (Boardman and Favis-Mortlock, 1993; Chambers et al., 1992; Chambers and Garwood, 2000; Evans, 1990b; Frost and Speirs, 1984; Fullen and Reed, 1986; Morgan, 1995; Reed, 1983; Reed, 1986; Skinner and Chambers, 1996). There are also practical issues involved with the indices such as availability of autographic rain gauge data. Morgan (1980) did overcome the problem of data by using those available in the Flood Studies Report to apply the  $KE > 25$ , yet the relationship between soil erosion and the intensity indices has been found to be poor for UK conditions (Bridges and Harding, 1971; Walling, 1974). In view of the inability of rainfall intensity to represent the UK climatic conditions relevant to erosion, the erosivity indices were excluded from the project.

Runoff calculation was considered as input to a potential model. An approach developed by Kirkby and Cox (1995) and DePloey et al. (1991) estimated mean monthly runoff based on the frequency distribution of daily precipitation depths. Account was also taken of soil storage capacity. The incorporation of magnitude-frequency analysis on a database of almost 50 daily rainfall stations emerged as a more appropriate way forward in view of the climatic conditions. The complex set of calculation procedures was developed for 26 stations spread across the

whole study area with unbroken records for >20 years. Significant time was allocated to this process, however it became clear later that runoff data also was unnecessary. Despite the obvious relevance of water to erosion careful consideration was given to whether or not rainfall characteristics have a role to play in the kind of model required for this project. Erosion/deposition predictions on an annual basis were required for the project and it became difficult to envisage runoff being integrated. Ultimately the dilemma of accounting for climatic driving forces was surrogated by the use of the upslope contributing area (Kirkby and Chorley, 1967).

#### 2.1.1.1.3 Soil

Le Bissonnais (1993) offers the definition of soil erodibility as being inherent tendency for soils to erode at different rates. Morgan (1980), states that erodibility defines the resistance of the soil to both detachment and transport. Generally 4 factors interact to control the overall resistance to erosion i.e. erodibility. Factors influencing erodability are shear strength, organic matter, aggregate stability and infiltration capacity. These variables are themselves in part controlled by topographic position as illustrated by various authors (Agassi and Ben-Hur, 1991; Agassi et al., 1989; Bryan and Poesen, 1989; Poeson, 1992).

In general, erodibility will increase as the fraction of silt and fine-sand increases and clay content decreases. Various authors have either concentrated on either the percentage of silt and sand or clay fractions as indicators of erodibility. In the UK, Evans (1980) preferred percentage clay noting that soils with 9-30 % clay content were the most erodible, yet Le Bissonnais, Singer, and Bradford (1993) failed to find a significant relationship between clay content and erosion. However, Morgan (1995) supported Evans in stating that clay and organic matter combine to strongly influence aggregate stability and that it is this that creates the soils' resistance to erosion. In the Scottish context, Frost and Speirs (1987) in their survey of eroded fields in eastern Scotland found that 62% were of loamy sand or sandy loam texture, with fine sand content being dominant in most cases. Also 68% of all instances were shown to be derived from Old Red Sandstone sediments. Evans in unpublished work has reportedly shown that

losses are far higher on coarser textured soils than on clays (quoted by Frost and Speirs, 1987).

Stability of aggregates is dependent on strength of the internal bonding between aggregates. Clay mineralogy has a clear effect on aggregate stability and therefore erosion. It is a more complex matter in that the type of clay present in a soil is always a mixture. Young and Mutchler (1977) found that smectitic clays are more efficient as aggregating particles than other clays due to their large specific surface and high physico-chemical interaction capacity. Trott and Singer in the USA (1983) found that kaolinitic soils were less eroded than soils containing montmorillonite. Clays behave very differently according to moisture content. Many clays become weaker when initially wetted, yet some under wet but non-saturated conditions will become stronger through time. Quansah (1981) found that soil with larger montmorillonitic fractions were less susceptible to splash detachment and that the clay maintained discrete aggregates that were visually larger than sand grains present after a simulated rainsplash event.

Organic matter content is thought to be one of the most effective stabilising agents in aggregates. Aggregate stability is strongly affected in turn by this factor. Most soils contain less than 15% organic matter but soils become more erodible as the 3.5% level is reached (Evans, 1980). Referring to mainly mineral soils, a decreasing linear relationship between soil erodibility and organic matter content between 0-10 % was reported by Voroney, van Veen, and Paul (1981). Frost and Speirs (1987) contest the argument that organic matter is of primary importance. They quote early soil surveys from Kay's 1934 work to illustrate that soils with less than 2% organic carbon content were widespread despite the incidence of low soil erosion. In their 1984 paper, they point out that differences in organic matter content can be the cause and not the result of soil erosion. Convincingly they use a nomograph to exemplify that relative erodibility decreases only 25% resulting from a drop in organic matter from 4 to 2% and by a further 15% with organic carbon decreasing further still to 0.5%. They argue that such small changes in erodibility were unlikely to have amplified the incidence of erosion cases in eastern Scotland. Fullen and Reed (1986) are not so certain and highlight that their results from Shropshire, England suggest that even

moderate increases in topsoil organic matter diminish runoff erosion.

Infiltration capacity defines the maximum rate at which rainfall can be absorbed by a given soil in a given condition (Gregory and Walling, 1973). It is influenced by the soil's pore distribution, size and connectivity. Infiltration can be reduced significantly by a surface sealing process, particularly on loamy sands of 80-90% sand. Considerable runoff will be generated across such soils (Poeson, 1992). It has, however, been suggested by Poeson (1992) that although a sealed soil surface decreasing the infiltration capacity is producing more erosive overland flow it will counterbalance itself by removing the seal further downslope. Consequently, infiltration increases. Infiltration varies widely with topographic position on a slope generally increasing with a corresponding increase in slope (Agassi and Ben-Hur, 1991; Agassi et al., 1989). However, the fact remains and is reported by Fullen (1986) that moderate amounts of precipitation (10-15mm) over 10-20 days are sufficient to cause the formation of a 1-4 mm thick cap which then markedly increase erosion on plots.

Regional assessment of runoff and erosion risk is based on an understanding of large-scale mechanisms and on the analysis of data that are easily available for such areas (King et al., 1993). Including such characteristics into such a regional study is a practical impossibility, so representative dominant factors need to be selected. Batjes (1996) used soil texture only in his global erosion assessment, Stocking (1987) also used texture, yet Le Bissonnais et al., (in press) used susceptibility to crusting and erodibility of parent material. In short, factors such as infiltration capacity and shear strength amongst others may be determined in lab conditions but are of little relevance to such regional-scale.

At the regional scale, integrating the resistance of soil to erosion into a modelling approach proved particularly difficult. The chosen model (Equation 2.4 and Equation 2.5) does offer the opportunity to spatially vary an appropriate soil factor through the use of parameter  $k_1$ . Descriptive soil texture data were considered as a possibility since they were available. However, the decision was eventually made not to vary  $k_1$  in an attempt to reflect the spatial variation in detachment resistance. The uncertainty in applying a subjective rating system

on very general descriptive soil texture data appeared to outweigh any possible advances in model performance. Furthermore, varying the  $k_1$  factor within the model would have certainly introduced more error which needed to be avoided or at least minimised.

#### 2.1.1.1.4 Vegetation / Land use

Ground cover is perhaps the most critical variable in controlling the frequency and intensity of surface runoff and erosion across the landscape. It plays a dual role by affecting both the erosivity of rainfall received at the soil surface and the soil being (potentially) eroded. Vegetation provides a mat of resistance in the following ways:

1. Precipitation interception - decreases the amount of and the energy of precipitation reaching the soil surface. Water is then held and usually lost to evaporation (Wiersum, 1985; Woo et al., 1997). Such properties are particularly evident in tree or shrub growth as opposed to cereal and other vegetable crops.
2. Infiltration - development of root networks allows infiltration to increase, therefore, attenuating surface runoff.
3. Resistance to flow - vegetation increases resistance to surface flow which therefore reduces soil detachment (Woo et al., 1997). The presence of surface litter such as leaves or post-harvest straw and grass will also have similar effects.

The latter two of the above points would appear to be more relevant to this project given the presence of crop-mark sites within arable areas. Evidence of erosion was noted across the study area exclusively on cultivated land. Runoff from cultivated land has also been noted encroaching areas of grassland or setaside where the effects of vegetation are sometimes demonstrated. Figure 2.1 illustrates how concentrated flow from a ploughed upslope area of a field enters the grass footslope area. The farmer left this portion of the field



enters the grass footslope area. The farmer left this portion of the field



Figure 2.1. Concentrated overland flow from upslope ploughed land depositing entrained sediment in a no-plough area of a field (N0016165).

unploughed due to the difficult complex topography. The flow upslope of the grass had established a rill channel which promptly disappeared inside the grass area. Sediment immediately began depositing. Work by Fullen (1991) in east Shropshire showed clearly the effectiveness of grass in yielding very little runoff and eroded soil. Runoff was an order of magnitude larger under bare surface conditions. He reports only some 0.12% of precipitation routed as runoff.

How effective is vegetation and at what point and form is it most effective at abating soil loss? Much of the work has been Mediterranean oriented but the underlying principle remains the same. Typical assumptions are based on a linear relationship between cover and soil loss, i.e. a decrease in cover equates to soil loss increase. The RUSLE assumes this. If we take this hypothesis and imagine a field of spring wheat immediately post-harvest (bare of vegetation), soil loss of the highest rate would be expected. Castillo et al., (1997) removed their test vegetation cover from a 23% slope against a control site and produced

the high vulnerability of this post-harvest period. Unfortunately the authors did not increment the cover levels between 0-30% to illustrate further its influence. This incremental influence has been well examined between this range (Rogers and Schumm, 1991). Cerda (1998) while focussing on runoff, soil loss and infiltration rates across variably vegetated slopes in Spain also supports such claims. His work produced an exponential decrease in runoff sediment concentration with increasing vegetation cover.

Equally important as percentage cover of the ground is the structure of the vegetation type, i.e. height, canopy structure, rooting depth. Quinton et al., (1997) investigated the effectiveness of plant cover type finding little difference between types, yet a distinct all-round reduction in soil loss. A pronounced effect was reported of between 0-30%.

Such pronounced differences in runoff under a simple grass treatment as illustrated by Fullen (1991; 1986) in the UK supports the exclusion of grasslands and other such like vegetated surfaces from erosion susceptibility assessments (De Roo, 1998). This project will not predict erosion rates for non-arable land uses but this does not preclude the exclusion of such areas as runoff contributors. Certain land use types will supply runoff despite possessing inherently low erosion susceptibility. Upland moorland is present towards the western and northwestern fringes of the study area and must supply substantial runoff. The same effect is assumed for all land use types across the study area. Ideally a dataset containing a recession-type runoff coefficient was required enabling the model to account for the varying vegetation effects on catchment hydrology. The Hydrology of Soil Types (HOST) (Boorman et al., 1995) dataset provides this in the form of a standard percentage runoff (SPR) value.

SPR is defined as the percentage of rainfall that causes the short-term increase in flow at the catchment outlet. SPR has been calculated firstly by separating the total flow hydrograph into quick response and baseflow components. The methodology takes into account whether or not the catchment is rural or urban, the catchment wetness and response due to direct rainfall. Mean SPR is calculated over a run of precipitation events and varies from 2 to 60%. Since SPR

is based on catchment flow hydrographs, topographical shape, land use, and soil hydrological characteristics are all considered. The data were available for the study area and was kindly provided by the Macaulay Land Use Research Institute (MLURI).

Land management practices or operations such as ploughing are now thought to play a major role in channelling overland flow in directions different to those defined by topography (Souchere et al., 1998; Takken et al., 2001). Patterns of flow induced erosion and deposition therefore can be strikingly different when routing flow along plough lines as opposed to along the direction of maximum slope. The 25m cell resolution use in this project does not allow for such small features to be modelled.

#### 2.1.1.1.5 Structure of landscape features

The network of linear features is composed mainly of hedges, stone walls, wooden and wire fences, ditches and dykes, although dry-stone walls are generally confined to upland regions. Regardless of type they form a topographic barrier on what would otherwise be a smooth landscape and in many cases produce a connected network of channels, ditches and furrows. In a sediment transport context, patterns of overland flow and consequent contributing areas may vary significantly in response to the structure of such channel/feature networks. The question ‘what effect, if any, do field boundaries have on erosion/deposition patterns and magnitude?’ is examined in this section and has been investigated to determine if further attention needs to be given to the modelling approach.

Field boundaries on the landscape play multi-functional roles in agriculture, ecology and administration. Evaluation of their importance appears heavily biased on standpoint, yet the Council for the Protection of Rural England (Select Committee on Environment, 1998) encompass the many assets as being central to the character and diversity of rural England. Some of the major functions are:

1. Division of land into management units or fields to satisfy the following:

- a. Cadastral property boundaries for landowners.
  - b. Livestock management.
  - c. Protection and shelter of livestock, crops, public rights of way and buildings.
2. Demarcation of soil boundaries - declining in importance since mechanization allows limitations in workability to be overcome.
  3. Prevention of soil erosion - claimed by MAFF Codes of Good Agricultural Practice for Soils (MAFF, 1998).
  4. Hunting and shooting.

The prevention of soil erosion claimed by MAFF (1998) as an important function of field boundaries has been poorly covered in the scientific literature. There appears to be no UK work focusing on determining magnitudes of the effect of such linear features on erosion/deposition budgets. The Houses of Parliament's Select Committee reported (1998) in great detail the values and functions of field boundaries as well as threats to them. Within the report, The National Trust quote boundaries as having beneficial shelter properties in preserving soil moisture and therefore soil erosion. Further, the Royal Commission provided evidence from their report on Sustainable Soil Use (1996) in supporting research on the effect of boundaries in reducing erosion.

This is not to say that field boundaries have been ignored in a wider sedimentation context. Work has been concentrated at the field and small catchment scale. Ludwig et al., (1995) highlighted the importance of a network of linear features on runoff delivery and state that the structure must be considered when assessing damage caused by concentrated flow. The interaction of natural runoff collectors such as thalwegs and depression lines with man-made features like drainage ditches, dead furrows, and parcel boundaries also needs to be carefully analysed. Although not strictly a modelling approach, Ludwig et al., (1995) demonstrated the link between the connectivity of upslope runoff generating areas, delivery features and the spatial patterns of erosion/deposition. Tillage direction and dead furrow orientation as a further in-field feature were recognized for the first time as major contributors to concentrated flow erosion/deposition. Significant research on this topic has

since emerged, in particular intra-field tillage direction.

Modelling of overland flow paths has traditionally been defined by topography, i.e. azimuth of steepest slope (aspect). Desmet and Govers (1997) modified a flow modelling approach to address tillage orientation claiming that the cultivation pattern has an important effect on the development of rill networks. Their approach calculates an average flow direction as an intermediate between topographic and tillage direction. Furthermore, they used an algorithm capable of distributing flow to two cardinal neighbouring downslope cells. This method of flow routing and average flow direction has since been disputed (Souchere et al., 1998; Takken et al., 2001). They claim flow will be either in a topographic or tillage direction depending on the angle between tillage and topographic direction. By forcing flow along cultivation lines, slope in the direction of flow may be significantly reduced. This will in turn reduce the erosion rate. In addition intra-field contributing areas will reduce in size when flow is routed by tillage patterns further reducing erosion rates. Incorporation of such a technique would be possible although assessing tillage direction in all fields would be rather labour intensive at the scale of this project. Takken et al.'s (2001) model also routes flow in respect to parcel boundaries, ditches, paths, roads or any other linear feature that may be accurately represented in a raster format. Using LISEM (DeRoo et al., 1995) as the erosion model, Takken et al., (2001) report a significant reduction in total erosion when using their new flow routing routine (1085 tonnes) in comparison to topographically routed flow (1550 tonnes). Flow is also noted to concentrate along parcel boundaries as well as along intra-field thalwegs. From this it is clear that the flow is being highly restricted during its journey downslope by linear features. Despite the evidence of erosion attenuation, Takken et al. (2001) are correct to state that modelled erosion will not always be reduced due to tillage and boundary forcing. Figure 2.2 shows a particularly relevant example that occurred in late February, 2000 just west of the town of Perth. Concentrated overland flow appears to flow in topographic direction across a field of winter cereals overriding tillage direction. The channel is approaching the fence-line at approximately 45° (Figure 2.2a). Approximately 1m in from the fence-line flow is redirected by a dead furrow and routed along the field boundary (Figure 2.2b). As the slope magnitude decreases

slightly, larger amounts of material have been subsequently deposited. Interestingly the photograph shows evidence of both flow and sediment overspill of the fence-line itself. Figure 2.2c is the topographic low-point of the field and illustrates the sediment trapping effect. The transport capacity of the flow has been modified sufficiently by the change in topography, i.e. the presence of the boundary feature such that deposition has taken place. Flowing right to left in the photograph is a small stream some 2m below the level of the field. Examination of the stream and bank revealed very little sediment overspill suggesting that the majority of the material had been deposited in the field itself.

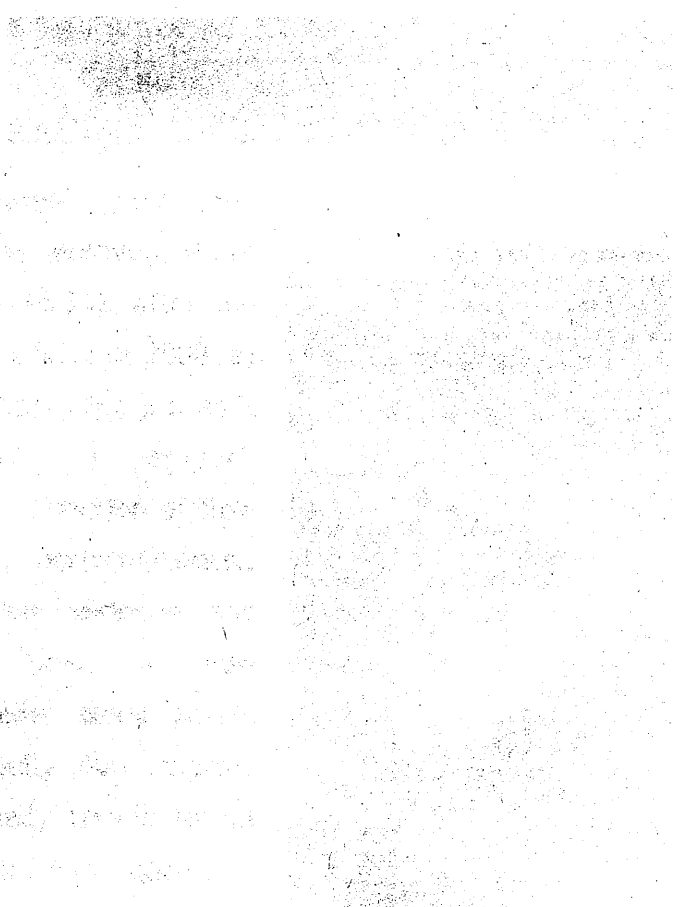


Figure 2.2c shows a topographic low-point of the field. The photograph shows evidence of both flow and sediment overspill of the fence-line itself. The stream is flowing from right to left. The sediment trapping effect is visible in the field.

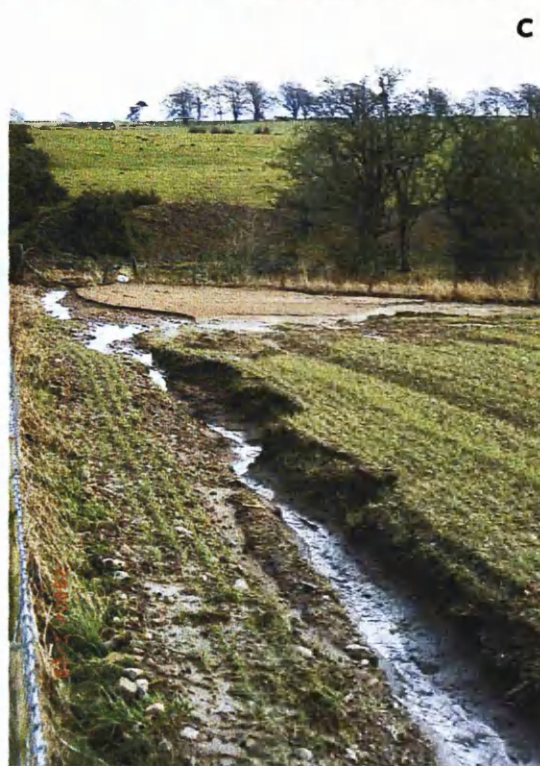


a



b

Figure 2.2. Large gully that appeared close to Methven, Perth and Kinross (NN999226), after the particularly wet winter of 2000. a) Gully on gentle backslope just as it begins to widen and approach parcel boundary. Direction of flow is approximately north-northeast. b) the gully has widened and direction of flow is now approximately east along parcel boundary. c) Gully now approx. 30cm deep. Finally terminates at lowest corner. Alluvium > 40cm.



c

Figure 2.3 further illustrates the barrier of dry-stone wall boundaries common in the Greens Burn catchment, bordering Loch Leven in Fife. This field



Figure 2.3 Sediment fans against a drystone wall in the Greensburn catchment, Loch Leven, Fife.

is a simple oblong shape some 500m long and 200m wide. The plough pattern is perpendicular to the contour except for the headland and the east portion of the field is a fairly uniform slope of approximately 10-15% gradually reducing towards the boundary seen in the photo. Both behind and in front of the person are two areas of deposition, the front one being the larger. This material had been removed from wheel tracks running the length of the field and only when in close proximity to the boundary wall did deposition begin. The whole width of the field had experienced medium-term accumulation resulting in a drop-off to the roadside. Almost certainly the height differential has been caused by the forced deposition of sediment coming off the upper slope segments over the medium term. In this case there was little evidence of material leaving the field unit. The structure of the field, i.e. location of the gate in terms of topography, is such that no evidence was found for overland flow focussing towards the



gate outlet. It has been common to find sediment on adjacent roads that are being regularly fed by either gaps in boundaries or gates. Contrary to the somewhat orthodox approaches to modelling runoff in the majority of previous erosion studies in the past, field boundaries and other linear features are slowly becoming recognized as further factors demanding consideration. Upslope and contributing areas cannot be accurately defined without such extra topographic features being included in the methodologies. Predicting soil erosion without the effects of the field boundary pattern will result in both incorrect patterns of erosion/deposition as well as magnitudes. However, MAFF's broad statement that field boundaries 'prevent soil erosion' needs to be examined closely since it may be false and more so, needs to be investigated further with regard to just what the effects are. Once sediment is entrained into flow, it is reported that gullies are efficient and important mechanism for sediment delivery and must be included when modelling (Nachtergaele et al., 2000; Poesen et al., 1996); Steegen et al., 2000). They reported seasonal variations in suspended sediment discharge at their catchment outlet are controlled mainly by the presence, formation and enlargement of such ephemeral gullies.

Strips of grass filters and hedges located at specific points in fields may have similar effects to some types of field boundary found in the UK. Many field boundaries within the study area are of the stake and wire and hedgerow type, which possess permeable attributes when flow is concerned. Filter strips, by which wire fence and low-density hedges may be classified, have been shown to significantly reduce levels of runoff and subsequently sediment and nutrients (Gilley et al., 2000). Gilley et al., (2000) report the effectiveness of grass hedges in initiating deposition on the upslope flanks of fields. Substantial deposition over a period of 6 years was evidenced by the development of berms. The hedges in Gilley's research were maintained at a height of 46cm, which is somewhat shorter than many hedges in the study area. Furthermore multiple rows of hedges were implemented. However, a parallel may be made with the effectiveness of a single such row and the field boundary hedgerow commonly found in the UK. The authors noted that during experimentation that backwater formed along the entire hedge width. As the head of runoff built up, the flow permeated the hedge, not uniformly, only in one or two locations. This



## 2.1.2 The basis for modelling erosion and deposition in a GIS environment

One of the problems preventing the transition from manual soil erosion modelling techniques to more automated fully 2D GIS approaches has been the difficulty in spatially explaining the hydrological characteristics driving erosion. Innovative work has since solved the problems and opened up many new opportunities for the application of GIS to sediment transport studies. The following is a brief outline of the foundations to modelling principles used in this study.

10 000 plot-years of erosion data led to the development of the Universal Soil Loss Equation (USLE) (Wischmeier and Smith, 1978), which despite its criticisms, became the standard global tool for assessing soil loss. In addition to being designed only for field or plot-scale studies, the USLE made no attempt to address depositional processes. Furthermore, uniform Hortonian overland flow generation was assumed, which is unlikely to be appropriate to the temperate humid environment of Scotland. Possibly one of the most important and key innovations that opened up the concept of catchment scale erosion modelling was the modification of the USLE. The Revised Universal Soil Loss Equation (RUSLE) (Moore and Wilson, 1992; Renard et al., 1991), addressed not only the problems with the representation of climatic factors, but more importantly the crucial roles of topography and hydrology when up-scaling to larger areas. A modified LS-factor was developed that allowed representation of the 3D terrain and how it affected catchment drainage patterns (Moore and Wilson, 1992). Their approach proposes the combination of the specific catchment area or upslope contributing area ( $\text{m}^{-2} \text{m}^{-1}$ ) and slope angle in the form of Equation 2.1, which they termed sediment transport capacity.

$$Tc^* = \left( \frac{As}{22.13} \right)^m \cdot \left( \frac{\sin \beta}{0.0896} \right)^n \quad \text{Equation 2.1}$$

Where:  $Tc^*$  = transport capacity (dimensionless)

$As$  = specific catchment area ( $\text{m}^{-2} \text{m}^{-1}$ ).

$\beta$  = slope (degrees).

$m, n$  = constants.

When optimised against the RUSLE-LS data, the constants  $m$  and  $n$  were set to 0.6 and 1.3 with ranges of 0.4-0.6 and 1.2-1.3 being also suitable. Use of this term rather than manually calculating the LS values introduces consideration of upslope hydrological conditions, e.g. flow paths, flow convergence and divergence and most importantly the magnitude of the accumulation of flow (drainage area).

Desmet and Govers (1996) offer a similar alternative to the  $L$  term in the RUSLE-LS parameter. Contributing area replaces the length to the upslope boundary/divide factor.

$$L_{i,j} = \frac{(A + D^2)^{m+1} - A^{m+1}}{D^{m+2} \cdot x^m \cdot (22.13)^m} \quad \text{Equation 2.2}$$

Where:  $L_{i,j}$  = slope length of cell  $i,j$

$A$  = contributing area ( $m^2$ ) at cell inlet

$D$  = cell size (m)

$x = (\sin\alpha + \cos\alpha)$  where  $\alpha$  = cell aspect (degrees)

$m$  = length exponent

This procedure requires coding within an iterative algorithm but drastically improves the original tedious and hydrologically incorrect procedure. Manually calculated LS values will be generally highest on steep slope sections since LS is dominated by the slope element. The LS input to the USLE/RUSLE model will then predict the highest rates of erosion simply on steep slope sections, which is not always evident in the field. Discharge is usually higher in concave zones where flow converges, readily causing rilling/gullyng. By applying a topographic based routine devised by Desmet and Govers (1996) and Moore and Wilson (1992), the resulting pattern of LS values will be vastly different from that produced via a manual approach. A more realistic catchment-wide response will be obtained. Furthermore, use of the contributing area to calculate LS has provided the opportunity to apply the USLE/RUSLE model to catchment scales within a 2D GIS environment. The USLE/RUSLE model still suffers seriously

from having to assess climate based on rainfall intensity (page 59), assuming factor independence through simple map multiplication and ignorance of deposition. The selected modelling approach was based on the work to replace the LS value. The replacement of LS with the unit contributing area has been the key to the development of new hydrologically based landscape erosion models and one of these has formed the foundation to this research.

### 2.1.3 The selected erosion model

This project needed a simple process-based model capable of predicting erosion and deposition based on readily available topographic and landuse data. Sediment transport due to overland flow in its simplest form (Equation 2.3) has been adapted by Desmet and Govers (1995) to account explicitly for the upslope contributing area (Equation 2.4). This simple hillslope storage model has been chosen due to its low demands on input data and opportunities for modification. The model implements a mass continuity calculation based on a proportional transport capacity parameter (Equation 2.5) allowing derivation of net erosion and deposition.

$$Q_s = kL^n s^m \quad \text{Equation 2.3}$$

Where:  $Q_s$  = sediment transport flux ( $\text{kg m}^{-1}$  unit time)

$k, m, n$  = constants

$L$  = distance from divide

$S$  = slope ( $\text{m m}^{-1}$ )

$$E_p = k_1 \cdot S^m \cdot Ro_s^n \quad \text{Equation 2.4}$$

Where:  $E_p$  = erosion potential ( $\text{kg m}^{-2}$ )

$Ro_s$  = Runoff = specific catchment area ( $\text{m}^{-2} \text{m}^{-1}$ ) \* SPR.

$S$  = slope ( $\text{m m}^{-1}$ )

$k_1$  = constant (set here to 4)

$m, n$  = constants

$$T_c = k_2 \cdot E_p$$

Equation 2.5

Where:  $T_c$  = transport capacity ( $\text{kg m}^{-1}$  of contour)

$k_2$  = proportionality factor (length)

$E_p$  = erosion potential ( $\text{kg m}^{-2}$ )

The model calculates 2 values at each point in the landscape:

1. Erosion rate ( $\text{kg m}^{-2}$ ) or detachment rate estimated using the erosion potential ( $E_p$ ) term, which is determined by the upslope contributing area, termed specific catchment area (sca) and slope.
2. Transport capacity ( $\text{kg m}^{-1}$ ) proportional to the erosion potential.

When calculating the  $E_p$  and  $T_c$  values, the following ranges for  $m$ ,  $n$ , and  $k_2$  were used when testing the model:

$$m = 1 - 1.8$$

$$n = 0 - 0.9$$

$$k_2 = 20 - 160$$

The ranges of parameters were selected from the literature. Equation 2.4 contains the specific catchment area variable and calculation of it required aspect and local slope information extractable from a high quality digital model of the landscape.

#### 2.1.3.1 The topographic model

The landscape was modelled with a digital terrain model (DTM) generated in ARC/INFO GRID. The OS Land-form Profile™ data set provided contours at 5m intervals in addition to spot elevation data as input. ARC/INFO GRID houses a very powerful interpolation routine, TOPOGRID, specifically developed to generate hydrologically correct digital elevation models from elevation and stream data. It is built around the ANUDEM program (Hutchinson, 1988;

Hutchinson, 1989), essentially a discretised thin plate spline technique (Wahba, 1990), where the routine has been modified to allow the fitted DEM to follow abrupt changes in terrain, such as streams and ridges. Desmet (1997) corroborates the use of splined approaches to DEM interpolation in a comprehensive examination of DEM interpolation techniques. TOPOGRID assumes that landscapes have few sinks and many hilltops or local maxima in elevation and using this assumption along with certain interpolation constraints, the routine generates a connected drainage structure and correct representation of ridges and streams. Two of the most attractive attributes of TOPOGRID are:

- low demands on the amount of input data - up to an order of magnitude less than normally required to adequately describe a surface with digitized contours.
- virtually eliminates the need for extensive post-processing of sinks and pits due to its global drainage conditions.

A digital data set of lochs was also input to TOPGRID to remove any interpolation within these areas and the NODATA attribute was subsequently assigned. Stream data provided extra topographical information to the interpolation routine by taking priority over all contour and point elevation data. This process allows any conflicting elevation data in flow paths to be ignored.

The grid cell size selected for the DTM was 25m. This was a compromise between computing power and spatial demands of representation at the regional and field scales. Quinn et al., (1995) suggest an absolute maximum cell size of 50m so as not to lose hydrological representation, yet fairly states an indication of macro-scale flow may well be adequately modelled with pixels of 50m or above. 50m in this case was viewed as too coarse. Schoorl et al., (2000) report a clear trend in erosion overestimation and sedimentation underestimation with increasing cell size, so the smallest possible was selected.

Slope was calculated for use throughout the modelling exercises using Equation 2.6 within GRID.

$$S = \sqrt{G_x^2 + G_y^2}$$

Where:  $S$  = dimensionless slope ( $m\ m^{-1}$ )

$G_x$  = slope in x-direction ( $m\ m^{-1}$ )

$G_y$  = slope in y-direction ( $m\ m^{-1}$ )

Profile curvature describing the rate of change in slope with aspect was calculated using Zevenbergen and Thorne's (1987) finite solution. It is very sensitive to sharp changes in topography (Desmet, 1997) and can be used to describe the acceleration of flow. Profile curvature has been used primarily in chapter 3 and 5.

Based on the above techniques it has been assumed that the DTM was as hydrologically correct as technically possible. The DTM was then utilized in the calculation of the contributing areas or specific catchment area (sca) for input into Equation 2.4. Within the last 20 years there have been a number of approaches proposed for the calculation of sca. A brief appraisal of the various techniques was carried out prior to selection.

### 2.1.3.2 Flow routing algorithms

Manual terrain analysis techniques have to-date been almost disregarded purely due to the emergence of fast cheap computing technology. Aiding the demise of manual approaches has been the transition from paper to digital formats in nationwide data sets and this now allows large areas of land to be processed and analysed within a few minutes using desktop PC software. Use of such computer aided processing created the digital terrain model (DTM) and using this as a platform, it becomes possible to calculate continuous topographic derivatives such as altitude, slope, aspect and curvature. In addition, topographic data in the form of a DTM possesses an area component, i.e. cell size. Cell size, which is always user defined, when used with altitude data allows calculation of two fundamentally important attributes, upslope area and specific catchment area. Upslope area  $A$  is defined as the total catchment area above a point or short



length of contour (Moore et al., 1991). The specific catchment area (sca), is defined as the upslope area ( $A$ ) per unit width of contour  $L$ , ( $sca = A/L$ ) (Moore et al., 1991). In essence each cell as an area must be transferred depending on topographic location to (lower) other points in the landscape. In effect a 'spread' of attributes is performed by the code/software. In the case of upslope contributing area,  $A$  can be estimated as the product of the number of draining cells in accordance with aspect plus the cell's own area. This distribution procedure may be applied to anything with a flow element (water, sediment, nutrients). It is this automated, iterative distribution procedure that is termed a flow routing algorithm and is most commonly used to define  $A$  and sca required for most hydrological and water quality models (Moore et al., 1993).

Two groups of flow routing algorithms have evolved over the last 20 years - single-direction flow (sdfa) and multi-direction flow algorithms (mdfa). The following review concentrates on only those using grid data structure, yet other contour based approaches exist (Panuska et al., 1991). Furthermore, any reference made to algorithms will be related to the flow of water as runoff. The key to the two differing algorithm types is how the flow is distributed or passed onto the next cell of the DTM. The procedure for analysing the digital terrain about a particular point in the DTM is common to both types of algorithm and a fairly standard technique. Inherent within ARC/INFO's GRID module is a technique called neighbourhood notation whereby cells adjacent to a cell being processed may be addressed individually via unique locators. Alternatively GRID also uses a standard 3x3 kernel of cells where the processing cell is central, to roam across all cells in a DTM. These neighbouring cells can be queried in relation to the processing cell and in a hydrological context used to define gradients of varying kinds.

## Single direction flow algorithms (D8 algorithms)

The steepest descent direction algorithm is by far the most frequently used in environmental modelling (Jenson and Domingue, 1988; Martz and De Jong, 1988; Panuska et al., 1991; Zevenbergen and Thorne, 1987). It was originally introduced by O'Callaghan and Mark (1984) and assigns *all* flow from each cell to only one of its eight neighbours (D8) in the direction of steepest downward slope. Lea (1992) developed an algorithm based on

cell aspect to define flow direction. It uses cell corner elevations averaged from the adjacent cell centres and fits a plane to its corners. Costa-Cabral and Burges (1994) modified Lea's algorithm further by treating flow as being uniform across a cell rather than traditionally from cell centre to centre. Their algorithm models flow as flow tubes yet still suffers from counter-intuitive and inconsistent flow directions under certain conditions (Tarboton, 1997). Modelling flow in a D8 manner generates strict discrete flow patterns as a result of the 45° 8 directions. Figure 2.4 is a sample from the D8 procedure. The output has a streaky appearance due to the rapid flow convergence. By assigning flow to only one neighbour, flow subsequently cannot diverge and respond to localised convexities where flow acceleration and spread would be expected. D8 is prone to predict permanent stream networks too early in the catchment due to this default flow convergence. Advantages of the algorithm include robustness, speed and efficient grid storage structure (Tarboton, 1997).

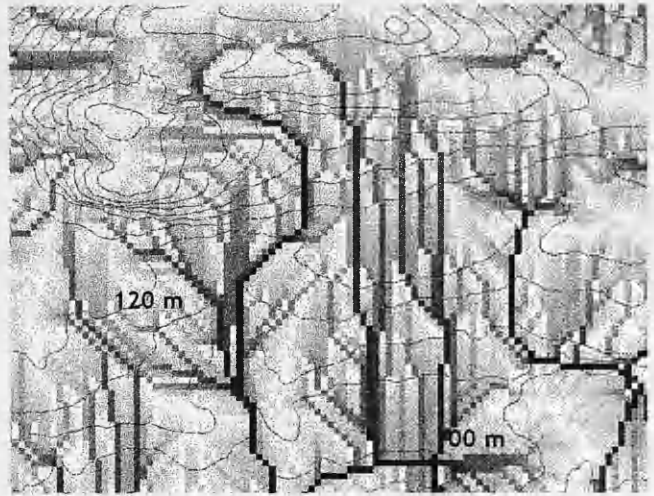


Figure 2.4. Specific catchment areas ( $\text{m}^2 \text{m}^{-1}$ ) calculated using the D8 algorithm (Jenson and Domingue, 1988).

is an important one to consider. Previously it has been only black and white in terms of what levels of dispersion was required until Tarboton (1997) introduced his approach.

## Multi-direction flow algorithms

Flow in such algorithms is distributed to a number of downslope cells proportionally to the slope magnitudes. Quinn et al., (1991) presented the first breakthrough in multi-direction flow routing. Their procedure assigns flow to *all* downslope neighbouring cells, each direction receiving a fraction of throughflow proportional to the gradient of each downhill flow path. The intuitive result is that steeper slope gradients tend to accumulate more flow. In theory of course there can be up to 8 receiving cells, therefore allowing divergent flow to be simulated. However, this can create problems with excessive spread of flow. Quinn et al., (1991) promote the procedure as being closer to reality having observed such flow behaviour in the field, particularly on the hillslope portions. Importantly they admit the algorithm performs a little strangely in valley bottoms where the flow begins a braiding pattern indicating flow to be leaving channels. Furthermore, they suggest that such a single-direction flow algorithm is desirable so that the flow reaches the permanent channel network.

Freeman (1991) used a similar approach. He represented flow draining through all downslope cells as being proportional to 1.1 power of the distance-weighted decrease in elevation through each direction. Holmgren (1994) developed a particularly flexible function into his flow algorithm. Correctly realising the lack of compromise between the single and multi-direction algorithms he offers a simplistic slope exponent  $\chi$  based approach allowing the user to vary  $\chi$  depending on the desired level of flow dispersion. Using  $\chi$  as 1 resulted in the same output as Quinn et al.'s (1991) and  $\chi$  as  $\infty$  forces the distribution towards single direction flow. Holmgren (1994) reported that the multi-direction pattern is too smooth (excessive dispersion/spread) and that the single-direction algorithm causes convergence much too early. The performance testing applied suggests that a  $\chi$  value of between 1 and 4 be used and varied depending on how flow is to be modelled. The problem of dispersal or spread when modelling flow is an important one to consider. Previously it has been fairly black and white in terms of what level of dispersion was required until Holmgren (1994) developed his approach.

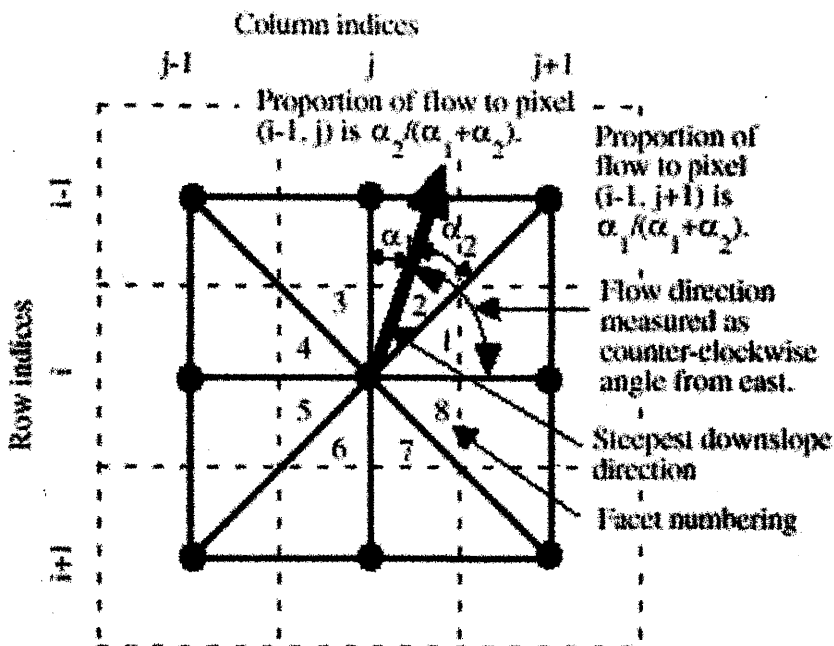


Figure 2.5. Definition of flow direction in the  $D_\infty$  algorithm (Tarboton, (1997)).

A further step has been taken towards a more realistic distribution by the work of Tarboton (1997). Tarboton (1997) developed his  $D_\infty$  (infinite number of possible single flow directions) algorithm with a view to incorporating the positive aspects of the previous approaches.  $D_\infty$  assigns flow direction based on the direction of steepest downwards slope, yet in a slightly different manner. Figure 2.5 shows how a standard moving 3x3 cell window split into 8 triangular facets.  $D_\infty$  calculates the local slope and flow direction of each facet. The facet with the largest local slope angle is then taken as the steepest downwards direction. This flow direction angle is then expressed as an angle counter-clockwise from east. If flow is in cardinal or diagonal directions, then flow is apportioned accordingly to that cell. Flow directions falling between cardinal and diagonal directions result in the splitting of flow between the 2 downslope cells adjacent to the steepest downslope direction. The amount of flow distributed to each cell is calculated depending on how close the angle of steepest downslope direction is to the direct angles to the 2 cell centres. The  $D_\infty$  procedure differs from Quinn et al.'s (1991) algorithm in that dispersion is

limited to a maximum of 2 cells in each iteration. Tarboton (1997) has been especially careful to maintain a certain amount of flow spread so as to model diversion, yet to stay consistent with definitive convergence of A and sca in catchments. Prior to flow direction processing,  $D_{\infty}$  initiates the D8 procedure primarily as a sink fill facility. It fills sinks to the level of the local overflow point to maintain the downslope movement of water hence preventing the formation of dams. In doing this D8 also performs a secondary function where  $D_{\infty}$  alone may fail to be able to assign a flow direction in flat areas or sink cells. After D8 sink fills, it is then capable of assigning flow direction albeit a single direction. The  $D_{\infty}$  procedure makes extensive use of D8's robustness.

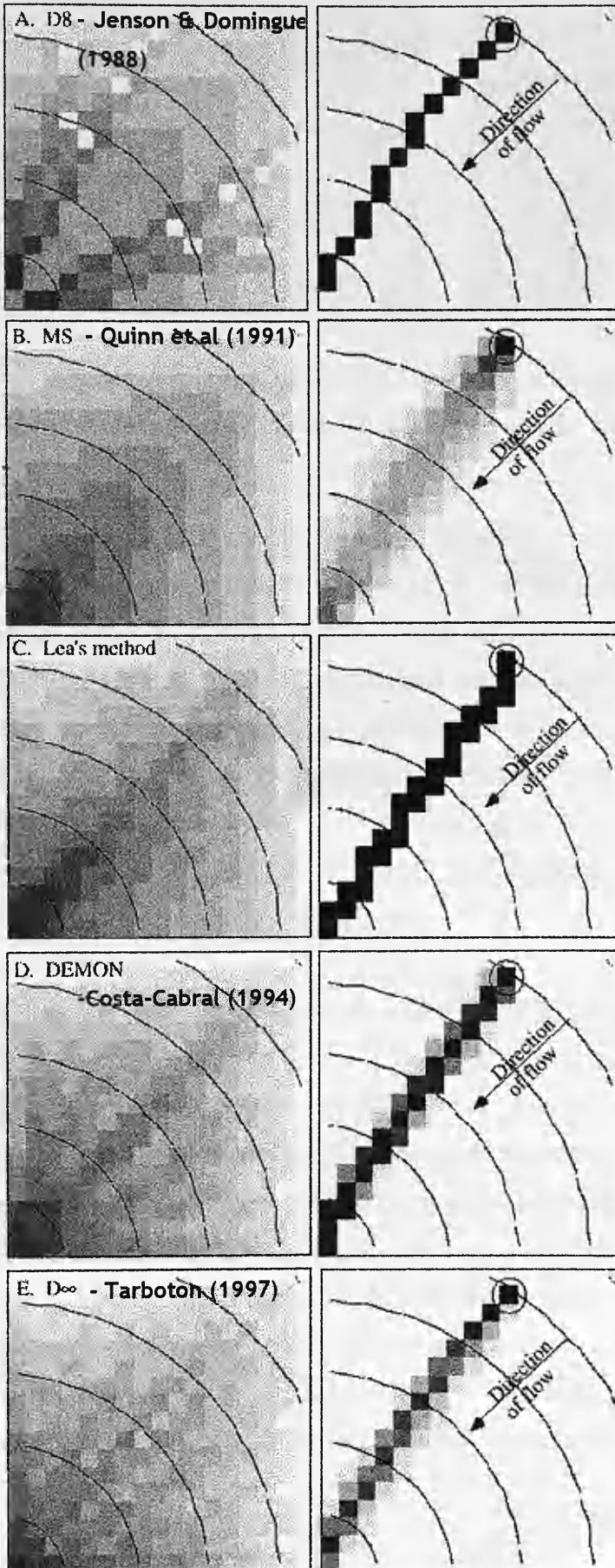


Figure 2.6. The inward cone shaped topography and how varying routing algorithms effect flow. Contours show elevation. Left panel is upslope area and right panel is how and which cells are influenced as a result of flow from the circled cell. (Tarboton, 1997).

recipe for Lea. The  
TARDEM. It contains  
and the catchment  
with its additions to  
creates hard-to-read  
viewer's GRID tool  
is found. TARDEM  
files for DEM data  
by TARDEM is freely  
etc.

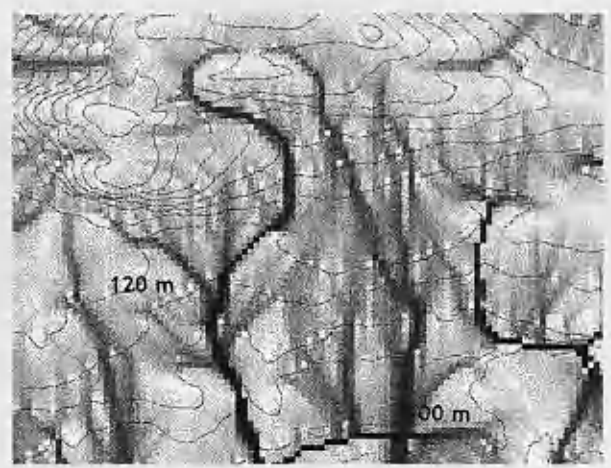
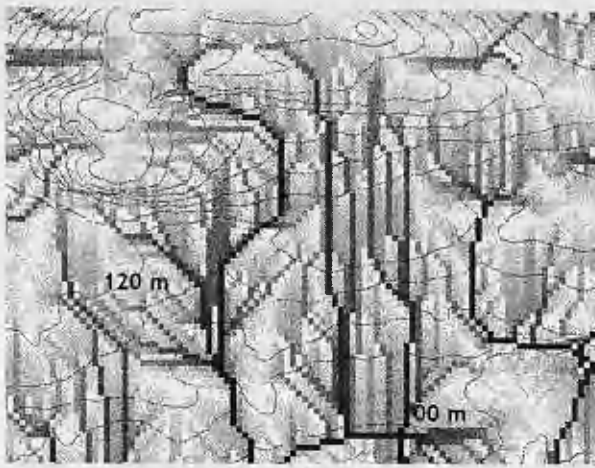


Figure 2.7. Comparison of specific catchment areas ( $\text{m}^{-2} \text{m}^{-1}$ ) calculated using a) the D8 algorithm and b) the  $D_{\infty}$  algorithm.

Figure 2.6 shows tests carried out by Tarboton (1997) on the algorithms of Jenson and Domingue's (1988), Quinn et al., (1991), Lea (1992), Costa-Cabral (1994) and Tarboton (1997). This is a final side-by-side comparison of some of the above-mentioned routing algorithms and displays the variation in flow behaviour across a top-right to bottom-left sloping inward cone. Note in particular the extreme convergence of the D8 and extreme dispersion of Quinn's MS whilst the  $D_{\infty}$  approach maintains general downslope convergence with a degree of spread. Figure 2.7 illustrates the striking differences in patterns produced from the D8 and  $D_{\infty}$  procedures.

Practical aspects of the  $D_{\infty}$  algorithm make it particularly attractive for use. The algorithm is neatly packaged into a suite of software named TARDEM. It contains a number of sub-modules for sink-filling, calculation of D8 and  $D_{\infty}$  catchment drainage areas (A and sca) and definition of drainage networks. In addition to the above positive technical/theoretical aspects, TARDEM operates hand-in-hand with ESRI GRID data. It does this by communicating with ArcView's GRID input-output libraries, hence reducing incompatibilities between GIS formats. TARDEM does however also accept and generate standard ASCII files for DTM data allowing smooth integration of other GIS platform data. Finally TARDEM is freely available for non-commercial use from David Tarboton's website<sup>2</sup>

<sup>2</sup> (<http://www.engineering.usu.edu/cee/faculty/dtarb/>).

After reviewing the above methods for routing flow and taking into consideration various other aspects, TARDEM was selected to deliver data on drainage areas. The package was put through a series of tests and trials to examine its performance and robustness when processing large data sets. In summary the package is extremely stable and consistently handled 80km x 60km grids at 25m resolution. Not only is TARDEM stable but computationally very fast.

The TARDEM  $D^\infty$  algorithm was modified to execute the mass continuity calculation for each cell. Sediment flux in the model was assumed to be transport limited, i.e. only by the magnitude of overland flow's capacity to transport. This has been reported by Moore and Wilson (1992), as being the dominant process influencing the pattern of erosion in landscapes. The following pseudo-code outlines how the new  $D^\infty$  algorithm works:

1.  $D^\infty$  accesses the erosion potential ( $E_p$ ) grid calculated using Equation 2.4. The  $E_p$  grid represents the amount of detachment due to overland flow.
2.  $D^\infty$  accesses the transport capacity ( $T_c$ ) grid using Equation 2.5.
3. In accordance with  $D^\infty$  routing procedure,  $E_p$  is then routed to the next downslope cell(s). For each cell the amount of sediment arriving (inflow) is calculated.
4. At each cell  $D^\infty$  executes the following to deposition and subsequent outflow:

$$\text{net loss/gain} = S_{\text{inflow}} - S_{\text{outflow}} \quad \text{Equation 2.7}$$

Where:  $S_{\text{inflow}}$  = sediment inflow to cell

$S_{\text{outflow}}$  = sediment outflow from cell

If the inflow of sediment to a cell is below the  $T_c$  value for that cell, then the erosion rate is assumed equivalent to a negative  $E_p$  value since the overland flow is further capable of transporting detached soil. Outflow from the cell is simply the value of  $E_p$  plus the inflow of soil. When cell inflow exceeds the  $T_c$  value, Equation 2.7 will result in the excess amount



of sediment being deposited (positive value). Sediment outflow in a deposition scenario can only be equal to  $T_c$  and never exceeded.

## 2.2 Pilot runs of the model

The model mechanics were initially examined in an Excel spreadsheet environment. A 350m x 25m slope transect was extracted from the DTM on the north slope of the river Earn close to Forgandenny, Perth and Kinross (NO032182). The transect is only 1 cell wide and therefore no flow divergence or convergence was modelled. The transect can be seen in Figure 2.8.

Figure 2.8 confirms that the model functioned correctly in the simple test environment. The accumulation of detached soil material resulting from overland flow continues to the 137.5m mark where a change in convexity lowers  $T_c$ . This change has sufficiently lowered  $T_c$  so as to trigger deposition (inflow > outflow). Sediment inflow to each cell then decreases along with  $T_c$  during the depositional phase until topography initiates a rise in  $T_c$  and  $E_p$  once more. The model does appear sensitive to topographic changes although it is unlikely that deposition would take place over a 50m distance. This is an artifact of restricting flow diversion and convergence. The  $D_\infty$  flow algorithm distributes flow to the 2 steepest downslope cells which widen and shortened a deposition zone.

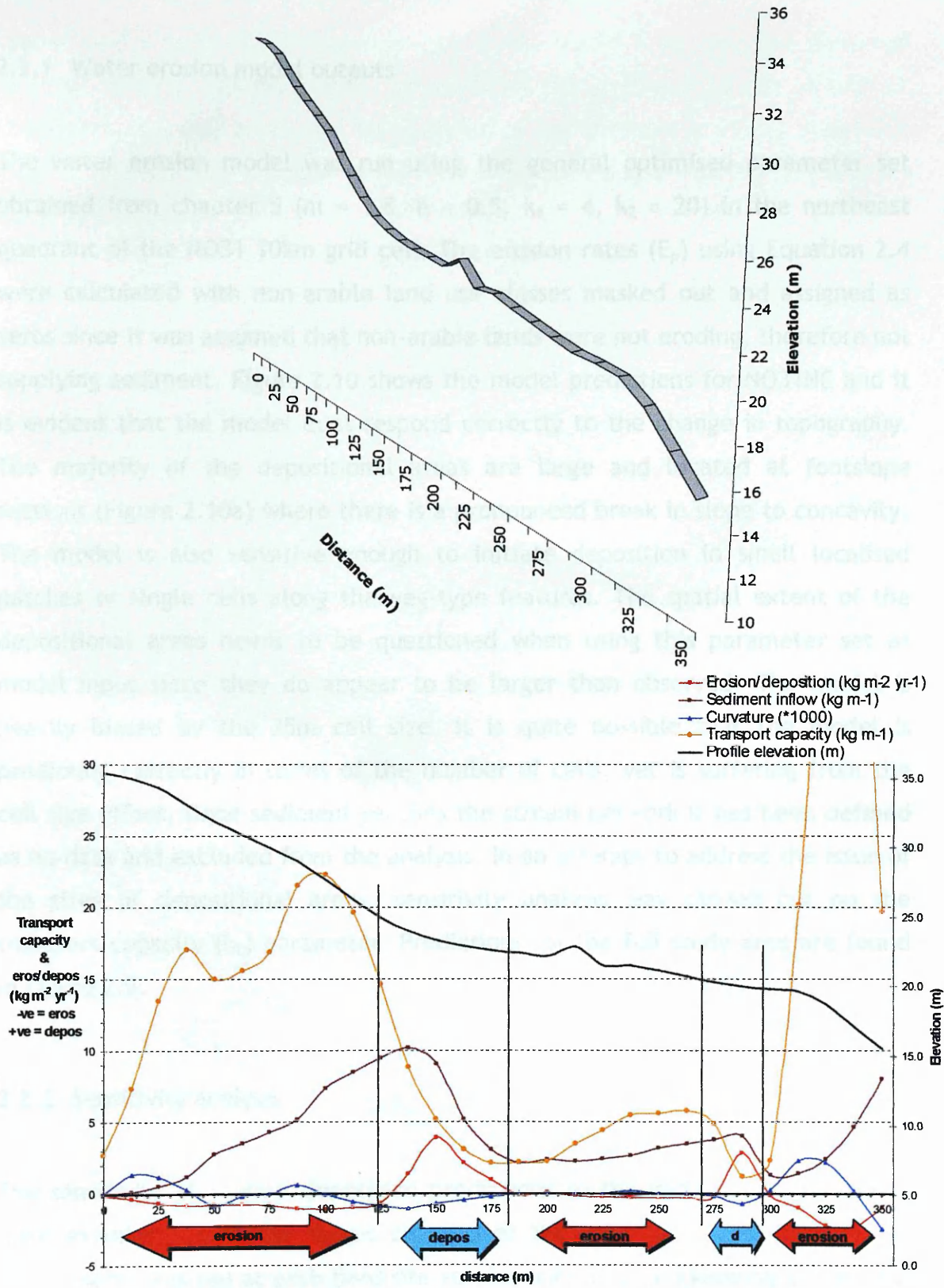


Figure 2.8. Results from a pilot run of the water erosion model in a spreadsheet environment along a 350m x 25m DTM extracted transect.

### 2.2.1 Water erosion model outputs

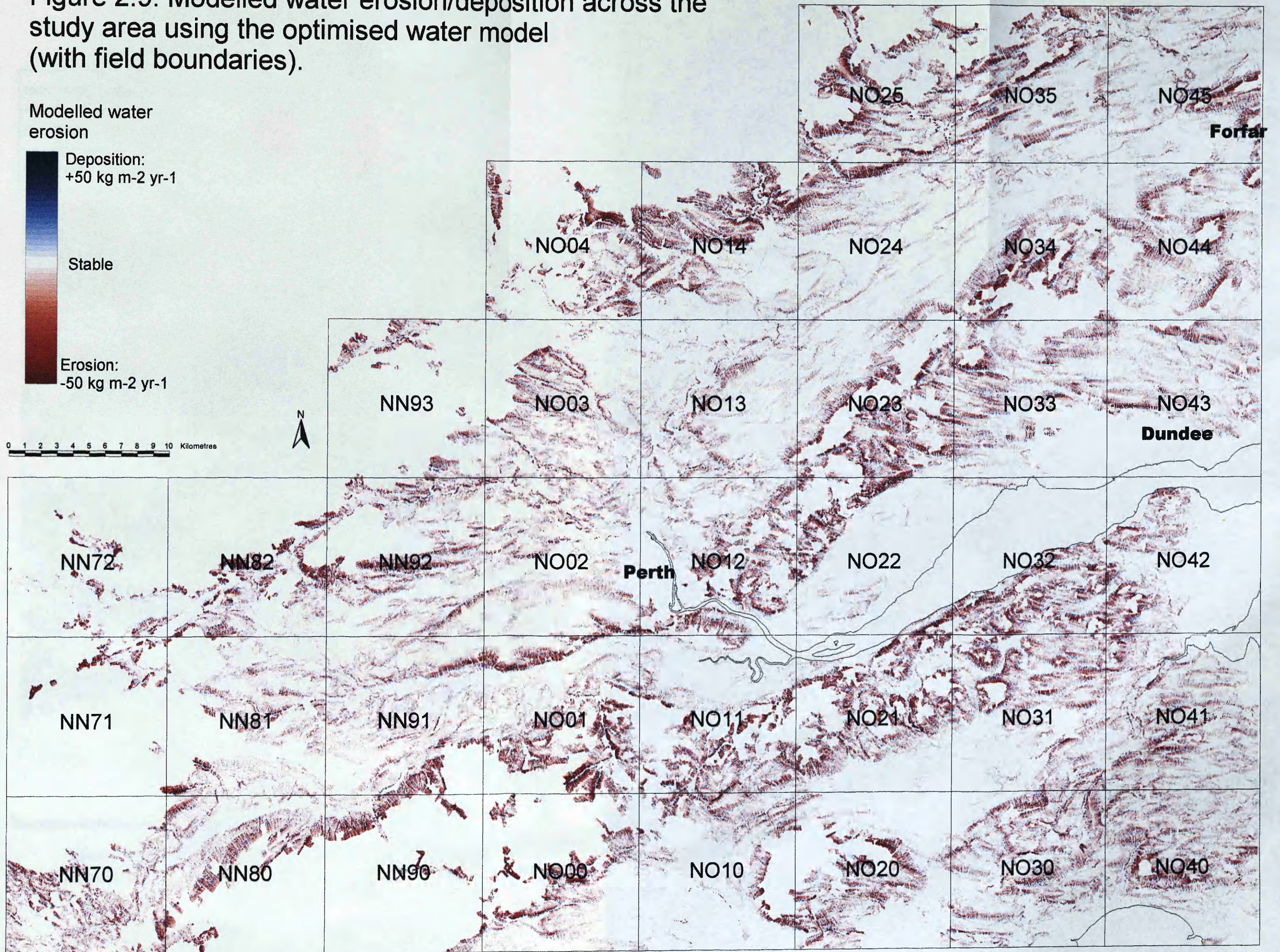
The water erosion model was run using the general optimised parameter set obtained from chapter 5 ( $m = 1.8$ ,  $n = 0.5$ ,  $k_1 = 4$ ,  $k_2 = 20$ ) in the northeast quadrant of the NO31 10km grid cell. The erosion rates ( $E_p$ ) using Equation 2.4 were calculated with non-arable land use classes masked out and assigned as zeros since it was assumed that non-arable lands were not eroding, therefore not supplying sediment. Figure 2.10 shows the model predictions for NO31NE and it is evident that the model does respond correctly to the change in topography. The majority of the depositional areas are large and located at footslope sections (Figure 2.10a) where there is a pronounced break in slope to concavity. The model is also sensitive enough to initiate deposition in small localised patches or single cells along thalweg-type features. The spatial extent of the depositional areas needs to be questioned when using this parameter set as model input since they do appear to be larger than observed. The model is heavily biased by the 25m cell size. It is quite possible that the model is predicting correctly in terms of the number of cells, yet is suffering from the cell size effect. Once sediment reaches the stream network it has been defined as no-data and excluded from the analysis. In an attempt to address the issue of the sizes of depositional areas, sensitivity analysis was carried out on the transport capacity ( $k_2$ ) parameter. Predictions for the full study area are found in Figure 2.9.

### 2.2.2 Sensitivity analysis

The sensitivity of erosion/deposition predictions to the variables  $m$ ,  $n$ , and  $k_2$  were examined using the ranges outlined at the four field sites. Initially the water model was run at each field site varying only  $m$ , and  $n$  keeping  $k_2$  constant at 20. The slope exponent  $m$  was kept constant at its most minimising or least influential (1.8) so as not to exaggerate the effect of  $n$ . The sca exponent  $n$  was held at zero. Outputs from the analysis are shown in Figure 2.11 to Figure 2.13. At all 4 field sites the water erosion/deposition model is more sensitive to changes in the sca  $n$  exponent than to changes in slope  $m$ . Selection of an

appropriate n exponent is therefore vital if the model is to resemble observed rates of erosion and deposition. In addition, the accuracy of the simulated catchment drainage areas and calculations of sca becomes a vitally important step in deciphering whether a point in the landscape will be eroding or accumulating soil.

Figure 2.9. Modelled water erosion/deposition across the study area using the optimised water model (with field boundaries).



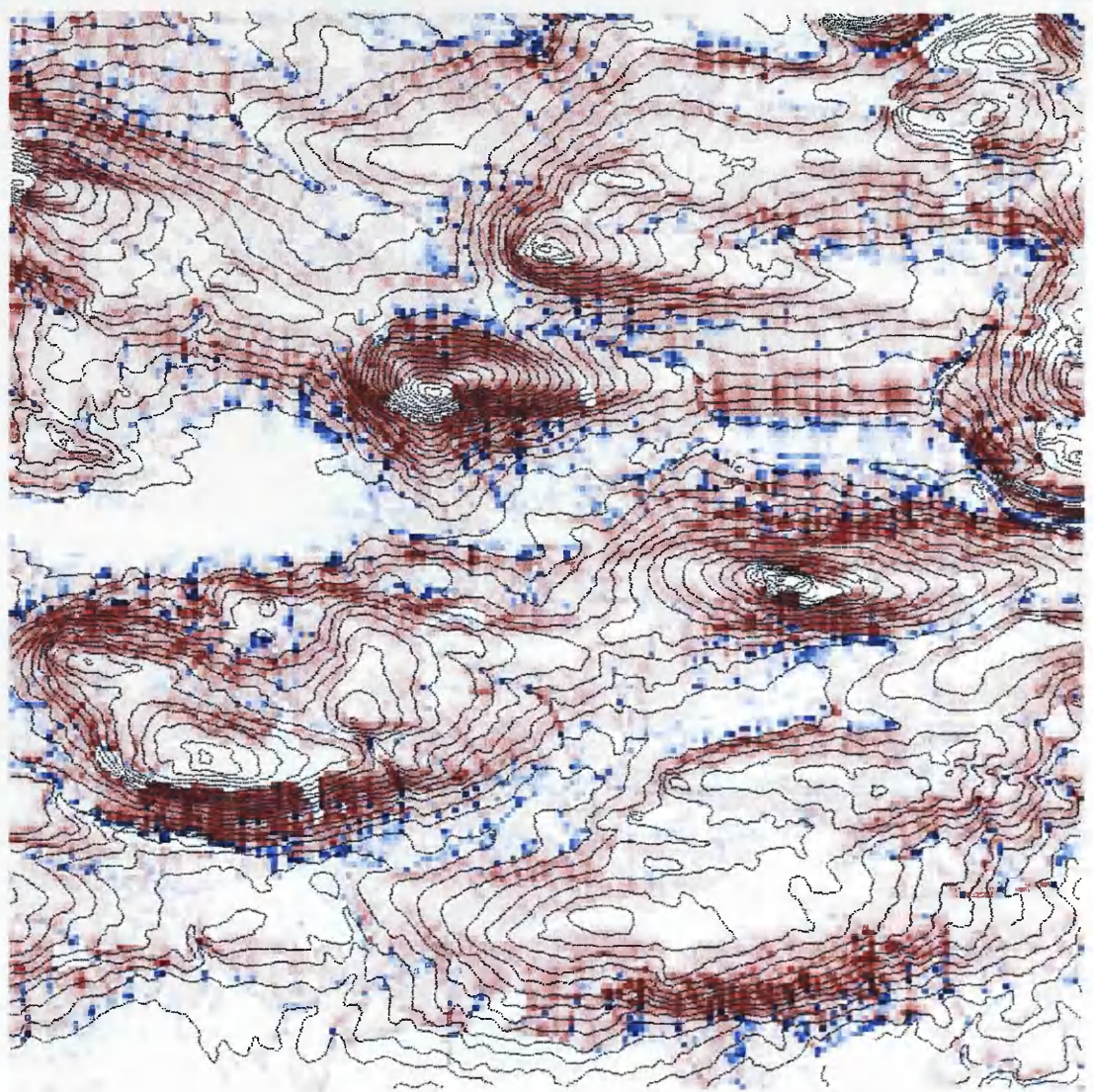
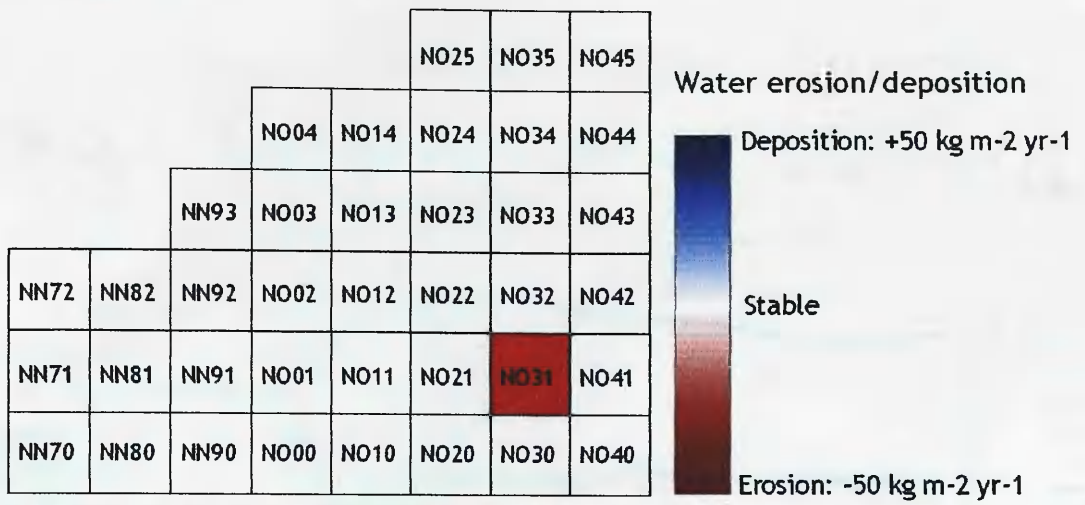


Figure 2.10. Water erosion model outputs for the northeast quadrant of N031

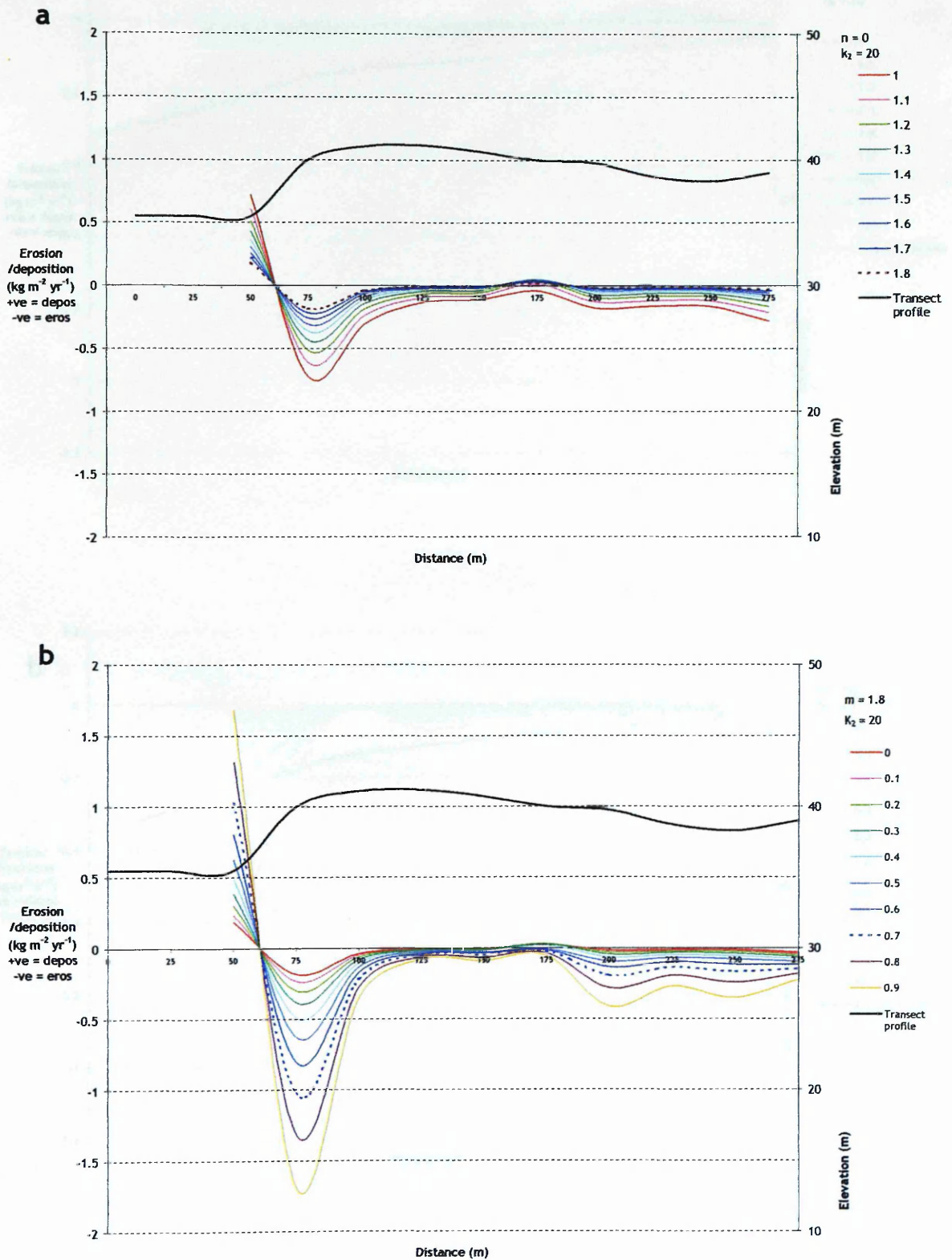


Figure 2.11. The sensitivity of the water erosion model at Loanleven to variations in the slope  $m$  (a) and sca  $n$  (b) parameters.

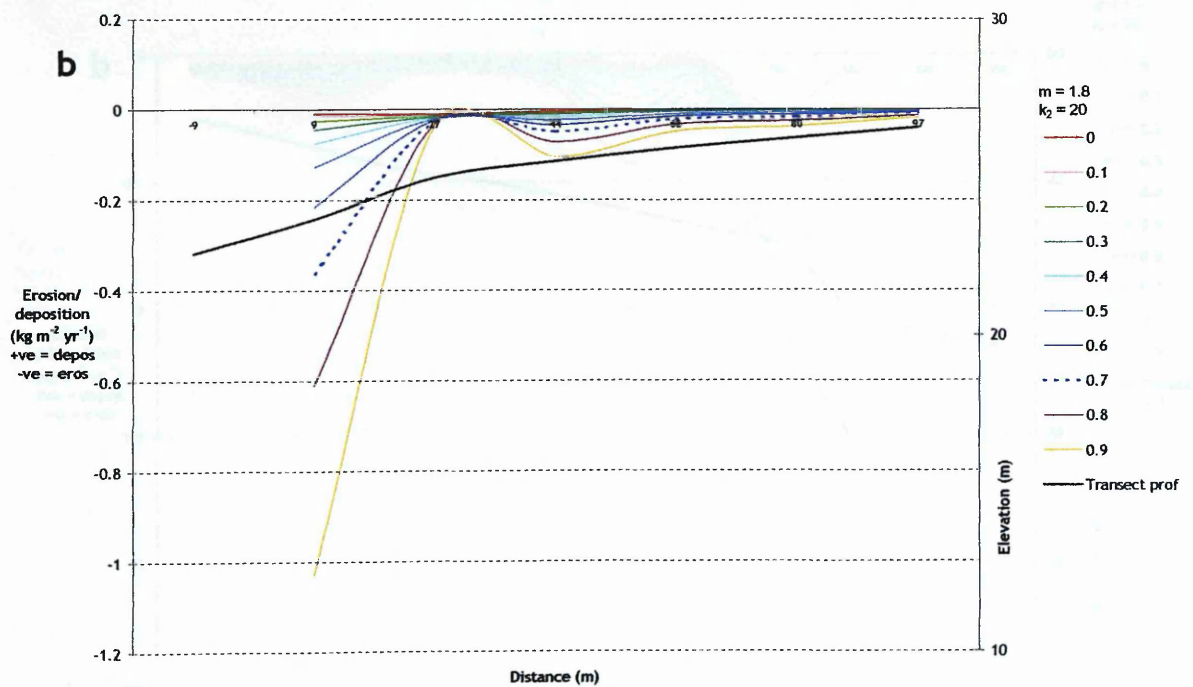
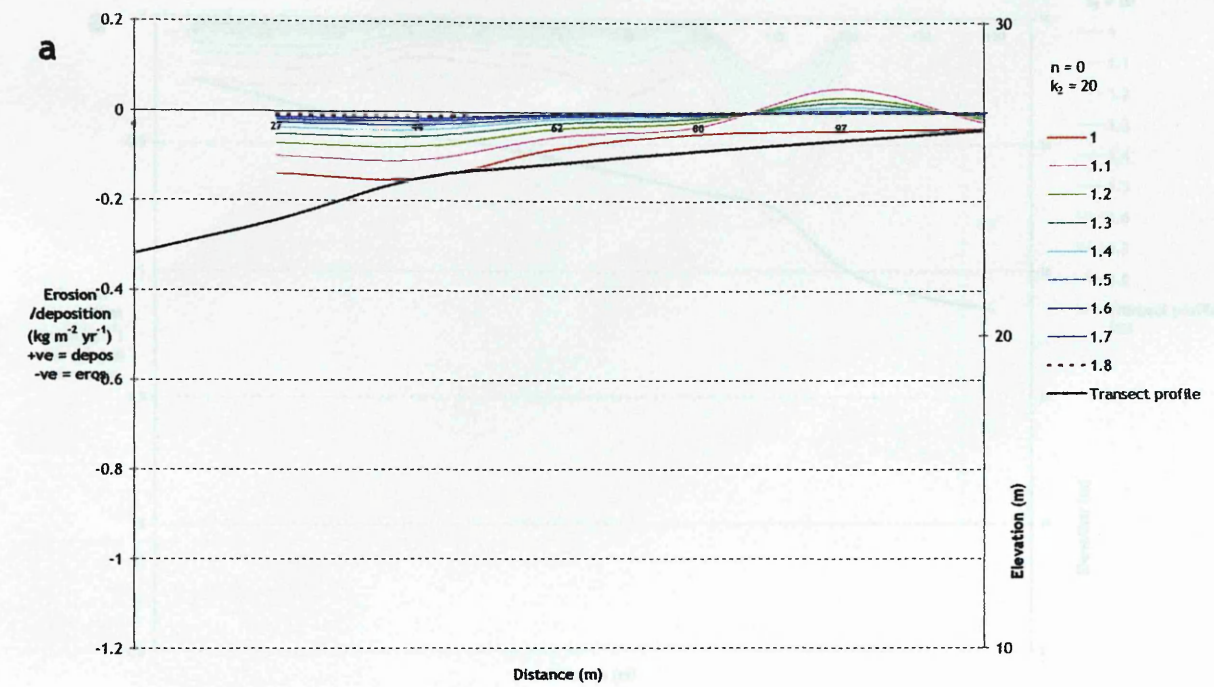


Figure 2.12. The sensitivity of the water erosion model at Blairhall to variations in the slope  $m$  (a) and scale  $n$  (b) parameters.



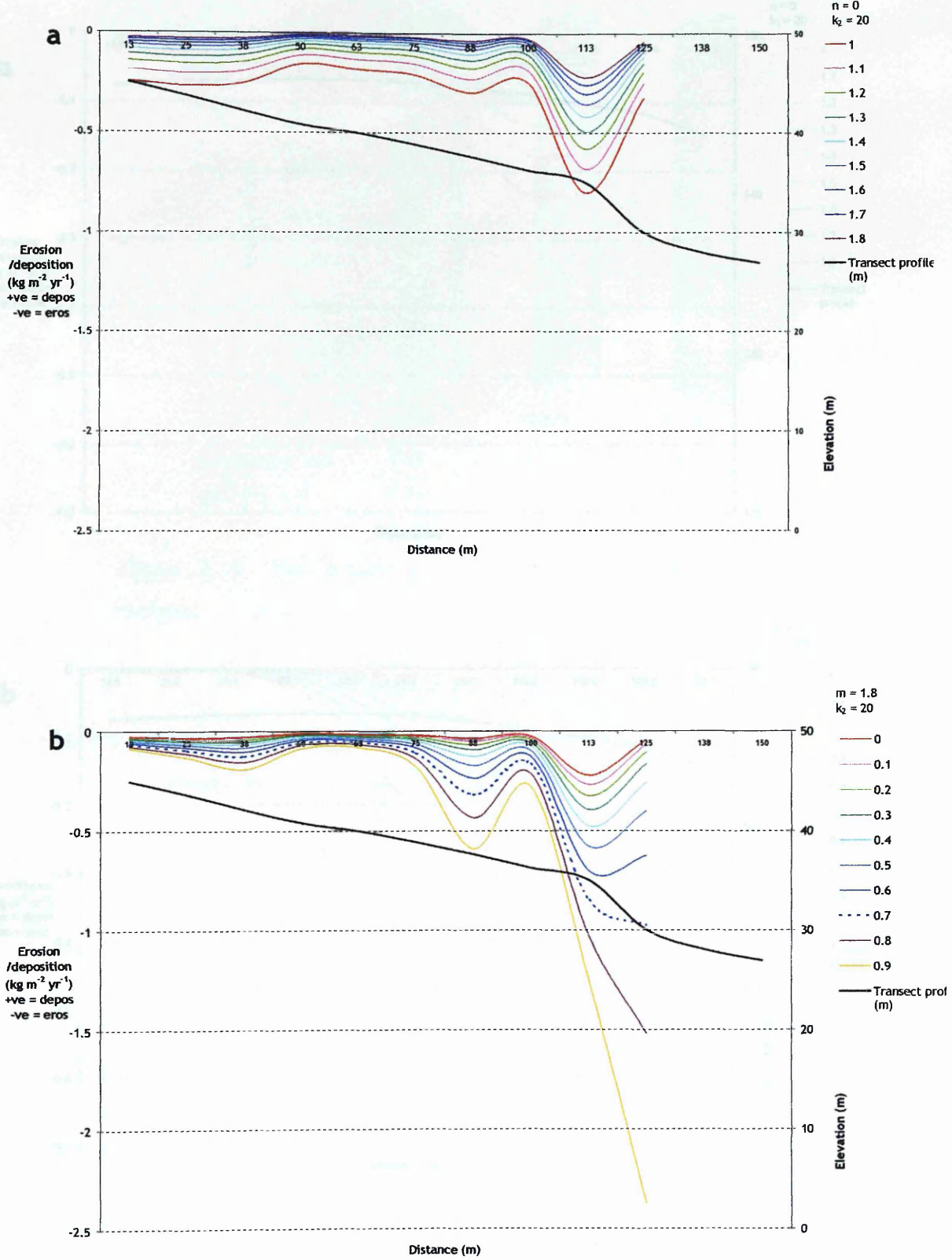


Figure 2.13. The sensitivity of the water erosion model at Leadketty to variations in the slope  $m$  (a) and sca  $n$  (b) parameters.

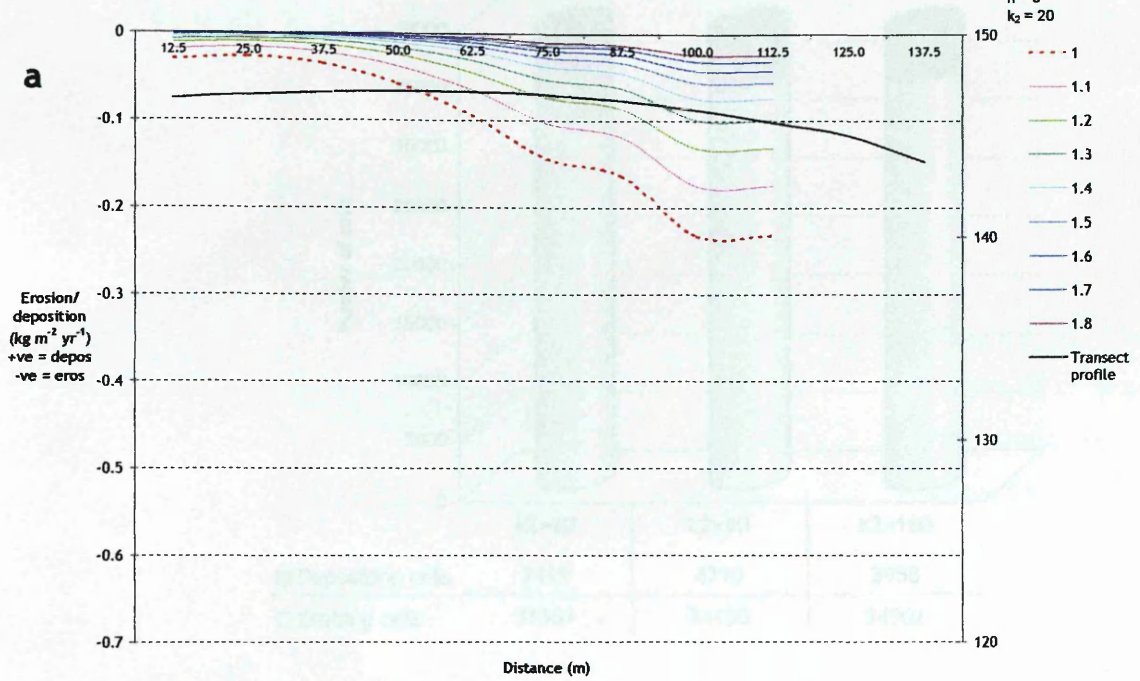


Figure 2.13. The effect of transport capacity on sediment budgets.

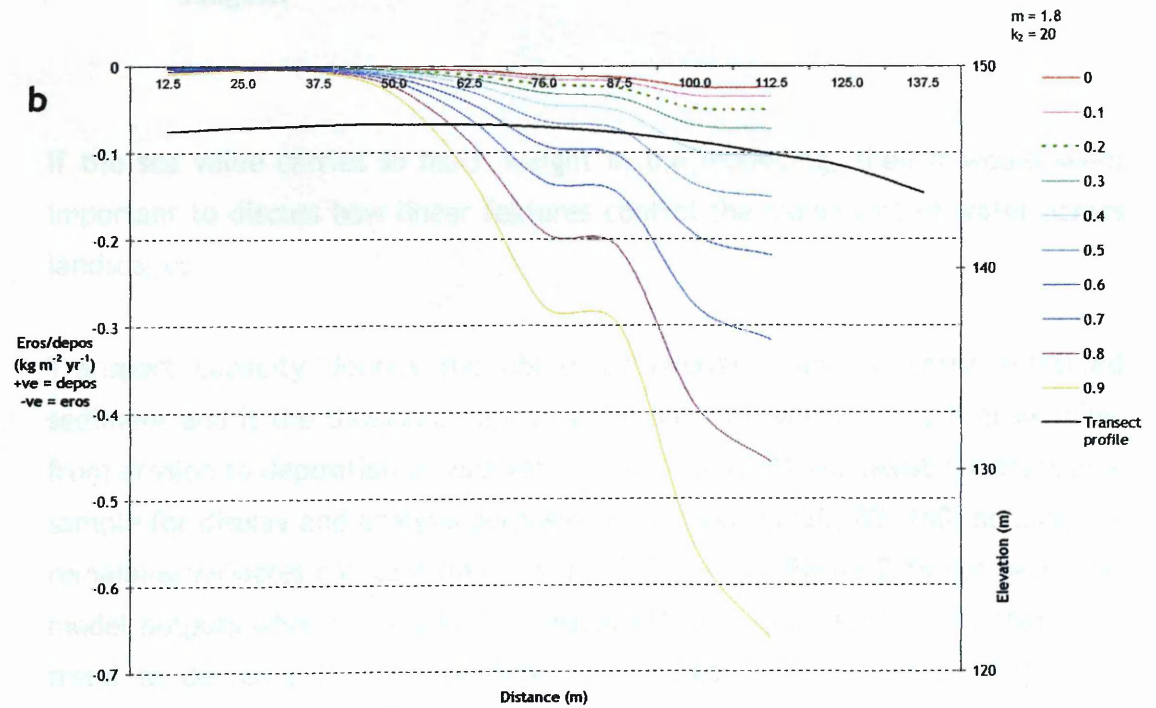


Figure 2.14. The sensitivity of the water erosion model at Littlelour to variations in the slope  $m$  (a) and scale  $n$  (b) parameters.

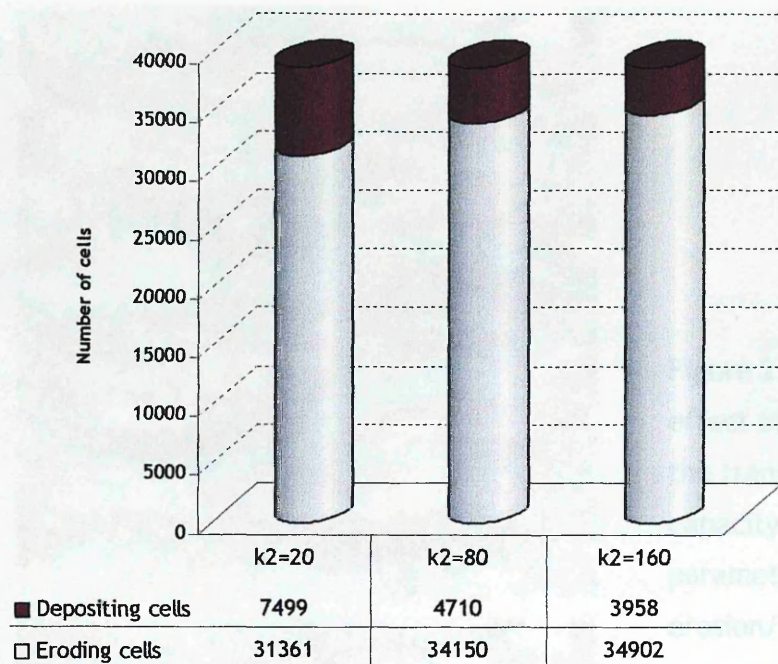
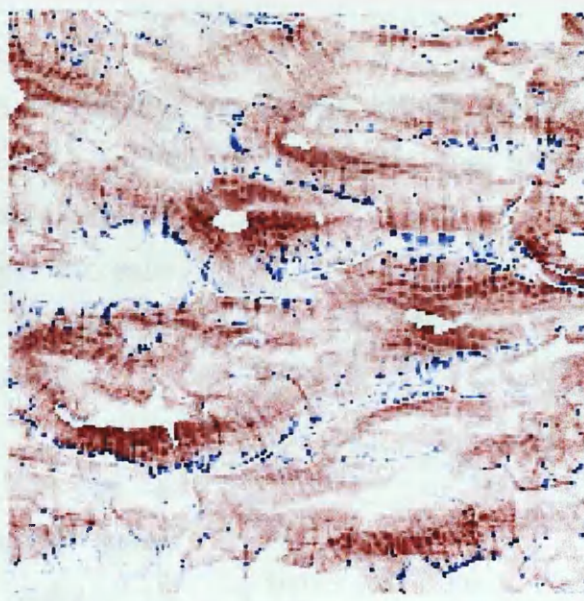


Figure 2.15. The effect of transport capacity on sediment budgets.

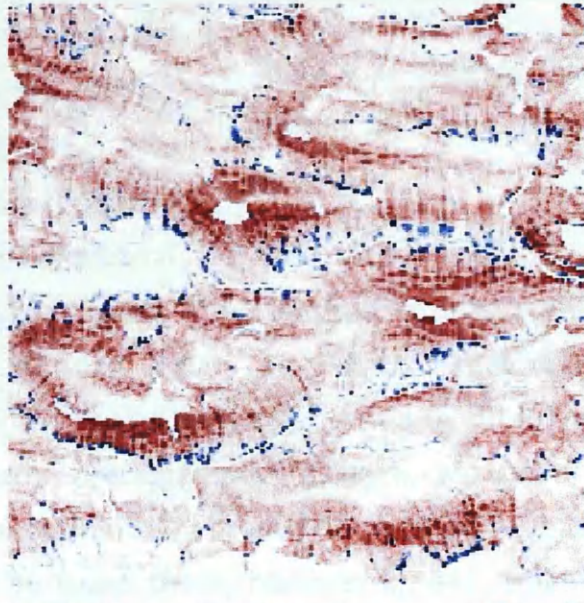
If the  $sca$  value carries so much weight in the modelling, then it would seem important to discuss how linear features control the movement of water across landscapes.

Transport capacity defines the ability of overland flow to carry entrained sediment and is the threshold depicting the point at which the system switches from erosion to deposition or vice versa. Using the NO31 northeast quadrant as a sample for display and analysis purposes,  $k_2$  was varied (20, 80, 160) holding the remaining variables constant ( $m = 1.8$ ,  $n = 0.5$ ,  $k_1 = 4$ ). Figure 2.16 compares the model outputs when varying  $k_2$ . The visual effect is quite subtle, but there is a trend to decrease the size of depositional areas as  $k_2$  increases. Table 2.1 supports this. High  $k_2$  ( $T_c$  value) causes deposition to occur in very intense localised patches where the  $T_c$  threshold is only exceeded at locations with sharper and more sudden change in topography. Also the increase in  $k_2$  allows more low gradient slope areas to be eroded due to high  $T_c$  values which otherwise would have been likely areas of deposition (Figure 2.15).

$k_2 = 20$



$k_2 = 80$



$k_2 = 160$

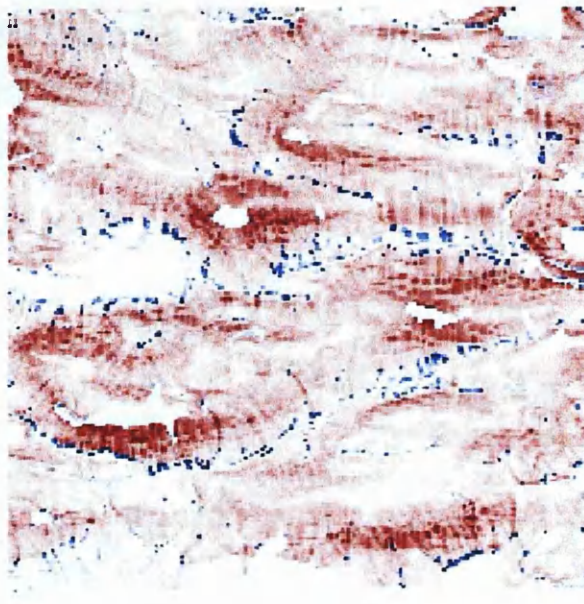
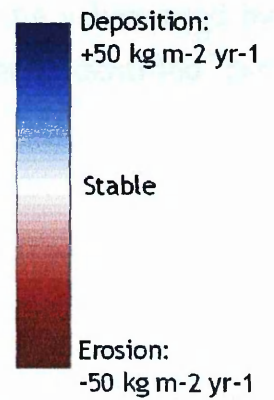


Figure 2.16. The effect of varying the transport capacity parameter ( $k_2$ ) on erosion/deposition patterns (NO31NE quadrant).

Water erosion /deposition



0 1 2 kilometres



Contrary to results in Desmet and Govers (1995) the mean erosion rate has slightly decreased with increasing  $k_2$  despite the number of eroding cells increasing. The median erosion rate does however increase with increase in  $k_2$ , though changes are very small.

$k_2$  should be used as a calibration parameter when comparing model outputs to observed field patterns. Desmet and Govers (1995) calibrated using  $k_2$  by comparing the model outputs against the locations of alluvial

soils on the Belgian soil map. They reported optimal agreement when using  $k_2$  set at between 48 and 120. They stated that the basic pattern of erosion/deposition was consistently reproduced by all  $k_2$  values. The process of calibrating the water erosion model using  $k_2$  alongside  $m$  and  $n$  has been implemented in the optimisation procedure outlined in chapter 5. Details on the procedures are to be found there, however  $k_2$  was optimised at 20 at all four field sites individually. 20 does appear low in view of the values used by Desmet and Govers (1995) and reasons for this have been identified and discussed in chapter 5.

$k_2$	Mean erosion rate (kg m <sup>-2</sup> yr <sup>-1</sup> )	Median erosion rate (kg m <sup>-2</sup> yr <sup>-1</sup> )	Mean deposition rate (kg m <sup>-2</sup> yr <sup>-1</sup> )
20	-0.383	-0.13503	+1.994
80	-0.362	-0.15384	+3.612
160	-0.356	-0.15671	+4.595

Table 2.1. Changes in mean and median erosion and deposition rates with varying  $k_2$ .

### 2.2.3 Modelling the effect of field boundaries

When conceptualizing the role a field boundary feature plays in the movement of water, the complexity and detail in which the final model would predict was heavily restricted by the selected cell size. Even assuming the existence of high resolution data on drainage ditches, dead furrows, position of gates etc, representing them with 25m cells cannot be justified. At this regional scale such data sets do not exist and collecting such data is an impossible task. Field boundaries have been mapped in vector format by the Scottish Executive Environment and Rural Affairs Department (SEERAD) and were kindly donated. The data set was rasterized to 25m.

The approach considers field boundaries as landscape features, so are considered as part of the terrain itself. To obtain this the raster field boundary dataset had to be assigned an elevation  $z$  value. This is the first in a number of assumptions within the modelling procedure. Due to the lack of detailed local information regarding the types of field boundaries in use in the SEERAD dataset, a uniform  $z$  value of 1m was assigned to all features. All other areas were assigned a value of zero. This was then simply added to the sink-free DTM. No further filling procedures were applied to the resulting raster. Since the field boundaries were solid features of the terrain, the procedure assumes that all boundaries are impermeable. As discussed earlier this is not always the case and reality exists somewhere between the solidity and porosity.

To facilitate data analysis and display 3 25km<sup>2</sup> clip areas (NO13SE, NO31NE, NO44NE) have been randomly selected. In addition one small 4km<sup>2</sup> clip (NO463 477: centre) is also included.

Tests for the effect of field boundaries were carried out on the following:

1. Calculation of specific catchment areas.
2. Patterns and magnitude of soil erosion/deposition.

The soil erosion model was run using parameters taken from the literature. Optimised parameters had not been obtained from the optimisation procedure at this stage so could not be used in this investigation but the effect of the field boundaries regardless of parameters would be same. Therefore, from each clip area, four output datasets have been generated - specific catchment areas and soil erosion/deposition with and without field boundaries.

## 2.2.4 Results and discussion

### 2.2.4.1 Specific catchment areas

The new terrain model was used as input for the calculation of specific catchment areas. The  $D_{\infty}$  (Tarboton, 1997) algorithm was used in specific catchment area calculation. Figure 2.17 to Figure 2.20 compare the impact field boundaries have on specific catchment areas in all 4 clips. The shape and size of drainage areas calculated without the presence of field boundaries are clearly influenced solely by topographic aspect. The deeper shades of blue are fingerprints for areas likely to generate high levels of concentrated overland flow and convergence of flow patterns into such zones is occurring fairly quickly. Comparing specific catchment areas calculated with and without field boundaries, the most striking difference is the overall general lighter blue appearance consistently generated when field boundaries are modelled. The attenuation in deep blues indicates, at least in a visual sense, an overall reduction in specific catchment area size. The corresponding frequency distributions corroborate this strongly in addition to the spread of values and descriptive statistics in Table 2.2. Not only are deep blue shades (large drainage areas) less common, but the dominance of topographic flow direction is also particularly reduced. Within field units, drainage areas continue to be defined by aspect, yet boundaries under certain conditions are forcing flow in non-aspect directions. In many fields high specific catchment area values have developed along the lower fringes. This is a simplistic analogy of that seen previously in Figure 2.2 so suggests that the redirecting properties of the boundaries is an improvement.

Ultimately this study focuses on whether the presence of field boundaries in the landscape has an attenuating effect on soil erosion/deposition. However, prior to this specific catchment areas were examined statistically using nonparametric Wilcoxon signed rank tests to ascertain whether or not they were being reduced by field boundaries (Table 2.3). The specific catchment area data was upon examination non-normally distributed so demanded testing using non-parametric statistical methods.

The following observations have been made:

1. In all 4 clips very strong statistical evidence ( $p < 0.05$  in all cases) indicates that modelled field boundaries have a statistically significant attenuating impact on how flow accumulates across the landscape (Table 2.3).
2. Field boundaries appear to have a squeezing effect on the frequency distribution of data and produce a sharper peak (sca standard deviation values for all clips are drastically reduced). The tails of the field boundary distributions are clipped indicating a general removal of larger sca values.
3. On average across the 4 clip areas, sca in 57% of cells was reduced. More important, however, is the >75% sca reduction figure. These data better highlight the larger differentials caused by field boundaries, which are more likely to have pronounced effects on erosion.
4. On average the presence of field boundaries caused sca attenuation > 75% in some 20% of cells. As discussed previously the channelling and forcing effect of field boundaries, which in some instances may lead to accelerated concentrated flow does appear to be consistently present within the analysis clip areas.
5. Sca doubling as a result of field boundary inclusion occurred on average in 7% of cells. In terms of real numbers this may at first seem quite low in consideration to the total population of cells, yet practically could produce quite extreme localised rilling/gullying. This will usually occur just down-catchment of the field boundary element as a 'pass-on' effect. In the case of the NO31NE quadrant, some 8% of cells experienced a doubling of sca size due to field boundaries. This equates to some 3168



cells or 198 ha. This of course assumes the total area of each cell is representing what in reality occurs in only a small proportion of this area on the landscape, i.e. a rill channel for example, which are not 25m wide as assumed in this project. Assuming this, cells with larger sca are usually clustered together along the linear field boundaries where flow is channelled against aspect.

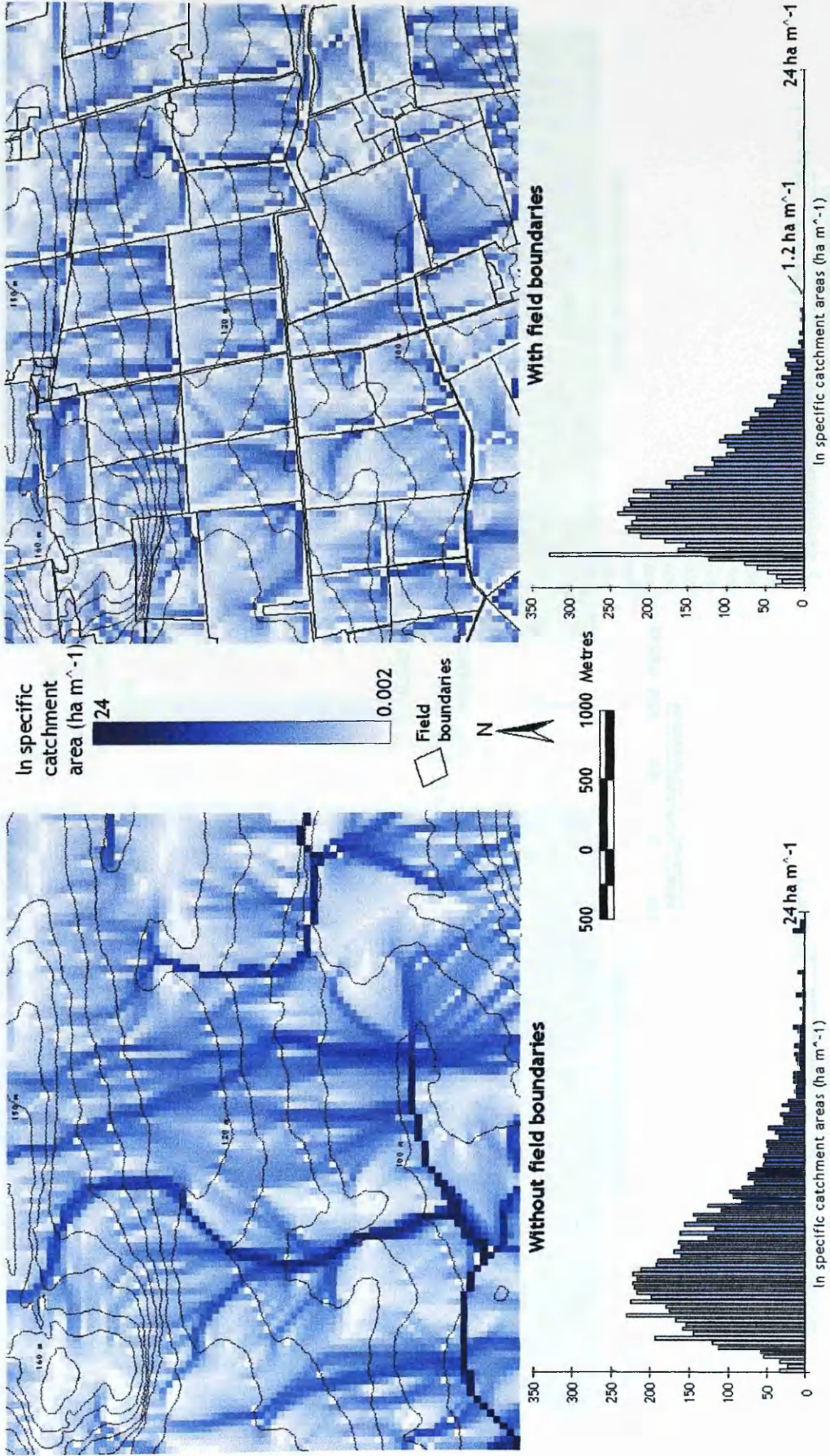


Figure 2.17. Patterns and frequency distributions of contributing areas calculated with and without the effect of field boundaries in the Forfar clip (NO463 477). 105

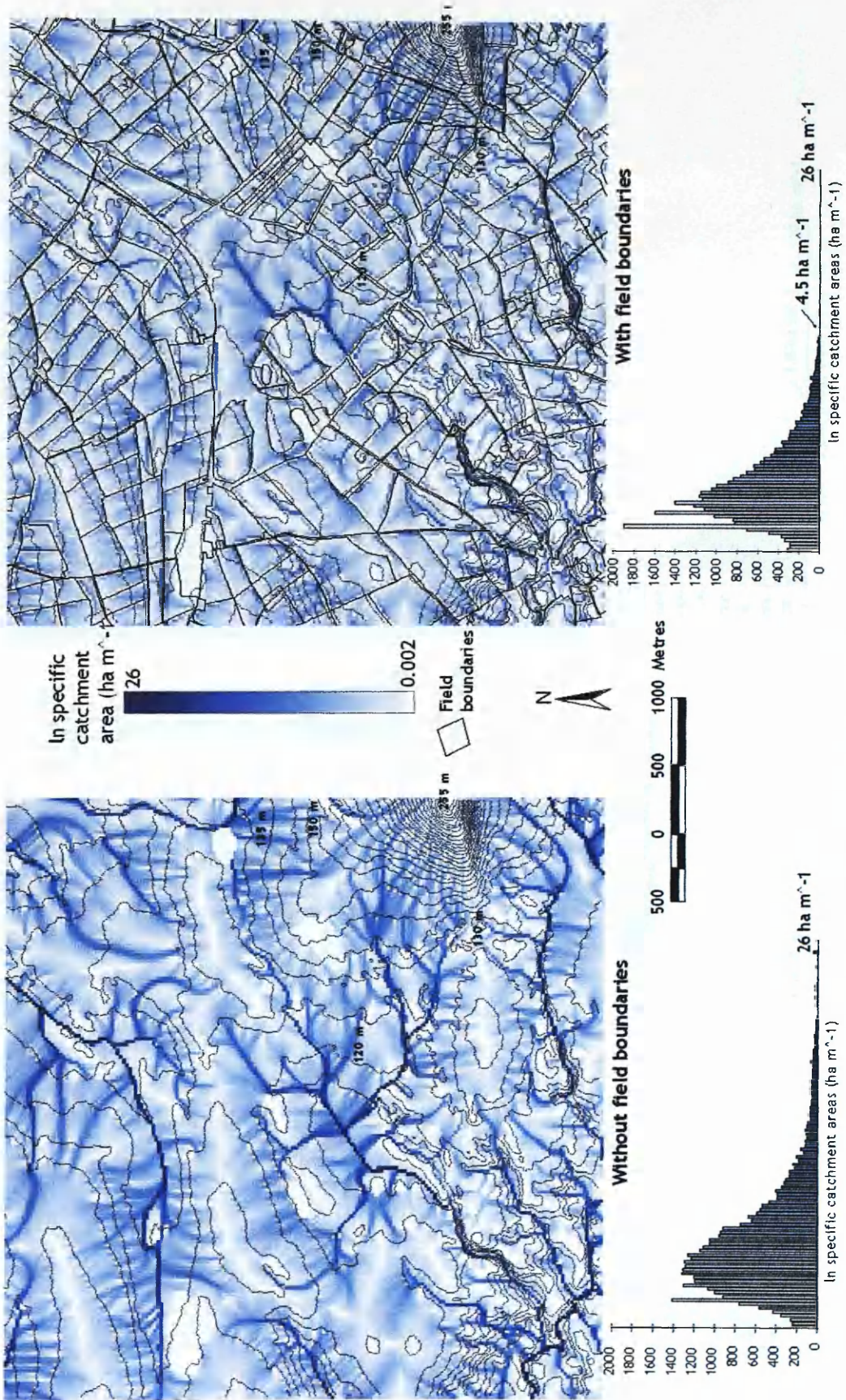


Figure 2.18. Patterns and frequency distributions of contributing areas calculated with and without the effect of field boundaries in the NO13SE OS grid quadrant. 106

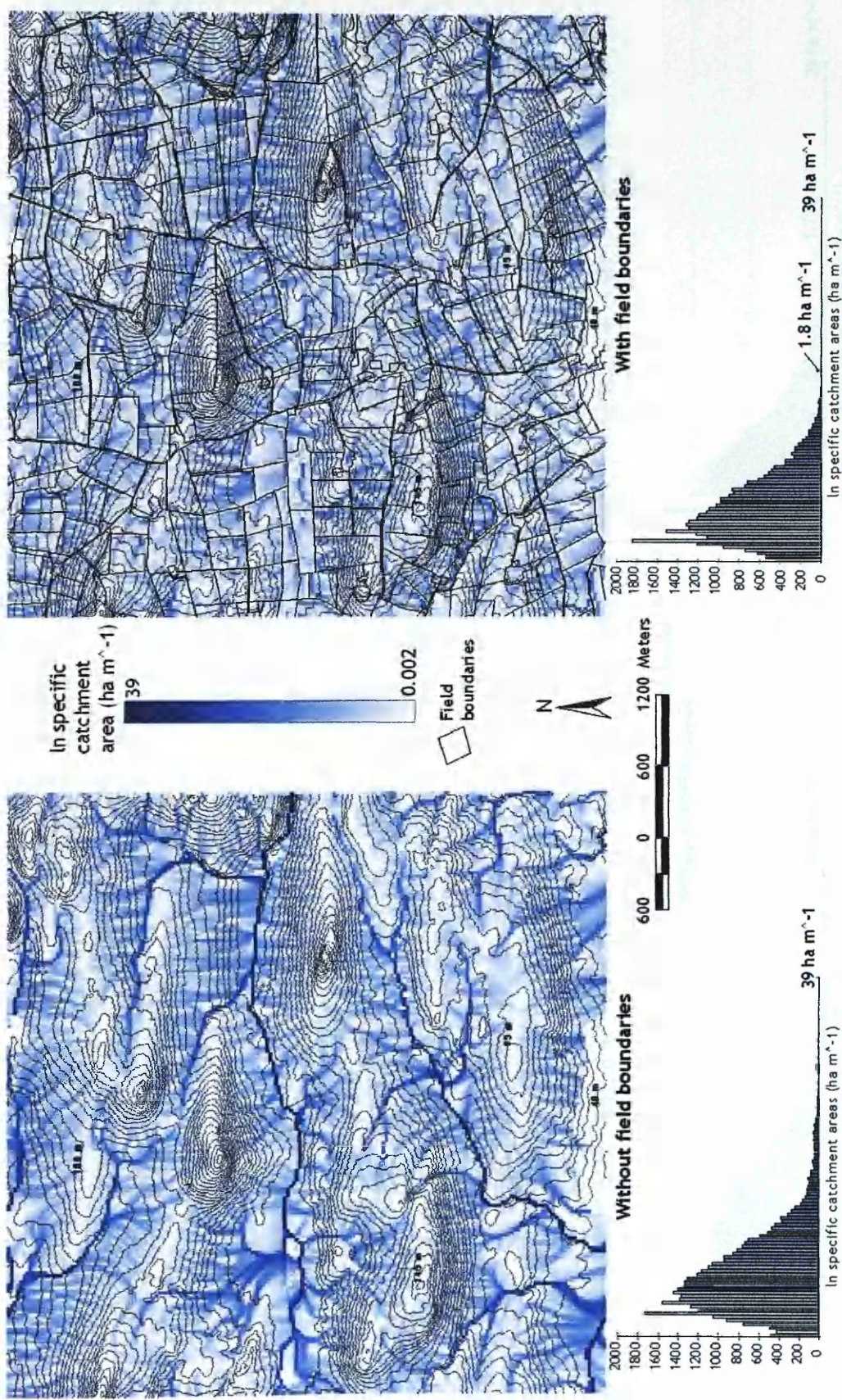


Figure 2.19. Patterns and frequency distributions of contributing areas calculated with and without the effect of field boundaries in the NO31NE OS grid quadrant.

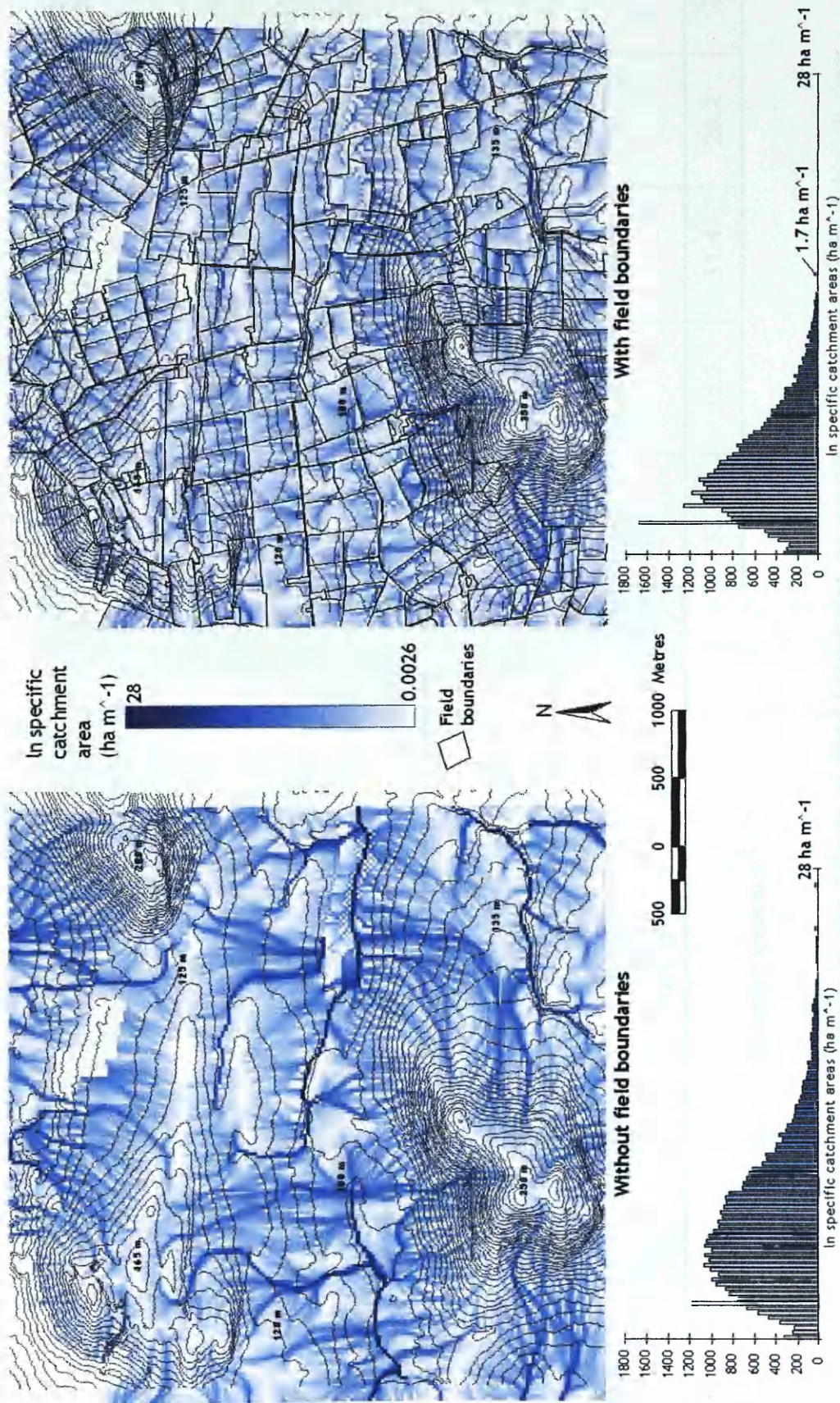


Figure 2.20. Patterns and frequency distributions of contributing areas calculated with and without the effect of field boundaries in the NO4NE OS grid quadrant. 108

Clip Area	No field boundaries				With field boundaries					
	Max	Min	Mean	Stdev	Max	Min	Mean	Stdev		
Forfar	235868.8	25	1870.8	12686.78	10896.82	25	248.6	534.91		
	264179.4	25	1941.5	14095.3	14989.99	25	251.3	899.29		
	388021.1	25	2184.5	17974.53	17661.02	25	286.6	678.91		
	284117.8	25	1330.4	9475.37	9775	25	289	670.16		
NO13SE	65.5	51.2	34	21.9	6.7	59.9	52.7	34.8	22	7.1
	50.3	41.3	24.5	15.4	8.1	55.1	47.9	32.4	21.4	7.4
	57.7	48.3	31.4	20.2	7.3					
NO31NE	65.5	51.2	34	21.9	6.7	59.9	52.7	34.8	22	7.1
	50.3	41.3	24.5	15.4	8.1	55.1	47.9	32.4	21.4	7.4
	57.7	48.3	31.4	20.2	7.3					
NO44NE	65.5	51.2	34	21.9	6.7	59.9	52.7	34.8	22	7.1
	50.3	41.3	24.5	15.4	8.1	55.1	47.9	32.4	21.4	7.4
	57.7	48.3	31.4	20.2	7.3					

Attenuating effect of field boundaries

Specific catchment areas in  $m^2 m^{-1}$

Table 2.2. Summary of the effects of field boundaries on specific catchment areas within all four clip study areas.

Clip Area		N	N FOR TEST	EST. MEDIAN	95% CI FOR DIFFERENCE	WILCOXAN STATISTIC	P
<b>Forfar</b>	Difference	7566	6743	96.16	87.5 - 105.5	1.83E+07	0.000
<b>NO13SE</b>	Difference	40023	33343	52.48	50.60 - 54.36	4.34E+08	0.000
<b>NO31NE</b>	Difference	39600	33089	18.46	17.27 - 19.63	3.62E+08	0.000
<b>NO44NE</b>	Difference	39687	31610	57.32	54.72 - 59.90	3.75E+08	0.000

Specific catchment areas in  $m^{-2} m^{-1}$

NB: for all of the above null hypothesis =  $n_1 = n_2$ , alternative hypothesis = sca with field boundaries < sca with field boundaries, i.e. median difference between pairs > 0.

Table 2.3. Results of the nonparametric Wilcoxon signed rank test to investigate the effects of field boundaries on specific catchment areas within all 4 clip study areas.

#### 2.2.4.2 Erosion/deposition magnitude and pattern

Outputs from the water erosion model using parameters taken from the literature are presented in Figure 2.24 to Figure 2.27. The large polygonal areas of white in the clip areas are zones of 'no data', which represent non-agricultural land classes such as lochs, roads, urban areas, sea etc. Streams have also been masked out of the model to avoid riverine erosion and depositional systems being modelled.

Common features of the model without field boundaries are extensive areas of deposition in flat valley bottoms. One particular 1.4 ha field in the Forfar analysis clip has c. 60% of its area as simulated deposition. In the NO44NE clip a 5.3 ha field (Figure 2.22) at the foot of a 10-18% 500+ m slope is predicted to be having c. 50% of its area as deposition. Such large accumulation features are rarely observed in agricultural landscapes in the UK, however this should not necessarily cast doubt on the processes operating in the model, at least when not considering field boundaries. By comparing the respective figures for each clip the influence of drainage patterns is clearly underpinning the main pattern and magnitude of erosion. On this basis therefore, it may be possible to use such a map to predict in a very approximate manner where gully and rill erosion is *likely* to take place. Predicting where sediment will deposit is more complex and this model attempts this by addressing changes in topographic form. When not considering field boundaries

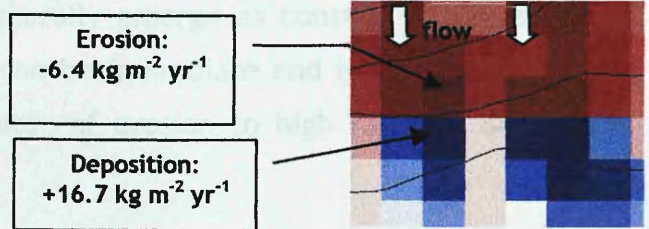


Figure 2.21. The transition from erosion to a depositional system as simulated by the model.

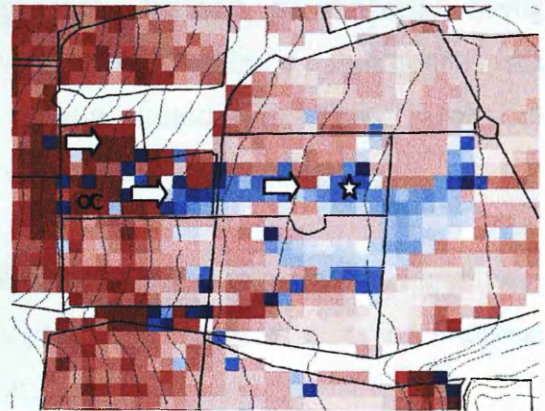


Figure 2.22. Unrealistically large zones of deposition when failing to consider field boundaries.

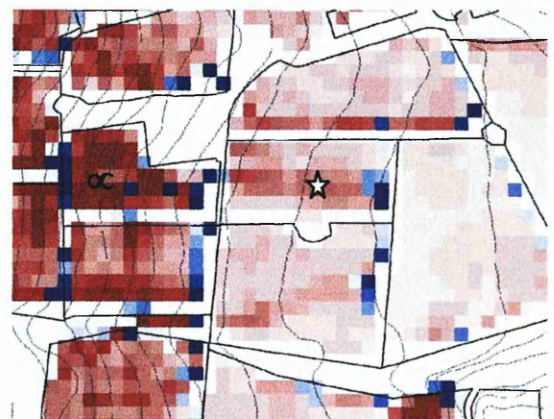


Figure 2.23. More realistic patterns generated by including field boundaries in the model.



depositional areas (blue shades) generally emerge as concavity increases. The change from erosion to deposition can be immediate and in many cases in the form of a large swing from high rates of erosion to high rates of deposition. Figure 2.21 is an example of this.

Figure 2.22 shows the same area this time after incorporation of field boundaries. Erosion on the steep backslope sections (marked  $\infty$ ) is similar both with and without field boundaries and is likely due to the influence of the slope angle despite field boundaries being present. Instead of material being deposited along the length of the gentle swale as marked by  $\star$ , sediment is left in small packets on the upslope side of the boundaries. These areas of accumulation are spatially much smaller and more probable in fields.

The performance of field boundaries in terms of influencing erosion budgets was investigated statistically using Wilcoxon signed rank tests due its non-normal distribution. Table 2.5 summarises the results.

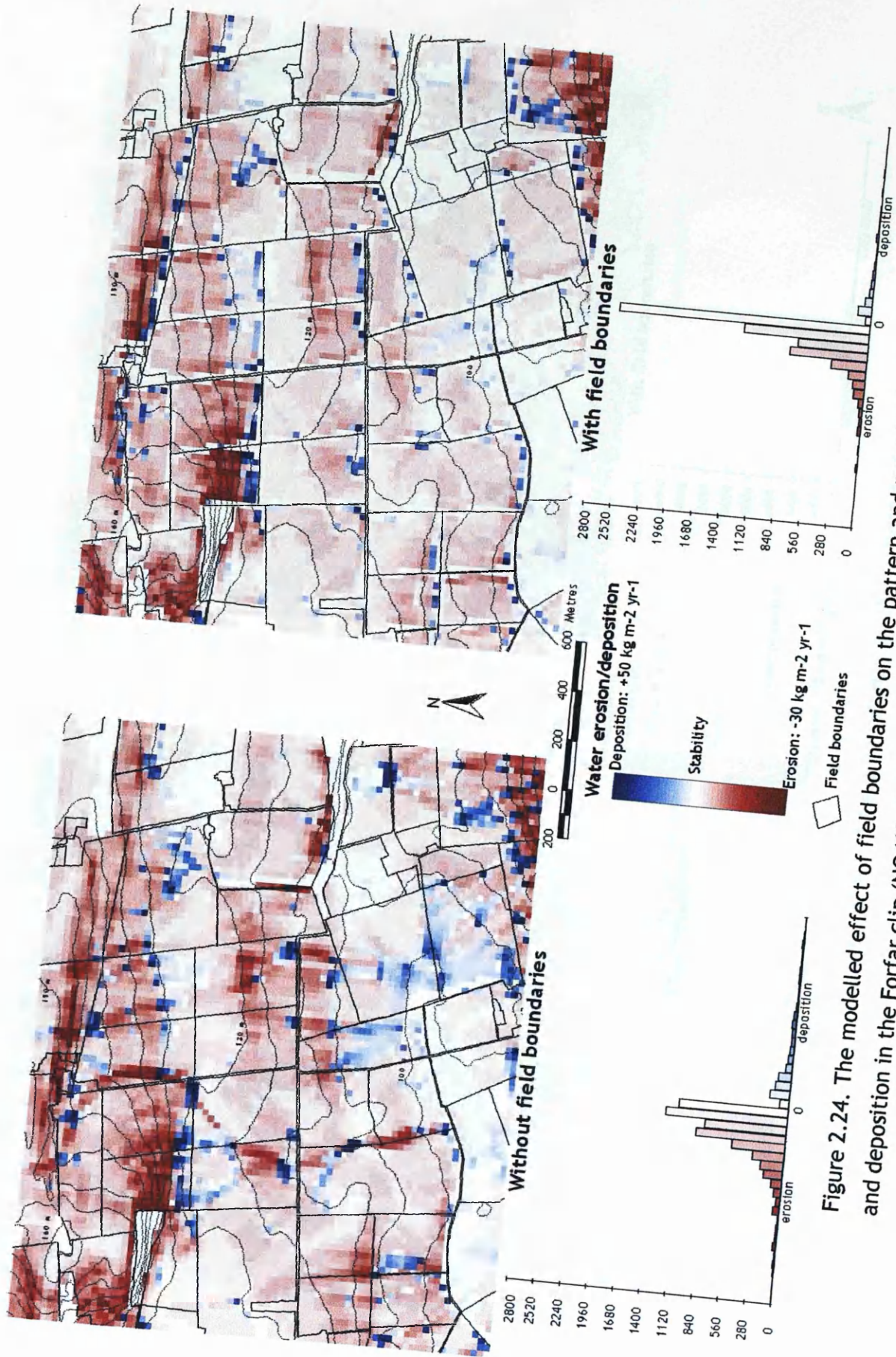


Figure 2.24. The modelled effect of field boundaries on the pattern and magnitude of erosion and deposition in the Forfar clip (NO463 477).

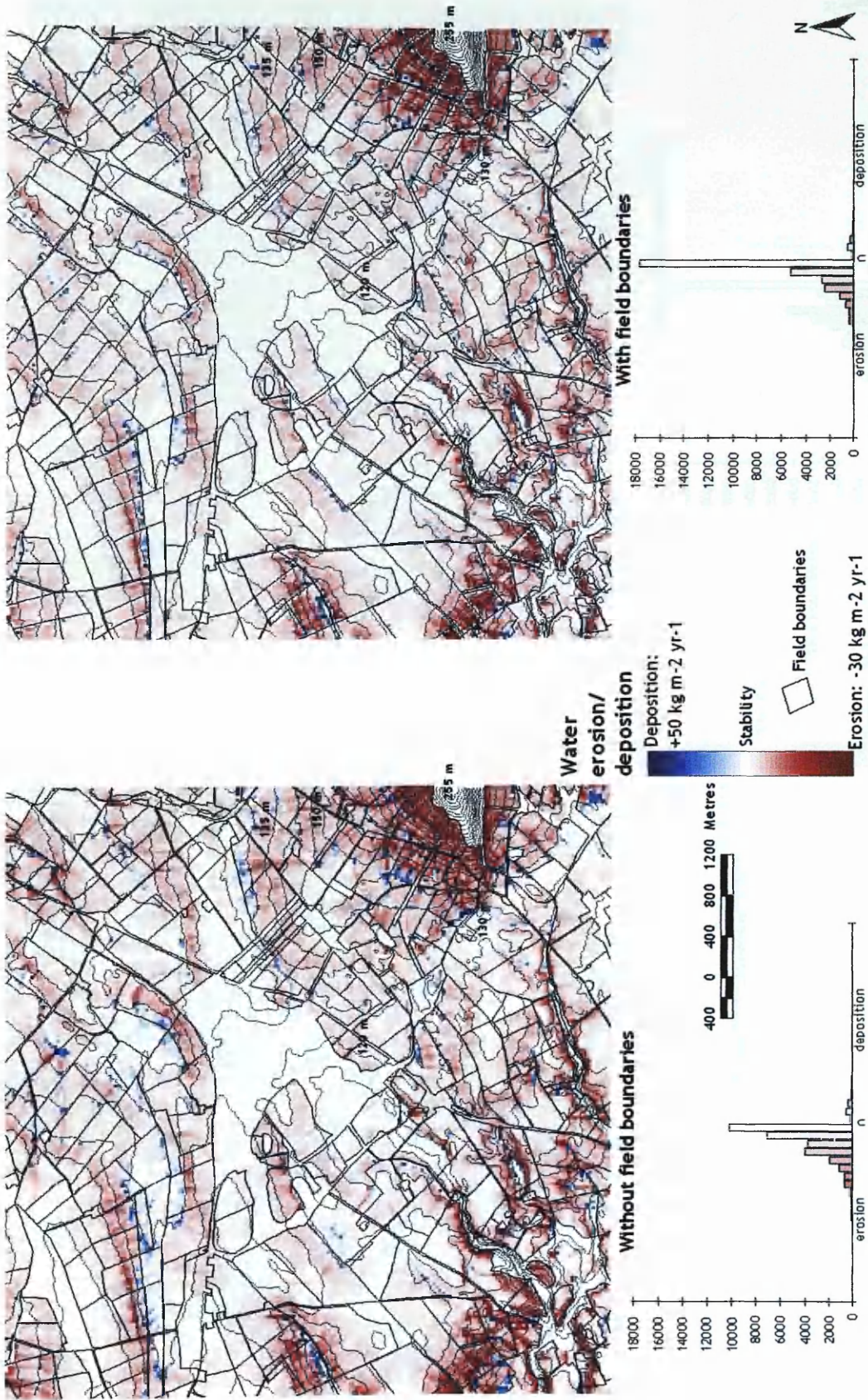


Figure 2.25. The modelled effect of field boundaries on the pattern and magnitude of erosion and deposition across the NO13 southeast OS grid quadrant. 114

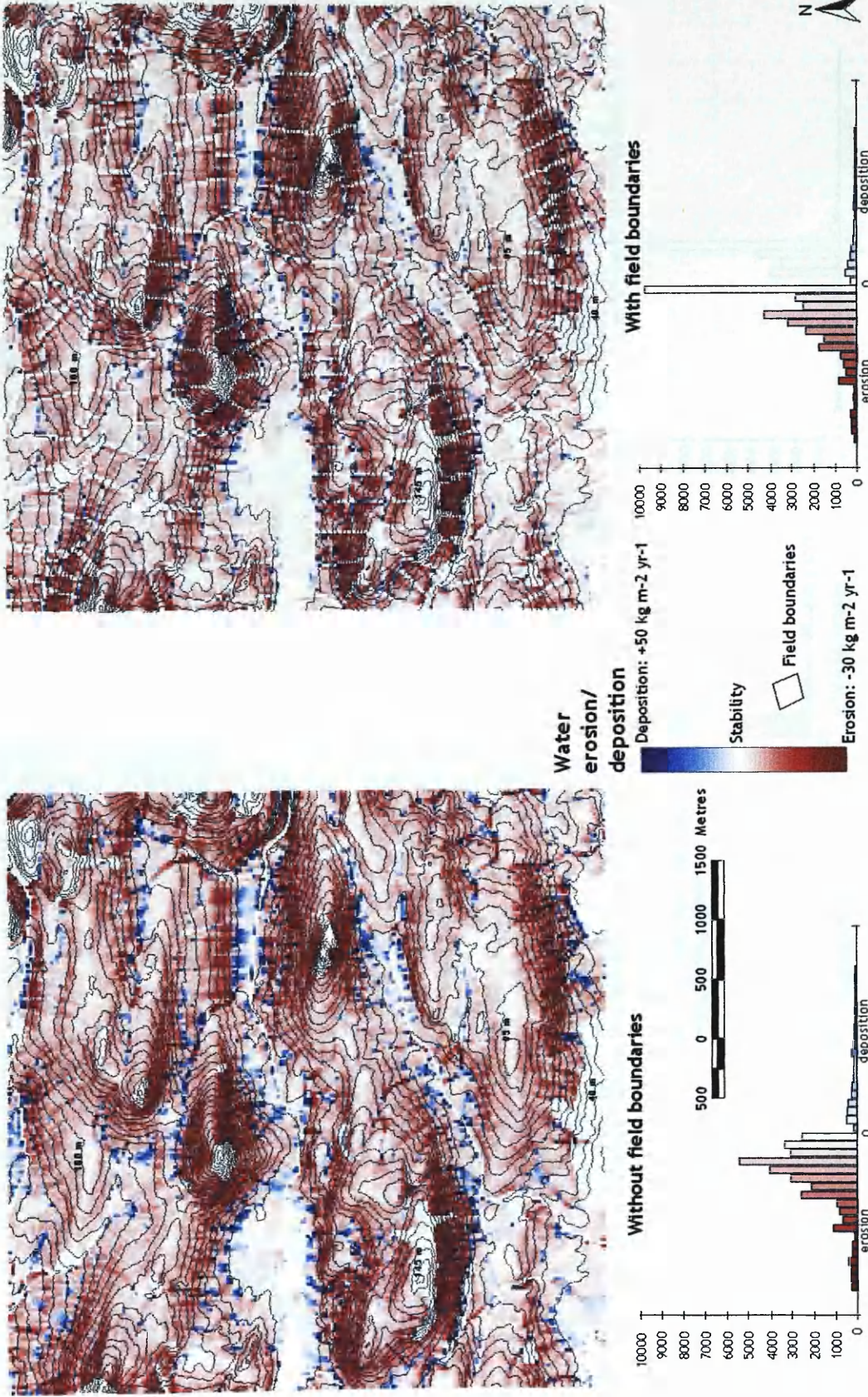


Figure 2.26. The modelled effect of field boundaries on the pattern and magnitude of erosion and deposition across the NO31 northeast OS grid quadrant.

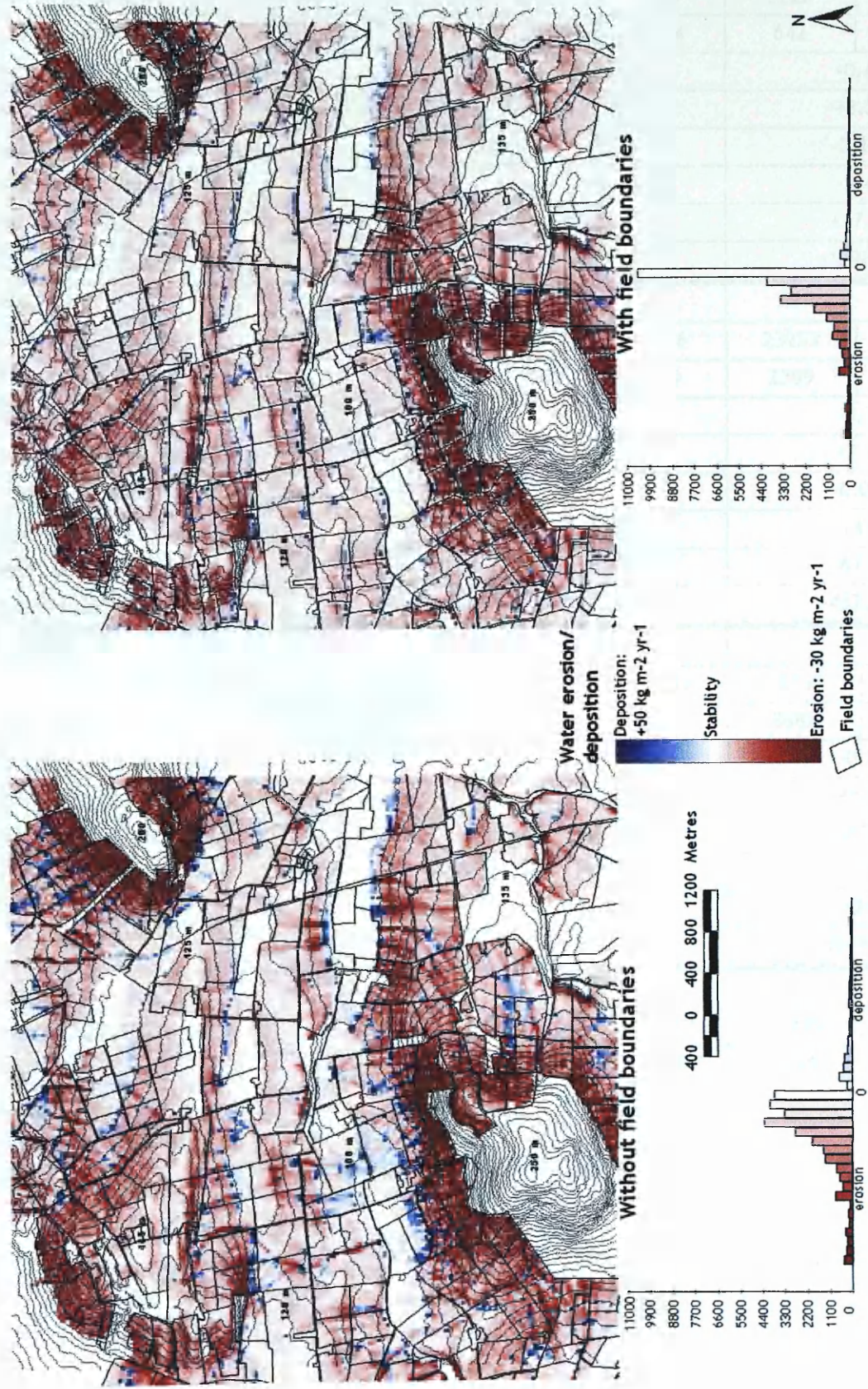


Figure 2.27. The modelled effect of field boundaries on the pattern and magnitude of erosion and deposition across the NO44 northeast OS grid quadrant. 116

FORFAR	Without FBs	Area (ha)	With FBs	Area (ha)
# of eroding cells	6082	380	5222	326
# of depositing cells	1127	70.4	642	40
Mean erosion rate (kg m <sup>-2</sup> yr <sup>-1</sup> )	-0.5		-0.4	
Mean deposition rate (kg m <sup>-2</sup> yr <sup>-1</sup> )	+3.4		+3.3	
Median erosion rate (kg m <sup>-2</sup> yr <sup>-1</sup> )	-0.2		-0.12	
Max erosion rate (kg m <sup>-2</sup> yr <sup>-1</sup> )	-15.6		-9.4	
Max deposition rate (kg m <sup>-2</sup> yr <sup>-1</sup> )	+60.7		+47.4	
Total detachment (t yr <sup>-1</sup> )	-1877.6		-1298.3	
<b>NO13NE</b>				
# of eroding cells	30989	1936	23253	1453
# of depositing cells	2877	179	2399	149
Mean erosion rate (kg m <sup>-2</sup> yr <sup>-1</sup> )	-0.4		-0.3	
Mean deposition rate (kg m <sup>-2</sup> yr <sup>-1</sup> )	+3.2		+2.9	
Median erosion rate (kg m <sup>-2</sup> yr <sup>-1</sup> )	-0.15		-0.07	
Max erosion rate (kg m <sup>-2</sup> yr <sup>-1</sup> )	-19.3		-14.0	
Max deposition rate (kg m <sup>-2</sup> yr <sup>-1</sup> )	+94.7		-67.0	
Total detachment (t yr <sup>-1</sup> )	-7222.6		-4522.9	
<b>NO31SE</b>				
# of eroding cells	32052	2003	25360	1585
# of depositing cells	4338	271	3882	242
Mean erosion rate (kg m <sup>-2</sup> yr <sup>-1</sup> )	-0.9		-0.8	
Mean deposition rate (kg m <sup>-2</sup> yr <sup>-1</sup> )	+5.6		+5.1	
Median erosion rate (kg m <sup>-2</sup> yr <sup>-1</sup> )	-0.48		-0.27	
Max erosion rate (kg m <sup>-2</sup> yr <sup>-1</sup> )	-19.5		-13	
Max deposition rate (kg m <sup>-2</sup> yr <sup>-1</sup> )	+88.8		+76	
Total detachment (t yr <sup>-1</sup> )	-17921.3		-13051.5	
<b>NO44NE</b>				
# of eroding cells	27531	1720	22125	1382
# of depositing cells	3765	235	2726	170
Mean erosion rate (kg m <sup>-2</sup> yr <sup>-1</sup> )	-0.8		-0.7	
Mean deposition rate (kg m <sup>-2</sup> yr <sup>-1</sup> )	+4.9		+5.3	
Median erosion rate (kg m <sup>-2</sup> yr <sup>-1</sup> )	-0.33		-0.16	
Max erosion rate (kg m <sup>-2</sup> yr <sup>-1</sup> )	-32.5		-24.3	
Max deposition rate (kg m <sup>-2</sup> yr <sup>-1</sup> )	+117.9		+127.0	
Total detachment (t yr <sup>-1</sup> )	-14415.3		-9899	

FBs = field boundaries

Table 2.4. Descriptive statistics demonstrating the effect of field boundaries on erosion/deposition in each clip area.

Clip Area		N	N for test	Est. median	95% CI for difference	Wilcoxon statistic	P
<b>Forfar</b>	Difference	7241	5821	-0.04	-0.0450 - -0.0350	5.95E+06	0.000
<b>NO13SE</b>	Difference	34298	26450	-0.045	-0.0450 - -0.0450	8.72E+07	0.000
<b>NO31NE</b>	Difference	36532	29772	-0.07	-0.0750 - -0.0650	1.50E+08	0.000
<b>NO44NE</b>	Difference	31688	26323	-0.08	-0.0850 - -0.0750	1.09E+08	0.000

NB: for all of the above null hypothesis =  $n_1 = n_2$ , alternative hypothesis = erosion with field boundaries < erosion with field boundaries, i.e. median difference between samples < 0.

Table 2.5. Results of the nonparametric Wilcoxon signed rank test to investigate the effects of field boundaries on erosion/deposition within all 4 clip areas.

Clip Area	Attenuating effect of field boundaries	% cells with eros. reduction	% cells with eros. reduction >10%	% cells with eros. reduction >50%	% cells with eros. reduction >75%	%cells with eros. increase.
<b>Forfar</b>		55.3	49.1	28.3	22.2	19.9
<b>NO13SE</b>		57.5	52	31.7	26.8	14.3
<b>NO31NE</b>		50.2	41.6	27	23.7	23.9
<b>NO44NE</b>		56.2	49.3	30.9	24.6	20.5
		<b>54.8</b>	<b>48.03</b>	<b>29.6</b>	<b>24.51</b>	<b>19.65</b>

Table 2.6. Summary of how erosion decreases and increases when field boundaries are integrated into the water erosion model.

The statistical test confirms that field boundaries similarly ( $p < 0.05$  in all cases) reduce erosion magnitudes. The 1-sample Wilcoxon test used with an alternative hypothesis (erosion without FBs  $>$  erosion with FBs) recognises a shift from erosion to deposition as being a reduction in erosion in addition to a simple attenuation of erosion. Imagining this within a field context, an eroding cell may be forced into deposition due to the presence of a boundary feature, therefore potentially eliminating further downslope erosion. Many of the following trends noticed in the sca data are present within the erosion data:

1. The attenuating influence of field boundaries on erosion is statistically significant in all clip areas.
2. Field boundaries reduce the standard deviation of erosion/deposition model outputs, hence creating a tighter and sharper frequency distribution peak. High tail values of erosion are removed from the distribution.
3. Erosion rates may also increase in response to modelled field boundaries. On average across the four clip areas almost 20% of cells experienced an increase in erosion rate.



2.2.4.2.1 The effect of field boundaries on erosion/deposition at the four field sites

	FBs	Mean erosion (kg m <sup>-2</sup> yr <sup>-1</sup> )	Median erosion (kg m <sup>-2</sup> yr <sup>-1</sup> )	Max erosion (kg m <sup>-2</sup> yr <sup>-1</sup> )	Max deposition (kg m <sup>-2</sup> yr <sup>-1</sup> )	# erod. cells	# dep. cells
<b>Loanleven</b>	x	-0.0288	-0.06	-0.63	+1.99	95	20
	✓	-0.0048	-0.05	-0.80	+1.71	90	15
<b>Blairhall</b>	x	-0.0057	0	-0.31	+0.34	308	46
	✓	-0.0096	0	-0.44	+0.1	283	31
<b>Leadketty</b>	x	-0.0560	-0.05	-2.74	+9.26	321	25
	✓	-0.0285	-0.04	-0.97	+3.56	269	39
<b>Littlelour</b>	x	-0.1011	-0.06	-0.45	0	183	0
	✓	-0.0857	-0.04	-0.63	+3.47	163	2

FBs = field boundaries  
 ✓ = present  
 x = not present

Table 2.7. Descriptive statistics on the effect of field boundaries at all four field sites.

Results from the four clips (Table 2.4) show a decrease in both mean and median erosion rates after integrating field boundaries into the water erosion model. Median erosion rates reduced by 40% in the Forfar clip, 53% in NO13SE, 43% in NO31NE and 51% in NO44NE. This trend is also evident in data taken from the four field sites, with the exception of Blairhall. Reductions in median erosion rates of 16% at Loanleven, 20% at Leadketty, and 33% at Littlelour were observed as a result of parcel boundaries. Furthermore, the data revealed reductions in eroding area of 5% at Loanleven, 8% at Leadketty and 11% at Littlelour. Statistically, however, the difference in median erosion rates (Wilcoxon signed rank test) with and without field boundaries was found to be insignificant at Loanleven (n =124, p = 0.907), Blairhall (n = 392, p = 0.996), and Littlelour (n = 183, p = 0.706). The attenuating effect of field boundaries at Leadketty was found to be significant (n = 351, p = 0.008). Data from the four clip areas revealed that erosion rates increased on average by almost 20% as a result of field boundary integration. This has been caused by the increases in sca values discussed on page 103. Although the number of eroding cells at each field site decreased due to field boundaries, the maximum rate of erosion increased by an average of 36%. The maximum erosion rate at Leadketty, however, decreased by

65%. Extents and rates of deposition have also been effected by field boundaries. The number of depositing cells with field boundaries present decreased by 25% at Loanleven, 33% at Blairhall and increased by 36% at Leadketty and 200% at Littlelour. With the exception of Littlelour, maximum rates of deposition reduced when field boundaries were modelled. In summary field boundaries have reduced the areal extent of erosion across all fields, yet locally have increased loss rates. Although statistically not significant, median soil erosion rates have decreased. Deposition appeared to be affected in a more complex manner and appeared to be linked with local topographic and hydrological conditions at each site.

Upon examining the summary statistical data closer, the statistically significant results produced by the tests (Table 2.4, Table 2.5, and Table 2.7) need to be evaluated in a practical sense. 95% confidence intervals for the differences between erosion/deposition with and without field boundaries for all four clip areas range from  $-0.085$  to  $-0.035 \text{ kg m}^{-2} \text{ yr}^{-1}$ . Is this range of values significant or noticeable to the farmer or archaeologist? Therefore the statistical results should be viewed with some caution. It is more suitable to evaluate the effectiveness of field boundaries in reducing erosion in a localised manner merely from model output maps rather than interpreting statistical trends from across a large dataset. Table 2.4 and Table 2.7 summarize the descriptive statistics with and without modelled field boundaries. Assuming the predictions are representative of observed erosion and deposition, the attenuating properties of the field boundaries are extremely consistent across all four clip areas. Mean erosion rates have been reduced by  $0.1 \text{ kg m}^{-2} \text{ yr}^{-1}$  ( $1 \text{ t ha}^{-1} \text{ yr}^{-1}$ ) in all cases equivalent to reductions of 20% (Forfar), 25% (NO13SE), 11% (NO31NE), and 12.5% (NO44NE). More importantly maximum erosion values were reduced by considerably more. On the other hand linear features have the tendency to exacerbate the magnitude of concentrated flow in very localised areas. The reduction in mean erosion rates actually may mask damaging increased rates of erosion. Table 2.6 presents data supporting this parallel increase alongside the general background attenuation of erosion.

### 2.2.4.3 The field boundary 'burst' effect

Whilst quality controlling the outputs from the field boundary model a burst effect was evident at irregular positions. Accumulation of flow appeared to have jumped across the field boundary and continued on its downslope path. Figure 2.28 illustrates this. Elevation data was extracted from the DTM before and after field boundaries had been integrated.

Figure 2.29 displays the two profiles. From Figure 2.29 it is clear that even once the 1.5m field boundary had been added to the DTM, the slope is still sufficiently steep enough upslope of the boundary to "trick" the flow routing algorithm.

The algorithm searches for the steepest downslope direction (0-360°) and then distributes flow to the 2 neighbouring cells proportionally. The band of 3 cells in Figure 2.28 centred on the transect line which bisects the boundary are

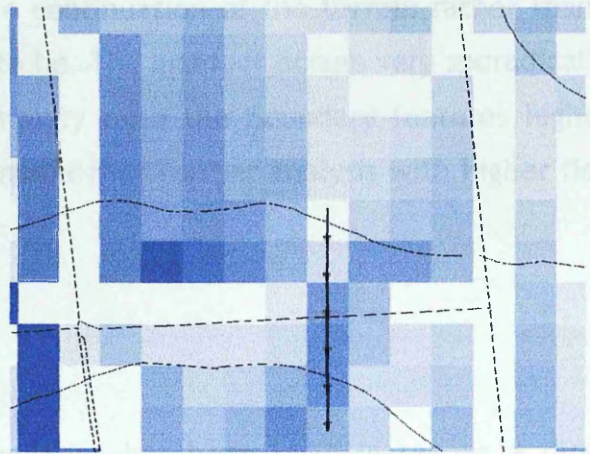


Figure 2.28. Field boundary 'burst' effect where flow crosses the boundary feature. Arrows indicate location of transect taken from Figure 2.29

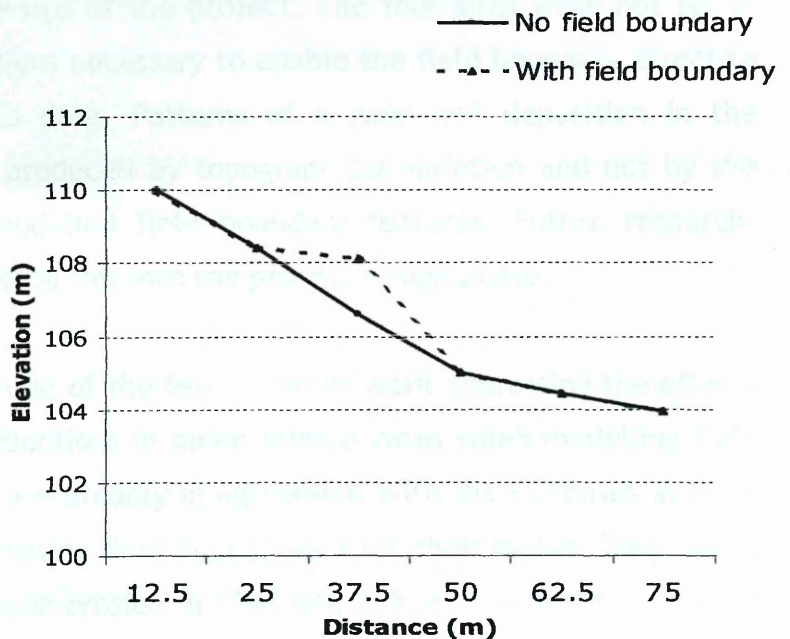


Figure 2.29 Graph showing profile of landscape with and without field boundaries integrated.

then distributes flow to the 2 neighbouring cells proportionally. The band of 3 cells in Figure 2.28 centred on the transect line which bisects the boundary are

therefore the lowest, despite having been raised by 1.5m. The algorithm assumes the 'new' boundary is just a continuation of the terrain rather than a physical obstacle as it was designed to be. The artefact occurs very sporadically. The solution to the problem is to simply raise the boundary features higher, ideally above 3m. Time constraints meant that further analysis with higher field boundaries was not possible.

## 2.3 Conclusions

The importance of linear field boundaries has been investigated as a direct result of frequent field observations and a realisation that the topic has in general lacked attention. In a way it has been a mini-project in itself and certainly demands closer study. This work was set at a very basic level in terms of its assumptions and techniques, yet results have been convincing and have provided a basis upon which further work can build. The biggest criticism is with the overall experimental design of the project. The four sites were not set in suitable hydrological conditions necessary to enable the field boundary effect to be tested against the  $^{137}\text{Cs}$  data. Patterns of erosion and deposition in the individual sites have been produced by topographical variation and not by the presence or absence of modelled field boundary features. Future research, therefore, needs to incorporate this into the project design phase.

Van Oost, (2000) published one of the few pieces of work addressing the effects of field boundaries. The reductions in mean erosion rates when modelling field boundaries generated here are broadly in agreement with the increases in rates in 3 catchments when eliminating field boundaries from their model. They noted a 58% overestimation of water erosion in 1947 and 20% in 1990 when excluding field boundaries from their model. This work proposes present day reductions of 20% (Forfar), 25% (NO13NE), 11% (NO31NE), and 12.5% (NO44SE) for the 4 clip areas, present day.

At the field sites the effects of field boundaries on the general optimised water erosion model were statistically insignificant. The small sample size was the cause as larger samples (four clip areas) produced highly significant results. The statistics further suggested that the differences in erosion rates before and after

field boundaries are of little practical relevance. The use of statistical tests should be cautioned when evaluating the overall effectiveness or boundaries. Field boundaries have a very localised impact on erosion/deposition patterns and rates and statistical analyses will tend to mask the importance of a field boundary at a particular location. For example, the presence of a dry-stone wall boundary along a stream at the slope base would be invaluable in halting the loss of sediment into the stream. The effectiveness of that boundary and enormous benefit brought to the field, farmer and water quality managers needs to be evaluated on a local and individual basis.

The disadvantage of field boundaries has also been demonstrated through the potential local increase in specific drainage area. This situation arises when overland flow is channelled and diverted away from natural topographic flow. The connectivity of the parcel boundaries over a large area in addition to topography can play a vital role in determining patterns and magnitudes of erosion/deposition. Increases in local concentrated flow erosion will be likely as a result, yet can be managed.

A further criticism of this modelling exercise is the assumption of impermeable field boundary features. In many situations parcel boundaries in the UK do act as non-porous structures but fences, hedges and gates do offer runoff exit or entry points. The location of these entry/exit points can have dramatic effects on the downslope erosion/deposition conditions. At the catchment scale gate positions can be easily mapped but the porosity is more complex. Research is needed on the trapping efficiency of the various types of agricultural parcel boundary.

Field boundaries have been accepted as vital within the modelling process if correct spatial patterns are to be predicted. Along side the changes in patterns, this exercise has reported that wide oscillations in erosion magnitude also occur particularly in a local sense, some of which may accelerate erosion damage. Data such as this can provide valuable input to archaeologists, conservation managers or farmers who may have accelerated drainage related erosion problems.

The model has further emphasized the strong driving influence of catchment hydrology on the erosion/deposition system and how linear features modify catchment connectivity. Therefore, field boundaries were implemented as a permanent feature of the water erosion model for optimisation in chapter 5.

not at least in terms of coverage of the whole or the  
part of the EU. It is not clear how the model is  
used and the model is not clear how it is used.

The model has approached erosion and sedimentation  
specific to that in this project. At the same time, it is  
not clear how the model is used and the model is  
not clear how the model is used. It is not clear how  
the model is used and the model is not clear how  
the model is used. It is not clear how the model  
is used and the model is not clear how the model  
is used.

- 1. Soil
- 2. Slope
- 3. Soil texture

The model is used to simulate the erosion and  
deposition of soil and sediment. The model is  
used to simulate the erosion and deposition of  
soil and sediment. The model is used to simulate  
the erosion and deposition of soil and sediment.  
The model is used to simulate the erosion and  
deposition of soil and sediment. The model is  
used to simulate the erosion and deposition of  
soil and sediment. The model is used to simulate  
the erosion and deposition of soil and sediment.

## 2.4 Comparison of the water erosion model outputs with the MLURI erosion risk model (Lilly et al., 2002).

Large-scale erosion projects and modelling in Scotland are very few. Work has concentrated on sporadic high magnitude events and consequently there has been a vacuum in the availability of general national erosion risk map. Lilly et al., (2002) of the The Macaulay Land Use Research Institute (MLURI) have modelled “The inherent geomorphological risk of soil erosion by overland flow in Scotland” under contract for Scottish Natural Heritage. It has been an ambitious project at least in terms of coverage as it spans the whole of Scotland. The appearance of the MLURI risk model has coincided with the research completed here and has therefore provided the opportunity for limited comparison of results.

The MLURI risk model has approached erosion risk modelling from a different perspective to that in this project. As the title indicates the MLURI risk model assesses the risk of water erosion assuming a vegetation free landscape. The authors claim it has delivered a baseline estimate of the sensitivity of Scottish soils to water erosion. Model inputs are:

1. Slope.
2. Runoff.
3. Soil texture.

At the model’s foundations lie a series of classifications nested within a set of rules, which ultimately define the risk. For example, erosive power of overland flow is defined as a function of slope and runoff. Slope is categorized (7 classes) and tabulated with the standard percentage runoff (SPR) used as a surrogate for runoff. Mineral and organic soil textures are categorized separately in a similar manner and tabulated with the erosive power deriving a set of 9 classes of erodibility for mineral soils and a set of 8 classes for organic soils. Most relevant to this project is the final risk classification for mineral soils (Table 2.9).

Percentage Runoff	Slope categories (degrees)					
	<2	2-4.9	5-9.9	10-17.9	18-30	>30
<20	a	b	c	d	d	
20-40	b	c	d	e	f	slopes unstable
>40	c	d	e	f	g	unstable

Table 2.8. Formulation of erosive power as a function of slope and SPR (Lilly et al., 2002).

Soil texture class	Erosive power						
	a	b	c	d	e	f	g
Fine	1	2	3	4	5	6	7
Medium	2	Low	4	Moderate	6	High	8
coarse	3	4	5	6	7	8	9

Table 2.9. Final risk classes for mineral soils in the MLURI risk model (Lilly et al., 2002).

The final erosion risk map was generated by integrating the set of rules in Table 2.9 into a GIS as a multiple query of the slope, soil texture and SPR datasets. The model has 9 classes of erosion risk from which non-arable land use classes and field boundary cells have been excluded. This was clipped to the extents of the study area of this project to allow direct comparison of the results of the two models.

The MLURI risk model predicts only erosion risk on a scale of 1 to 9, 9 being the highest risk equivalent to 18-30° slopes, runoff >40% on coarse textured mineral soils. In contrast the water erosion model used in this project produces continuous floating-point values both for erosion (negative) and deposition (positive). To allow direct comparability, the predicted water erosion map was modified by removing all depositing cells and then used as a template to clip the MLURI map further to exactly the same extents. As with previous statistical analyses the northeast quadrant of the NO31 OS grid cell was selected to reduce the volume of data to manageable levels. Model outputs for the full study area are shown in Figure 2.31 and Figure 2.32.



MLURI EROSION RISK CLASS	Count	Area (m <sup>2</sup> )	Mean erosion (kg m <sup>-2</sup> )						Median rank
			Min	Max	Range	Mean	Stdev	Sum	
3	2740	1712500	-4.78	-0.0004	4.78	-0.12	0.20	-336.64	20292
4	11782	7363750	-5.13	-0.0002	5.13	-0.21	0.27	-2503.15	15323
5	8818	5511250	-7.19	0	7.199	-0.49	0.55	-4393.28	8721
6	2290	1431250	-5.93	-0.0009	5.93	-0.95	0.816	-2190.29	3630
7	59	36875	-2.21	-0.0014	2.21	-0.58	0.61	-34.44	10133

Table 2.10. Descriptive data on erosion rates within the MLURI erosion risk classes.

The water erosion data was non-normally distributed, therefore the Kruskal-Wallis test was applied to investigate whether the median predicted erosion rate within each MLURI risk class was statistically different. In other words the test examined whether the increase in MLURI erosion risk class corresponds with increases in modelled erosion rates. Differences were found in the erosion rate medians within each MLURI class in addition to being highly significant ( $H = 5945.31$ ;  $DF = 4$ ;  $n = 25689$ ;  $P = 0.000$ ). There are, however, problems with the correspondence between the two models since the highest modelled erosion rate is contained within class 5 not 7 as would be expected. More importantly, the ranges of modelled rates within each class are very similar and therefore suggest overlap. This is, of course, inevitable but the broad agreement between the two models is present.

The coefficient of explanation when predicting erosion rate from MLURI risk class was very poor ( $r^2 = 0.19$ ,  $n = 25689$ ;  $p = 0.000$ ) suggesting that the relationship is not linear. It is acknowledged that from a pure statistical standpoint the regression model should not have strictly been applied using ordinal data (MLURI model classes), however it served a broad-brush approach to examining spatial disagreement between the models. Analysis of the spatial distribution of the residuals could not be carried out due to the poor performance of the regression model.

The MLURI approach to erosion risk differs primarily in the way it is built around the slope-based erosive power of runoff. It assumes a greater erosion risk results

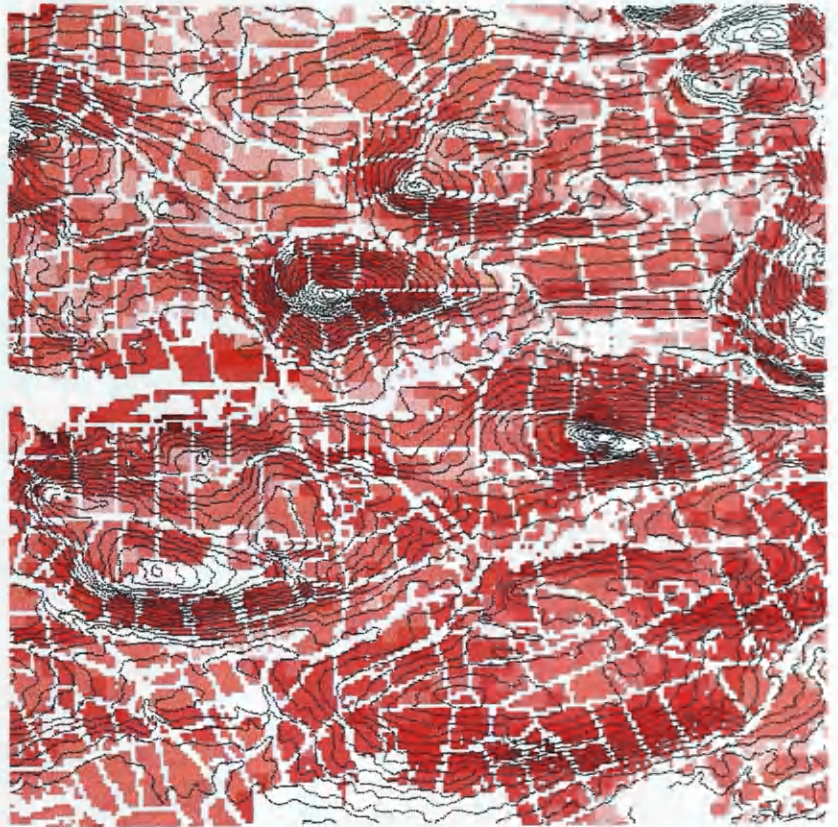
from increases in slope gradient. This may not be the case. Slope is indeed vital for estimating the transporting capacity of overland flow or ability to erode but more importantly the sizes and distribution of drainage catchments controls erosion processes. This variable is absent from the MLURI model and is probably the most important flaw. By not addressing how flow diverges and converges across the landscape, the MLURI model cannot capture low slope/high contributing area zones of the catchment where concentrated erosion is highly probable as being high-risk class. In addition, high slope gradients do not always generate equivalent high rates of erosion since catchment contributing areas here are generally low. The MLURI model has been designed to highlight large areas or regions where risk is high and not at the field scale. Making direct comparisons of observed values at the field scale with such national scales predictions should be resisted and any inferences made based on these should not be taken too seriously. The risk predictions generated by the MLURI model should be considered as what could be *generally expected* in terms of erosion. Focussing on fields or small catchment areas the model becomes more unrepresentative because it has not satisfied the extra modelling detail required for processes at these scales. The lack of catchment contributing areas or even field boundaries are good examples of this.

When comparing the results inside the northeast quadrant of NO31 (Figure 2.30), the MLURI model has no 1 or 2 classes present as well as having very few in class 3 (Table 2.10). The frequency distribution is too sharp to be normally distributed, therefore the model must be over-sensitive to one of the variables which is subsequently causing the class biasing. If the MLURI model had addressed tillage processes in determining risk, then such a clustering within 2 or 3 classes would have been more likely.

At the general visual level and assuming the predictions made here are acceptable, the MLURI erosion risk model has proved capable of identifying erosion susceptible areas. Most noteworthy are the areas running northeast-southwest between Perth and Dundee around the Sidlaw Hills and the large areas of Fife. The water erosion model overall corresponds quite well with these. The biasing effect noted in NO31NE is present throughout the whole study area.

Ultimately it must be remembered that the MLURI model is nation wide and aimed only to assess risk therefore simplification has been necessary.

MLURI  
risk class

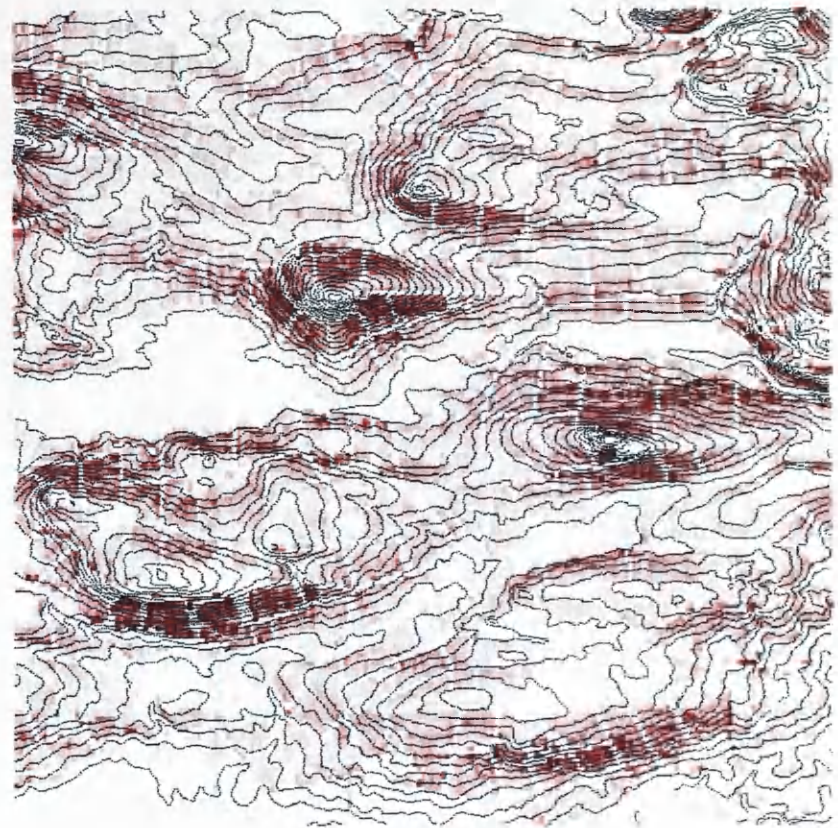


Modelled  
water  
erosion

Stable:  
 $0 \text{ kg m}^{-2} \text{ yr}^{-1}$



Erosion:  
 $-50 \text{ kg m}^{-2} \text{ yr}^{-1}$



0.0 0.2 0.4 0.6 kilometres



Figure 2.30. Comparison of MLURI risk model and modelled soil

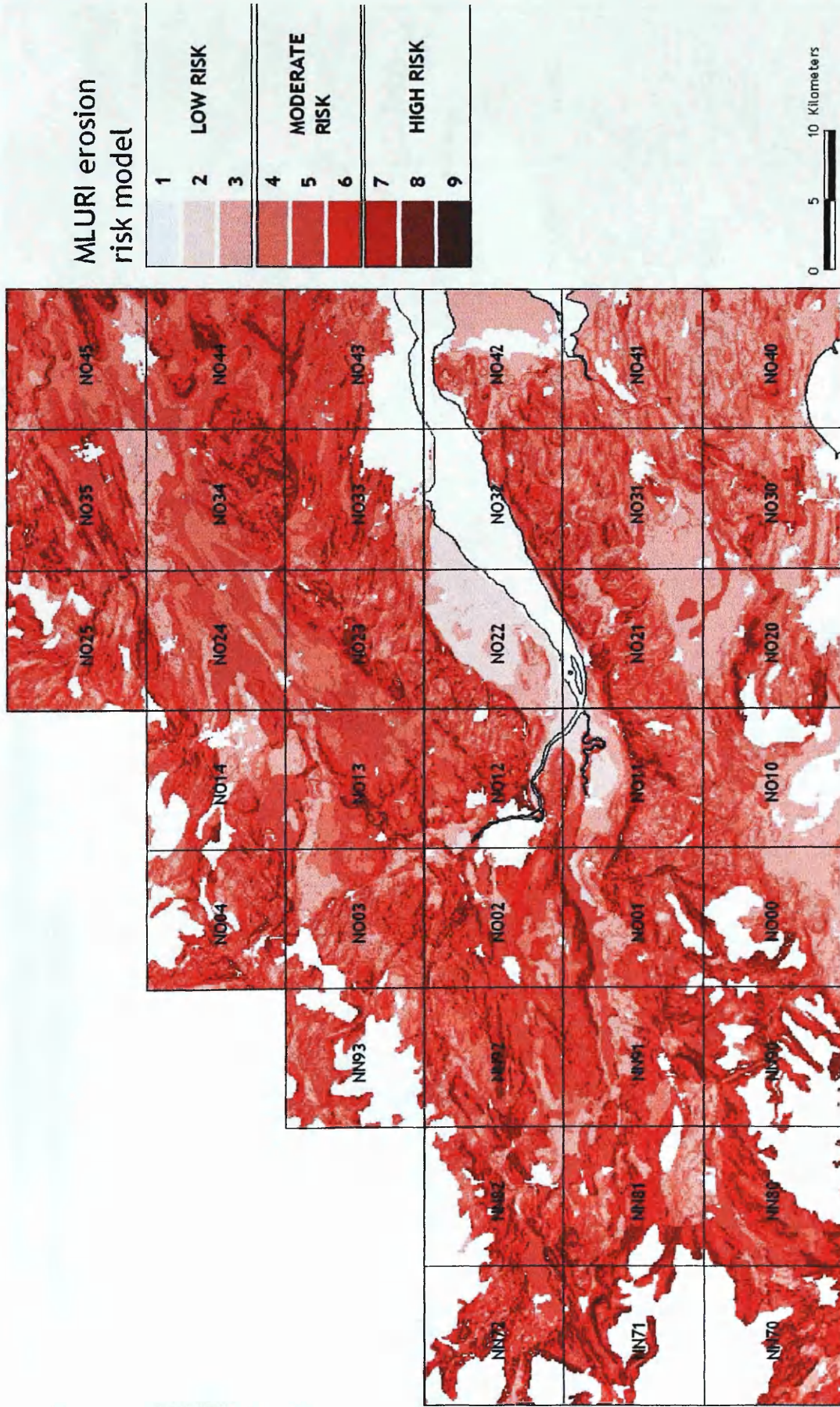
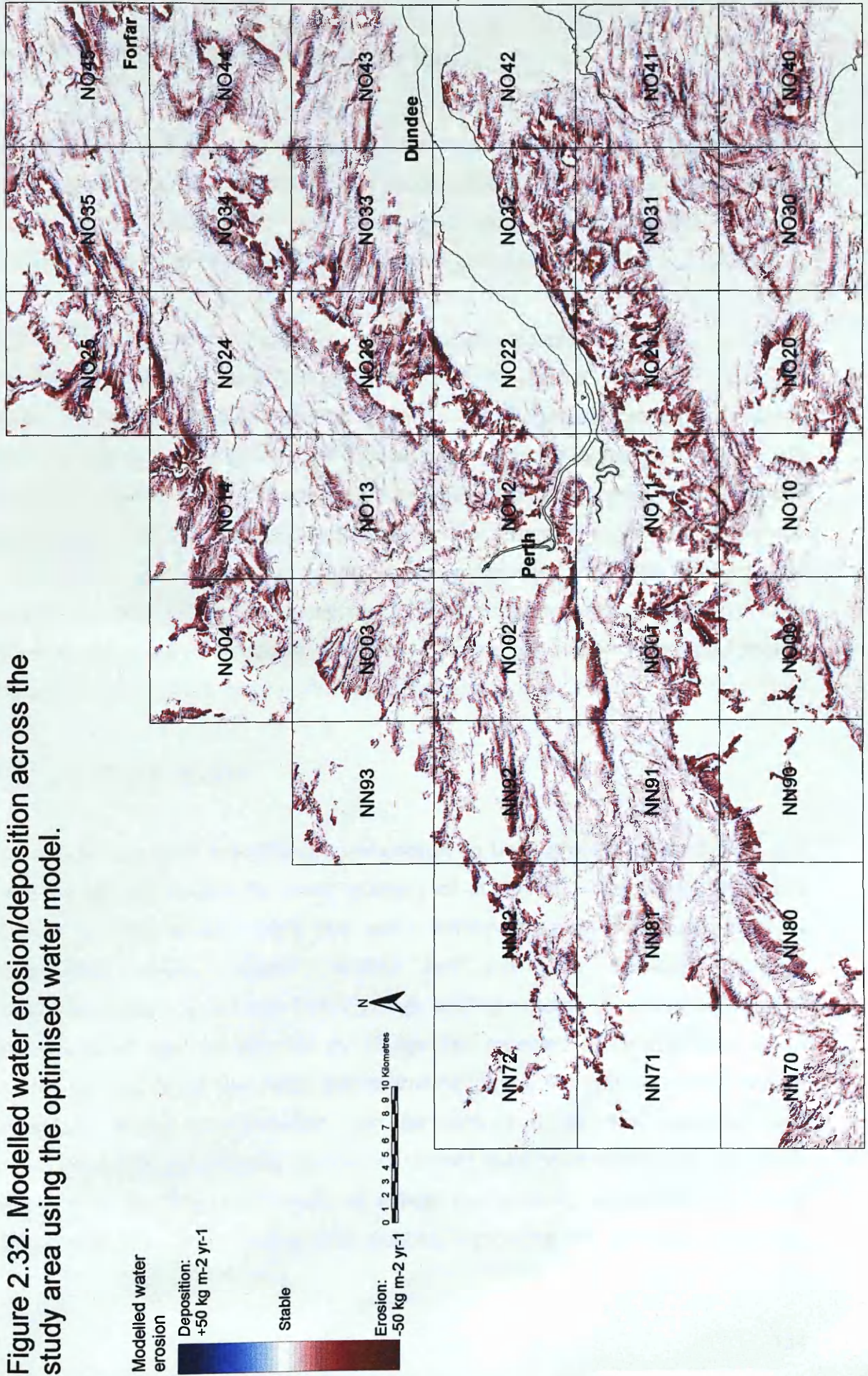


Figure 2.31. Output from the MLURI erosion risk model (Lilly et al., 2002) for the study area.

Figure 2.32. Modelled water erosion/deposition across the study area using the optimised water model.



# Chapter 3.

## 3. Modelling Tillage translocation.

This chapter reviews current literature surrounding tillage translocation, highlights its emerging significance in its contribution to the erosion-deposition budget, and presents the processes involved. Finally, details of pilot experiments in modelling tillage translocation are presented.

For both practical and map/data presentation reasons a small 5 km<sup>2</sup> area immediately west of Methven (NN979 254), Perthshire was selected. This provided a suitable visual resolution when viewing the spatial patterns of erosion and deposition, particularly at the field scale. Initially a test 1-D model was formulated within Excel allowing valuable experimentation with mechanics and parameters. This served as an introduction to the structure and mechanics of the model before augmenting the 2-D algorithm within ARC/INFO. The final steps of calibration and validation necessary in modelling are not included in this chapter; these are covered in chapter 4, where the whole integrated model (tillage and water) has been optimised as one unit.

### 3.1 Literature review

Soil tillage has been traditionally considered to be a process exacerbating soil susceptibility to erosion by water (Govers et al., 1994). This break up of the surface is claimed to reduce the soil's ability to resist raindrop and flow detachment, reduce organic matter and aggregate stability, increase infiltration, and expose low fertility/high acidity subsoil (Kosmas, 2001). The physical movement of material by tillage has received little attention as an erosive process in its own right, but is now becoming a major focus of research attention. Tillage translocation can be described as the transport and displacement of soil incurred by any implement used to condition the soil. Such implements are dragged through or across the topsoil, sometimes at depths >25cm, with the aim of mixing crop stubble, increasing soil aeration, improving

drainage, and preparing a suitable soil structure as a seedbed. The soil is generally subjected to combinations of overturning, breaking or rolling.

An increasing body of literature over the last 10 years has highlighted the issue of soil redistribution due to tillage operations. To date it should certainly be seen as a paradigm shift when attempting to model sediment transport as a whole in agricultural systems. Failing to do so appears to warrant results only akin to that of 'guesstimation'. Prior to this transition in thinking, however, a mere handful of researchers had investigated tillage operations as a potential erosive action. Reasons why early work by Mech and Free (1942) and Papendick and Miller (1977) remained somewhat unnoticed are not difficult to understand. First and foremost, post-war soil degradation research was focussed almost solely on the action of water. The development of the USLE from the 1930s onwards (Wischmeier and Smith, 1978) restricted research for the following five decades to rill and sheet erosion processes. Secondly, tillage processes generate almost no readily recognizable signs or features commonly associated with erosion. The land is perceived almost as being well maintained after fresh ploughing and seedbed preparation. In many cases it may be fair to state that tillage processes may actually shield the farmer's public image in that erosion damage is biannually erased from view by his ploughing. Despite this evidence of tillage operations, albeit subtle, can be readily observed in tilled fields particularly over a long-term period by simple topsoil depth measurements and variation in crop growth vigour.

Tillage erosion has been reported as being responsible for at least 70% (estimated via  $^{137}\text{Cs}$ ) of the total erosion budget (Lobb et al., 1995). Govers et al., (1994) corroborate by estimating that during a mouldboard plough operation across a field set to a depth of 0.3m, the whole plough horizon is inverted and horizontally displaced by at least 0.3m. When assuming a bulk density of  $1350 \text{ kg m}^{-3}$ , approximately  $4000 \text{ t ha}^{-1}$  of soil are moved. Therefore, by not addressing such a mechanism when predicting patterns of erosion and deposition will result in significant gaps between expected and observed values. Govers et al., (1993) investigated precisely this void between model predictions and field observations. Their work established that in the short-term, a simple topographic based water erosion model was capable of accurately mirroring the



patterns of erosion rates across fields in Belgium and the UK. When simulating long-term hillslope dynamics, agreements were weak, yet by adding a diffusive component into the model (representing rain splash and creep), agreements were regained. The authors point out that the rates required by diffusive processes were too large to be associated with soil creep and splash processes. They attribute such shifts in soil material to tillage action, yet major soil erosion models such as EUROSEM (Morgan et al., 1998), WEPP (Laflen et al., 1991) as well as the USLE suite (Wischmeier and Smith, 1978) all ignore it.

Field evidence of tillage translocation is widespread. In topographically complex field systems, contrasting adjacent land uses such as grass set-aside and cereals will often generate soil berms at field boundaries. In the Palouse region of the Pacific Northwest, the U.S. Soil Conservation Service (SCS) reported drop-offs (steps between adjacent contrasting land uses) between 0.41-0.91m developing over 10 years between ploughed and non-ploughed land. In the same locations the SCS also document soil berms of between 1.2 - 3.1m against lower boundaries of ploughed fields (Montgomery, 1999). 3-4m high soil banks were also noted by Papendick and Miller (1977) both up and downslope of fence lines in the Palouse. Lighter coloured soils are commonly observed along ploughed ridges/knolls where subsoil material is persistently incorporated into the topsoil creating lighter coloured islands. Throughout the last three years across Perthshire and Kinross-shire such features have been regularly observed (evidence from fieldwork visits, conversations with farmers).

Variation in crop yield due to tillage is further evidence of its detrimental effect. Kosmas et al. (Kosmas, 2001) found that leaf area index changed from 2.6 on convex slope portions to 3.6 on concave portions. The tenant farmer at the Littlelour fieldsite provided some anecdotal evidence of yield variation across the field. He claims to consistently gain higher yields of rape and cereals from the western base of the field adding that the contrast in growth vigour is usually visible with that of the eastern top section.

### 3.1.1 The translocation process

Tillage aims to invert the topsoil or alter the topsoil's structure. The inversion of the topsoil is of primary concern and is widely accepted as being the most erosive, but other tillage tools contribute in varying ways (Govers et al., 1994; Lobb, 1999b). The implement used to turn the soil is the mouldboard plough. The process of tillage translocation is driven by gravity, which exerts a vertical downwards force on the soil, on the mouldboard plough, and on the tractor pulling the plough. Assuming a perfectly flat field, uniform soil, constant plough depth, and constant tractor velocity, the soil displaced (perpendicular to plough direction) will be uniform along the plough pass. Remove the perfectly flat field in place of an undulating field and any variation in slope gradient affects the downslope movement the soil, plough and tractor mass. By dragging fixed-frame ploughing implements across an uneven landscape, valley and ridge topography in the landscape will over time become gradually planed (Lobb, 1999a). This process is readily visible as lighter coloured topsoils on the subtlest of convex ridge features.

During mouldboard ploughing the operator will nearly always plough in the direction of longest 'run'. This way he has less time wasted with turning around at the parcel boundaries and provides a more efficient run for subsequent seeding, spraying and harvesting operations. Such decisions often ignore the aspect of the slope and fields in the UK are commonly tilled in an up-downslope manner. The topsoil during up and downslope ploughing is always inverted in the same direction so as to prevent the development of ridge and furrow. The PTO (power take-off) tractor connections allow reversible ploughs to flip at the end of each run to maintain this yet, during up-down slope ploughing it is incorrect to assume that soil displacement on the upslope run entirely offsets that of a downslope run. If, however, our theoretical flat uniform field was being tilled, then the net budget would be zero. Various investigations have confirmed this as well as the mean throw distance resulting on varying slopes (Govers et al., 1994; Lindstrom et al., 1990; Lindstrom et al., 1992). Lindstrom, (1990) discovered a strong relationship between throw distance perpendicular to plough direction and slope. Soil movement perpendicular to plough direction was almost twice during a downslope run than that during upslope runs. Gerontidis et al.

(Gerontidis et al., 2001) reports similar findings. Subsequent to downslope (22 % slope) ploughing, a displacement distance of 0.92m resulted, which was reduced to 0.69 m under contour ploughing. Lobb (1995) used  $^{137}\text{Cs}$  as a tracer to reveal mean forward throw distances of 0.38 m due to a single conventional tillage pass (1 mouldboard pass, 2 tandem disc passes, 1 field cultivator pass) with some material displaced by up to 2.5m. Lobb et al., (1999a) further report a single pass of a chisel plough resulting in forward displacement of 0.21m and 0.22 m for a mouldboard plough, 0.26 m for a tandem disc, and 0.32 m for a field cultivator.

Although the term translocation does not explicitly imply any net erosion, any variation in the magnitude of the translocation may result in a net loss (erosion) or gain (deposition) of soil material at a particular location. Various authors have detailed the strong positive relationship between the magnitude of soil displacement and slope gradient, i.e. a larger slope angle will generate a larger unit flux of soil. Consequently areas of convexity will display higher tillage soil fluxes relative to a flat surface in line with the increasing slope gradients. Areas of concavity (decreasing slope gradient) will display lower tillage soil fluxes. A state of equilibrium exists when slope gradients are constant (or zero) despite a soil flux being present based on the magnitude of the slope gradient at the point (Lindstrom, 2000). If mass continuity principles are applied, the change in slope gradient and hence soil flux across a field will ultimately control whether a location is experiencing net loss or gain of material. A net loss of soil material is termed tillage erosion. Convex shoulder slopes were the focus of work carried out in Ontario, Canada by Lobb et al. (1995). A mean loss of  $3.9 \text{ kg m}^{-2}$  or  $39 \text{ t ha}^{-1}$  per pass of mouldboard plough, tandem disc (2 passes), and field cultivator occurred, which exceeds the established loss tolerance limit of  $0.6 \text{ kg m}^{-2} \text{ a}^{-1}$  for south west Ontario. Lindstrom et al. (1992) determined soil loss due to tillage on a convex slope to be approximately  $3 \text{ kg m}^{-2}$  or  $30 \text{ t ha}^{-1} \text{ a}^{-1}$  from mouldboard ploughing alone. The two major processes of erosion and deposition are clearly operating at different portions of the hillslope. Tillage erosion can be anticipated in areas of positive slope change or convexity (shoulders/ridges), deposition in areas of negative slope change or concavity (footslopes). Water erosion occurs in regions of high flow accumulation i.e. shallow backslopes and thalweg/valleys eventually depositing in flat valley bottoms. If this is the case,

then tillage erosion may be contributing to the supply of erodible sediment via deposition in the very portions of the hillslope that water erosion operates (Govers et al., 1996).

Besides the main driving force of slope, other factors have been identified as having major impacts on the intensity of soil displacement. (Lobb, 1999b) found slope to be a major controlling factor, yet alone it seemed unable to fully explain variability in translocation. Slope curvature was noted to play a role in the planing action of the mouldboard plough on non-uniform curved surface features. He also highlights factors that in essence can be controlled and therefore minimised in their impact. Plough depth and speed were highly variable in response to the change in topography. Tractor velocity during the experiment was set to  $1.6 \text{ m s}^{-1}$  but during upslope runs velocity decreased by between 20-60%, increasing to between 10-30% on downslope runs. Lobb (1999b) points out that the relationship between speed and translocation is fairly weak and varies for different tools. An increase in speed when using a mouldboard plough according to Lobb may only result in the displacement occurring faster. Displacement distance must surely also increase when plough speed increases on a sloping surface. Plough depth controls the volume of soil to be inverted. Variation in depth in response to topography is expected but this depends on the operator's skill and local knowledge of the field. Mouldboard plough depth may increase by up to 33% whilst passing over convex features (Lobb, 1999b) allowing a decrease in plough depth in concave areas. Gerontidis et al. (Gerontidis et al., 2001) discovered that by reducing the plough depth by 50% tillage displacement was reduced by > 75%. Depending on the size of the plough frame and curvature of the surface over which it is pulled a variation of a few centimetres between the middle and the front and back of the tool can be evident. A particularly interesting fact to note was that the tractor operator unknowingly and regularly ploughed to depths (mean 0.23m) greater than 0.17m (as originally set) with the mouldboard plough as well as to mean depths of 0.17m (originally set to 0.13m) with a chisel plough. These factors compounded will cause further increases in translocation. A further implication of the tillage machinery unit or train is the presence of a so-called lead effect. Lobb has been the only author to identify this and may be seen in Figure 3.1.

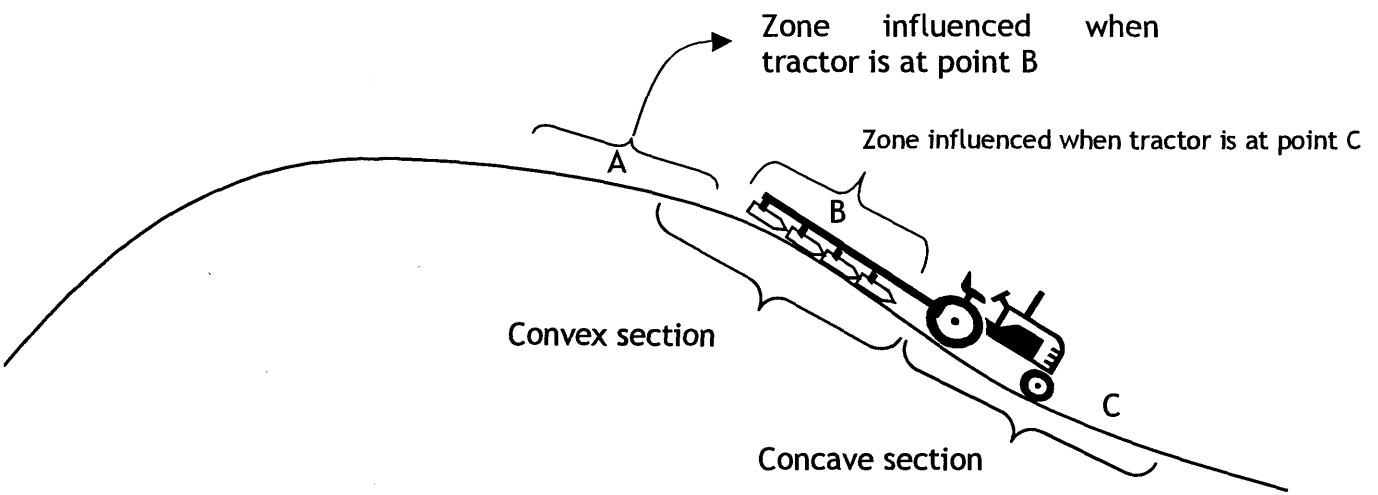


Figure 3.1. Illustration of the lead effect present across the tillage train.

Translocation by the plough is related to tractor location in addition to all of the above factors. Since the gap between the centre of the tillage tool and the centre of the tractor's mass may be between 3-6m, loss or accumulation of soil will vary before and after the point at which the change in slope would suggest, i.e. soil loss occurs before slope increases and accumulation occurs before slope decreases (Lobb, 1999b). From this it is possible to conclude that the pattern of distribution and not the magnitude of translocation is being driven by the lead effect. In Figure 3.1 the tractor is exposed to less accelerative forces since the slope gradient is decreasing (concavity), yet the plough is still passing a progressively steepening slope segment. When the tractor is influenced by site conditions at B, the pattern of soil translocation is reflected at point A.

Despite this, tillage erosion should not be considered as an absolute soil loss, rather as a redistributive process within the field unit. Fields are usually enclosed by some form of fence-line or wall to keep livestock out and a zone of zero flux immediately adjacent to the field boundary is usually present. Here the farmer ploughs a headland parallel to the boundary allowing unploughed land during tractor turn-arounds to be attended to at the end of ploughing (Figure 3.2). It is here that the soil banking is likely to occur since the repeated action of ploughing headlands will see a net accumulation of soil, especially up against

lower boundaries. This of course depends on which direction the soil is thrown by the plough.

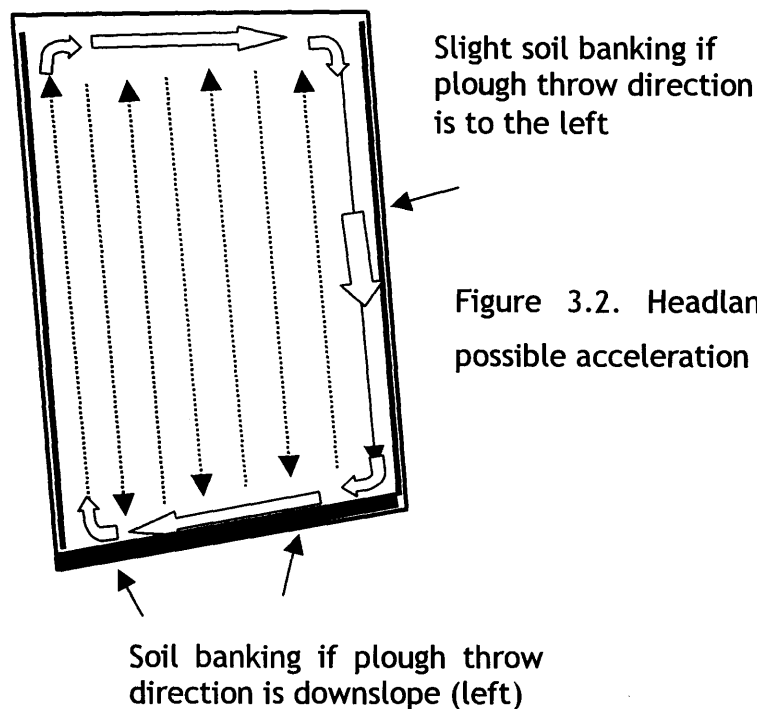


Figure 3.2. Headland ploughing and its possible acceleration of soil banking.

Flux of soil material to adjacent fields is physically obstructed therefore zero. By examining a cluster of cultivated fields a fairly consistent pattern of tillage erosion at the downslope side of parcel boundaries and deposition on the upslope sides is normally evident. Van Oost et al., (2000) claim that tillage erosion immediately adjacent to a boundary can be extreme; on a 0.01 slope assuming a flux value of  $800 \text{ kg m}^{-1}$ , soil loss exceeds  $8 \text{ kg yr}^{-1}$  or  $80 \text{ t a}^{-1}$  or  $6 \text{ mm yr}^{-1}$ .

Advances in technology have and will continue to undoubtedly physically impact the soil. Since the Second World War there has been a trend in increasing size and power of tractors, and from 2 wheel to 4 wheel-drive units. In the mid 1960s the average UK tractor power was 45 kW (60 hp), which increased to 55 kW (75 hp) in the early 1980s (Hinchliffe and Schadler-Hall, 1980). Table 3.1 shows the changes in tractor power and design between 1998 -1999 (SEERAD, 2000).

Tractor power (kW)	1998	1999	% Change
60-80	15033	14483	-3.7
80-100	2902	3325	+14.6
100+	656	858	+30
4 wheel drive in total (Scotland)	20328	21060	+3.6

Table 3.1. Trends in tractor engine performance for Scotland (Scottish Executive, 1998, 1999).

Tractor power has increased dramatically in Scotland (Table 3.1). Such increases in power allow longer, wider and multiple tillage tools to be carried in addition to cultivating steeper land. The intensification of modern arable farming, in particular the reduction in farm workforce, can only imply continuation of such trends and that ploughing is here for some time to come (Hinchliffe and Schadler-Hall, 1980). Evidence from across the central belt of Scotland during fieldwork suggests that on the larger estates there is a move towards larger 100+ kW tractors capable of operating larger frame plough implements and more commonly complex single-pass systems.

Hilly topography may therefore be continuously planed down and concavities being infilled through ploughing action. This may have serious implications for archaeological remains within arable field systems and more so if bias towards a certain hillslope location were found to exist. Sites located at foot and toe-slope locations would likely to be in long-term receipt of material and demand a lower classification of risk by default. Interestingly, recent research in Greece has highlighted that simple upslope reversion of the furrow when ploughing along the contour is capable of significantly reducing tillage displacement to 2-33cm (Gerontidis et al., 2001). If this is the case then there may be a strong case for contour cultivation, at least in a tillage erosion context.

Evidence that a significantly damaging process associated with soil cultivation is modifying the landscape at a faster rate than water erosion rates has been presented. It appears that recognition is now being given to tillage as a key process in agricultural erosion/deposition systems whereas before it was

overlooked. In this project specific effort was made to include tillage in modelling spatial patterns and rates of erosion..

### 3.1.2 Modelling tillage erosion

The relatively small body of literature on tillage erosion modelling has focussed on a diffusion-type equation (Kirkby, 1971). Slope has been statistically related to soil translocation. Lindstrom et al. (1992) investigated displacement distance resulting from a mouldboard plough on varying slopes to develop a predictive regression model. Displacement perpendicular to the direction of ploughing (Y) in centimetres was strongly related ( $r^2 = 0.81$ ) to percentage slope (G; positive for upslope, negative downslope):

$$Y = 44.28 - 1.12G \quad \text{Equation 3.1}$$

Where: Y = displacement (m)

G = slope ( $m\ m^{-1}$ , positive for upslope, negative downslope)

Govers et al., (1994) found a slightly weaker relationship ( $r^2 = 0.68$ ) between throw distance and slope gradient across steeper slopes (0-25%) for a mouldboard plough:

$$Y = - 0.62G + 0.28 \quad \text{Equation 3.2}$$

Where: Y = displacement (m)

G = slope (% , positive for upslope, negative downslope)

Work by Montgomery et al., (1999) produced an even weaker relationship ( $r^2 = 0.52$ ):

$$Y = 42.73 - 0.366G \quad \text{Equation 3.3}$$

Where: Y = displacement (m)

G = slope (%)



Slope coefficients from any of the above may then form the basis of a diffusion coefficient introduced by Govers et al., (1994) describing the intensity of soil displacement per tillage operation ( $\text{kg m}^{-1}$ ):

$$k_{\text{till}} = -D \cdot \rho b \cdot \beta \quad \text{Equation 3.4}$$

Where:  $k_{\text{till}}$  = tillage transport coefficient ( $\text{kg m}^{-1}$ ) per operation

$D$  = plough depth (m)

$\rho b$  = bulk density ( $\text{kg m}^{-3}$ )

$\beta$  = regression coefficient from above equations representing soil displacement (m) at a slope gradient of 1

Table 2. shows representative tillage transport coefficients ( $k_{\text{till}}$ ) taken from the literature for various tillage tools and methods of implementation.

The flux ( $\text{kg m}^{-1}$ ) of material at a position in the landscape can be expressed as follows:

$$Q_s = -k_{\text{till}} \frac{\partial h}{\partial x} = k_{\text{till}} \cdot S \quad \text{Equation 3.5}$$

Where:  $k_{\text{till}}$  = tillage transport coefficient ( $\text{kg m}^{-1}$  per operation)

$\partial h$  = change in elevation (m)

$\partial x$  = change in horizontal distance (m)

$S$  = slope ( $\text{m m}^{-1}$ )

The first stage in modelling tillage erosion is determining a  $k_{\text{till}}$  value, representative of the various cultivation practices at the sites of research. Figure 4 includes a number of compound  $k_{\text{till}}$  constants in an attempt to reproduce contemporary multi-pass tillage systems.

Source	Tillage depth (m)	Tillage speed (m/s)	Implement, soil condition	$k_{till}$ (kg/m per tillage operation)
<b>Up- and downslope tillage</b>				
Govers et al., (1994)	0.15	1.25	Chisel	111
Govers et al., (1994)	0.28	1.25	Mouldboard	234
Lindstrom et al., (1992)a	0.24	2.1	Mouldboard	330
Lobb et al., (1995)(b)	0.15	1.1	Mouldboard	184
Lobb et al., (1995)(b)	0.11	1.12	Mouldboard+2 disc+cultivator	473 - 734
Lobb et al., (1999)	0.17	2.66	Chisel plough	275
Lobb et al., (1999)	0.23	1.71	Mouldboard	346
Lobb et al., (1999)	0.17	0.84	Tandem disc	369
Lobb et al., (1999)	0.15	1.92	Field cultivator	13
Poesen et al., (1997)	0.16	0.65	Duckfoot chisel	282
Quine et al., (1999)	0.19	2.3	Duckfoot chisel	605 - 660
<b>Contour tillage</b>				
Lindstrom et al., (1992)a	0.24	2.1	Mouldboard	363
Montgomery et al., (1999)	0.23	1.0	Mouldboard	110

Table 3.2. Variation in tillage transport coefficients ( $k_{till}$ ) reported in the literature.

For the purpose of this simulation,  $k_{till}$  values were selected from work carried out in conditions analogous to those found in lowland Scotland. Van Oost et al., (2000) quote a range of typical values expected in Western Europe ca. 500-1000  $\text{kg m}^{-1} \text{a}^{-1}$ . Values applied within this range include 700-900  $\text{kg m}^{-1} \text{a}^{-1}$  in Belgium (Van Oost, 2000), 400-600  $\text{kg m}^{-1} \text{a}^{-1}$  in the same field (Govers et al., 1994), 348 and 397  $\text{kg m}^{-1} \text{a}^{-1}$  in 2 fields in central England (Govers et al., 1996). In North America, Montgomery et al., (1999) determined  $k_{till}$  values of 105 - 113  $\text{kg m}^{-1}$ . Once selected, simulation of the fluxes downslope and the calculation of erosion and deposition rates can be relatively simply estimated in accordance with mass balance accounting. Conceptually it may be written as follows:

$$\text{Net loss or accumulation}_{x,y} = \text{inputs}_{x,y} - \text{outputs}_{x,y}$$

Where: inputs = inflow of soil to cell x,y

Outputs = outflow of soil from cell x,y

A vitally important aspect of this project is the ability to predict spatial distribution of areas of high and low risk. Lindstrom et al.'s (2000) visual basic model used mass continuity principles to model tillage movement, both as blocks of soil down a single transect and in 2-D across a field. The model is very flexible allowing any number of tillage operations as input as well as user definable  $k_{\text{till}}$  values. However, the model is capable more importantly of simulating tillage translocation over x number of years, and constantly recalculating profile morphology after each pass of the plough(s). This model was kindly provided by Lindstrom et al., as a means of validating performance of the ARC/INFO based tillage translocation model developed here (ARCTILL). The program is somewhat physically restricted in its applicability due to the 65000 row limit in Excel, but application to individual fields is what the model is really designed for, therefore, was run a number of times across each of the 4 field sites.

## 3.2 Development of a tillage translocation model

From the Land Cover of Scotland database (1988), non-arable land uses were omitted from the analysis. From the 3800 km<sup>2</sup> study area, 1631 km<sup>2</sup> remained as cultivated land. Considering the low resolution and somewhat outdated landuse data, assumptions regarding the type of tillage operations had to be made. Use of the mouldboard plough is commonplace throughout Scotland. A standard tillage procedure was defined as 1 mouldboard pass, 2 PTO field cultivator passes, 1 power harrow pass. As a result  $k_{\text{till}}$  values of 397 kg m<sup>-1</sup> (Govers et al., 1996) and 550 kg m<sup>-1</sup> (Quine et al., 1997) were assumed to be most representative of conditions in the study area.

### 3.2.1 The Excel pilot model

The model developed simply requires derivatives of the topography: slope and slope aspect. To test the model's 1-D behaviour it was integrated into Excel along various hypothetical slopes profiles as well as a real slope profile taken from the DTM. The model was run using  $k_{\text{till}}$  values of 550 and 397 kg m<sup>-1</sup> with topographic data being taken from the DTM. These along with other attributes are found in table 3. At 212.5 m (point X) from the top of the transect, a very simple representation of a 1.5m field boundary was introduced. The topographic rise feature was assigned a zero slope and  $k_{\text{till}}$  values so as to prevent the rise generating and receiving sediment to and from adjacent cells. By following the table data and the graph it is clear that the model is consistently tilted from erosion to deposition and vice-versa by slope curvature. The model is somewhat unrealistic in that all soil translocated does so to the next downslope cell, i.e. there is no diversion or dispersion of translocated soil to multiple neighbouring cells. The simplistic field boundary appears to be simulating the boundary of zero flux reported in the literature and seen in the field. The downslope side of the boundary receives no soil from the upslope cell to offset soil its outflow hence a net loss in material, i.e. tillage erosion. Upslope of the boundary, outflow is effectively blocked due to the fence/wall, rather no ploughing takes place, therefore soil accumulates over time. For the purpose of testing the

mechanics of the model such a simple spreadsheet implementation sufficed and allowed the effect of field boundary presence to be experimented with.

### 3.2.1.1 Results from the Excel pilot model

Figure 6 shows the Excel model outputs along the chosen transect and the corresponding raw data is presented in figure 5. When examining the results it should be borne in mind that the Excel model operates only in one dimension and transports either all output material from one cell to another or does not transport material at all depending on its topographic location. There is no diversion to multiple cells. Erosion and deposition rates have been calculated using  $k_{\text{till}}$  values of  $397 \text{ kg m}^{-1}$  and  $550 \text{ kg m}^{-1}$ . Figure 5 lists the fundamental topographic characteristics of each transect cell utilised by the model. At each cell using equation 4, soil outflow (flux) is calculated using its corresponding slope value and the selected tillage transport coefficient ( $k_{\text{till}}$ ). It is assumed that there is no inflow of material into the first cell in the transect. At each subsequent cell the total amount of material moving through (kg) is first calculated by multiplying the tillage flux per unit length (m) by cell size (25m). This is then followed by a mass balance (inputs minus outputs) and converted into a rate per unit area ( $\text{kg m}^{-2}$ ) by dividing by cell area ( $625\text{m}^2$ ). Outflow from this cell then becomes inflow to the next cell. This continues along the transect. The first cell can only output material providing the slope gradient is high enough to generate outflow. Clearly at this cell a 0.028 slope is sufficient to generate a flux and, although the flux magnitude is relatively low, the second highest erosion rates of  $-0.616 \text{ kg m}^{-2}$  and  $-0.444 \text{ kg m}^{-2}$  (for  $k_{\text{till}}$   $550 \text{ kg m}^{-1}$  and  $397 \text{ kg m}^{-1}$  respectively) were found, due mainly to the zero inflow of material and its impact on the mass balance. The simple field boundary halfway down the transect produced interesting results in line with what was expected in the field. Outflow of material from the cell immediately upslope of the boundary was restricted and hence causes a net accumulation of soil ( $+0.19 \text{ kg m}^{-2}$   $+0.143 \text{ kg m}^{-2}$ ). On the downslope side of the boundary once again inflow is blocked in the same manner as in the first transect cell, which produces an area of net loss or erosion. Slope curvature (exaggerated by 1000 for graphing purposes) describes the rate of change of slope (positive = convex, negative = concave). Patterns of erosion-

Z (m)	Distance (m)	Slope (m m <sup>-1</sup> )	(curvature) d <sup>2</sup> e/dx <sup>2</sup>	k <sub>till</sub> (550 kg m <sup>-1</sup> )	Soil outflow (kg m <sup>-1</sup> )	Soil inflow (kg m <sup>-1</sup> )	eros/depos (kg m <sup>-2</sup> ) k <sub>till</sub> = 550 kg m <sup>-1</sup>	eros/depos (kg m <sup>-2</sup> ) k <sub>till</sub> = 397 kg m <sup>-1</sup>
35.380	0	0.028	0.0000	550	385.00	0.00	-0.6160	-0.4446
35.000	12.5	0.045	1.3600	550	618.75	385.00	-0.3740	-0.2700
34.280	25	0.060	1.2000	550	825.00	618.75	-0.3300	-0.2382
33.118	37.5	0.064	0.3200	550	880.00	825.00	-0.0880	-0.0635
31.912	50	0.054	-0.8000	550	742.50	880.00	0.2200	0.1588
30.941	62.5	0.052	-0.1600	550	715.00	742.50	0.0440	0.0318
30.000	75	0.052	0.0000	550	715.00	715.00	0.0000	0.0000
29.047	87.5	0.059	0.5600	550	811.25	715.00	-0.1540	-0.1112
27.694	100	0.058	-0.0800	550	797.50	811.25	0.0220	0.0159
26.269	112.5	0.051	-0.5600	550	701.25	797.50	0.1540	0.1112
25.000	125	0.040	-0.8800	550	550.00	701.25	0.2420	0.1747
24.012	137.5	0.027	-1.0400	550	371.25	550.00	0.2860	0.2064
23.339	150	0.018	-0.7200	550	247.50	371.25	0.1980	0.1429
22.910	162.5	0.012	-0.4800	550	165.00	247.50	0.1320	0.0953
22.633	175	0.009	-0.2400	550	123.75	165.00	0.0660	0.0476
22.420	187.5	0.009	0.0000	550	123.75	123.75	0.0000	0.0000
22.189	200	0.009	0.0000	550	0	123.75	0.1980	0.1429
23.700	212.5	0	0	0	0	0	0	0
21.550	225	0.014	0.1600	550	192.50	0	-0.3080	-0.2223
21.550	237.5	0.016	0.1600	550	220.00	192.50	-0.0440	-0.0318
21.157	250	0.016	0.0000	550	220.00	220.00	0.0000	0.0000
20.745	262.5	0.016	0.0000	550	220.00	220.00	0.0000	0.0000
20.347	275	0.014	-0.1600	550	192.50	220.00	0.0440	0.0318
20.000	287.5	0.005	-0.7200	550	68.75	192.50	0.1980	0.1429
19.868	300	0.008	0.2400	550	110.00	68.75	-0.0660	-0.0476
19.658	312.5	0.037	2.3200	550	508.75	110.00	-0.6380	-0.4605
18.732	325	0.064	2.1600	550	880.00	508.75	-0.5940	-0.4288
17.130	337.5	0.066	0.1600	550	907.50	880.00	-0.0440	-0.0318
15.578	350	0.035	-2.4800	550	481.25	907.50	0.6820	0.4923

Table 3.3. Attributes from DTM derived profile used in 1D pilot run of tillage model.

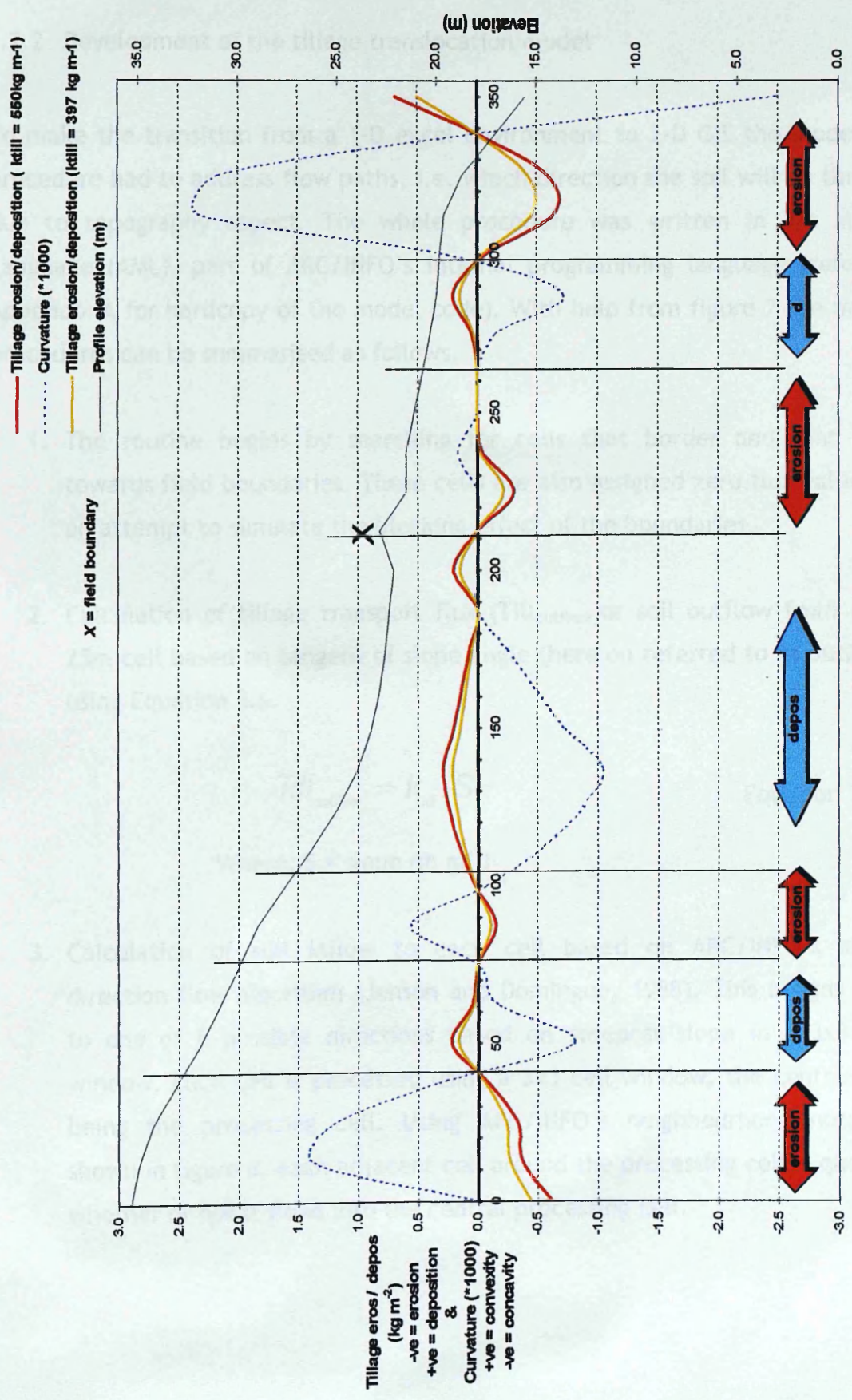


Figure 3.3. Pilot run of a 1-D tillage translocation model across a sample DTM transect (25m v 350m)

deposition follow the curvature curve closely along the transect. All convex slope sections display erosion and concave areas display deposition.

### 3.2.2 Development of the tillage translocation model

To make the transition from a 1-D excel environment to 2-D GIS the modelling procedure had to address flow paths, i.e. which direction the soil will be thrown due to topography aspect. The whole procedure was written in Arc Macro Language (AML), part of ARC/INFO's internal programming language (refer to Appendix A for hardcopy of the model code). With help from figure 7 the model procedures can be summarised as follows:

1. The routine begins by searching for cells that border and that flow towards field boundaries. These cells are also assigned zero flux values in an attempt to simulate the blocking effect of the boundaries.
2. Calculation of tillage transport flux ( $Till_{outflow}$ ) or soil outflow from each 25m cell based on tangent of slope angle (here on referred to as outflow) using Equation 3.6.

$$Till_{outflow} = k_{till} \cdot S \quad \text{Equation 3.6}$$

Where:  $S$  = slope ( $m\ m^{-1}$ )

3. Calculation of soil inflow to each cell based on ARC/INFO's single direction flow algorithm (Jenson and Domingue, 1988). This assigns flow to one of 8 possible directions based on steepest slope in a 3x3 cell window. Each cell is processed using a 3x3 cell window, the central cell being the processing cell. Using ARC/INFO's neighbourhood notation shown in figure 8, each adjacent cell around the processing cell is queried whether or not it flows into the central processing cell.



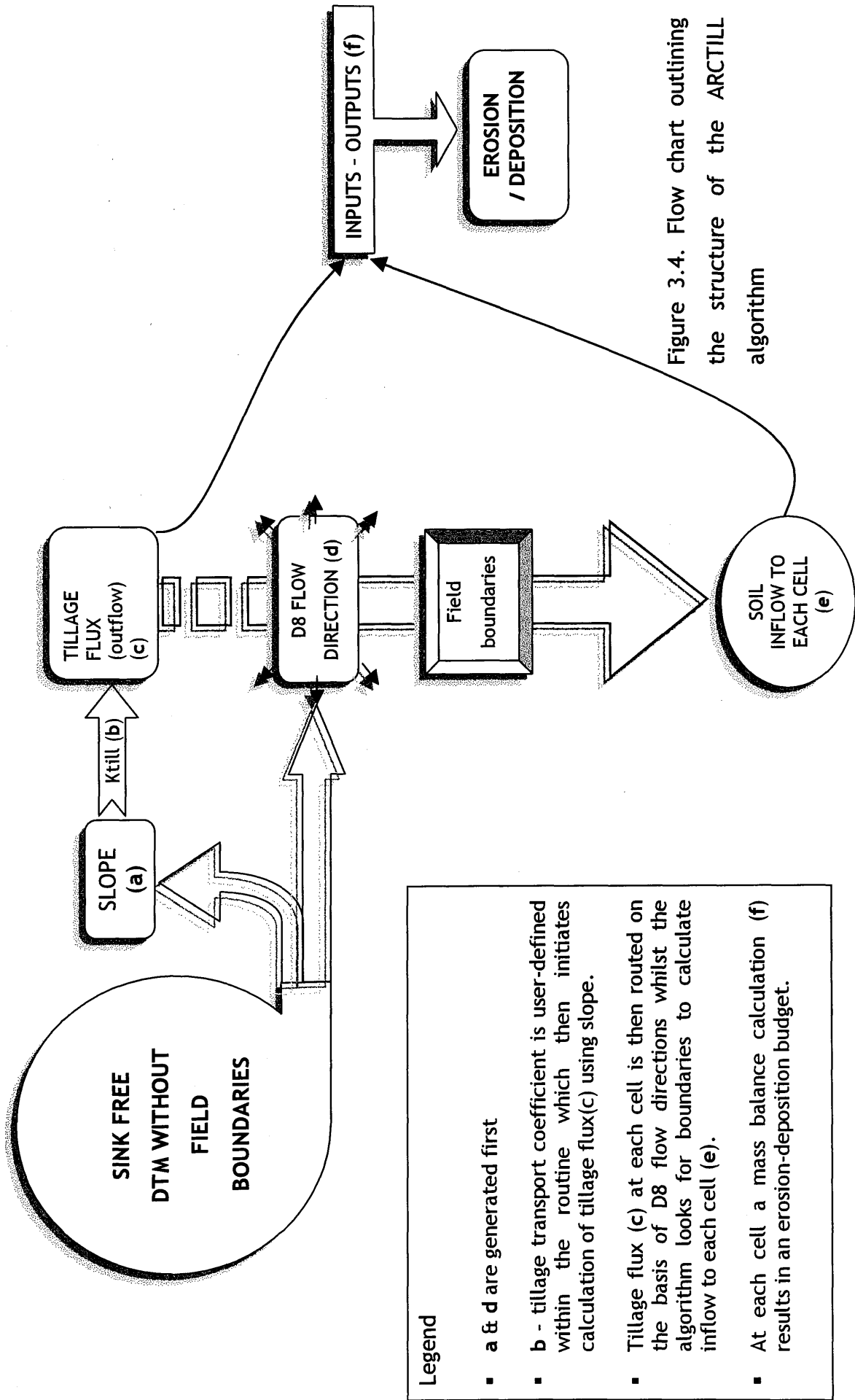


Figure 3.4. Flow chart outlining the structure of the ARCTILL algorithm

	0	0	
	-1,1	0,1	1,-1
0	-1,0	X	1,0
	-1,1	0,1	1,1
	0	0	

25

321

298

Figure 3.5. Use of ARC/INFO neighbourhood notation (x is processing cell) and method of calculating inflow to each cell

If for example the NE (1,-1), E (1,0) and SE(1,1) cells are flagged as flowing into the processing cell, their corresponding outflows calculated in step 1 are added and placed into the processing cell portraying inflow. Cells not flowing into x are given zero. Figure 3.5 illustrates that inflow to x is therefore  $298 + 321 + 255 + 0 + 0 + 0 + 0 + 0 = 874$ . This routine repeats at every cell and although the 3x3 roaming window 'looks' at some of the same cells analysed in the previous iteration as it overlaps, soil may flow only in a single direction so multi-counting of a cell's outflow into 2 different cells will never occur. The flux values above are all per unit metre of cell width. Total sediment flux per cell was obtained by multiplying unit fluxes by cell size (25m). It is assumed cell size (25m) as being representative of contour length despite diagonal flow lengths in this case being approximately 35.35m.

4. Rates of tillage erosion and deposition at each cell are calculated using Inputs - outputs. Units of total soil shift per cell are converted to kg per unit area by dividing by cell area (625 m<sup>2</sup>).

The  $k_{till}$  value of 550 kg m<sup>-1</sup> was used as preliminary input for the tillage model. The model was run for the complete study area (arable lands only). Results at each field site were then clipped from the regional scale model run and used in combination with water erosion model results for direct comparison with field based <sup>137</sup>Cs investigations. To test whether the performance of the spatially distributed ARCTILL tillage erosion model was acceptable, Lindstrom et al.'s (2000) Tillage Erosion Prediction model (TEP) was run across the 4 field sites

using the a  $k_{till}$  parameter of  $550 \text{ kg m}^{-1}$  and used as a benchmark. Although a fairly new model TEP was designed based on the extensively researched empirical relationship between slope gradient and soil displacement distance. Various authors (Govers et al., 1994; Lindstrom et al., 1992; Montgomery, 1999) have established the relationship all with similar results.

		N	MEAN	DIFF	STDEV	SE MEAN	t	P
Loanleven	ARCTILL	94	-0.000	-0.0183	1.757	0.181	-0.31	0.757
	TEP	94	0.018		1.760	0.182		
Blairhall	ARCTILL	300	-0.001	-0.00624	0.439	0.025	-0.86	0.391
	TEP	300	0.005		0.446	0.026		
Leadketty	ARCTILL	280	0.000	-0.1173	1.233	0.074	-2.49	0.013
	TEP	280	-0.117		1.003	0.060		
Littlelour	ARCTILL	177	-0.000	0	0.725	0.055	-0.00	1.0
	TEP	177	0.000		0.556	0.042		

$$H_0: \mu_{ARCTILL} = \mu_{TEP}$$

Table 3.4. Summary of paired t-tests comparing performance of the ARCTILL and TEP tillage models at each field site.

$K_{till} = 550 \text{ kg m}^{-1}$		MIN	MAX	% CELLS ERODING	% CELLS DEPOSITING
Loanleven	ARCTILL	-3.96	5.81	63.8	36.2
	TEP	-4.46	4.76	60.6	39.4
Blairhall	ARCTILL	-2.33	3.82	56.0	44.0
	TEP	-3.06	2.79	54.0	46.0
Leadketty	ARCTILL	-4.07	6.11	56.4	43.6
	TEP	-5.17	5.39	60.4	39.6
Littlelour	ARCTILL	-2.2	2.64	62.1	37.9
	TEP	-2.5	2.2	60.5	39.5

Table 3.5. Summarised data from both tillage models

The TEP model on these grounds was assumed to be as scientifically sound as possible.

Results of paired t-tests are presented in Table 3.4. The tests were applied to confirm whether ARCTILL had been designed correctly at least in a rough and ready way. In no way is it assumed that the TEP is the most accurate model nor that it had been selected over other models. It was obtained on the basis that the authors have established considerable research experience in the subject area and the user-friendliness of the software and applicability was particularly suitable. The null hypothesis assumes that the two models are functioning and performing the same. It is clear that at Loanleven, Blairhall and Littlelour there is strong statistical evidence suggesting that TEP and ARCTILL are generating significantly similar results ( $p > 0.05$ ). The two models at Leadketty, however, performed statistically differently ( $p = 0.013$ ). Table 3.5 contains descriptive statistics of both models side-by-side at each field site. Figure 3.7 and Figure 3.8 further exemplifies the strong correlation between the TEP and ARCTILL models at each field site. Figure 3.9 to Figure 3.12 are outputs from both models at all four sites allowing comparison of spatial patterns.

Figure 3.6 is a sample model output from a ca 5 km<sup>2</sup> area immediately west of Methven village, Perthshire. The most striking prediction from ARCTILL is that tillage erosion-deposition pattern can be highly variable across field units. Deep red areas (erosion) are clearly highlighting zones of convexity and blue areas zones of concavity. In addition to the strong topographic related pattern, the model is also sensitive to the structure of field boundaries in conjunction with slope aspect. The model requires boundary location as input and allocates them all zero flux, therefore, acting as barriers. This was successfully modelled in the simple 1-D Excel model and has been successfully implemented into the 2-D version. As a rule of thumb the bases of fields are accumulating and field heads are losing soil the boundaries functioning as traps. They do not function in the same way against water borne erosion/deposition. Surface runoff may penetrate a field boundary since in reality it is not impermeable, such as a hedge. If flow is carrying sediment, the variation in roughness or slope as it makes the transition across the boundary could trigger the sediment to be deposited within the hedge. The flow may continue downslope depending upon local conditions, yet with the same hedge boundary tillage will rarely throw soil up against/into the boundary. The farmer leaves a buffer strip usually less than a metre wide, so soil accumulating at a slope base will tend to do so just short

of the actual boundary feature. ARCTILL has been developed so that any cell defined as a field boundary cannot receive material.

Examining all figures relating to the models outputs it is fair to conclude that ARCTILL has performed well both in terms of quantitatively predicting erosion/deposition to remarkably similar levels of a more established model and simulating as technologically feasible as possible the way in which linear features fundamentally influence the spatial patterns of soil translocation.

No optimisation techniques have been applied to ARCTILL at this point. Both the water and tillage erosion models have been combined and optimised individually within the singular model against  $^{137}\text{Cs}$  inventories.

ARCTILL has been optimised in chapter 4 to best-fit all  $^{137}\text{Cs}$  erosion/deposition estimates for the 4 field sites. The tillage transport coefficient ( $k_{\text{till}}$ ) was set at  $400 \text{ kg m}^{-1}$  and the ARCTILL predictions for the whole study area are shown in Figure 3.13.

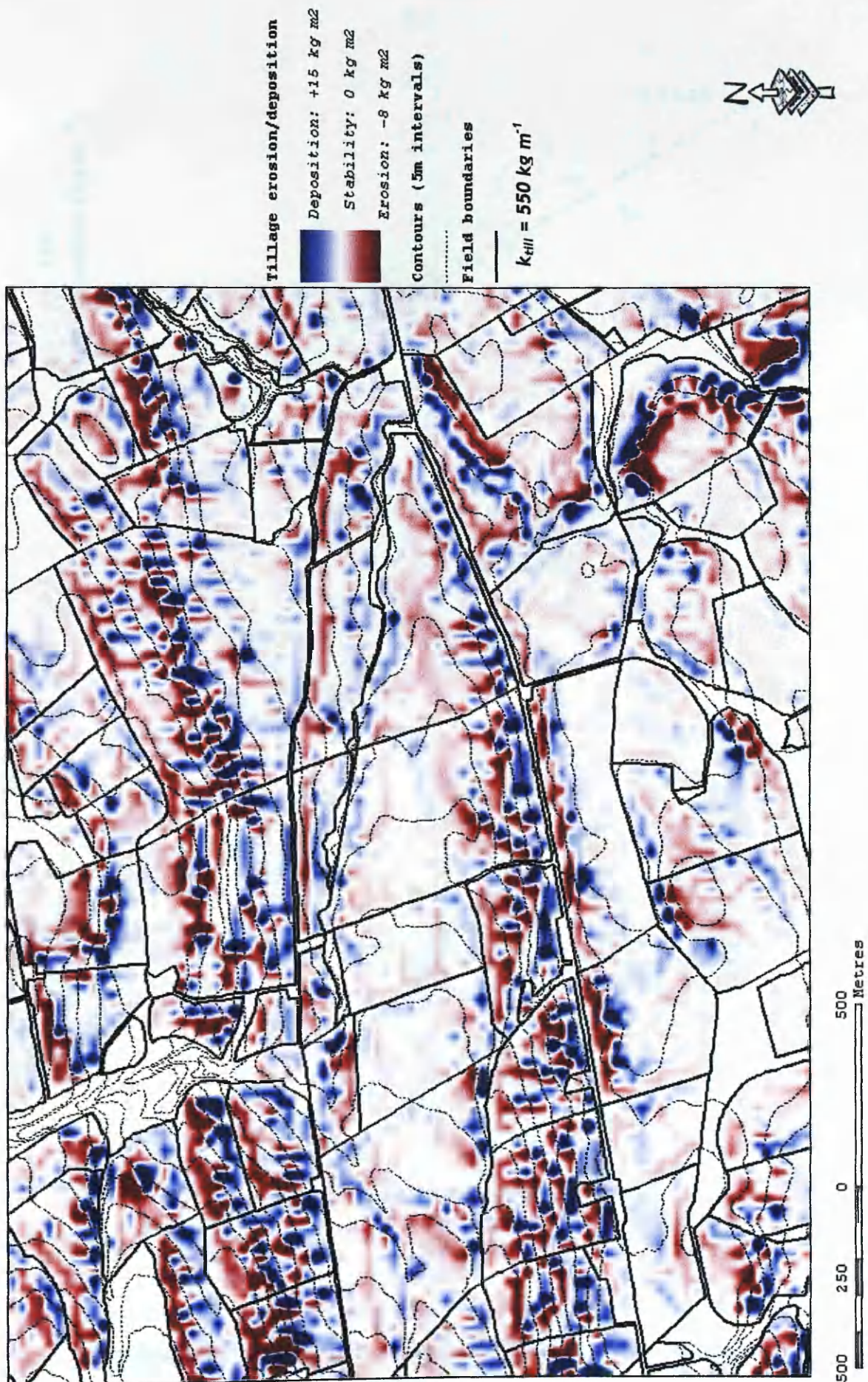


Figure 3.6. Sample output from the ARCTILL model 2km west of Perth.

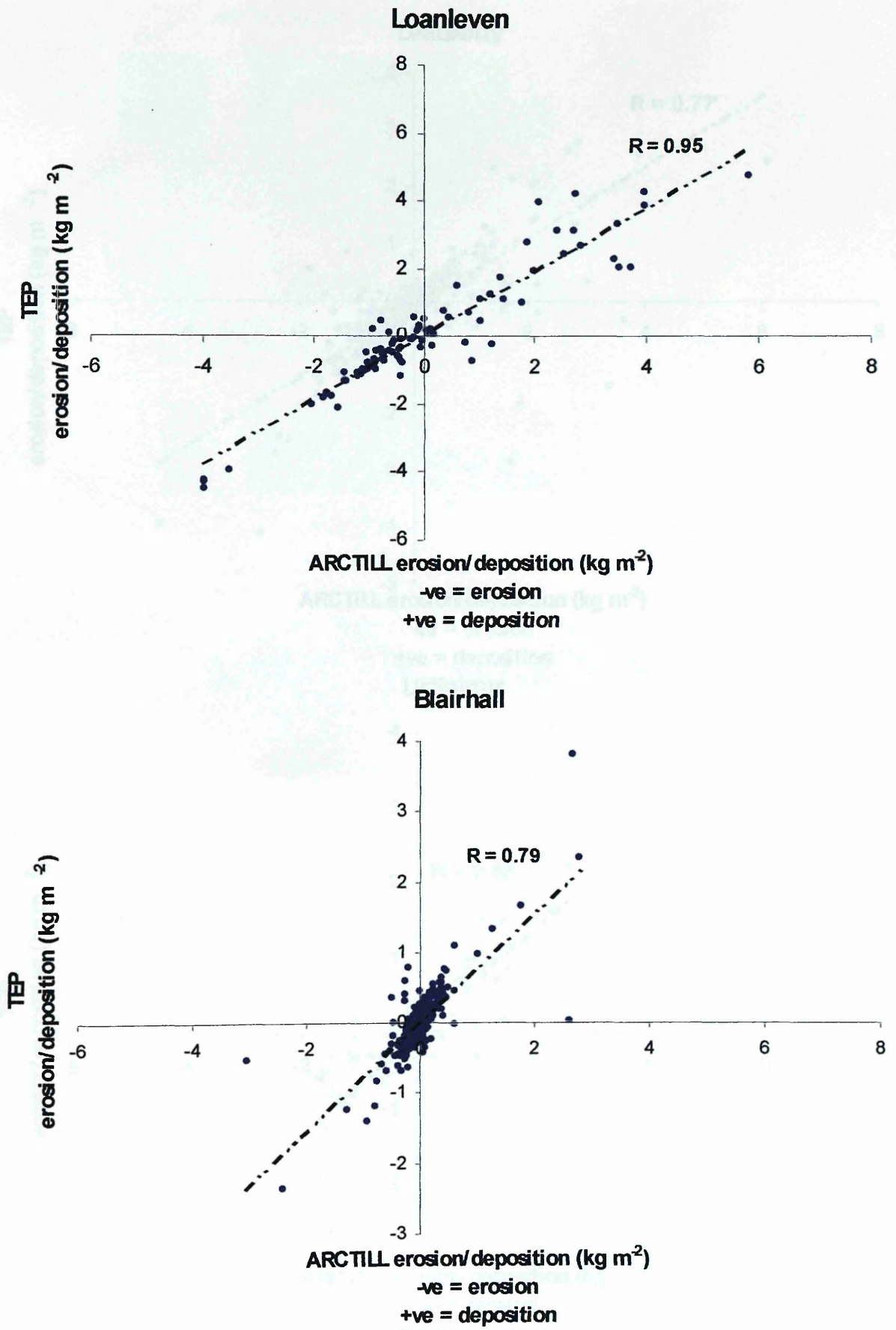


Figure 3.7. Relationship between the TEP model (Lindstrom et al., 2000) and the ARCTILL tillage model across the Loanleven and Blairhall field sites.

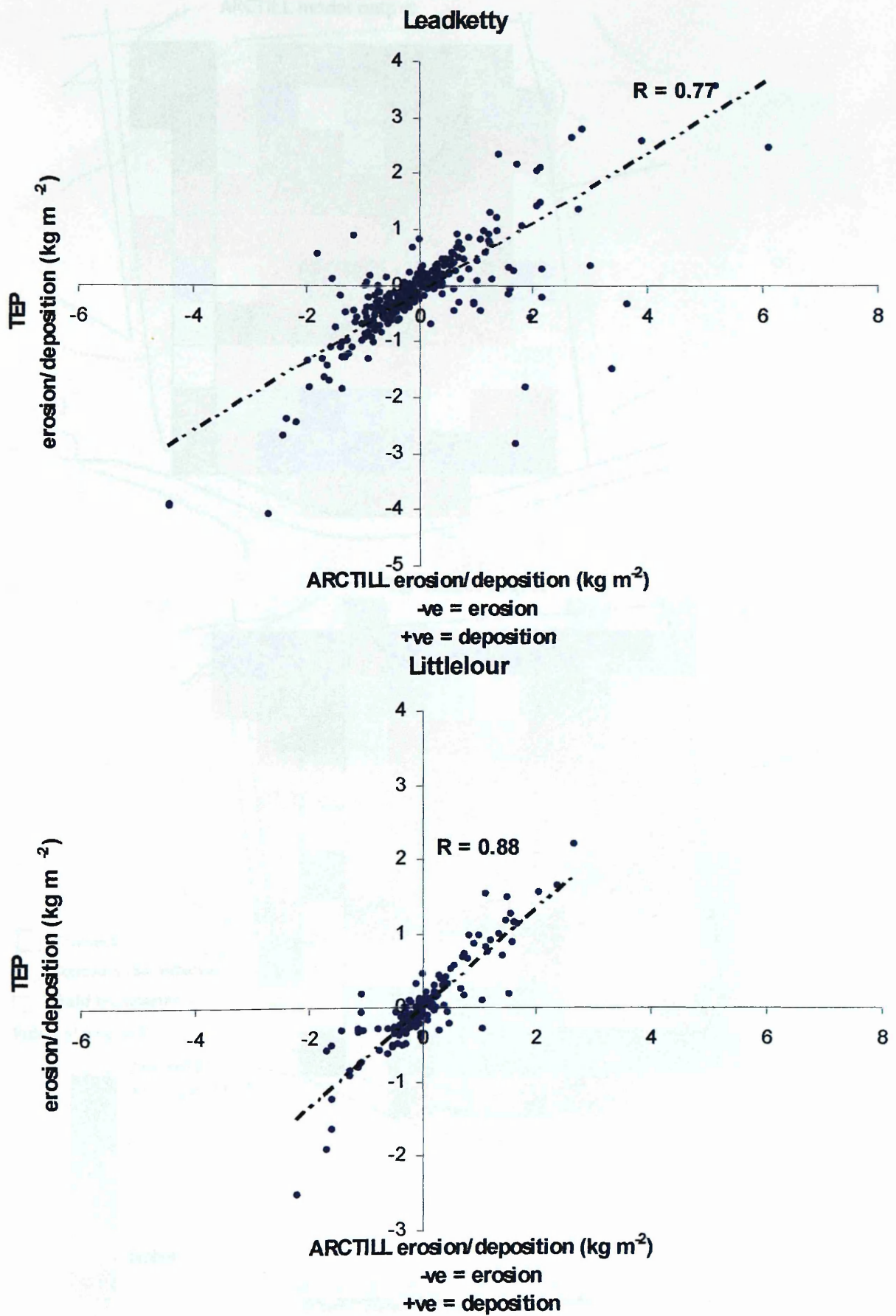


Figure 3.8. Relationship between the TEP model (Lindstrom et al., 2000) and the ARCTILL tillage model across the Leadketty and Littlelour field sites.



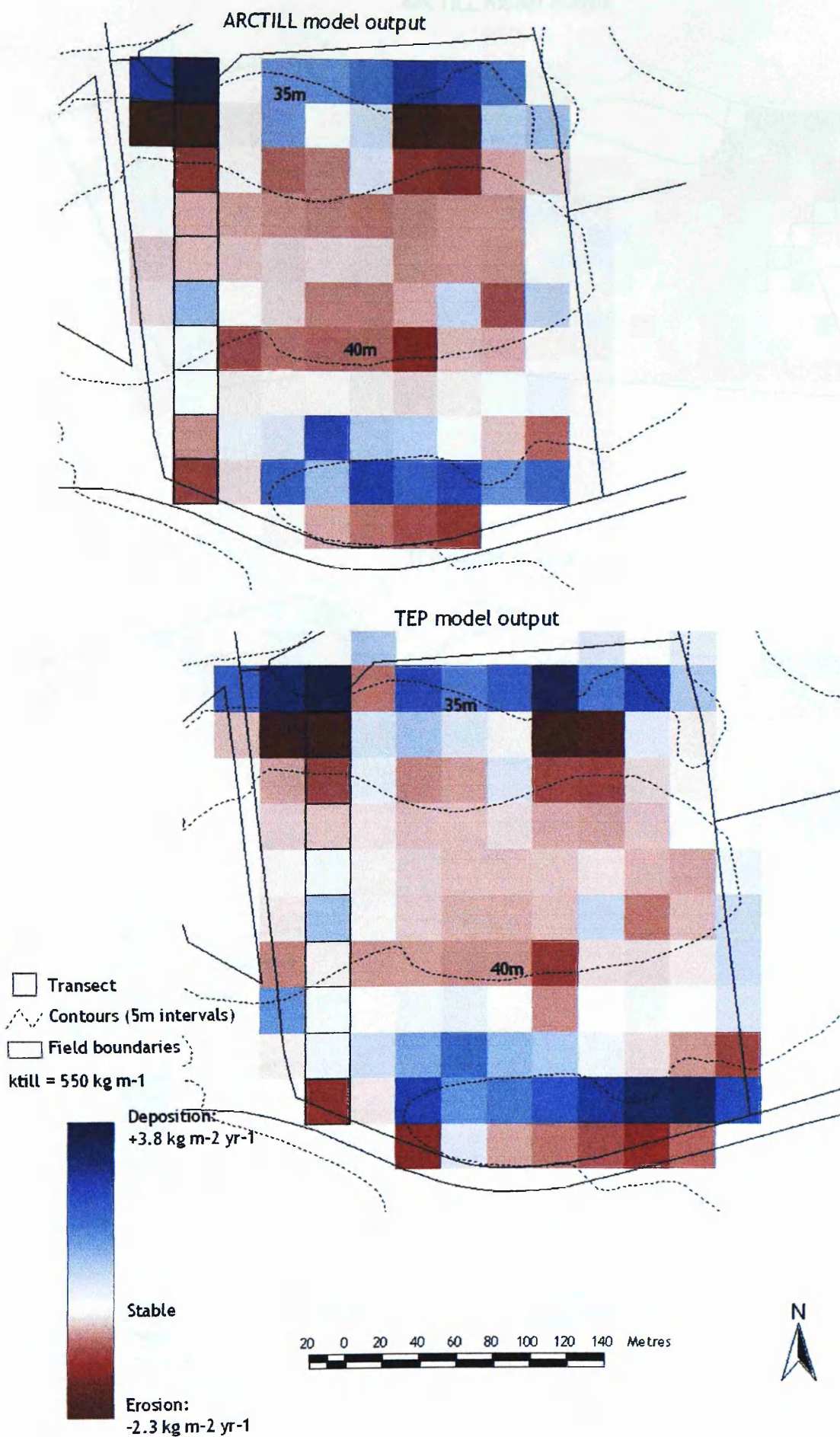
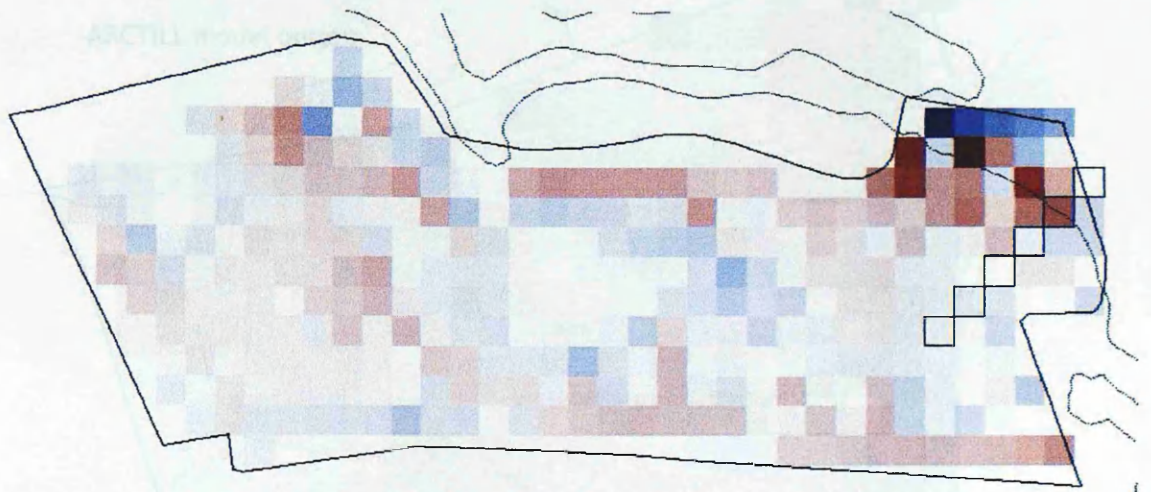
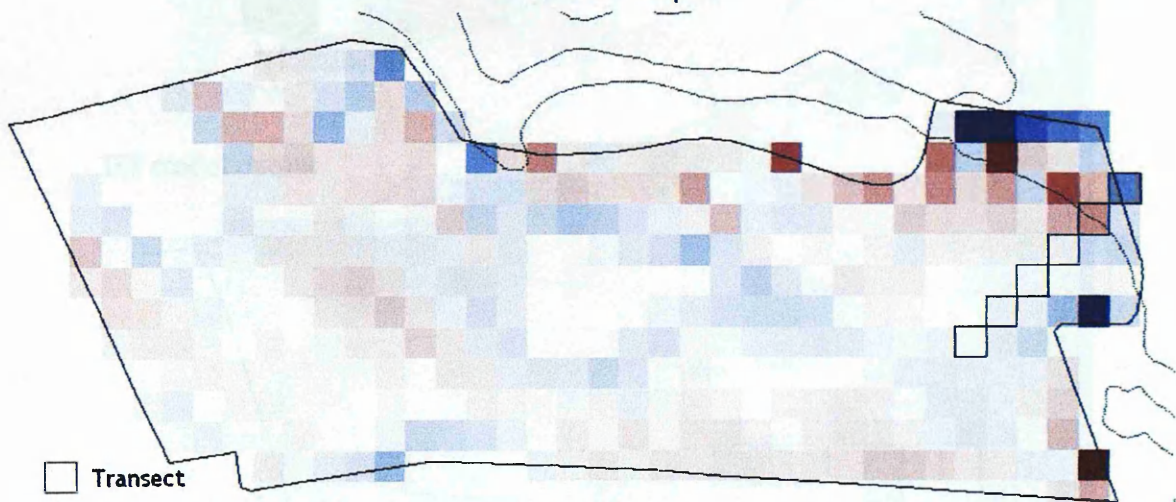



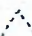

Figure 3.9. Tillage erosion/deposition as predicted by the ARCTILL and TEP (Lindstrom et al., 2000) across the Loanleven field site.

ARCTILL model output



TEP model output



-  Transect
-  Contours (5m intervals)
-  Field boundaries
- ktill = 550 kg m<sup>-1</sup>

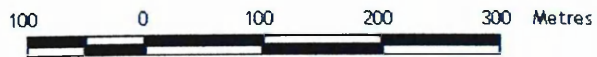
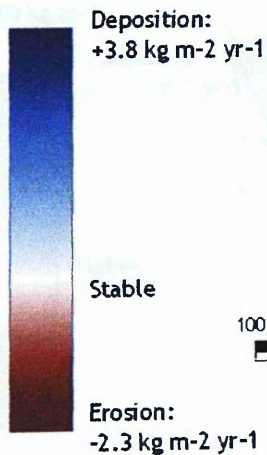


Figure 3.10. Tillage erosion/deposition as predicted by the ARCTILL and TEP (Lindstrom et al., 2000) across the Blairhall field site.

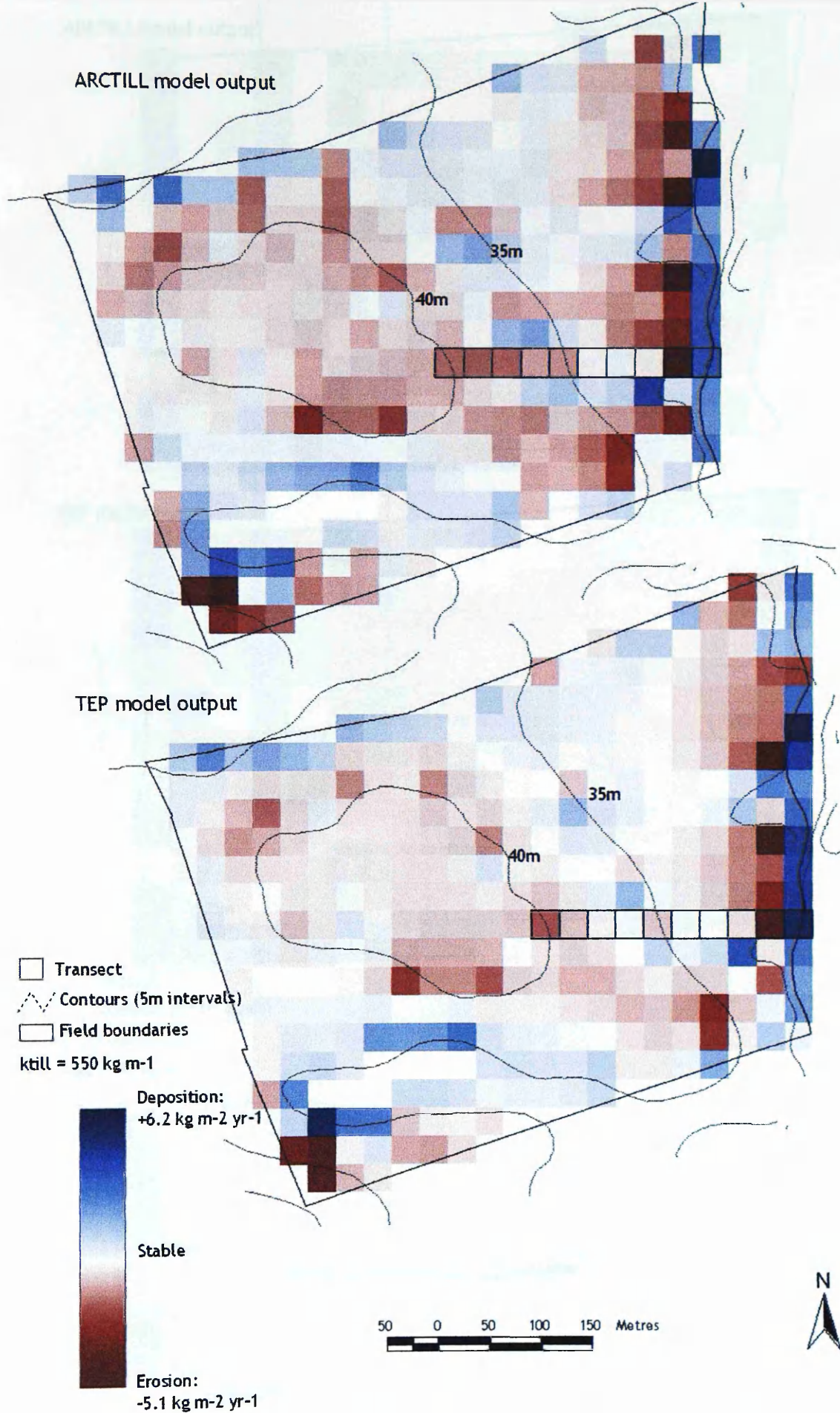
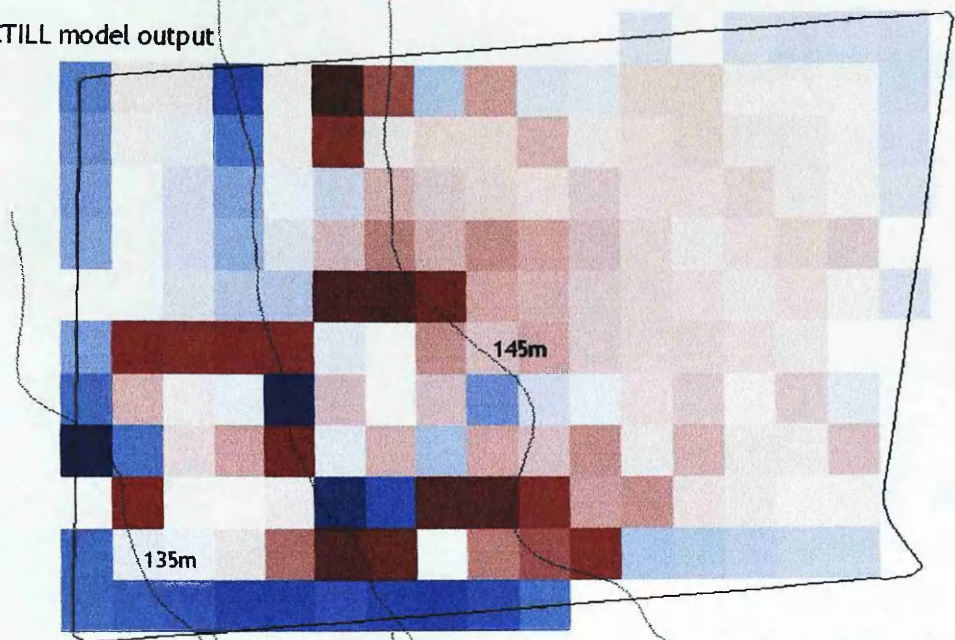
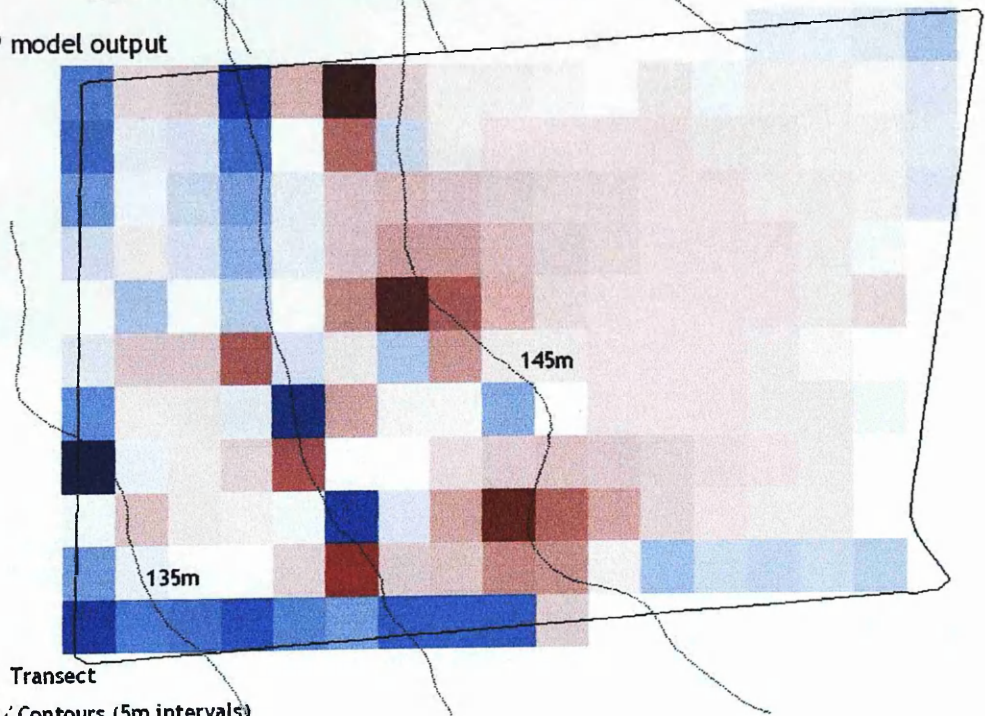


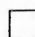

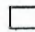
Figure 3.11. Tillage erosion/deposition as predicted by the ARCTILL and TEP (Lindstrom et al., 2000) across the Leadketty field site.

ARCTILL model output



TEP model output



-  Transect
  -  Contours (5m intervals)
  -  Field boundaries
- ktill = 550 kg m<sup>-1</sup>

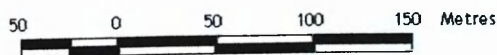
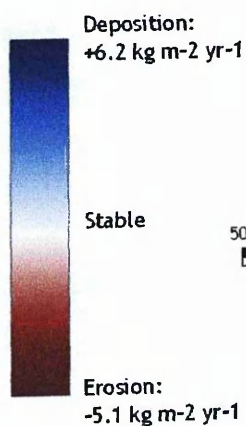
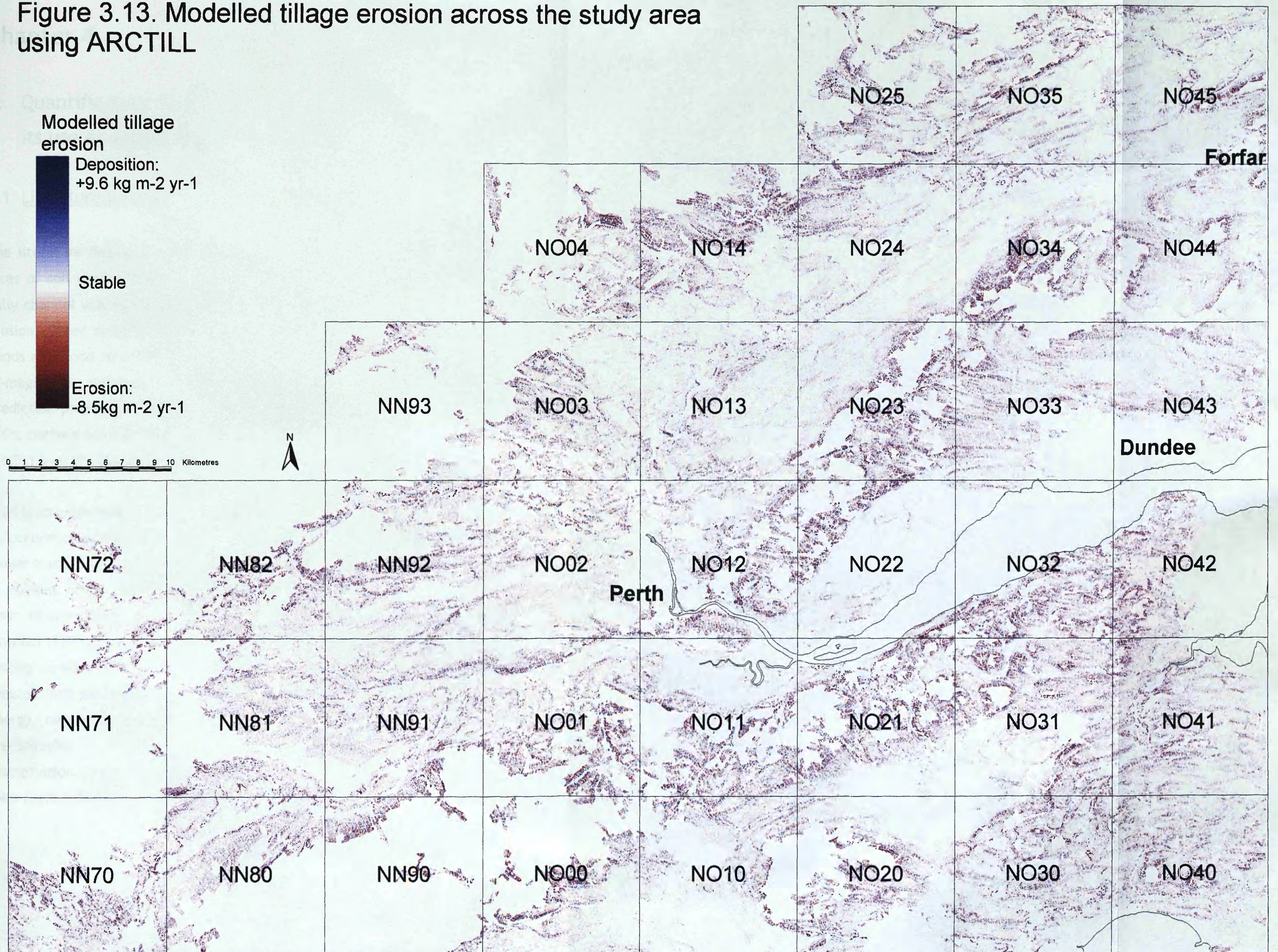


Figure 3.12. Tillage erosion/deposition as predicted by the ARCTILL and TEP (Lindstrom et al., 2000) across the Littlelour field site.

Figure 3.13. Modelled tillage erosion across the study area using ARCTILL



# Chapter 4

## 4. Quantification of soil loss using the $^{137}\text{Cs}$ technique and its use as a modelling optimisation tool.

### 4.1 Literature review

The literature details a wide range of techniques have been used to estimate rates of soil erosion. Field-scale monitoring such as plot experiments, rill and gully channel volumetric measurement, have traditionally provided estimates of erosion. Other methods include monitoring sedimentation rates of reservoirs, ponds and flood retention basins. Many of the methods used provide only order-of-magnitude estimations and encompass inherent spatial and temporal prediction problems. Mapping the redistribution of radioactive tracers such as  $^{137}\text{Cs}$ , derived from fallout, has provided a further method by which to quantify erosion over the medium term.

$^{137}\text{Cs}$  is an anthropogenic radionuclide derived from nuclear fission. Consequently its occurrence in the environment is a result of licensed discharges from nuclear power stations, atmospheric nuclear weapons testing, and accidents or incidents at nuclear power stations. Isolated reports as early as 1945 of  $^{137}\text{Cs}$  releases close to sites used for nuclear weapons tests are documented by Carling and Moghissi (1977). Global dispersion of  $^{137}\text{Cs}$  commenced as a result of super-power testing in November 1952 (Figure 4.1).  $^{137}\text{Cs}$  along with other isotopes were ejected into the upper troposphere or stratosphere, depending on detonation energy, eventually returning to the earth's surface as wet or dry fallout via precipitation. It has been noted that  $^{137}\text{Cs}$  fallout is strongly linked both to precipitation patterns and magnitudes. Ritchie and McHenry (1990) quote in their review that fallout measurement data taken by the New York Health and

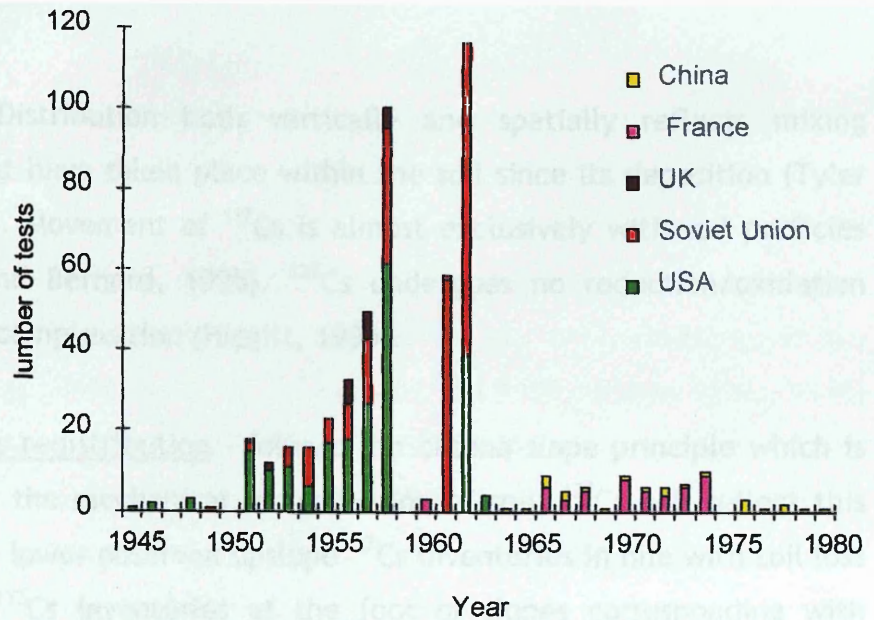


Figure 4.1. Frequency of atmospheric nuclear weapons tests and countries responsible (Wright et al., 1999).

Safety Laboratory in 1972 indicate the start of  $^{137}\text{Cs}$  fallout in  $1952 \pm 2$  years (Robbins, 1978), the emergence in detectable levels of  $^{137}\text{Cs}$  in 1954 (Wise, 1980) and major periods of deposition in 1958, 1963/64.

Further input of material in to the atmosphere was halted due to the Test Ban Treaty signed in 1963 and since this date levels of  $^{137}\text{Cs}$  fallout rates have decreased steadily until further 'localised' events such as Chernobyl. Distribution of  $^{137}\text{Cs}$  across the UK particularly after the Chernobyl event of 1986 was rather heterogeneous. The main factor controlling this was precipitation scavenging and topographic controls on the radioactive cloud (Tyler and Heal, 2000). Tyler et al., (1996) also state that variability of Chernobyl deposition occurs at all spatial scales.

The main properties and behavioural aspects of  $^{137}\text{Cs}$  are outlined below:

1. Soil association -  $^{137}\text{Cs}$  is a positively charged ion, and can become irreversibly sorbed to fine illite clay and strongly adsorbed to the organic fraction after deposition similar to K ions (Walling and Quine, 1991). Coleman and Le Roux (1965) and Sawny (1972) suggested that the retention of  $^{137}\text{Cs}$  is primarily due to the illite and mica clay content in

the soil. Distribution both vertically and spatially reflects mixing activities that have taken place within the soil since its deposition (Tyler et al., 2001). Movement of  $^{137}\text{Cs}$  is almost exclusively with soil particles (Wicherek and Bernard, 1995).  $^{137}\text{Cs}$  undergoes no reduction/oxidation reactions or complexation (Higgitt, 1995).

2. Soil and  $^{137}\text{Cs}$  redistribution - follows the catena slope principle which is enhanced by the mechanical redistribution of soil.  $^{137}\text{Cs}$  will reflect this accordingly - lower observed upslope  $^{137}\text{Cs}$  inventories in line with soil loss and higher  $^{137}\text{Cs}$  inventories at the foot of slopes corresponding with deposition.
3. Rate of distribution - given that the peak input of  $^{137}\text{Cs}$  was in 1962,  $^{137}\text{Cs}$  offers the opportunity to determine the rate of spatial soil erosion/deposition rates. The rates represent the mean time integrated estimate of erosion/deposition since c. 1962.
4. Depth distribution - Undisturbed sites display a near exponential decrease in  $^{137}\text{Cs}$  activity from the soil surface with increasing depth. Ploughing action simply mixes  $^{137}\text{Cs}$  activity into a homogeneous band in accordance with plough depth. This relative uniform distribution makes estimation of soil loss relatively easy.
5. Spatial uniformity - at the local scale (c. 1km) the initial distribution of weapons testing  $^{137}\text{Cs}$  following deposition can be assumed to relatively uniform.

#### Issues of soil incorporation of $^{137}\text{Cs}$

Soil is covered for the majority of time with varying types of vegetation which must influence the sorption process of  $^{137}\text{Cs}$  in soil. The majority of sorbed  $^{137}\text{Cs}$  is washed off vegetation and deposited directly on the soil (Davis, 1963 as quoted in Ritchie and McHenry, 1990). Rogowski and Tamura (1970a) claim that 93% of  $^{137}\text{Cs}$  applied to grass washed off during the first year. Absorption takes place as vegetation dies and is incorporated into the soil and released. Uptake of



$^{137}\text{Cs}$  is reported by various authors in the review of Ritchie and McHenry (Fredrickson et al., 1958; Davis, 1963; Dahlman et al., 1975).

Evidence in the last decade has ascertained the importance of cultivation practices on the spatial distribution of soil (Govers et al., 1993; Lindstrom et al., 1990; Lindstrom et al., 1992) and  $^{137}\text{Cs}$  (Govers et al., 1996; Govers et al., 1994; Quine, 1999a; Quine, 1999b; Quine et al., 1997; Quine and Zhang, 2002). Ploughing the soil acts as a mixing agent, therefore the exponential decrease in  $^{137}\text{Cs}$  with increasing depth over time becomes homogenised. The potential redistribution of  $^{137}\text{Cs}$  following deposition on to bare soil is likely to be minimal given the time of exposure and the proportion of  $^{137}\text{Cs}$  input compared to the total inventory. In addition, much of the soil is physically translocated by the plough implement in accordance with plough direction and slope gradient and aspect. In the short-term, spatial patterns of  $^{137}\text{Cs}$  activity develop and these offer a valuable insight into the erosion processes operating.

In summary,  $^{137}\text{Cs}$  is assumed to irreversibly couple to soil clay and therefore reflect patterns of soil movement both in a spatial sense across the landscape and with depth.

#### 4.1.1 Evolution of the $^{137}\text{Cs}$ tracer technique

The 1960s saw work begin on monitoring radionuclides alongside soil loss.  $^{90}\text{Sr}$  redistribution was related to soil loss (Menzel, 1960) and  $^{137}\text{Cs}$  was used for the first time by Rogowski and Tamura (1965) on small grass test plots. From this work a logarithmic relationship between soil loss and  $^{137}\text{Cs}$  was ascertained. Early work by Ritchie et al. (1974) developed a methodology for measuring soil loss from percentage loss of fallout  $^{137}\text{Cs}$ . Using the USLE (Wischmeier and Smith, 1978) soil loss was predicted and found to be strongly logarithmically related to fallout  $^{137}\text{Cs}$  loss from varying catchment land uses. The data was pooled with that of Menzel (1960), Rogowski and Tamura (1970a; 1970b) and others to gain an  $r$  value of 0.94 between soil loss ( $\text{t ha}^{-1} \text{yr}^{-1}$ ) and percentage  $^{137}\text{Cs}$  loss. They concluded that soil loss could be reliably measured via  $^{137}\text{Cs}$  loss. On the basis of these findings research within catchments to assess sediment redistribution patterns and how sediment leaves catchments became focused on  $^{137}\text{Cs}$  as a tool.

It emerged that at undisturbed sites, i.e. untouched non-eroded sites, the soil  $^{137}\text{Cs}$  inventory was equal to that of the fallout  $^{137}\text{Cs}$  deposited in that area and resided in the top of the soil profile (Ritchie and McHenry, 1990). Furthermore, it became clear that eroding sites consistently displayed lower  $^{137}\text{Cs}$  levels than amounts initially input through fallout. On the other hand depositional sites showed increased  $^{137}\text{Cs}$  levels when compared to fallout deposition and in addition  $^{137}\text{Cs}$  levels were found to increasing depth. Mapping the patterns of  $^{137}\text{Cs}$  activity therefore allowed erosion/deposition to be confidently estimated across the catchment (McHenry and Ritchie, 1977a). They also highlighted the possibility of building up a picture of soil movements at various scales.  $^{137}\text{Cs}$  was used to confirm that flat areas experienced little soil loss, and concave footslope zones frequently displayed deposition.

The cornerstone of the whole technique is the selection of a reference site to act as a baseline of total activity for the area studied. The site must be undisturbed, i.e. unmanaged and should display a total activity equivalent to that of total atmospheric input from fallout minus losses associated with radioactive decay

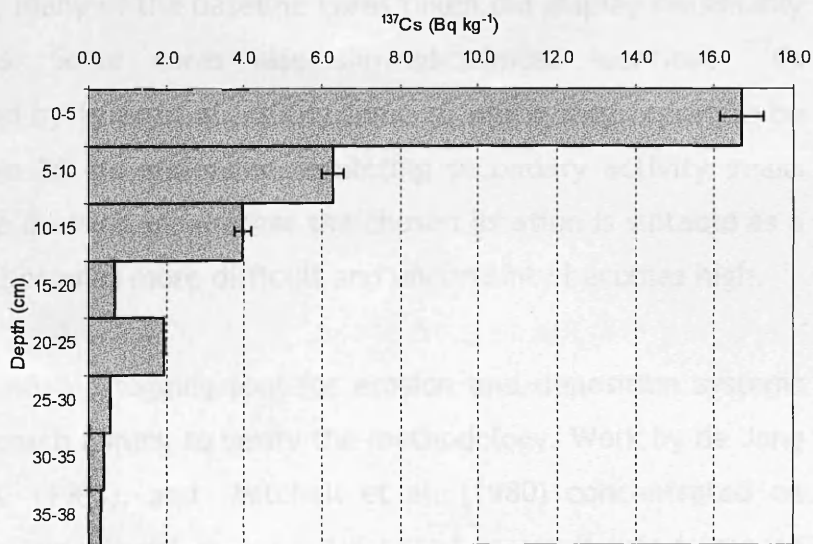


Figure 4.2. A typical  $^{137}\text{Cs}$  activity depth profile from the undisturbed site adjacent to the Loanleven research field, Perth and Kinross (NO 058 252).

(Quine and Walling, 1993) and be as close as possible to the area of interest. Any fluctuations of  $^{137}\text{Cs}$  activity level both spatially and with depth can therefore be attributed to soil movement since the pre-Test Ban Treaty era of deposition. The process of defining the baseline inventory plays a vitally important role in obtaining erosion/deposition values (Sutherland, 1991), yet has proved a

particularly difficult task in this study. Early work discovered that with depth in a stable uncultivated soil profile,  $^{137}\text{Cs}$  exhibits an exponential decrease in activity. Figure 4.2 shows such a site used as the reference for the baseline  $^{137}\text{Cs}$  inventory for the Loanleven research field used in this study. It is generally assumed that such a depth distribution is analogous to a stable uncultivated soil. Locating one close enough to the site of interest has been consistently difficult and taken up a considerable proportion of fieldwork as a whole. Further problems arise when distributions begin to depart from the exponential-like profile seen in Figure 4.2. Recent research carried out by Tyler et al. (2001), appears to throw further doubt over the assumption. Work carried out in southern Scottish upland soils clearly demonstrated how undisturbed soils are being homogenized up to depths of 20 cm by earthworm populations. Although it may be argued that upland soils are different to lowland agricultural soils in terms of faunal activity, many of the baseline cores taken did display reasonably rich worm populations. Some cores also showed almost identical  $^{137}\text{Cs}$  distributions as published by Tyler et al. (2001) some of which they report to be fully homogenized above 20 cm and some exhibiting secondary activity peaks lower in the profile. The decision of whether the chosen location is suitable as a reference/baseline site becomes more difficult and uncertainty becomes high.

Establishing  $^{137}\text{Cs}$  as a reliable tagging tool for erosion and deposition systems produced a surge of research aiming to verify the methodology. Work by de Jong (1982), Longmore et al. (1983), and Mitchell et al. (1980) concentrated on sediment distribution in agricultural systems. UK based research was triggered into action when Walling (1982) demonstrated that the  $^{137}\text{Cs}$  methodology had potential.

#### 4.1.2 Methodology of the $^{137}\text{Cs}$ tracer technique

Quine (1995) summarises the approach by proposing a number of necessary steps when applying the  $^{137}\text{Cs}$  tracer technique:

1. Collection of soil samples from the study field and a selected undisturbed reference site close by.

2. Ascertaining the  $^{137}\text{Cs}$  inventory (remaining  $^{137}\text{Cs}$  per unit area) both at points in the research field and at the reference site.
3. Calculation of  $^{137}\text{Cs}$  loss and gain at each sampled point in the field by comparison of  $^{137}\text{Cs}$  activity at the reference site.
4. Development of site-specific calibration relationships between  $^{137}\text{Cs}$  losses and gains with erosion and deposition rates.
5. Use of calibration relationships from point four to calculate estimates of soil erosion/deposition rates for each soil sample.

The crux of the technique is selection of a suitable calibration relationship. Empirically relating actual soil erosion/deposition with  $^{137}\text{Cs}$  loss/gain (Ritchie and McHenry, 1975) formed the basis upon which much of today's  $^{137}\text{Cs}$  work is carried out.

Such an approach demands detailed medium-term erosion/deposition monitoring records, which are generally rare. More importantly any resultant relationship established between the field and the reference site activity are very site specific and only transferable to other areas with identical land use history.

Approaches are two-fold - the directly proportional method and the mass-balance model. The directly proportional method takes the following form:

$$E_t = \frac{C_t - C_{t-1} - C_f}{C_e} \quad \text{Equation 4.1}$$

Where:  $C_t$  =  $^{137}\text{Cs}$  inventory at time t ( $\text{Bq m}^{-2}$ )

$C_f$  = Fallout input between time t-1 and t ( $\text{Bq m}^{-2}$ )

$C_e$  =  $^{137}\text{Cs}$  specific activity of soil between time t-1 and t ( $\text{Bq kg}^{-1}$ )

$E_t$  = Erosion rate between time t-1 and t ( $\text{Bq m}^{-2}$ )

D = decay constant.

Despite the obvious attractiveness Quine (1995) criticizes the assumption that all  $^{137}\text{Cs}$  input to the soil is subsequently mixed evenly throughout the plough profile. Loss of  $^{137}\text{Cs}$  from the surface during the period of deposition prior to erosion taking place is not accounted for in the directly proportional method.

When used in regions dominated by water and wind erosion this method will generate overestimates.

The mass balance approach attempts to simulate  $^{137}\text{Cs}$  loss and gain with erosion and deposition. It was developed by Kachanoski and de Jong (1984) and is expressed as:

$$E = M \left( \frac{C_i - C_r}{C_r} \right) \quad \text{Equation 4.2}$$

Where: E = total soil loss (per unit area) since start of  $^{137}\text{Cs}$  fallout.

M = mass of plough layer per unit area

$C_i$  =  $^{137}\text{Cs}$  at sample point

$C_r$  =  $^{137}\text{Cs}$  input at reference site

When applied Kachanoski and de Jong (1984) concluded that erosion rates between 0.5 and 10  $\text{kg m}^{-2} \text{yr}^{-1}$  could be estimated with reasonable precision. Erosion rates are also higher than those generated from the directly proportional method despite considering  $^{137}\text{Cs}$  deposition and tillage dilution. The term  $C_e$  (Equation 4.2) representing  $^{137}\text{Cs}$  content in eroded soil has become an area of intense debate in the literature. Estimating erosion/deposition accurately via which ever method therefore necessitates comprehensive and careful consideration of all  $^{137}\text{Cs}$  sources, sinks, and pathways.

De Jong et al. (1983) proposed what Lobb (1999) called a linear method of estimating soil loss rates.

$$A^* = \frac{\rho_c D_c (C_{s_0} - C_{s_i})}{Y C_{s_0}} \quad \text{Equation 4.3}$$

Where:  $A^*$  = mean annual soil loss ( $\text{kg m}^{-2} \text{yr}^{-1}$ )

$D_c$  = depth of  $^{137}\text{Cs}$  distribution in soil (m)

$\rho_c$  = Bulk density ( $\text{kg m}^{-3}$ )

$C_{s_i}$  = measured  $^{137}\text{Cs}$  activity in soil ( $\text{Bq m}^{-2}$ )

$C_{s_0}$  =  $^{137}\text{Cs}$  activity of undisturbed land ( $\text{Bq m}^{-2}$ ) (decay corrected)

Y = duration of erosion period considered (yr)

This method was compared by Lobb and Kachanoski (1996) with the methodology proposed by Walling and Quine (1990) in terms of estimative ability.

The Walling and Quine (1990) approach (power approach) is expressed as follows:

$$A^* = \frac{\rho_c D_c}{\eta} \left( 1 - (C_{si} / C_{so})^{1/Y} \right) \quad \text{Equation 4.4}$$

Where:  $A^*$  = mean annual soil loss ( $\text{kg m}^{-2} \text{yr}^{-1}$ )

$D_c$  = depth of  $^{137}\text{Cs}$  distribution in soil (m)

$\rho_c$  = Bulk density ( $\text{kg m}^{-3}$ )

$C_{si}$  = measured  $^{137}\text{Cs}$  activity in soil ( $\text{Bq m}^{-2}$ )

$C_{so}$  =  $^{137}\text{Cs}$  activity of undisturbed land ( $\text{Bq m}^{-2}$ ) (decay corrected)

$Y$  = duration of erosion period considered (yr)

$\eta$  = enrichment ratio ( $^{137}\text{Cs}$  in transported soil v till-layer)

Both approaches were applied to cultivated soils where tillage processes were dominant. The linear method (de Jong, 1983) delivered accurate measures of total redistribution but overestimated the extent of soil loss and underestimated maximum soil loss rate. The power method (Walling and Quine, 1990) estimated the maximum soil loss rate more accurately but over-estimated the extent of soil loss. Lobb (1996) attributed such errors to the fact that  $^{137}\text{Cs}$  poor subsoil is incorporated into the plough layer and subsequently translocated.

#### 4.1.3 Uncertainty and error

As with any sampling technique and laboratory work, there are many sources of inherent error resulting from assumptions or experimental technique. Sources of  $^{137}\text{Cs}$  contributing to soil activity include atmospheric fallout, input via water/wind sediment deposition, and influx due to tillage. Loss of  $^{137}\text{Cs}$  occurs via sediment water/wind erosion, vegetation uptake, outflux due to tillage, radioactive decay and loss via harvesting (removal of soil from field). Tillage mixing, both vertical and horizontal, and sediment transport processes are

pathways influencing distribution of  $^{137}\text{Cs}$ . These must be addressed in any calibration technique.

Potentially one of the most important discoveries is that of particle size selectivity. The first attempt to integrate particle size selectivity into the calibration process (Kachanoski and De Jong, 1984) was done through the use of an enrichment factor. Walling and Woodward (1992) found that  $^{137}\text{Cs}$  preferentially adsorbed to the finer fraction of soil. This may lead to the technique tracking the movement of finer material as opposed to the soil as a whole. Research carried out by Quine and Walling (1991) did expose a slight bias towards the finer fractions (30% of  $^{137}\text{Cs}$  content in <1mm fraction) after wet sieving the mass of the <1mm fraction was reduced by a third and the  $^{137}\text{Cs}$  content by 50%. The authors tentatively suggest that despite the skew towards finer material the overall redistribution picture will not be significantly affected. However, upon examining differing topographic locations within fields (slope and ridge segments)  $^{137}\text{Cs}$  inventories were statistically significantly different when compared with swale  $^{137}\text{Cs}$  inventories.

One of the largest uncertainty factors is that caused by  $^{137}\text{Cs}$  variability in non-eroding sites. Higgitt (1990) notes that coefficients of variation at such sites in the UK are generally <15%. In the light of such variability in  $^{137}\text{Cs}$  activity at undisturbed sites, the question of how many samples are required to estimate the local  $^{137}\text{Cs}$  baseline inventory must be addressed. Sutherland (1991) attempted to calculate this allowing an error of 10% at 95% CI. Estimating the mean  $^{137}\text{Cs}$  baseline activity requires 4 samples under a 10% variation (CV), 16 samples with a 20% CV and 35 samples with a 30% CV. It seems fair that the distribution of bomb-derived  $^{137}\text{Cs}$  has been uniform across the area research (Walling and Quine, 1991) to due to long-term deposition. However, further inputs of  $^{137}\text{Cs}$  generated from the 1986 Chernobyl disaster were not uniform. Walling, (1991) presented maps of Chernobyl deposition, which exhibits strong relationship with topography. Fallout from this event was highly spatially heterogeneous (Tyler et al., 1996) being controlled by synoptic meteorological circulation and rainfall and over, in many cases, one event. Although a general map, northern parts of the study area could possibly have been affected by such deposition. In such cases Walling, (1991) cautions the use of the technique.

#### 4.1.4 Applications

The number of published research projects using the  $^{137}\text{Cs}$  technique is particularly high and therefore it is not possible to review them all. Selected applications either in the archaeological context or in other closely related themes are considered.

Use of  $^{137}\text{Cs}$  as a monitoring tool is generally applied only at large-scales, i.e. fields, or small catchments. The method requires high-density sampling, which in the case of archaeological sites is particularly unfavourable due to site disturbance (Davidson et al., 1998; Tyler et al., 1998). Furthermore, time limitations often become severe when sampling since laboratory processing and analysis demands periods of months for a field (Tyler et al., 2001b; Walling and Quine, 1991). Sampling may be reduced to compensate for time available but at the cost of spatial resolution, so careful planning is required.

Studies in Quebec, Canada examined both the loss of  $^{134}\text{Cs}$  under simulated conditions and more interestingly the redistribution of  $^{137}\text{Cs}$  in some 63 fields under varying conditions of slope, soil texture, and land use (Bernard and Laverdiere, 1993). It was found that mean soil loss was not significantly different between the 4 textural classes studied. The effect of slope was more clear; 4.1, 6.1, and 7.2 t ha<sup>-1</sup> yr<sup>-1</sup> were estimated for slopes of <2%, 2-5% and >5% respectively and losses of 3 t ha<sup>-1</sup> yr<sup>-1</sup> on dairy farms and 10.9 t ha<sup>-1</sup> yr<sup>-1</sup> on horticultural farms were observed. As a summary the researchers summarise a rapid decrease in  $^{137}\text{Cs}$  within the first 30-150m of the slope, followed by a smaller rate with erratic oscillations in levels, representative of alternative erosion and deposition. Beyond 150m  $^{137}\text{Cs}$  activity increased, indicating redeposition.

Across many agricultural areas the basic landscape unit is the field. Hedges and fences, act as physical boundaries to the movement of soil and thus complete removal of soil from the field rarely occurs. Therefore, 'soil loss' as so commonly termed should possibly be termed more realistically 'soil redistribution' within an agricultural context. Froehlich et al. (1993), investigated field plots in southern Poland which were segmented by terraces.



From their study there were striking amounts of  $^{137}\text{Cs}$  in the cores sampled at the terrace edges as well as the depth to which  $^{137}\text{Cs}$  was found in comparison to average levels inside the plots.  $^{137}\text{Cs}$  levels immediately below the terrace were similar to mid-plot levels. Froehlich, (1993) noted also from his 2 year monitoring that even in the presence of high levels of soil movement it did not represent a significant transfer of sediment to the streams. Tyler, (2001b) and Davidson et al, (1998) using traditional soil core derived  $^{137}\text{Cs}$  and in-situ spectrometry have also examined the spatial pattern in erosion rates within a field unit in Perth and Kinross, Scotland in the context of archaeological cropmark sites. They confirm maximum soil loss rates of  $2\text{mm yr}^{-1}$  just downslope of the shoulder convexity and maximum deposition levels at the slope base ( $2\text{mm yr}^{-1}$ ). Use of the  $^{137}\text{Cs}$  method successfully quantified the gradual truncation of the soil profile. The threat of damage presented to the cropmark site was in this case increased both by the accelerated net loss of soil due to the plough and physical planing of the cropmark itself.

Zhang, (1998) measured erosion rates on a Chinese loess plateau by comparing a conventional rill volume technique and the  $^{137}\text{Cs}$  technique. They concluded that the two techniques produced results in close agreement and reiterate caesium's solid potential. Quine et al. (1997) in similar studies showed that  $^{137}\text{Cs}$  derived water erosion patterns also strongly reflected patterns from field rill measurements. The  $^{137}\text{Cs}$  technique has also received mixed appraisals on occasion (Wicherek and Bernard, 1995) whereby comparison of rill volumes and  $^{137}\text{Cs}$  erosion estimates in a small Parisian catchment highlighted  $^{137}\text{Cs}$  overestimating erosion by approximately 50%.

The  $^{137}\text{Cs}$  technique has been specifically applied to archaeological sites under cultivation to assess rates of erosion (Davidson et al., 1998; Tyler et al., 1995; Tyler et al., 1998; Tyler et al., 2001b) within lowland Central Scotland. Traditional techniques of extracting soil cores may not be appropriate at such sites due to their invasive nature. In addition, many of the sites are protected as Scheduled Ancient Monuments, therefore it is paramount to avoid damage. Tyler (1999; 1996b) has developed an innovative technique allowing in-situ measurements of  $^{137}\text{Cs}$  to be taken, removing any threat of site damage. Results indicate that  $^{137}\text{Cs}$  inventories detected using the in-situ method agree closely to

inventories gained by conventional coring techniques. Variability of  $^{137}\text{Cs}$  activity has been further highlighted in these studies and that high-resolution sampling is necessary if an accurate and precise picture of erosion is required. Such a technique also reduces tedious man-hours involved with laboratory sample preparation.

The  $^{137}\text{Cs}$  technique offers a great opportunity to monitor intra-field soil movement active within the last 40 years and more so, to validate and calibrate performance of distributed soil erosion models. The application of the  $^{137}\text{Cs}$  technique is innovative and offers great potential for archaeological site damage risk assessment.

## 4.2 Sampling methodology

The topography and general sampling layout of the 4 research fields have been detailed in chapter 1. Each field has a 25 x 25 m grid overlay which corresponds exactly to the layout of the grids used for GIS modelling purposes. Each grid cell surveyed on the field represents a cell in all modelling grids allowing direct comparison between model layers within a GRID stack (Figure 4.3).

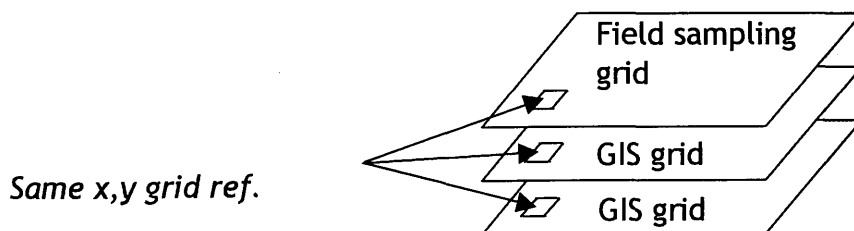


Figure 4.3. Layout and comparability of the field sampling grid and the GIS grids.

Before devising a sampling grid the topography and location of the archaeological features within each field was studied carefully (Figure 1.17, Figure 1.19, Figure 1.21, Figure 1.23). Since the project aims to estimate soil erosion directly threatening buried archaeological features, the sampling grid had to bisect/encroach the main body of the archaeological features. Transects have been laid across the archaeological site(s) in such a way as to then follow

the line of steepest slope. Using a grid (Figure 4.3) system for sampling may pose restriction on the orientation of the final transect due to bias in eight directions, however in all cases it caused no restriction. The main reason for grid sampling was to allow full integration with the GIS modelling outputs.

To address the problem of variability within each 25 x 25 m cell, 5 samples were taken in the form of a five on a dice. Each corner sample point was taken exactly 12m out from the centre point (approximately 5.5m in the from the corner).

Cores were taken using a manual golf hole corer developed by Tyler (1994) with extended cutting blades to a length of 40cm and a core diameter of 10.5cm (Figure 4.4). The corer was hammered into the soil as far as physically possible, the sample extracted, sealed in an airtight bag and returned to the lab for preparation. Note was taken of the depth of the topsoil at each core. Initially the core was split into half (top and bottom) and then:



Figure 4.4. Golf hole corer used throughout the project to obtain soil cores.

1. Oven dried at approx. 100°C for 24 hours
2. Manually sieved to < 2mm.
3. Manual homogenisation.
4. All <2mm soil ground using a Gyromill
5. sub-sample taken from each half placed in small beaker.

The samples were then counted for between 30 000 and 80 000 seconds in an n-type, 35% relative efficiency HPGe gamma spectrometer. Specific activities were corrected for stone content. After completing gamma spectrometry at the first site (Loanleven) using the top and bottom sectioning technique, it became clear that a less time-consuming way of obtaining a representative core  $^{137}\text{Cs}$  activity had to be used. There would have been insufficient time to complete

the second half of the sites. Therefore, at the three remaining sites each core was homogenized thoroughly from which sub-samples were then taken. Although not ideal, this reduced the detector time by approximately 50% securing analysis of all 4 sites. However, by taking one 200g sub-sample from a core of on average 3 kg increases the risk of inaccurately representing the mean specific concentration. Furthermore, it demands a robust system of homogenisation to limit variability. To test the methodology used and examine  $^{137}\text{Cs}$  variability after bulking and mixing, two cores were selected and five replicate sub-samples were taken from each. Table 4.1 summarises the results from the investigation. The main encouraging aspect of the results was that variability was low (<7%, only marginally larger than percentage analytical error in table 4.1) and that both cores exhibited good consistency in  $^{137}\text{Cs}$  activity. The method of homogenising the whole core, taking one sub-sample as representative, was therefore justified.

Mapping of the sampling grids in the field was accomplished using digital field boundary datasets within the surveying software LISCAD, EDM surveying techniques and field tapes.

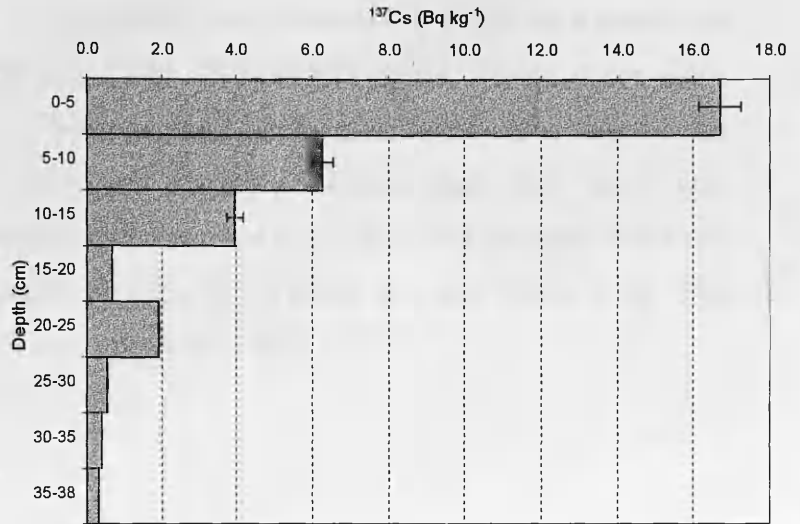
Cell	Bulk wet weight (g)	Bulk dry weight (g)	<2mm (g)	Spectrometer sampe size (<2mm in g)	Top soil depth (cm)	Cs-137 Bq kg <sup>-1</sup>	% Error	Corrected Cs-137	Cs Bq m <sup>-2</sup>
4NE a	3491	2715	2110	221.1	34	9.98	4.3	7.754	2431.45
b				226.03		9.52	5.4	7.402	2320.97
c				214.42		10.61	3.9	8.242	2584.27
d				219.67		10.65	4.7	8.274	2594.26
e				217.89		11.28	3.2	8.766	2748.51
								mean	2535.89
								stdev	164.36
								cv	6.48
								% error	2.90
8SW	3611	2888	1988	189.65	37	9.31	4.3	6.407	2137.06
8 SWa				214.55		9.85	3.4	6.780	2261.36
8 SWb				221.03		9.43	3.5	6.494	2165.85
8 SWc				201.11		10.50	4.8	7.227	2410.51
8 SWd				217.01		9.46	5.5	6.514	2172.79
								mean	2229.51
								stdev	111.35
								cv	4.99
								% error	2.23

Table 4.1. Results of the investigation into variability of  $^{137}\text{Cs}$  within cores after bulk homogenisation.

### 4.3 Baseline $^{137}\text{Cs}$ activity at reference sites

#### 4.3.1 Loanleven

Figure 4.5.  $^{137}\text{Cs}$  depth profile at the Loanleven field site.



Depth	$^{137}\text{Cs}$ Bq kg <sup>-1</sup>	$^{137}\text{Cs}$ Bq m <sup>-2</sup>	Total Bq m <sup>-2</sup>
North top (0-15cm)	8.92	1441.33	1503.65
Bottom (16-30)	0.32	62.32	
Central top (0-15cm)	8.17	1365.16	1813.82
Bottom (16-30)	2.1	448.66	
South top (0-15cm)	7.45	1258.56	1743.37
Bottom (16-30)	2.54	484.81	

Table 4.2.  $^{137}\text{Cs}$  inventories at the Loanleven reference site.

Depth (cm)	$^{137}\text{Cs}$ Bq kg <sup>-1</sup>	$^{137}\text{Cs}$ Bq m <sup>-2</sup>
0-5	16.69	1126.20
5-10	6.28	328.73
10-15	3.96	265.84
15-20	0.67	37.93
20-25	1.93	98.80
25-30	0.55	32.82
30-35	0.39	23.48
35-38	0.32	12.50
		<b>1926.29</b>

Table 4.3. Depth incremented  $^{137}\text{Cs}$  activity.

Table 4.4. Summary of variability measurements between the 3 reference cores at Loanleven.

Mean total ref. activity (Bq m <sup>-2</sup> )	1746.79
St. Dev	178.74
CV	10.23
St. Err	89.37
% error	5.12

Immediately adjacent to the Loanleven field was a small field of permanent grass used for sheep grazing. 3 preliminary bulk cores were taken as a means of quickly testing for disturbance in a rough and ready manner. These cores were split into two (top and bottom), homogenized, and sub-samples were taken from both. Analysis of specific activities strongly hinted that the land was undisturbed. Subsequently a depth-incremented core (5cm increments) was then taken to confirm the  $^{137}\text{Cs}$  depth distribution (Figure 4.5 and Table 4.3). The mean activity of all reference cores was  $1746.79 \text{ Bq m}^{-2}$ .

### 4.3.2 Blairhall

Undisturbed sites representing fieldsite two at Blairhall were located at Perth Racecourse (Figure 4.6 and Table 4.5, Figure 4.7 and Table 4.6). Three cores were taken and a further check was carried out with core three taken from the Perth racecourse to examine how effective the depth incremented sampling was at defining the overall  $^{137}\text{Cs}$  inventory of a core. The whole core was prepared in the way described, however, this time all of the gyromilled soil was placed into pots. The core produced some 2.065kg of < 2mm fraction, which was equivalent to 12 sample pots. The  $^{137}\text{Cs}$  activity of all 12 pots was counted. This provided a high confidence benchmark activity level totally devoid of any heterogeneity involved in the mixing of each depth increment.

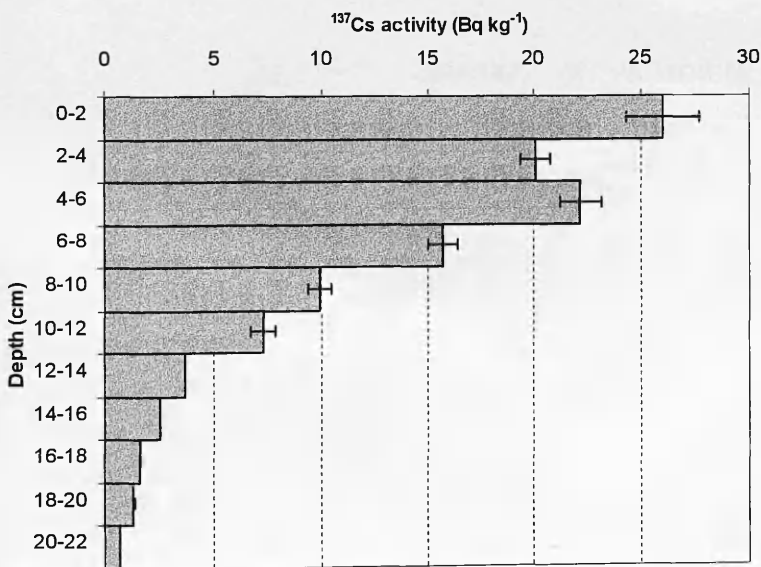


Figure 4.6.  $^{137}\text{Cs}$  depth profile of core 1 at the Blairhall reference site.

Depth (cm)	$^{137}\text{Cs}$ Bq kg <sup>-1</sup>	$^{137}\text{Cs}$ Bq m <sup>-2</sup>
0-2	26.02	158.43
2-4	20.03	235.31
4-6	22.16	271.96
6-8	15.72	403.57
8-10	9.94	284.53
10-12	7.3	232.11
12-14	3.66	106.99
14-16	2.53	59.27
16-18	1.65	43.14
18-20	1.34	20.17
20-22	0.70	20.30
		1834.78

Table 4.5.  $^{137}\text{Cs}$  inventory of core 1 at the Blairhall reference site

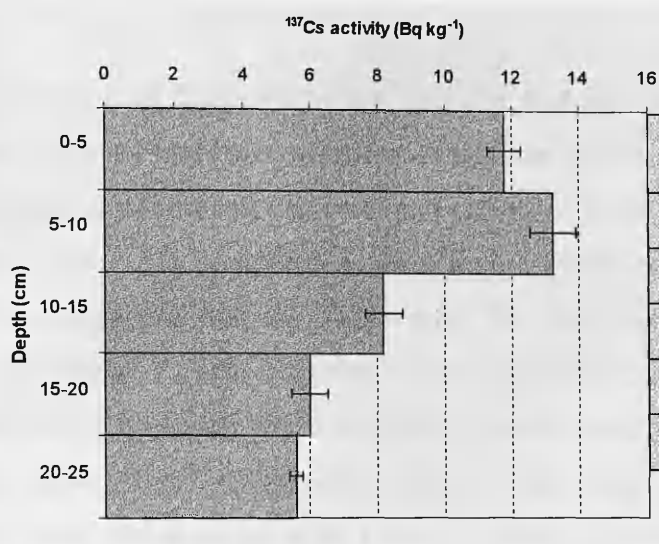


Figure 4.7. <sup>137</sup>Cs depth profile of the core 2 at the Blairhall reference site.

Table 4.6. <sup>137</sup>Cs inventory of core 2 at the Blairhall reference site.

Depth (cm)	<sup>137</sup> Cs Bq kg <sup>-1</sup>	<sup>137</sup> Cs Bq m <sup>-2</sup>
0-5	11.79	357.77
5-10	13.22	712.01
10-15	8.19	462.42
15-20	6	275.91
20-25	5.58	158.25
		1966.37

Table 4.7. Summary of variability measurements between the 3 reference cores at Blairhall.

Mean total ref. activity (Bq m <sup>-2</sup> )	1879.60
St. dev	75.15
CV	4.00
St. error	37.58
% error	2.00



Comparison of this benchmark activity and the other two total inventory cores was made to highlight whether or not the depth incremented sub-sampling was capable of accurately determining the total core  $^{137}\text{Cs}$  inventory. Once again the intra-core  $^{137}\text{Cs}$  variability is very low, further confirming the efficiency of the homogenisation method (Table 4.8). The total activity inventory compared well to the other 2 cores creating a mean reference site activity of  $1879.60 \text{ Bq m}^{-2}$ . Variability between the 3 reference cores taken is presented in Table 4.7. Core one and two did reveal differences in the shape of the depth activity profiles. Both sites were assumed to be undisturbed on the basis of information provided by the racecourse manager. The racecourse has been established just over 100 years and since that time no modification or development has taken place. The only likely explanation for the difference maybe increased bioturbation.

Core	Depth	Bulk wet weight (g)	Bulk dry weight (g)	<2mm (g)	Spectrometer sampe size (<2mm in g)	Measured Cs-137 Bq kg-1	% Error	Corrected Cs-137 Bq kg-1	Cs Bq m-2
Core 3	whole core	2748.9	2148.9	2065.8					
subsamples	1				162.89	7.1589	8.1	6.88	129.47
	2				157.01	8.5819	3	8.25	149.60
	3				163.53	8.5091	6.5	8.18	154.49
	4				174.69	7.8831	5.9	7.58	152.89
	5				173.94	8.2254	6.8	7.91	158.84
	6				162.97	8.0926	5.8	7.78	146.42
	7				170.99	7.8072	6.7	7.51	148.21
	8				174.79	8.0388	5.6	7.73	156.00
	9				175.28	8.4575	6.9	8.13	164.59
	10				174.82	7.6302	5.9	7.34	148.10
	11				179.7	8.5981	6.3	8.27	171.54
	12				163	8.7035	2.7	8.37	157.51
								<b>Total</b>	<b>1837.65</b>
								<b>mean</b>	<b>153.14</b>
								<b>stdev</b>	<b>10.44</b>
								<b>cv</b>	<b>6.82</b>
								<b>%error</b>	<b>1.97</b>

Table 4.8. Examination of baseline  $^{137}\text{Cs}$  core activity by counting gamma activity in *all* <2mm material.

### 4.3.3 Leadketty

This site proved the most difficult to define. Many attempts all revealed disturbance or suspiciously high levels of activity. Table 4.9 summarises the depth incremented activity.

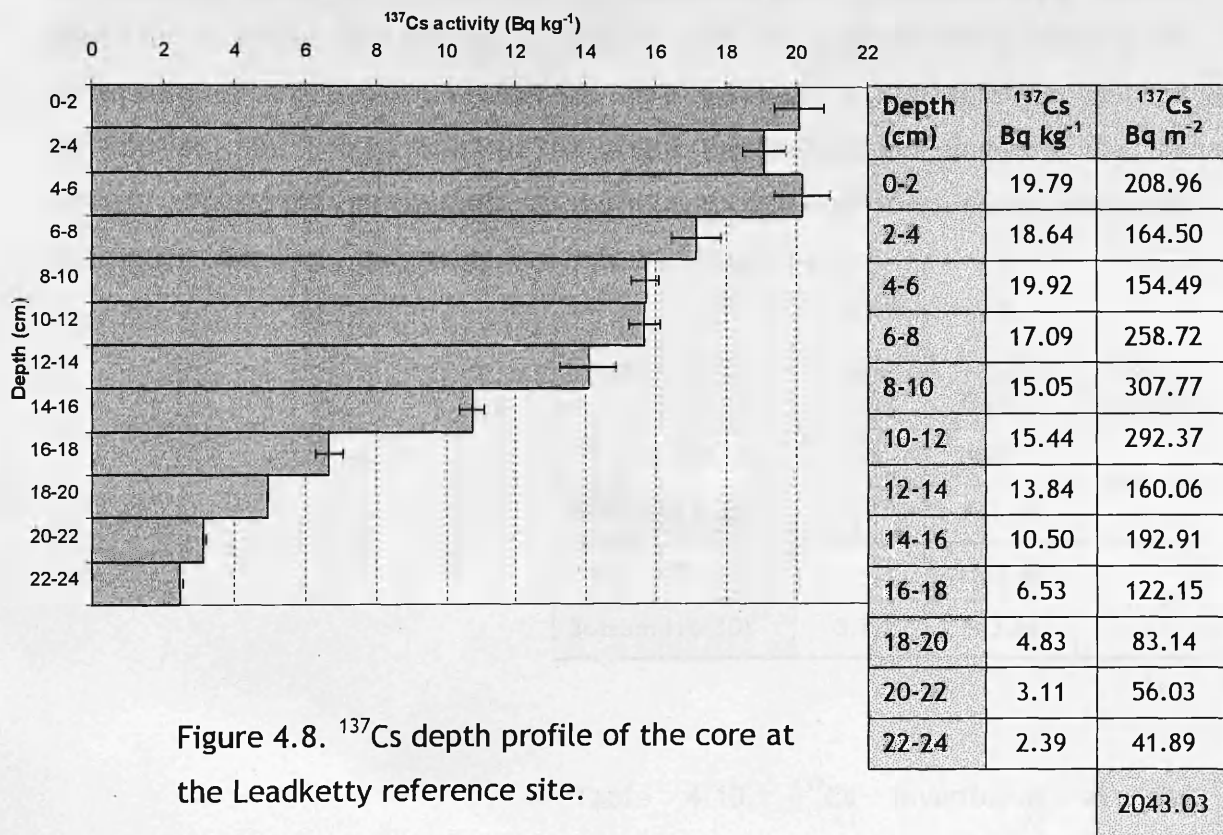


Figure 4.8. <sup>137</sup>Cs depth profile of the core at the Leadketty reference site.

Table 4.9. <sup>137</sup>Cs inventory of the core at the Leadketty reference site.

The <sup>137</sup>Cs depth profile again has not shown the expected exponential-like decrease. The reference site could have in no way been cultivated due to its dimensions and guarantee was given by the farmer that no cultivation had taken place in his generation (aged mid to late fifties). Bioturbation could be responsible although the profile does appear to have a slight bias in activity towards the top. Six potential reference sites were tested for suitability and all proved to be disturbed. This site was the seventh and last tested and possessed the closest exponential-like activity profile.

#### 4.3.4 Littlelour

To gain preliminary results of disturbance, two cores were taken and simply split into top and bottom sections as with the Loanleven site. The  $^{137}\text{Cs}$  inventories are presented in Table 4.10. Both strongly suggested non-disturbance so a further depth incremented core was taken. Results from this analysis are in Table 4.11. By examining the depth incremented core in Figure 4.9 it is clear that its distribution does not conform to the classic exponential-like decrease in  $^{137}\text{Cs}$  activity as is normally expected. Activity levels between the 3 cores were very consistent once more exhibiting less than 8% variability (cv).

Depth	$^{137}\text{Cs}$ Bq kg <sup>-1</sup>	$^{137}\text{Cs}$ Bq m <sup>-2</sup>	Total Bq m <sup>-2</sup>
1 top (0-15cm)	7.72	1405.35	2246.73
Bottom (16-30)	4.15	841.37	
2 top (0-15cm)	7.40	1347.60	2111.29
Bottom (16-30)	3.77	763.68	

Table 4.10.  $^{137}\text{Cs}$  inventories at the Littlelour reference site.

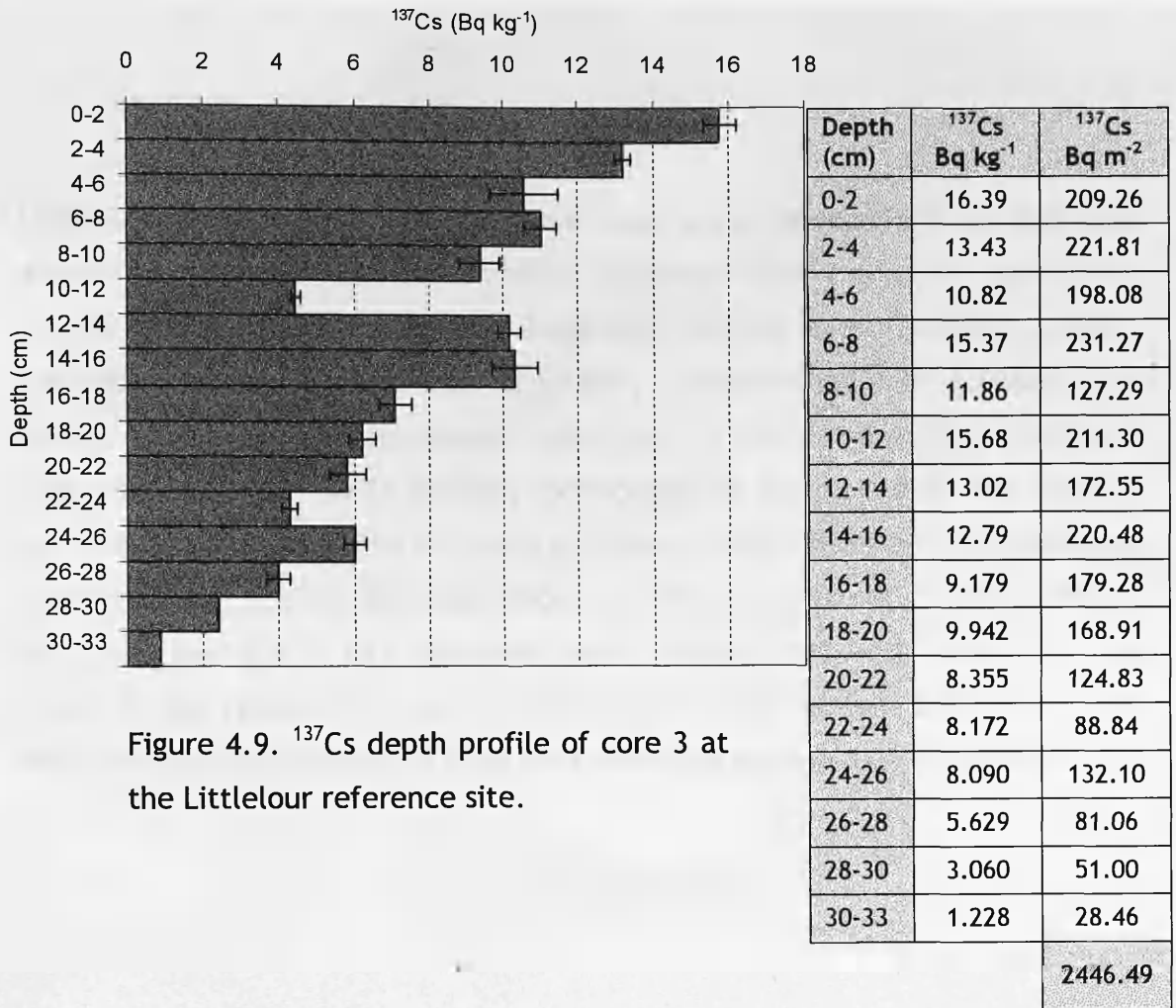


Figure 4.9. <sup>137</sup>Cs depth profile of core 3 at the Littlelour reference site.

Table 4.11. <sup>137</sup>Cs inventory of depth incremented core 3 at the Littlelour reference site.

Table 4.12. Summary of variability measurements between the 3 reference cores at Littlelour.

Mean total ref. activity (Bq m-2)	2268.17
St. Dev	168.63
CV	7.43
St. Err	97.36
% error	4.29

#### 4.3.5 Summary

At the Loanleven, Blairhall and Littlelour fields undisturbed reference sites were successfully located and subsequently displayed the expected exponential activity with depth in the profiles. Tests were carried out to examine whether the sub-sampling of cores was accurately representing  $^{137}\text{Cs}$  activity after homogenisation. Variability between reference site cores at the three mentioned sites was very low (<7%) allowing confidence to be placed in the results. Uncertainty surrounding the representativeness of depth increment sub-sampling from cores can also be dismissed since variability between all three cores was also very low (CV = 4%). Problems were encountered with Leadketty and therefore the results there need to be treated with caution. Reference cores demonstrated some departure from the theoretical exponential-like profile.

#### 4.4 Estimation of soil erosion/deposition (calibration).

Total  $^{137}\text{Cs}$  activity per unit area for each point per cell of each transect was calculated accounting for stone content. A mean value (from five cores) was taken to represent the activity at each cell. Conversion of point  $^{137}\text{Cs}$  activity per unit area to unit area soil erosion/deposition values was facilitated by the mass balance model developed by Zhang et al. (1990).

$$\text{Re} = H\nu \left( 1 - \left( \frac{X}{Y} \right)^{1/N-1963} \right) \quad \text{Equation 4.5}$$

Where: Re = soil erosion rate ( $\text{kg m}^{-2} \text{yr}^{-1}$ )  
H = depth of plough layer (m)  
 $\nu$  = bulk density of soil ( $\text{kg m}^{-3}$ )  
X = measured  $^{137}\text{Cs}$  activity in field ( $\text{Bq m}^{-2}$ )  
Y = local  $^{137}\text{Cs}$  reference activity ( $\text{Bq m}^{-2}$ )  
N = year of sampling

This model requires minimum parameterisation, yet has well documented assumptions. One of the requirements is a uniformly homogenised plough layer. Furthermore, where water erosion has been active this model is reported to overestimate soil loss (Zhang et al., 1998). Figure 4.10 to Figure 4.12 illustrate the spatial distribution of  $^{137}\text{Cs}$  activity, calibrated erosion/deposition budgets and error analysis across the 4 field site transects. Negative values quoted throughout represent erosion and positive values deposition.

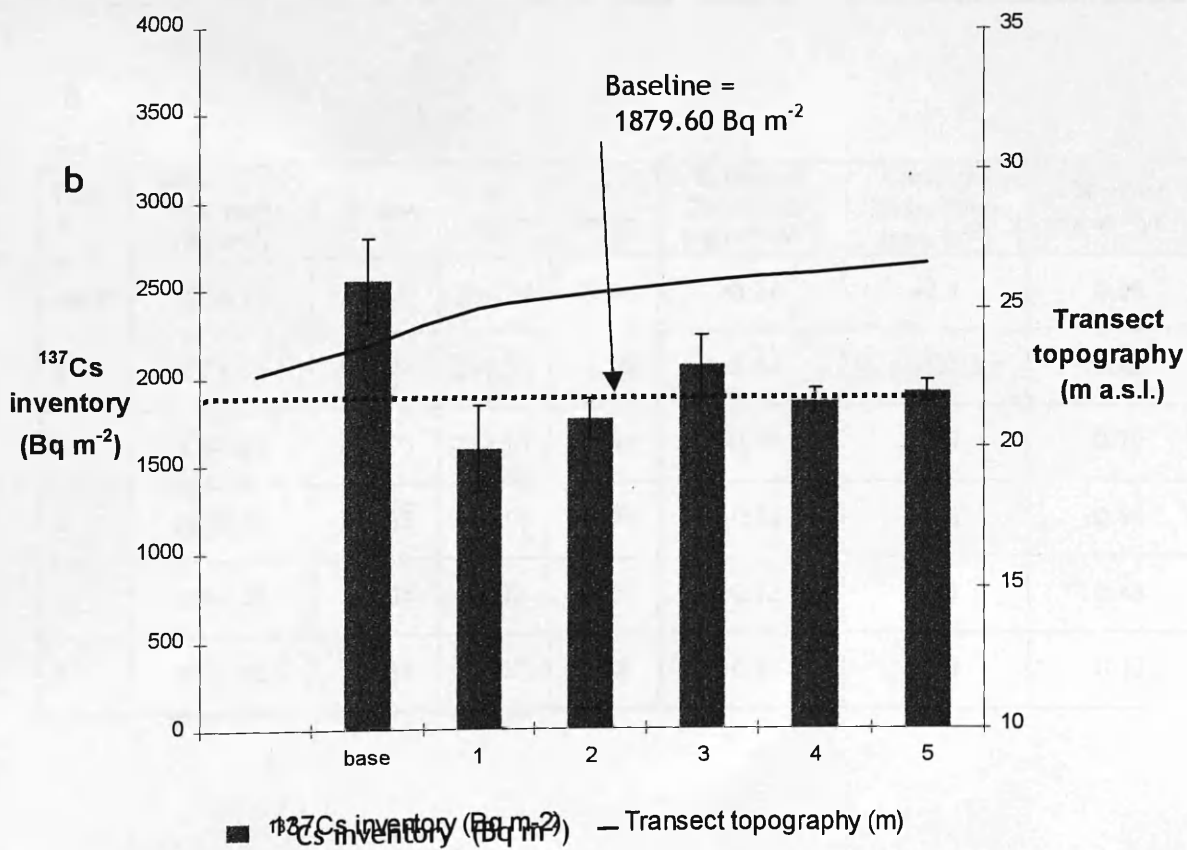
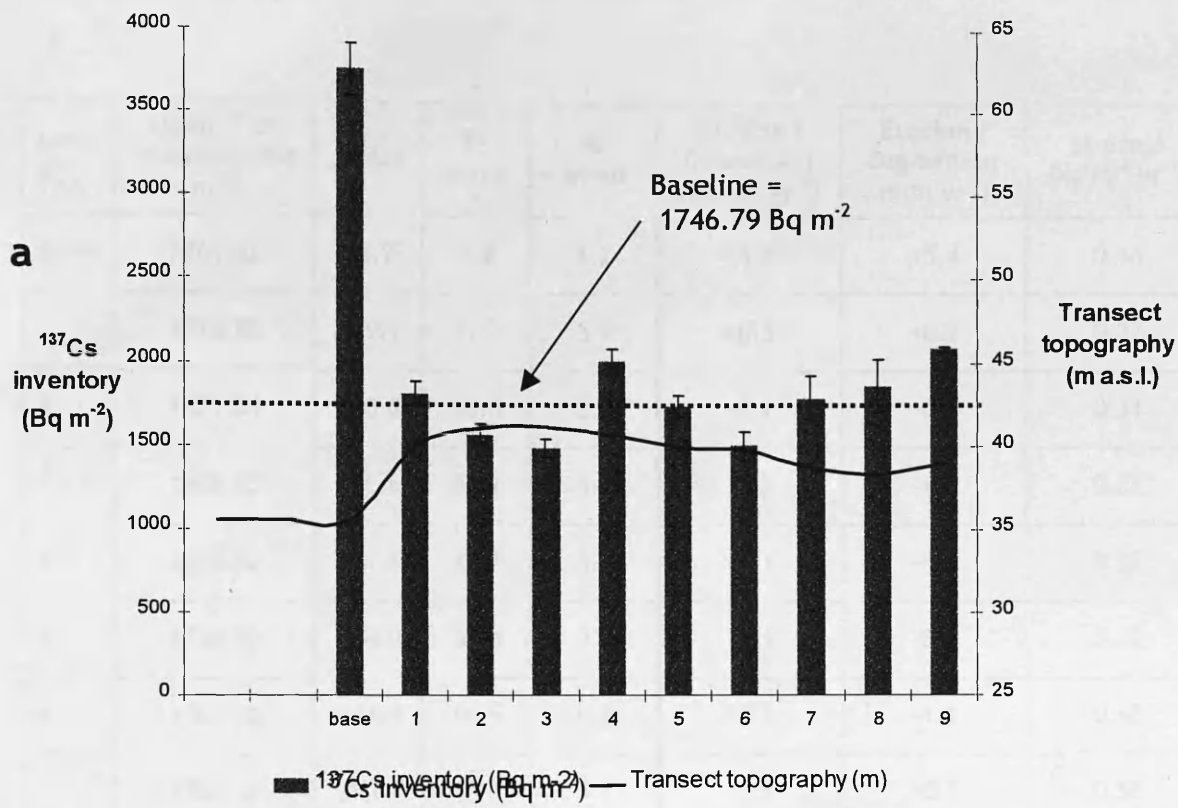


Figure 4.10. Distribution of  $^{137}\text{Cs}$  inventories across the Loanleven transect a) and Blairhall transect b).

a

Cell #	Mean <sup>137</sup> Cs inventory (Bq m <sup>-2</sup> )	St dev	St error	% error	Erosion / Deposition (kg m <sup>-2</sup> yr <sup>-1</sup> )	Erosion / Deposition (mm yr <sup>-1</sup> )	St error (kg m <sup>-2</sup> yr <sup>-1</sup> )
Base	3761.42	43.9	1.2	1.2	+6.4	+5.4	0.46
1	1815.82	159.1	71.2	3.9	+0.3	+0.2	0.32
2	1571.54	130.8	58.5	3.7	-0.9	-0.8	0.31
3	1486.83	125.6	56.2	3.8	-1.3	-1.1	0.31
4	2010.52	171.6	76.7	3.8	+1.1	+1.0	0.32
5	1739.15	144.0	64.4	3.7	-0.1	-0.1	0.32
6	1501.30	193.4	86.5	5.8	-1.3	-1.1	0.48
7	1791.32	285.1	127.5	7.1	+0.1	+0.1	0.58
8	1862.49	264.3	158.5	8.5	+0.4	+0.3	0.72
9	2081.94	33.3	14.9	14.9	+1.4	+1.2	0.49

b

Cell #	Mean <sup>137</sup> Cs inventory (Bq m <sup>-2</sup> )	St dev	St error	% error	Erosion / Deposition (kg m <sup>-2</sup> yr <sup>-1</sup> )	Erosion / Deposition (mm yr <sup>-1</sup> )	St error (kg m <sup>-2</sup> yr <sup>-1</sup> )
Base	2558.73	62.83	241.24	2.5%	+3.34	+2.1	0.09
1	1598.61	539.44	241.24	33.7%	-2.14	-1.3	1.43
2	1763.25	256.05	114.51	14.5%	-0.78	-0.5	0.70
3	2068.12	393.68	176.06	19.0%	+0.88	+0.6	0.92
4	1864.47	161.04	72.02	8.6%	-0.12	-0.1	0.43
5	1923.06	129.84	58.07	6.8%	+0.23	+0.1	0.33

Table 4.13. <sup>137</sup>Cs activity and derived erosion/deposition estimates for a) Loanleven and b) Blairhall.



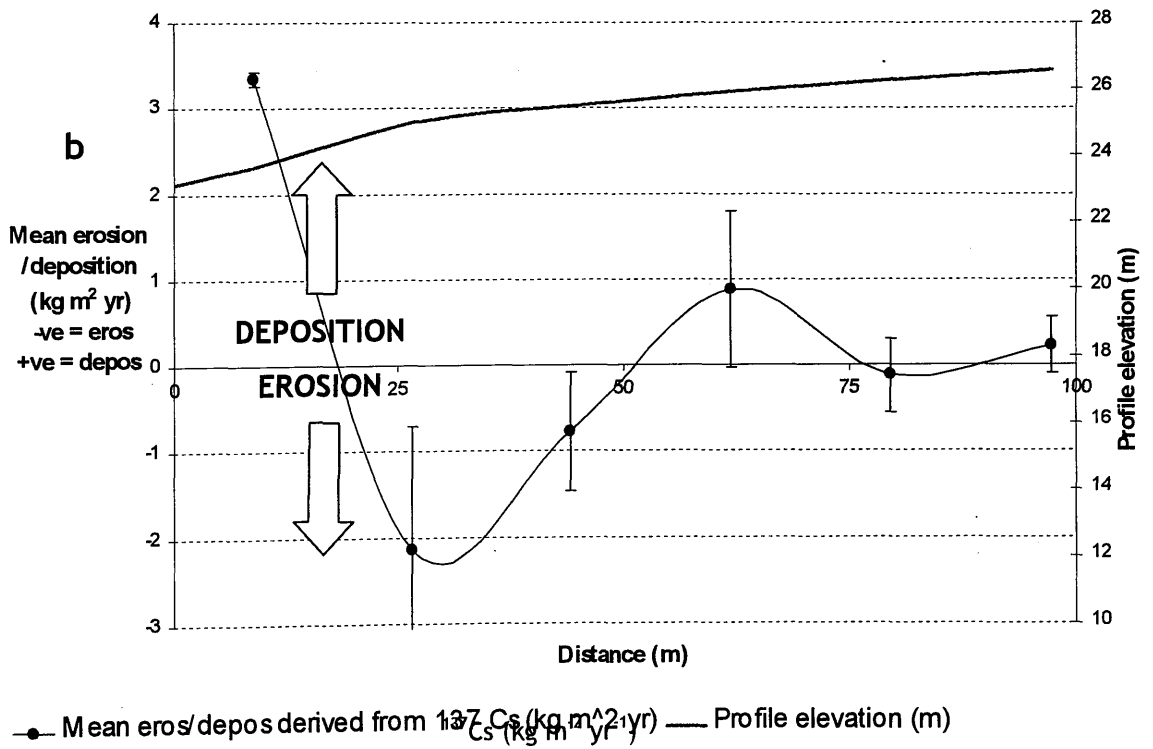
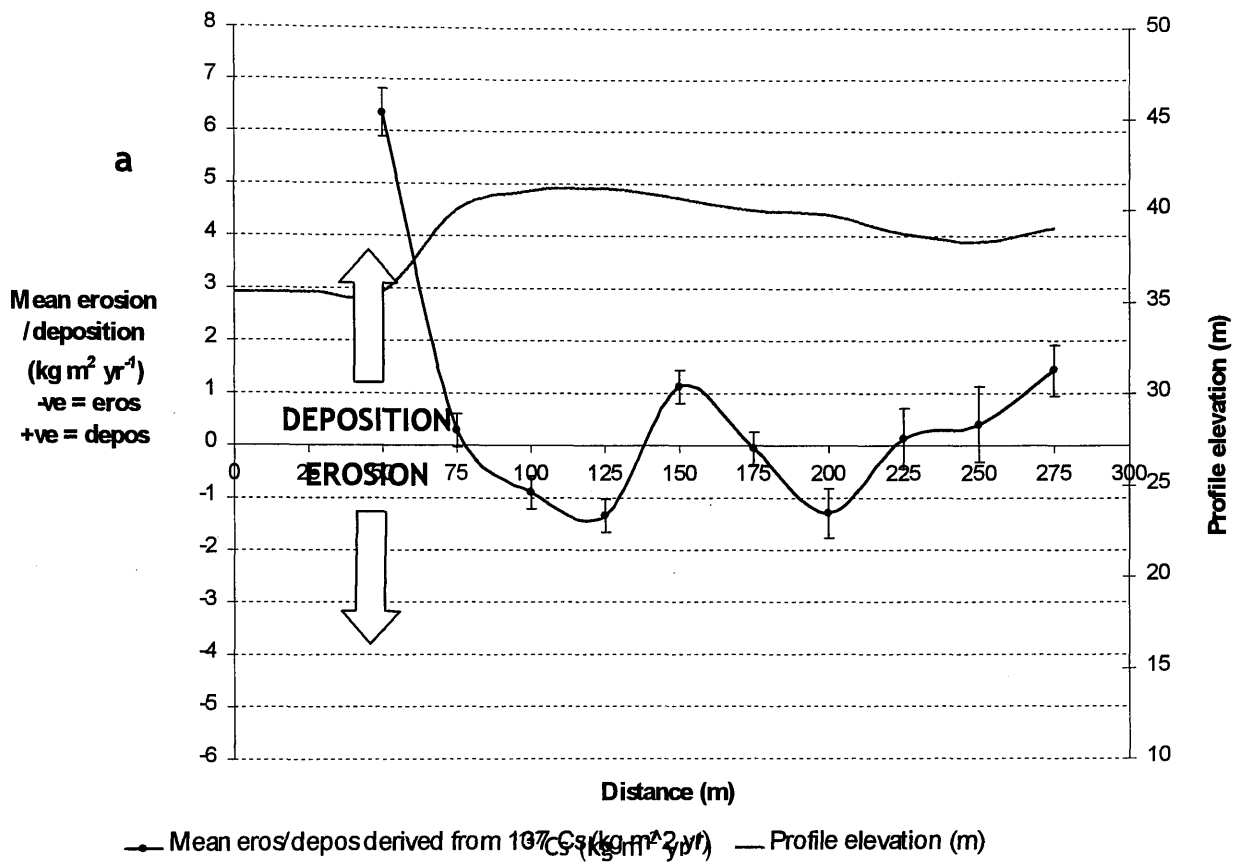


Figure 4.11.  $^{137}\text{Cs}$  derived erosion/deposition estimates across the Loanleven transect a) and the Blairhall transect b).

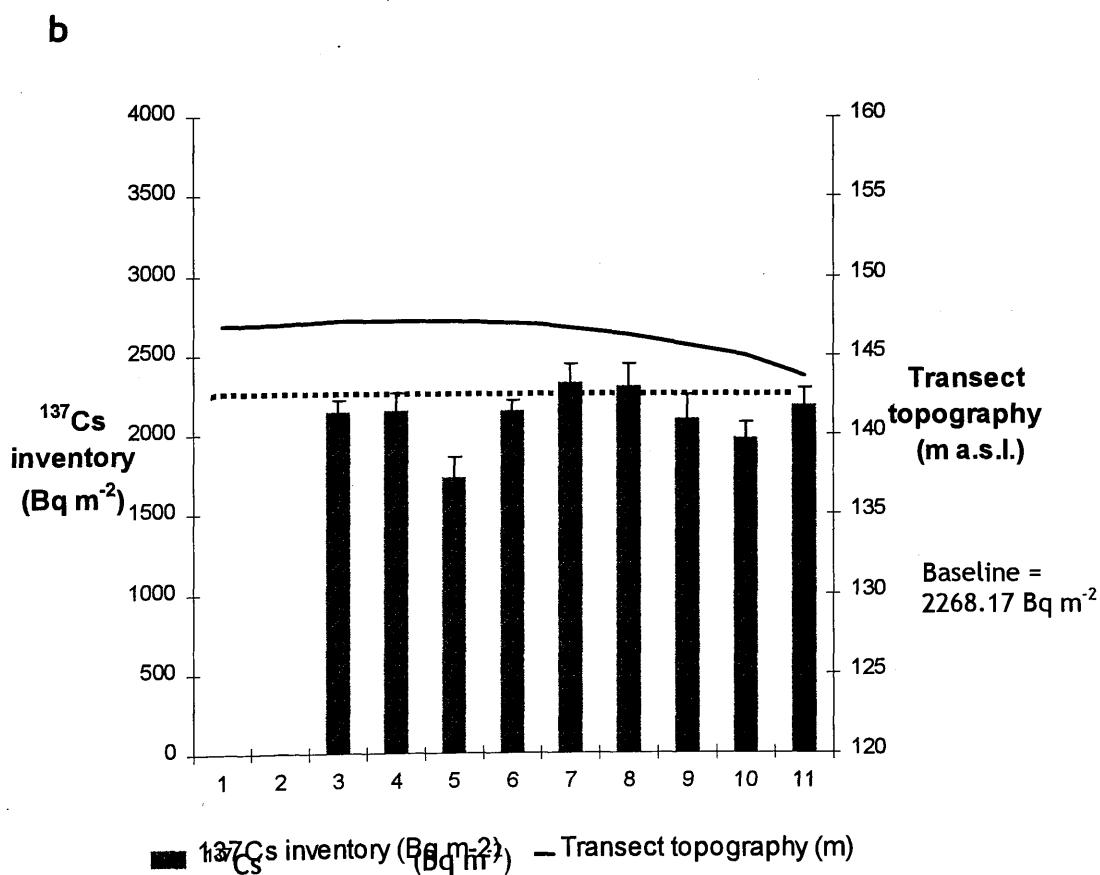
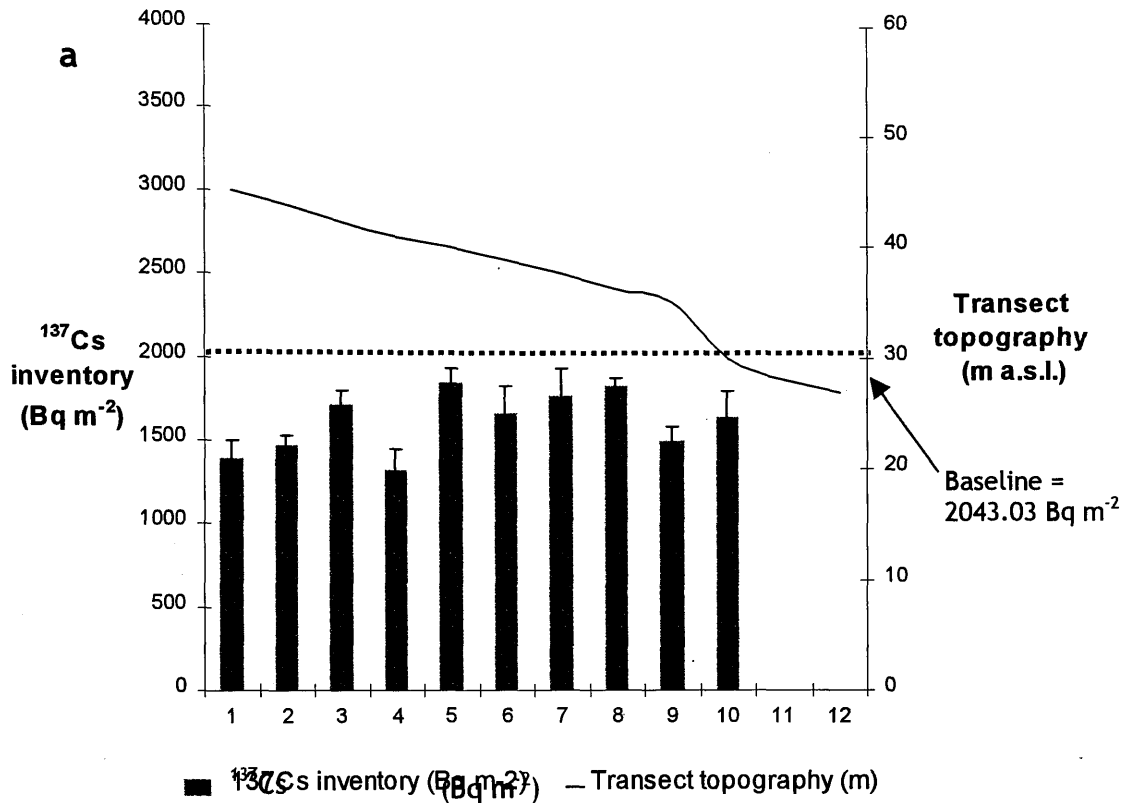


Figure 4.12. Distribution of  $^{137}\text{Cs}$  inventories across the Leadketty a) and Littlelour transect b).

Cell #	Mean <sup>137</sup> Cs inventory (Bq m <sup>-2</sup> )	St dev	St error	% error	Erosion / Deposition (kg m <sup>-2</sup> yr <sup>-1</sup> )	Erosion / Deposition (mm yr <sup>-1</sup> )	St error (kg m <sup>-2</sup> yr <sup>-1</sup> )
1	1389.21	234.59	104.91	16.9%	-4.33	-2.7	0.84
2	1473.03	109.24	54.62	7.4%	-3.58	-2.2	0.36
3	1711.45	202.21	90.43	11.8%	-1.96	-1.2	0.59
4	1326.85	275.74	123.32	20.8%	-4.89	-3.1	1.02
5	1848.18	204.40	91.41	11.1%	-1.10	-0.7	0.55
6	1667.17	360.39	161.17	21.6%	-2.42	-1.5	1.18
7	1775.71	349.77	156.42	19.7%	-1.66	-1.0	0.98
8	1828.66	117.96	52.76	6.5%	-1.18	-0.7	0.32
9	1496.93	191.71	85.74	12.8%	-3.46	-2.2	0.68
10	1647.90	335.72	150.14	20.4%	-2.48	-1.5	1.06

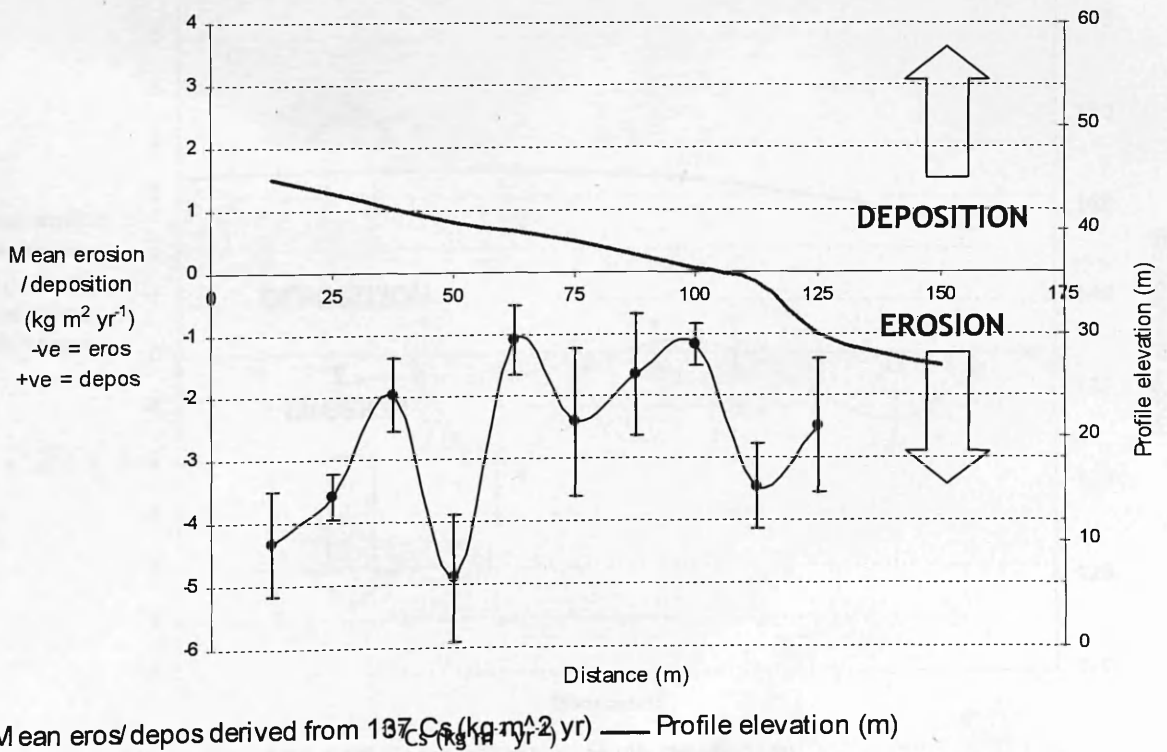


Table 4.14 and Figure 4.13. <sup>137</sup>Cs inventories and derived erosion/deposition estimates across the Leadketty transect.

Cell #	Mean $^{137}\text{Cs}$ inventory ( $\text{Bq m}^{-2}$ )	St dev	St error	% error	Erosion / Deposition ( $\text{kg m}^{-2} \text{yr}^{-1}$ )	Erosion / Deposition ( $\text{mm yr}^{-1}$ )	St error ( $\text{kg m}^{-2} \text{yr}^{-1}$ )
3	2140.32	166.4	74.4	7.8%	-0.50	-0.4	0.31
4	2150.14	236.5	105.8	11.0%	-0.08	-0.1	0.46
5	1727.58	290.2	129.8	16.8%	-2.88	-2.2	0.68
6	2148.65	143.8	64.3	6.7%	-0.46	-0.3	0.27
7	2329.54	246.1	110.1	10.6%	+0.25	+0.2	0.43
8	2297.93	329.4	147.3	14.3%	+0.09	+0.1	0.58
9	2102.07	335.1	149.8	15.9%	-0.72	-0.5	0.60
10	1980.52	222.5	99.5	11.2%	-1.22	-0.9	0.51
11	2179.44	242.6	108.5	11.1%	-0.36	-0.3	0.53

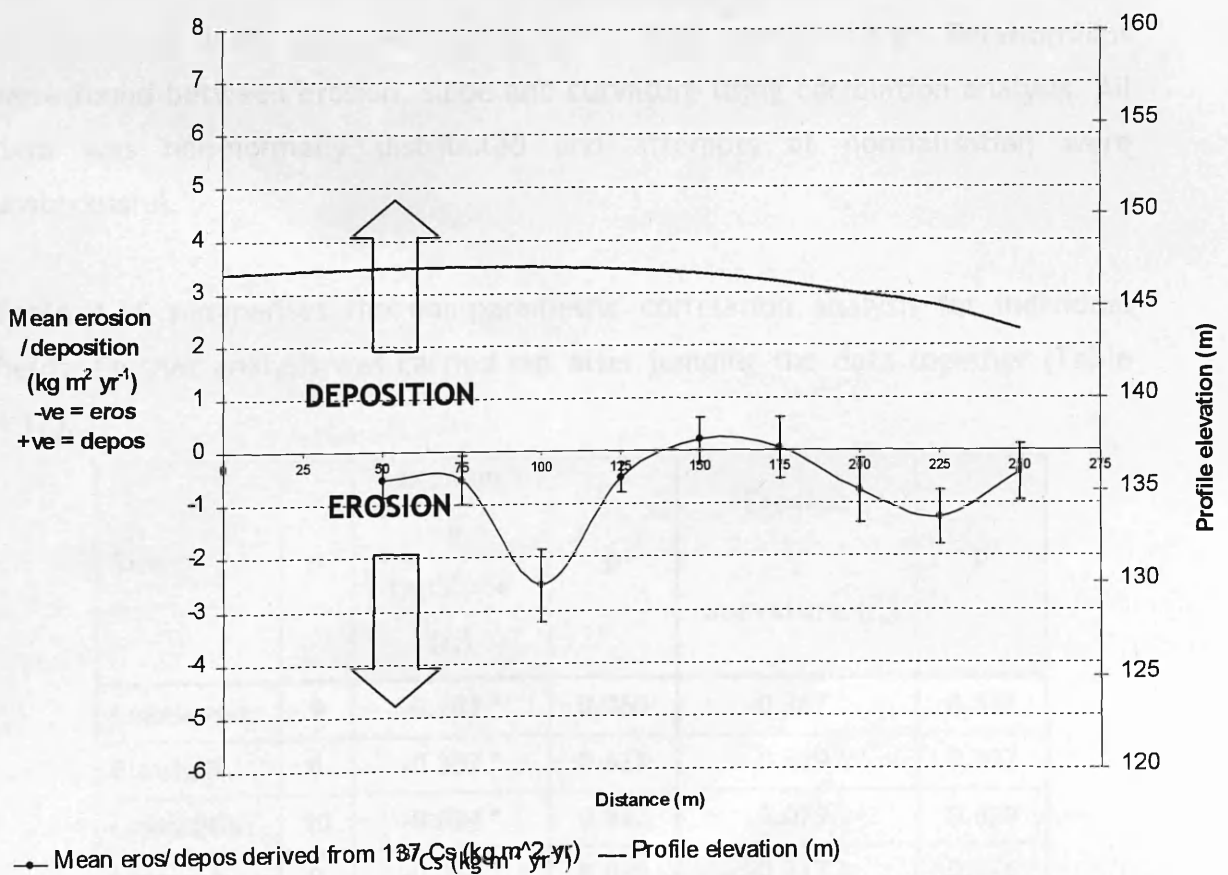


Table 4.15 and Figure 4.14.  $^{137}\text{Cs}$  inventories and derived erosion/deposition estimates across the Littlelour transect.

#### 4.4.1 Discussion of erosion/deposition rates

Net erosion /deposition across the landscape and the control of various topographic properties has been widely studied (Agassi et al., 1989; Cerda and Garcia-Fayos, 1997; Fox and Bryan, 1999; Kirkby, 1971; Kirkby and Morgan, 1980; Laflen et al., 1991; Nearing, 1997; Wischmeier and Smith, 1978). Change in the shape of topography (slope angle) is considered one of the most influential, however the *rate* of change in topography is now being viewed equally as important. The  $^{137}\text{Cs}$  derived erosion/deposition rates for all of the 4 transects show strong visual correspondence with the shape of the terrain. Within the transects the erosion/deposition rates are highly variable, often alternating from erosion to deposition regularly within short distances (adjacent cells). Erosion is predicted almost exclusively on areas of positive slope gradient (uniform backslope sections) and areas of changes in the slope gradients (curvature). The highest rates of  $^{137}\text{Cs}$  derived erosion appear related not to the steepest slope gradients but to the zones where the rate in slope change is high. Relationships were found between erosion, slope and curvature using correlation analysis. All data was non-normally distributed and attempts at normalisation were unsuccessful.

Table 4.16 summarises the non-parametric correlation analysis for individual fields. Further analysis was carried out after lumping the data together (Table 4.17).

Site	n	Erosion v tanSlope ( $r_s$ )	P	Erosion v curvature ( $r_s$ )	P
Loanleven	9	-0.283 *	0.460	-0.367 *	0.332
Blairhall	6	-0.257 *	0.623	-0.429 *	0.397
Leadketty	10	-0.024 *	0.947	-0.079 *	0.829
Littleour	9	-0.050 *	0.898	-0.217 *	0.576

\* insignificant at 0.05 level

Table 4.16. Relationships (Spearman rank  $r_s$ ) between  $^{137}\text{Cs}$  derived erosion/deposition rates and topographic parameters at each field site.

Site	n	Erosion v tanSlope ( $r_s$ )	p	Erosion v curvature ( $r_s$ )	P
Lumped	34	-0.476*	0.004	-0.350**	0.043

\* significant at 0.01 level

\*\* significant at 0.05 level

(critical value = 0.336)

Table 4.17. Relationship (Spearman rank  $r_s$ ) between  $^{137}\text{Cs}$  derived erosion/deposition rates and topographic parameters using all data lumped together.

Loanleven, Blairhall and Littlelour have the most visually intuitive erosion/deposition patterns. The main breaks of slope and backslope sections are experiencing the maximum rates of erosion and maximum deposition is estimated at the footslopes.  $^{137}\text{Cs}$  does appear to be very sensitive to small variations in topography or other factors not identifiable from Figure 4.11, Table 4.14 and Figure 4.13, Table 4.15 and Figure 4.14. Good examples of this are seen at 150m at Loanleven, and 67.5m at Blairhall where no local significant topography is apparent. There are also loci where high rates of erosion are estimated counter-intuitive to where overland flow could be responsible for such levels of soil loss (100m at Littlelour). Tillage translocation is likely to be dominant in these positions.

Individually the fields produced consistently poor slope-erosion relationships and curvature provided only marginal improvements. Slope gradient shows the best statistical agreement with erosion/deposition rates although does not appear to be playing a dominant role. When bulked (Table 4.17) the slope was more capable of explaining erosion/deposition-erosion and is negative in direction (increasing positive slope causes an increase in negativity, i.e. erosion). Slope is providing the conditions for water flux, however, the gradient of the slope alone is clearly not capable of explaining the  $^{137}\text{Cs}$  derived erosion/deposition rates. Curvature is slightly less capable of explaining erosion/deposition with the same directionality. Upon analysing data (correlation) from individual fields, the

results were statistically non-significant, however the consistent general trend of the curvature-erosion relationship (inverse) is viewed as being otherwise too coincidental. Certainly the sample size of the individual transects is small and has therefore played a decisive role in the poor levels of explanation at individual sites. These limited tests at least suggest that the level of convexity/concavity does have an underlying role in modelling soil erosion rates.

#### 4.4.2 Error

Few researchers explicitly discuss and have examined the topic of spatial variability and sampling error when attempting to estimate  $^{137}\text{Cs}$  activity. Throughout the project there has been consistent evidence of significant spatial variability within the ploughed field environment in  $^{137}\text{Cs}$  even over distances of a few metres. This has inevitably influenced inventory and erosion/deposition estimation and its presence and implications are discussed.

There are three sources of data error: 1) heterogeneity of the sampled site, 2) sampling technique, and 3) analytical error. Analytical error is associated with the efficiency of the n-type HPGe gamma spectrometer and random error (points 1 and 2) coupled to sampling and laboratory error.

##### 4.4.2.1 Variability

The techniques used at the field-scale attempted to reproduce a 37-year mean erosion/deposition rate per cell. The sampling system was designed to maximise the number of samples taken within each cell versus time available for fieldwork. This was vitally important given the area of the cell ( $625\text{m}^2$ ). The size of the cell also allowed for quite wide variation in intracell topography and this may have caused problems. This was evident in particular at the 75m point, Loanleven where a mean net deposition was estimated on the steep convex shoulder. It is this topographic variability within each cell that controls the flux of water and soil due to tillage and possibly water. Therefore, since the  $^{137}\text{Cs}$  activity at these locations is extremely point specific, use of a mean may mask the actual erosion/deposition status. This effect was particularly noticeable in

cell 3 at the Blairhall site. Of the 5 samples taken from the cell the northeast core was located on an increasingly concave section of slope, the central core being on the shoulder. Bearing in mind the baseline  $^{137}\text{Cs}$  activity of the site ( $1879.60 \text{ Bq m}^{-2}$ ), values of  $1184.53 \text{ Bq m}^{-2}$  (NW corner),  $2527.13 \text{ Bq m}^{-2}$  (NE corner),  $1486.30 \text{ Bq m}^{-2}$  (centre),  $1533.34 \text{ Bq m}^{-2}$  (SW corner),  $1261.73 \text{ Bq m}^{-2}$  (SE corner)  $\text{Bq m}^{-2}$  were calculated with a standard error of  $241.41 \text{ Bq m}^{-2}$  or  $1.43 \text{ kg m}^{-2} \text{ yr}^{-1}$ . The issue of cell resolution is therefore serious and the results here strongly suggest that a  $25 \times 25\text{m}$  cell at the field scale is incapable of correctly reflecting spatial patterns of  $^{137}\text{Cs}$  at points in the landscape where erosion/deposition may be particularly important. Such sampling errors were investigated by Tyler (1994) in a  $2\text{m} \times 2\text{m}$  grid after taking seven samples. He noted  $^{137}\text{Cs}$  activity to range from  $5.82\text{-}14.23 \text{ kBq m}^{-2}$  equivalent to a CV of 30%. Very similar variability has been noted in the  $25\text{m} \times 25\text{m}$  cells as shown in Table 4.18.

Loanleven	Blairhall	Leadketty	Littlelour
1.17%	2.46%	16.89%	7.8%
8.76%	33.74%	7.42%	11.0%
8.33%	14.52%	11.81%	16.8%
8.45%	19.04%	20.78%	6.7%
8.53%	8.64%	11.06%	10.6%
8.28%	6.75%	21.62%	14.3%
12.88%		19.70%	15.9%
15.92%		6.45%	11.2%
19.02%		12.81%	11.1%
1.60%		20.37%	

Table 4.18. Summary of intracell  $^{137}\text{Cs}$  activity variability (CV) at each field site.

Using Gaussian statistics it is possible to calculate the number of samples required for the experimental mean to be within X % of the true mean with 95% confidence. Applying the equation Tyler (1994) found that 133 samples would be required to be within 5% of the mean and 33 samples within 10%. Rather than increasing the number of samples Tyler (1994) increased the sample size (from a



38mm corer to a 105mm corer) based on Ingamells' (1974) approach. CV was reduced from 10.4% to 5.8% after using the larger corer. By comparing the variability noted in 25m x 25m cells at the four field sites and within the 2m x 2m cell used by Tyler, a reduction in sampling resolution is not likely to see an equivalent reduction in  $^{137}\text{Cs}$  variability.

#### 4.4.2.2 Reproducibility

The sub-sampling technique used for obtaining representative activity involved a manual process of homogenisation. Soil cores were typically up to 3 kg and were either split in to top and bottom sections or bulked prior to homogenisation. Sub-samples of 150 cm<sup>3</sup> were taken for counting. This technique of sub-sampling was tested whether it could reproduce representative  $^{137}\text{Cs}$  activity in replicate samples. Table 4.1 shows the results from the bulking of two cores and subsequent reproducibility. CV from the sub-samples of the two cores were 6.5% and 5% indicating the homogenisation process was capable of high reproducibility. A further test was applied to compare how representative sub-sample activity was against the actual core  $^{137}\text{Cs}$  activity. Table 4.8 presents the results and clearly shows the low variability in sub-sample activity. More importantly the total inventory of the core compares well with the other two reference cores of 1966.37 Bq m<sup>-2</sup> and 1834.78 Bq m<sup>-2</sup> to produce a low CV of 4%. Tyler (1994) examined variability of six 150 g sub-samples taken from a 1 kg sample. He concluded that for  $^{137}\text{Cs}$  the CV was lower than or comparable with analytical error produced inherent within the counter. These results corroborate those of Tyler (1994) and given the natural heterogeneity of the soil and the many factors affecting variability of radionuclides the methodology has performed well.

### 4.5 Evaluation of the model outputs

The consensus of geomorphologists that the  $^{137}\text{Cs}$  technique can provide mean annual soil erosion/deposition rates since the mid 1960's provides an invaluable opportunity against which to quantitatively evaluate erosion model outputs.

Montgomery et al. (1997) and Busacca et al. (1993), both used  $^{137}\text{Cs}$  derived erosion/deposition rates to validate the performance of RUSLE in cultivated fields in a similar way to that applied here. This section concentrates on examining the erosion/deposition rates calculated using Zhang et al.'s (1990)  $^{137}\text{Cs}$  calibration model with the landscape erosion model used here.

The aim is to optimise the four calibration parameters, slope (m) and specific catchment area (n) exponents,  $k_2$  (transport capacity) of the water erosion model and  $k_{\text{till}}$  of the tillage translocation model to generate the best-fit scenario. The optimisation procedure has taken elements from the Generalised Likelihood Uncertainty Estimation (GLUE) methodology (Beven and Freer, 2001; Beven and Binley, 1992) in that a 10% threshold of acceptance was defined. Outside the threshold model predictions were deemed non-behavioural and not considered. At each field site an optimum parameter set from the 10% acceptance band was selected. However one general optimised parameter set for the whole study area was defined from the four parameter sets. From within the threshold for each field site a best-fit general parameter was formulated. GLUE assumes that applying the range of optimised parameters taken from the Loanleven 10% threshold for example, should predict observed erosion/deposition values of other fieldsites. This of course will depend on how well the model represents the actual general processes operating in the field and not field specific processes/conditions. GLUE proposes that the optimum dataset dogma be dismissed and in its place a *range* of acceptable parameter values deemed as behavioural installed. GLUE recognises the theory of equifinality whereby any x number of parameter combinations can and are likely to produce very similar results. In theory if the model is any 'good' then one application of GLUE methodology will suffice in providing behavioural parameters for further model applications elsewhere. Such an approach would be idealistic, yet the remit of the project is tightly defined both in terms of content and time. Furthermore GLUE is somewhat complex.

A classical optimisation approach was chosen that hybridises slightly with GLUE in that the procedure has determined 4 best-fit models from which a general net model has evolved. Parallel to this, observations have been made relating to any ranges or trends in parameter values and evidence for equifinality.

#### 4.5.1 The optimisation routine

Net erosion is considered to be the sum of water and tillage erosion. Although the optimisation procedure deals with net erosion in a slightly different way, graphical output of net erosion is considered as a summation of the water and tillage model. The procedure was coded in AML within ARC/INFO GRID and the following pseudo-code outlines how it functions.

1. The code takes a text file of *all* model parameter combinations (5040) as basic input.
2. The code reads each quadruplet of model parameters ( $m$ ,  $n$ ,  $k_1$ ,  $k_2$ ) and takes the first 3 and feeds them into the water model. The water model runs in ARC/INFO GRID.
3. The fourth parameter feeds in to the ARCTILL tillage model, which also runs in ARC/INFO GRID.
4. ARCTILL outputs are then subtracted from the  $^{137}\text{Cs}$  derived erosion/deposition rates to produce 'goal' values that the water model must meet for best-fit.
5. Water model outputs are compared to the 'goal' values to produce an error squared value at each cell in the transect.
6. Error squared values and erosion/deposition rates are dumped to text file, along with associated model parameters.
7. Code cleans up and returns to (2) to read second line of parameter quadruplets. Subsequent model runs and outputs in (6) are appended to the text file created in 6.

Steps 1 through 7 are equivalent to one model run using a specific set of parameters. The model iterates until all parameter combinations have been read, input, and model outputs produced.

## 4.6 Optimisation of the models.

This section details the how the water and tillage models were optimized and then combined into a generalised optimised model. The models were optimized at each field using the developed application outlined in 4.5.1 (page 202).

### 4.6.1 Loanleven

Whilst processing the raw outputs from the optimisation routine, it soon became apparent that one particular cell invariably produced the highest error squared value. Cell 1 (second in the transect from the north end) is located on the shoulder section of the slope as the central plateau area breaks to the north. The cell is strongly convex (0.48) and has a slope gradient of  $10^\circ$  (18%) yet the calculation of the erosion/deposition rates using the calibration technique developed by Zhang et al. (1990) resulted in an unexpected amount of intracell variability. Figure 4.15 illustrates the results of the calculations for the 5 intracell replicates.

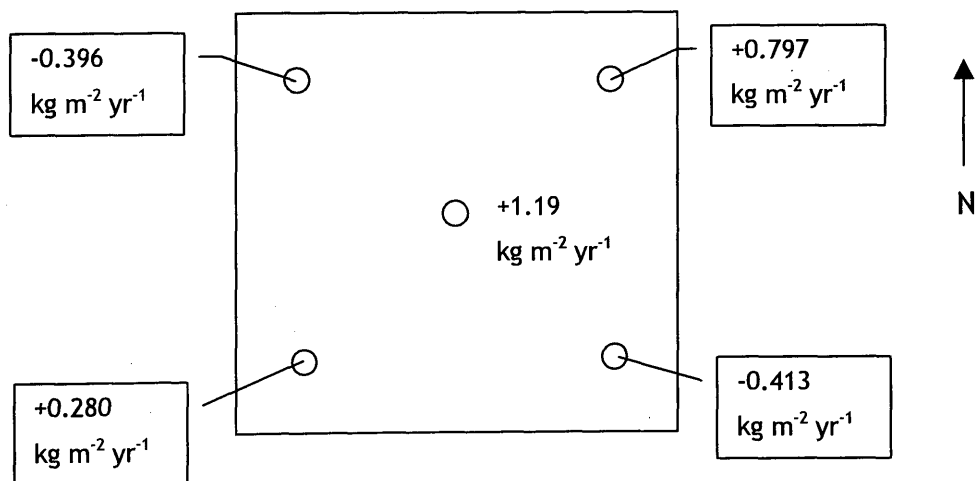


Figure 4.15. Details of the intracell erosion/deposition rates derived from  $^{137}\text{Cs}$  for cell 1 at Loanleven.

It was expected that this cell is dominated by net losses of soil mainly due to tillage translocation. Since the specific catchment area at this point is only

25m<sup>-2</sup> m<sup>-1</sup> (lowest possible - indicative of a topographic peak receiving no flow), erosion/deposition processes due to water could therefore be assumed to be negligible. From Figure 4.15 the situation within cell 1 is not uniform or even consistent. This must be attributable to the fact that the topography north to south across the cell was not uniform, yet GIS assumed uniformity. While the <sup>137</sup>Cs technique is addressing conditions and processes taking place at specific positions in the cell, the water erosion and ARCTILL models are not and instead also assume homogeneity in cell conditions. The mean soil erosion/deposition rate calculated from the 5 samples is +0.293 kg m<sup>-2</sup> yr<sup>-1</sup>, i.e. a net deposition. ARCTILL predicts the following rates in Table 4.19 for corresponding k<sub>till</sub> values for cell 2.

K <sub>till</sub> used	500	450	400	350	300	250	200
Eros/depos rates (kg m <sup>-2</sup> yr <sup>-1</sup> )	-3.604	-3.243	-2.883	-2.523	-2.163	-1.802	-1.442

Table 4.19 Erosion rates predicted by ARCTILL at cell 1, Loanleven using various k<sub>till</sub> coefficients

Once any of the tillage erosion budgets from Table 4.19 have been subtracted from the <sup>137</sup>Cs derived budgets leaving the required water erosion goal budget, it was impossible to parameterise the water erosion model to predict any of the required deposition at this point in the landscape. For example, the erosion rate of -2.163 kg m<sup>-2</sup> yr<sup>-1</sup> generated by the optimised k<sub>till</sub> parameter 300 is subtracted from the <sup>137</sup>Cs observed budget (+0.293 kg m<sup>-2</sup> yr<sup>-1</sup>). The goal erosion/deposition rate for the water model is therefore +2.456 kg m<sup>-2</sup> yr<sup>-1</sup>, net deposition. As explained the topography is such that this scenario will never be attained. The effect of this problem cell on the optimisation was investigated for a possible workaround solution.

Optimisation was initially achieved using all cells in the transect. Secondly, optimisation was rerun excluding cell 1. One major concern arose once the squared errors across the transect for both optimisation runs had been plotted (Figure 4.16). The water model was performing well at the cell base 1 where it predicted large net deposition, corroborated well by over deepened topsoil

(90cm) and field evidence of small alluvial fans. The  $^{137}\text{Cs}$  derived deposition rate here was  $+6.35 \text{ kg m}^{-2} \text{ yr}^{-1}$ . Using the optimised parameter set including cell 1 the deposition rate attained by the net model is  $+3.53 \text{ kg m}^{-2} \text{ yr}^{-1}$ . Excluding cell 1 from the optimisation routine the predicted deposition is  $+4.85 \text{ kg m}^{-2} \text{ yr}^{-1}$  considerably closer to the  $^{137}\text{Cs}$  derived value. The corresponding error values are plotted in Figure 4.16. In conclusion the suspicion surrounding cell 1 justified the decision to ignore cell 1 in the optimisation procedure. The effect of varying the three parameters on error values is presented in Figure 4.17 and Figure 4.18.

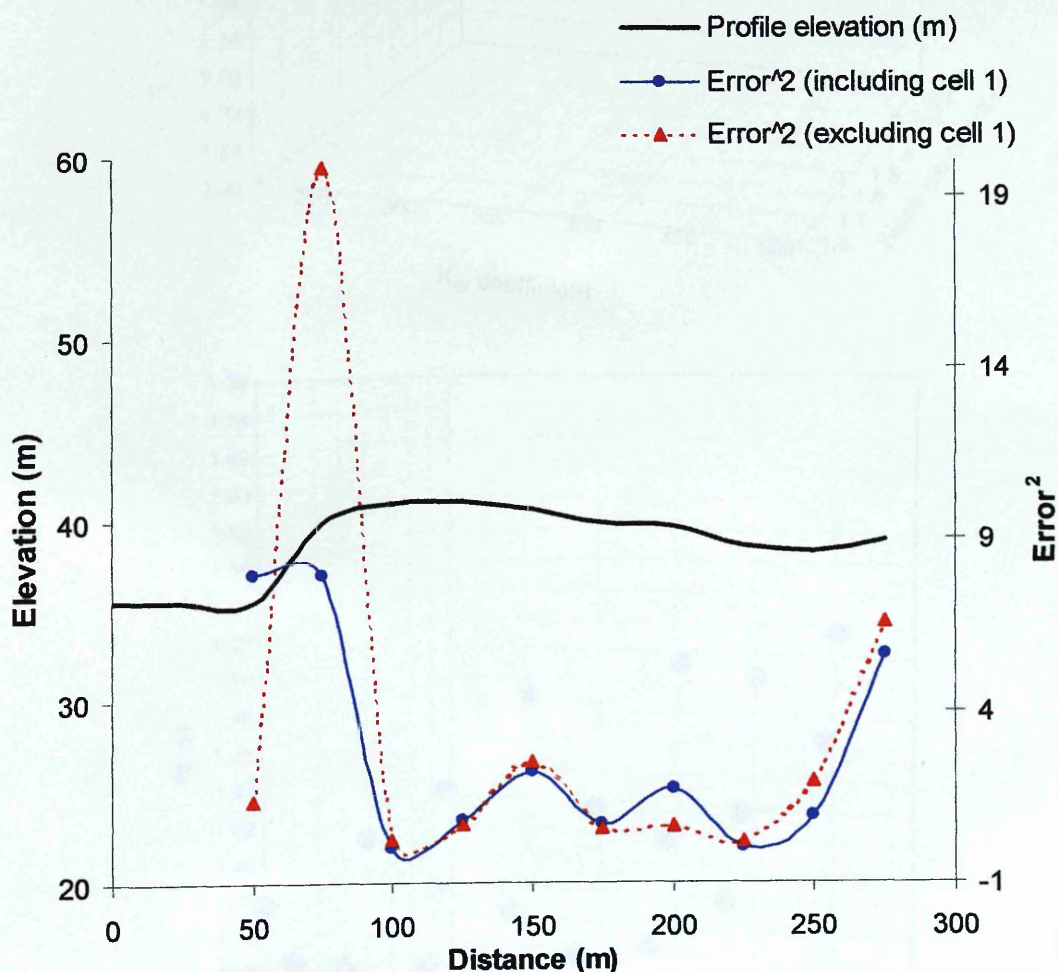
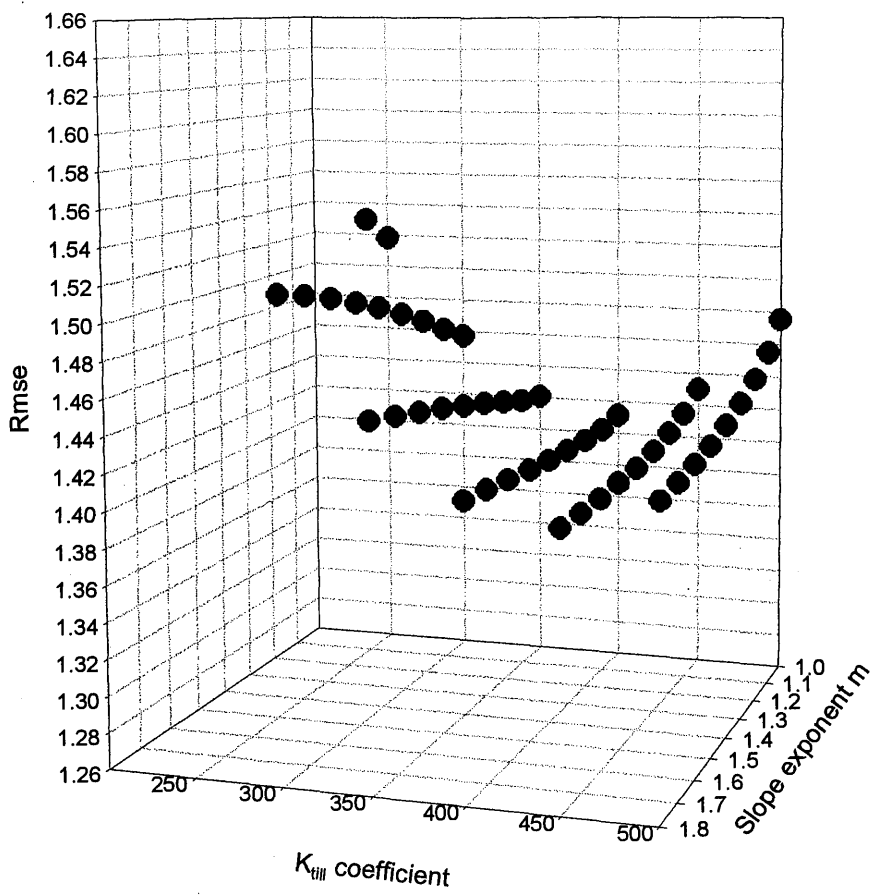
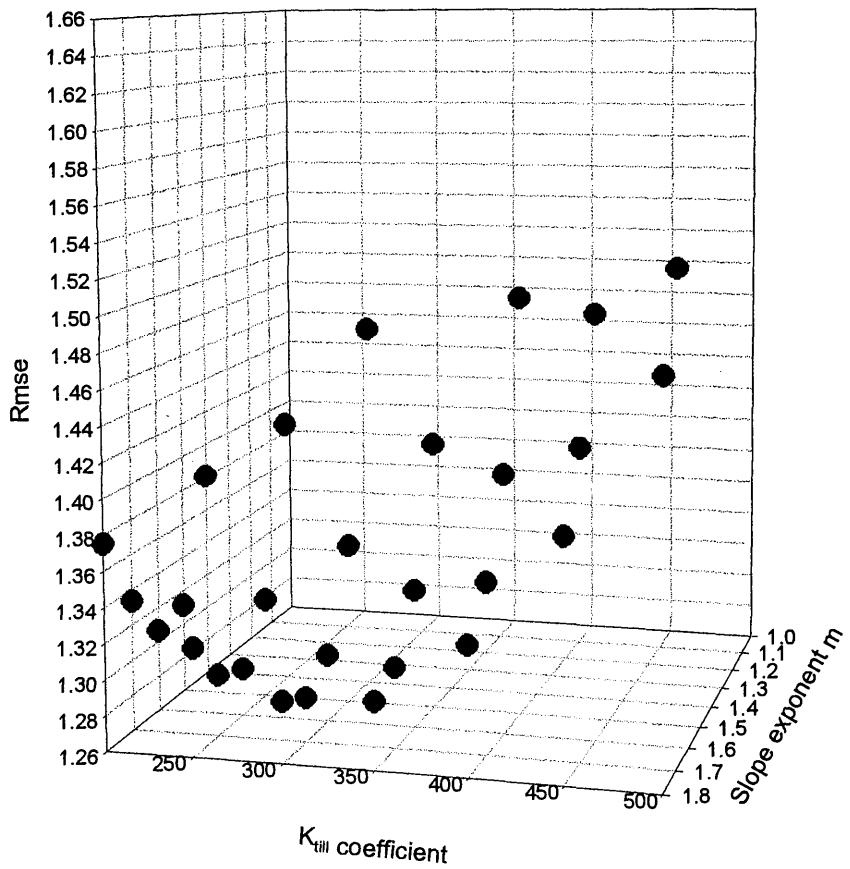


Figure 4.16 Changes in error squared values when running the optimisation routine including and excluding cell 1 at Loanleven.

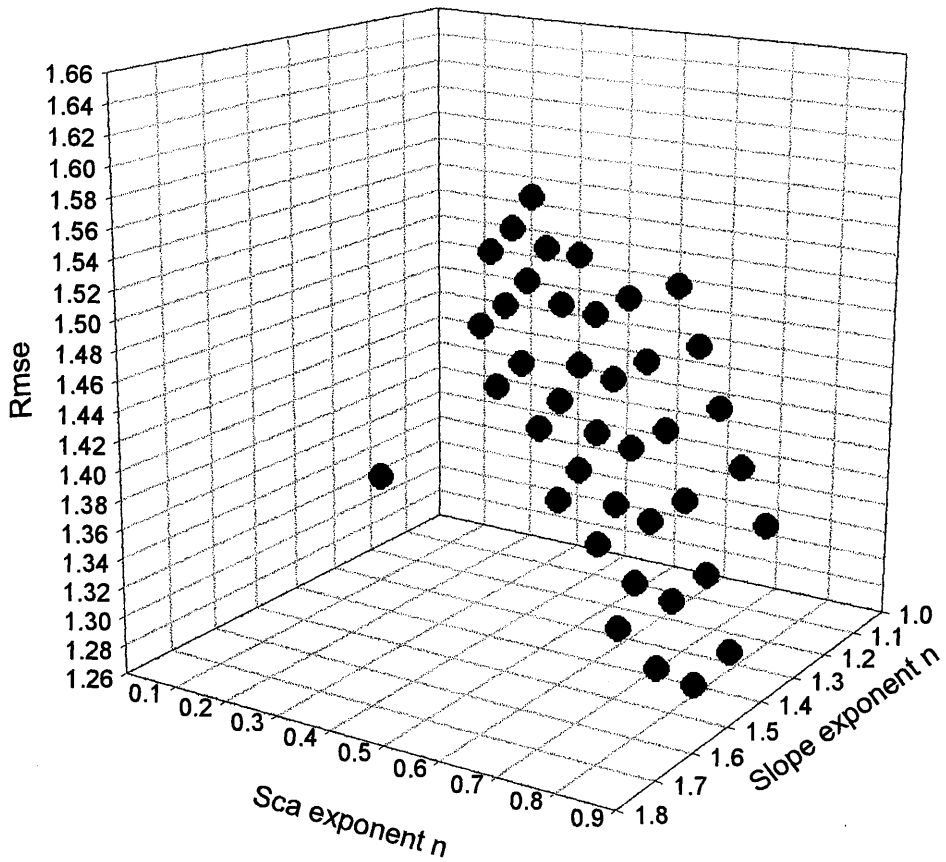


a

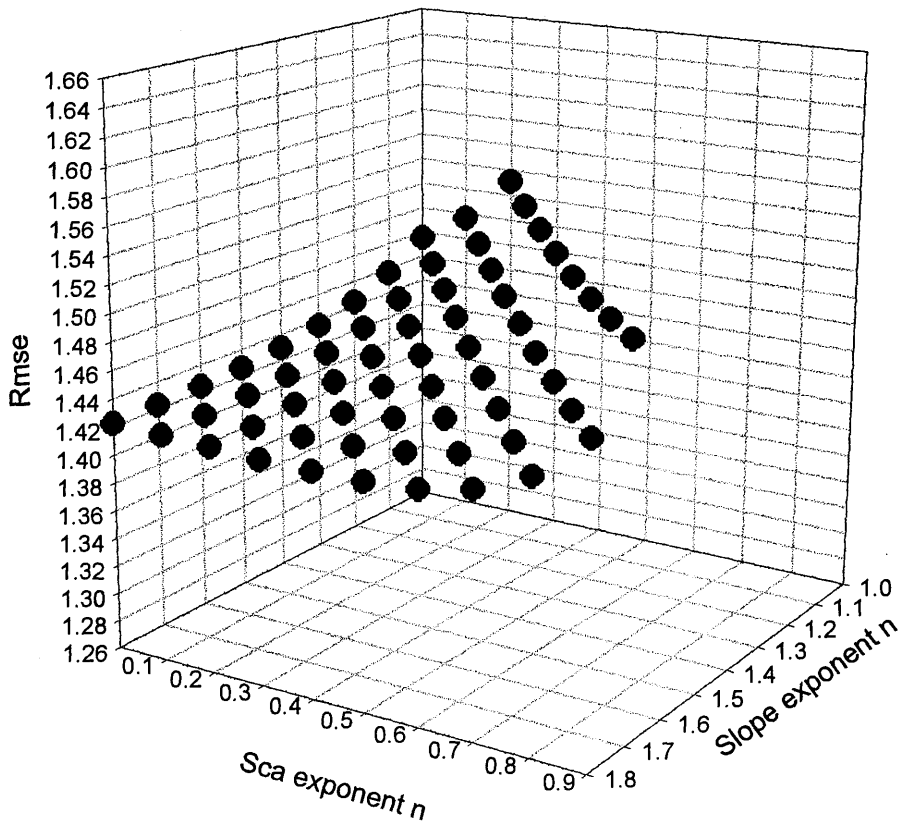


b

Figure 4.17. Error response for Loanleven by varying the slope exponent  $m$  and  $k_{till}$  variables, whilst holding the specific catchment area exponent  $n$  and  $k_2$  at (a) minimum and (b) maximum.



a



b

Figure 4.18. Error response for Loanleven by varying the slope exponent  $m$  and the specific catchment area exponent  $n$ , whilst holding variables  $k_{till}$  and  $k_2$  at (a) minimum and (b) maximum.



The optimised parameter set for the Loanleven net erosion/deposition model is:

Slope  $m = 1.7$   
 Sca  $n = 0.9$   
 $k_2 = 20$   
 $k_{till} = 300$   
**Rmse = 1.2852**

To investigate the interaction, sensitivity and influence of parameters within this model application error distribution under various scenarios was plotted in Figure 4.17 to Figure 4.18. From these trends, explanations and reference back to earlier work have been attempted.

#### 4.6.1.1 Effects of varying $m$ , $n$ , $k_{till}$ and $k_2$

Figure 4.17 primarily plots error response resulting from varying  $k_{till}$  and slope with the sca  $n$  and  $k_2$  held at minima and maxima. Figure 4.17 and Figure 4.18 hint at the strong influence of the sca  $n$  exponent. The lowest 5 errors in Figure 4.17a were very tightly clustered and are presented below in Table 4.20.

$m$	$n$	$k_2$	$k_{till}$	rmse
1.6	0	20	450	1.408807
1.7	0	20	450	1.40882
1.8	0	20	450	1.409222
1.5	0	20	450	1.409361
1.1	0	20	400	1.409491

Table 4.20. The lowest 5 rmse values taken from Figure 4.17a

With  $n$  minimised (Table 4.20), the lowest error attained was far from the lowest rmse value of the optimised parameter set. The optimised  $k_{till}$  value was also not contained within this dataset. When  $n$  was maximised as in Figure 4.17b the error curves dropped substantially and spread containing a wider range of  $k_{till}$  values. The lowest 5 values from Figure 4.17b are shown in Table 4.21.

m	n	$k_2$	$k_{till}$	rmse
1.7	0.9	160	300	1.285192
1.6	0.9	160	250	1.28727
1.8	0.9	160	300	1.294604
1.7	0.9	160	250	1.294883
1.8	0.9	160	350	1.298179

Table 4.21. The lowest 5 rmse values taken from Figure 4.18a.

After maximising  $sca_n$ , the optimised  $k_{till}$  coefficient was contained in the lowest error dataset (Table 4.21).  $k_2$  has however been selected at 160. The error value actually remained the same since  $k_2$  had at least in the bounds of this optimisation procedure no effect.

The transport capacity parameter  $k_2$  had no influence on the outcome of the model. This was fairly surprising. Sensitivity analysis was carried out on  $k_2$  but is not presented. Unfortunately it is suspected that the design of the project may be the cause of the failure to resolve  $k_2$  as a valid controlling parameter. At the catchment scale,  $k_2$  is the threshold defining the transition from erosion to deposition and vice versa, therefore, must be key to the whole foundations of this project.  $k_2$  was optimised to 20 at the Loanleven site, albeit on the basis of the other 3 parameters. 20 when input to the water model does in fact correspond very closely to field evidence of deposition, in particular at the north end of the transect. Increasing  $k_2$  allows more detachment to occur at a point in the landscape since the flow responsible for detaching material is defined as being able to carry more sediment. In respect to a hillslope, an increase in  $k_2$  advances or pushes downslope the point at which deposition will initiate. Lowering  $k_2$  triggers the point of deposition to retreat upslope or initiate earlier.

During test runs of the water erosion model, variation in  $k_2$  had quite marked impact on the erosion/deposition patterns (Figure 2.16, chapter 2), so by insufficiently testing  $k_2$  could have quite serious implications once an optimised set of parameters are applied to a larger area. One possible explanation as to why the procedure seems to be unable to detect the importance of  $k_2$  is that the Loanleven transect is hydrologically insignificant in terms of runoff. The general shape of the field section bisected by the transect can be described as a low

knoll or plateau. Specific catchment areas along the transect are low (Figure 4.19). The transect certainly is not being influenced by hydrological conditions up-catchment, so Loanleven would be a poor candidate for testing  $k_2$  within large catchments. The transect is therefore displaying areas of deposition caused by tillage translocation and not by surface flow accumulation therefore the optimisation procedure has not detected the influence of  $k_2$  and has simply selected the first lowest error value in the column, which corresponds to a  $k_2$  value of 20. In the outputs from the optimisation procedure the same parameter set with a  $k_2$  value of 40 through to 160 produces exactly the same rmse value. This is an artefact of the way in, which the code for the optimisation procedure has firstly generated all possible combinations of parameters and secondly how it then outputs the runs to file. This artefact may be seen in Table 4.22. Selecting a smaller range of  $k_2$  with finer increments would have possibly allowed the  $k_2$  signal to be received better.

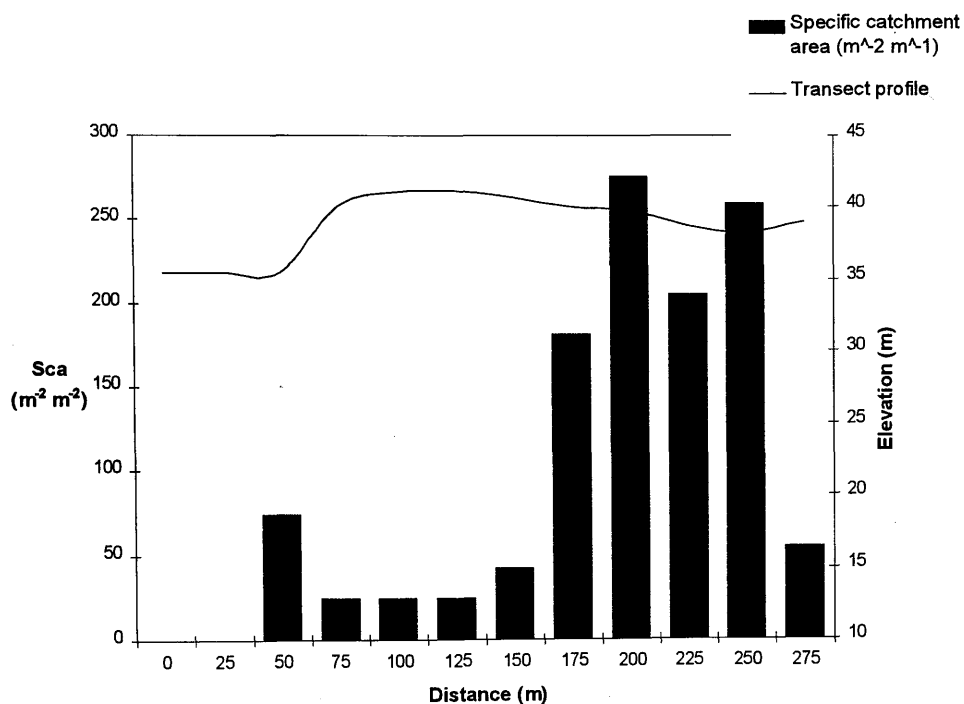


Figure 4.19. Variation in specific catchment area across the Loanleven transect

The  $k_{till}$  coefficient when translated into the ARCTILL model shows little influence on the shape of the error surfaces both when minimising and maximising the other constants.  $k_{till}$  with slope gradient define the magnitudes of soil fluxes due to tillage operations. Variation in modelled net erosion/deposition rates across the transects by using five  $k_{till}$  coefficients (0, 200, 300, 700, 1000  $\text{kg m}^{-1}$ ) was examined to check sensitivity during which the slope ( $m$ ),  $sca$  ( $n$ ) and  $Tc$  ( $k_2$ ) parameters were held at their optimised values. Net erosion/deposition budgets across the Loanleven transect certainly displayed the highest level of sensitivity to tillage translocation ( $k_{till}$ ), but this may be somewhat misleading. The range of  $k_{till}$  used for this sensitivity analysis was considerably larger than that used in the model optimisation procedure (200-500  $\text{kg m}^{-1}$ ). The range for the  $k_{till}$  coefficient was set based on work carried out in Northwest Europe and the assumption made that Scottish agriculture would be analogous of such conditions. Examining the error response across Loanleven as  $k_{till}$  varies reveals the minimum as 400  $\text{kg m}^{-1}$  and 300  $\text{kg m}^{-1}$  when the other parameters were minimised and maximised respectively. Interestingly the error is generally low across the whole  $k_{till}$  range suggesting the selection of a particular  $k_{till}$  value may not be necessarily vital in this case.

$k_{till}$	MIN	MAX
200	1.603117	1.376032
250	1.51922	1.321135
300	1.45765	1.294604
350	1.421311	1.298179
400	1.412153	1.331617
450	1.430696	1.392769
500	1.475898	1.478201

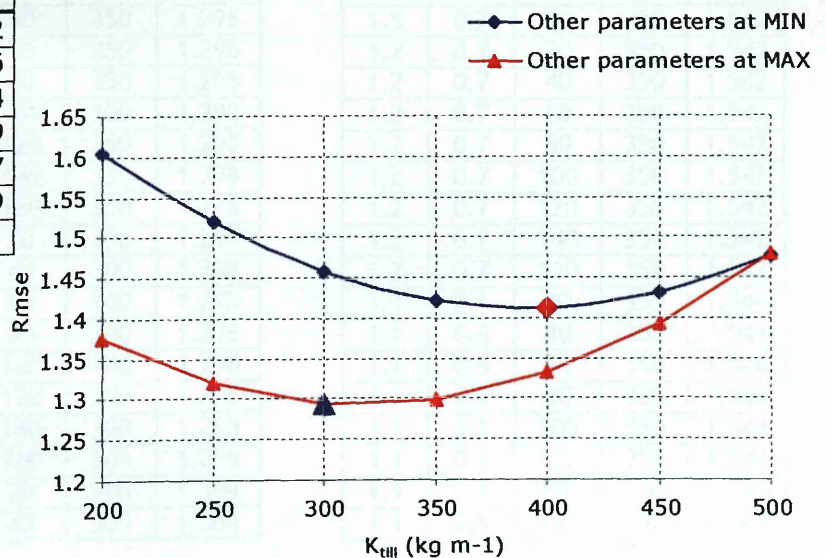


Figure 4.20. Best fit  $k_{till}$  coefficient for the Loanleven site and error sensitivity either side of it.

**a**

m	n	k <sub>2</sub>	k <sub>till</sub>	rmse
1.7	0.9	20	300	1.285
1.7	0.9	40	300	1.285
1.7	0.9	60	300	1.285
1.7	0.9	80	300	1.285
1.7	0.9	100	300	1.285
1.7	0.9	120	300	1.285
1.7	0.9	140	300	1.285
1.7	0.9	160	300	1.285
1.6	0.9	20	250	1.287
1.6	0.9	40	250	1.287
1.6	0.9	60	250	1.287
1.6	0.9	80	250	1.287
1.6	0.9	100	250	1.287
1.6	0.9	120	250	1.287
1.6	0.9	140	250	1.287
1.6	0.9	160	250	1.287
1.8	0.9	20	300	1.295
1.8	0.9	40	300	1.295
1.8	0.9	60	300	1.295
1.8	0.9	80	300	1.295
1.8	0.9	100	300	1.295
1.8	0.9	120	300	1.295
1.8	0.9	140	300	1.295
1.8	0.9	160	300	1.295
1.7	0.9	20	250	1.295
1.7	0.9	40	250	1.295
1.7	0.9	60	250	1.295
1.7	0.9	80	250	1.295
1.7	0.9	100	250	1.295
1.7	0.9	120	250	1.295
1.7	0.9	140	250	1.295
1.7	0.9	160	250	1.295
1.8	0.9	20	350	1.298
1.8	0.9	40	350	1.298
1.8	0.9	60	350	1.298
1.8	0.9	80	350	1.298
1.8	0.9	100	350	1.298
1.8	0.9	120	350	1.298
1.8	0.9	140	350	1.298
1.8	0.9	160	350	1.298
1.6	0.9	20	300	1.298
1.6	0.9	40	300	1.298
1.6	0.9	60	300	1.298
1.6	0.9	80	300	1.298
1.6	0.9	100	300	1.298
1.6	0.9	120	300	1.298
1.6	0.9	140	300	1.298
1.6	0.9	160	300	1.298
1.6	0.8	20	300	1.304
1.6	0.8	40	300	1.304

**b**

m	n	k <sub>2</sub>	k <sub>till</sub>	rmse
1.1	0	160	250	1.532
1.4	0.4	20	200	1.533
1.4	0.4	40	200	1.533
1.4	0.4	60	200	1.533
1.4	0.4	80	200	1.533
1.4	0.4	100	200	1.533
1.4	0.4	120	200	1.533
1.4	0.4	140	200	1.533
1.4	0.4	160	200	1.533
1.1	0	20	250	1.534
1.3	0.1	40	250	1.535
1.3	0.1	60	250	1.535
1.3	0.1	80	250	1.535
1.3	0.1	100	250	1.535
1.3	0.1	120	250	1.535
1.3	0.1	140	250	1.535
1.3	0.1	160	250	1.535
1.8	0.4	40	250	1.537
1.8	0.4	60	250	1.537
1.8	0.4	80	250	1.537
1.8	0.4	100	250	1.537
1.8	0.4	120	250	1.537
1.8	0.4	140	250	1.537
1.8	0.4	160	250	1.537
1.3	0.1	20	250	1.537
1.8	0.4	20	250	1.538
1.5	0.2	40	250	1.540
1.5	0.2	60	250	1.540
1.5	0.2	80	250	1.540
1.5	0.2	100	250	1.540
1.5	0.2	120	250	1.540
1.5	0.2	140	250	1.540
1.5	0.2	160	250	1.540
1.5	0.2	20	250	1.542
1.2	0.7	20	350	1.542
1.2	0.7	40	350	1.542
1.2	0.7	60	350	1.542
1.2	0.7	80	350	1.542
1.2	0.7	100	350	1.542
1.2	0.7	120	350	1.542
1.2	0.7	140	350	1.542
1.2	0.7	160	350	1.542
1.1	0.6	20	350	1.544
1.1	0.6	40	350	1.544
1.1	0.6	60	350	1.544
1.1	0.6	80	350	1.544
1.1	0.6	100	350	1.544
1.1	0.6	120	350	1.544
1.1	0.6	140	350	1.544
1.1	0.6	160	350	1.544

Table 4.22. The 50 lowest (a) and highest (b) rmse values with associated parameters taken from the whole set of Loanleven model runs.

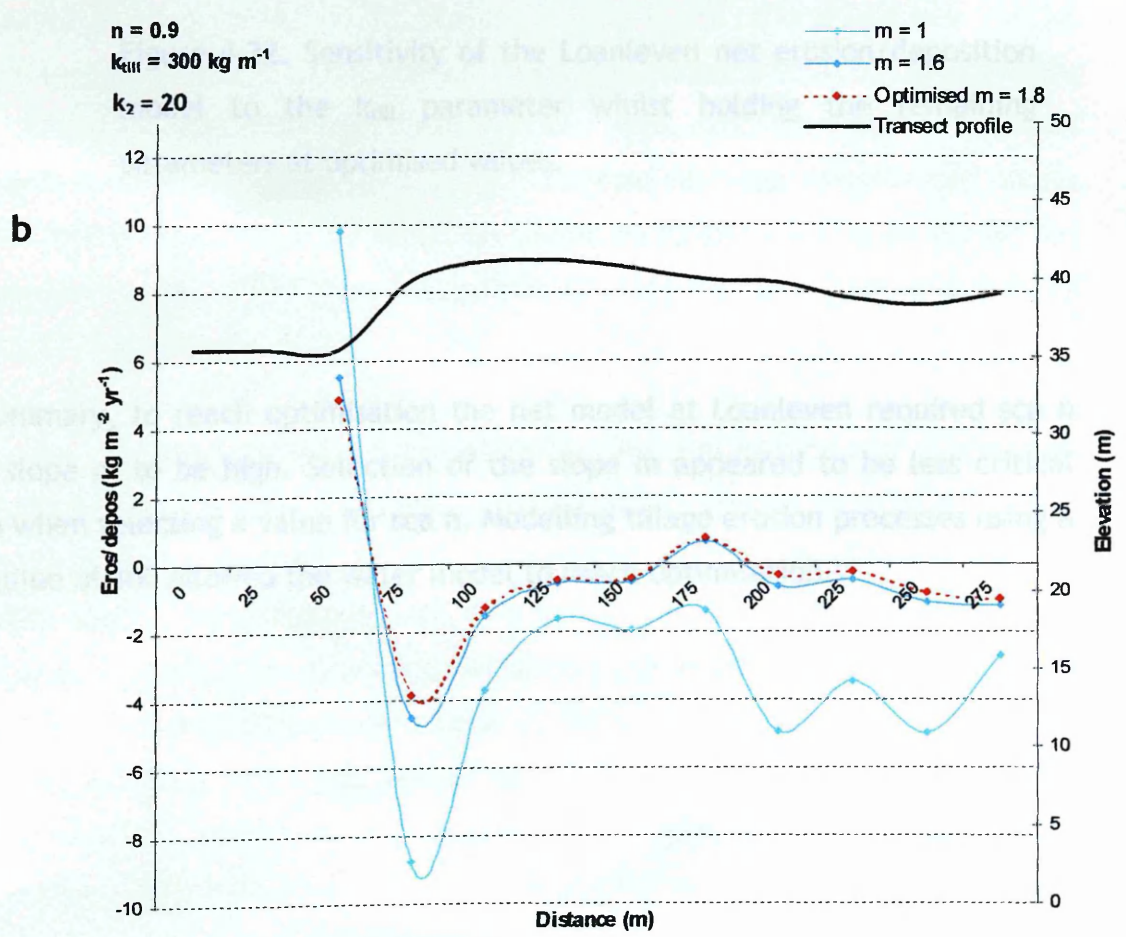
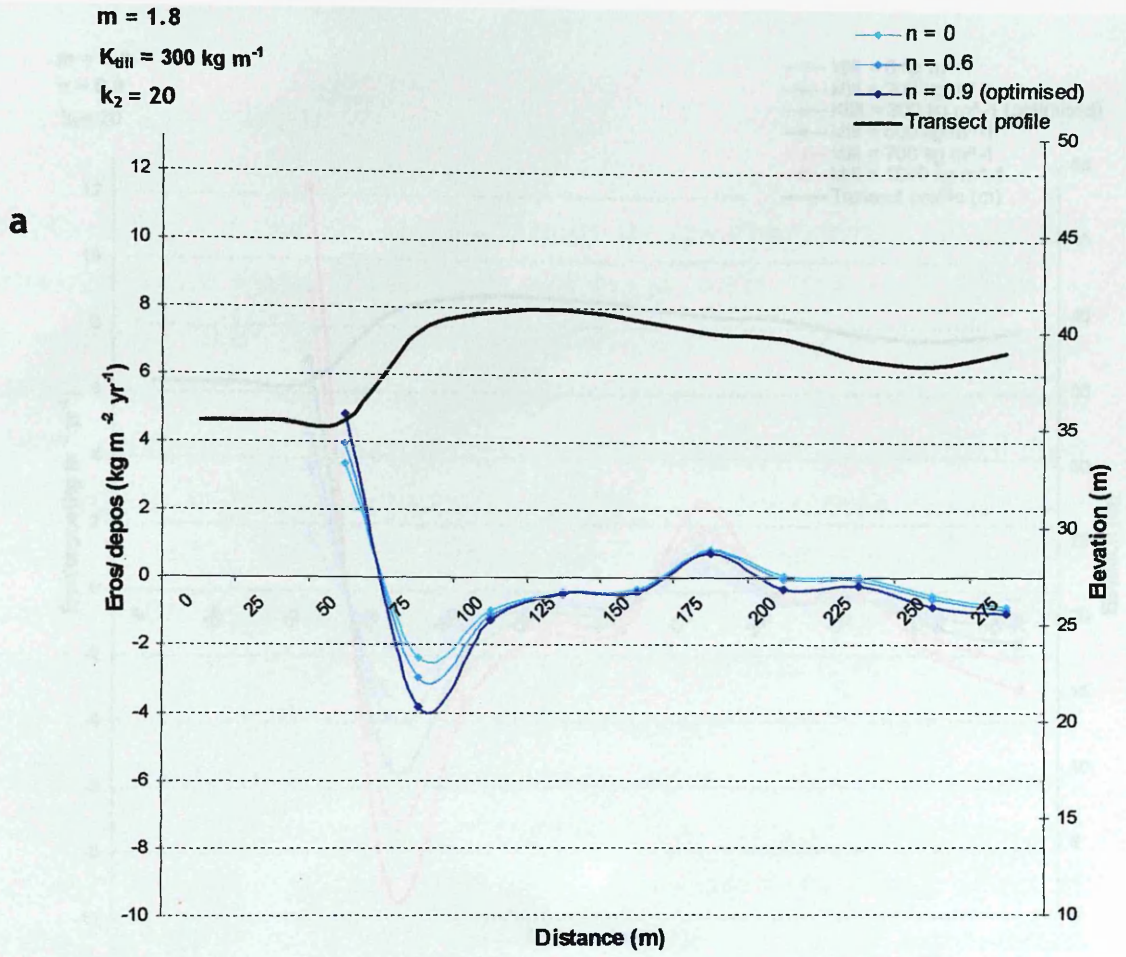


Figure 4.21. Sensitivity of the Loanleven net erosion/deposition model to the sca  $n$  (a) and slope  $m$  (b) parameters whilst holding the remaining parameters at optimised values.

$m = 1.8$   
 $n = 0.9$   
 $k_2 = 20$

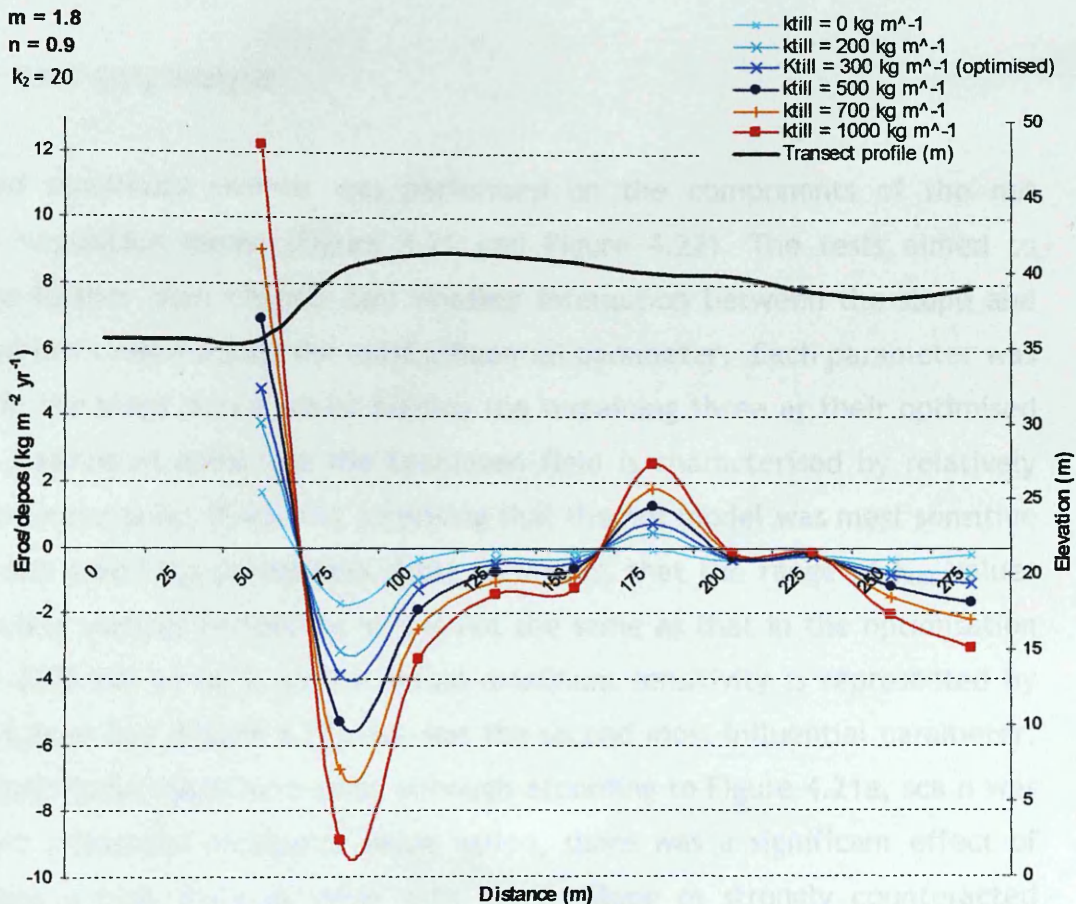


Figure 4.22. Sensitivity of the Loanleven net erosion/deposition model to the  $k_{\text{till}}$  parameter whilst holding the remaining parameters at optimised values.

In summary, to reach optimisation the net model at Loanleven required  $sca$  and slope  $m$  to be high. Selection of the slope  $m$  appeared to be less critical than when selecting a value for  $sca$ . Modelling tillage erosion processes using a  $k_{\text{till}}$  value of 300 allowed the water model to reach optimisation.

#### 4.6.1.2 Sensitivity analysis

Standard sensitivity analysis was performed on the components of the net erosion/deposition model (Figure 4.21 and Figure 4.22). The tests aimed to examine further from chapter two whether interaction between the slope and sca n exponents was masking the most influential parameter. Each parameter was varied in the steps shown whilst holding the remaining three at their optimised values. Bearing in mind that the Loanleven field is characterised by relatively complex topography, it was not surprising that the net model was most sensitive to the sca n and  $k_{till}$  parameters. Note, however, that the range of  $k_{till}$  values used in this analysis (0-1000  $\text{kg m}^{-1}$ ) is not the same as that in the optimisation routine (200-500  $\text{kg m}^{-1}$ ), so the actual maximum sensitivity is represented by the dark blue line (Figure 4.22).  $k_{till}$  was the second most influential parameter. Care needs to be taken here since although according to Figure 4.21a, sca n was the least influential parameter when varied, there was a significant effect of combining a high slope m value with sca n. Slope m strongly counteracted influence of sca n in the model outputs (Figure 4.21). This effect was evident when examining sensitivity of the water erosion model in chapter two. Varying the sca n exponent when combined with the slope exponent held at 1.8 (least influential) highlighted the control the catchment drainage variable had on the water model. The reason for slope appearing so influential (Figure 4.21a) was simply due to the effect the combination of slope and sca n set at 0.9 (most influential) had on the result.

By taking a 50 run sample from the data within the 10% threshold of acceptance, sorted according to ascending rmse value it became clearer still the roles each parameter played. Rmse during 50 runs increased only by 1.5%. Slope m was very flexible and in comparison to sca n it would seem far less important when selecting an appropriate value.  $k_{till}$  displayed a fair amount of variation although there was a clear trend towards a value of 300  $\text{kg m}^{-1}$ . Despite this, whether the  $k_{till}$  is set at 250 or 350  $\text{kg m}^{-1}$  would appear fairly trivial due to the oscillation around the 300  $\text{kg m}^{-1}$  value. Analysis of the high end of the rmse scale uncovered that combinations of low n, m and  $k_{till}$  were most likely to produce high rmse values. It is also worth mentioning that the lowest 50 rsme values are dominated by n values  $< 0.2$  even alongside  $k_{till}$  values of 250.



#### 4.6.1.3 Model performance at Loanleven

	kg m <sup>-2</sup> yr <sup>-1</sup>	mm yr <sup>-1</sup>
<b>Mean water erosion</b>	-0.50	-0.42
<b>Max water erosion</b>	-1.99	-1.69
<b>Max water deposition</b>	+1.99	+1.69
<b>Mean tillage erosion</b>	-0.85	-0.72
<b>Max tillage erosion</b>	-2.16	-1.83
<b>Max tillage deposition</b>	+3.53	+2.99
<b>Mean net erosion</b>	-1.18	-1
<b>Max net erosion</b>	-4.16	-3.53
<b>Max net deposition</b>	+5.17	+4.38

Table 4.23. Summary of modelled erosion/deposition rates across the Loanleven transect using the optimised parameter set.

Transect summary erosion/deposition rate data are displayed in Table 4.23. Predictions of the water, tillage and net erosion/deposition models following optimisation have been plotted in Figure 4.25. There has been some prior discussion and comment in the previous section regarding various aspects of the models behaviour and why that may have been. Figure 4.25 draws together the final best fit scenario that the modelling and optimisation routines have been capable of producing and relates it to the topography of the transect. Of particular value here is the sense of proportionality that Figure 4.25 uncovers within the overall net erosion/deposition budget or put another way, the contributions of tillage and water to the net erosion/deposition package.

There are instances where the net model has predicted the contrary to that of the <sup>137</sup>Cs derived observed. Cells 1 (75m), 4 (150m), 8 (250m) and 9 (275m) fall into this category. Explanations relating to cell 1 have already been proposed (page 203), however for the others it has proved rather more complex. Cell 4 is located on the southern break of slope off the plateau area. Although much less convex than cell 1 once again deposition here would not be expected from a topographical standpoint. The standard error at cell 4 of 0.32 kg m<sup>-2</sup> yr<sup>-1</sup> provides

no room for overlap with the net model's predictions. This is also the case with cell 9. Error margin in cell 8 provides a very close convergence of observed and modelled predictions which is encouraging. Unfortunately failure of the net erosion/deposition model to accurately predict the observed values cannot be blamed on the inherent intracell error when using a multi-sample approach to using means. Cells 2, 6, and 7 all have standard errors equal to or greater than cell 4 ( $0.32 \text{ kg m}^{-2} \text{ yr}^{-1}$ ), yet have delivered good agreements. The strong increasing trend in deposition across cells 8 to 9 could only be attributed to a local tillage pattern. An unlikely but possible explanation is that the plough throw may have been turned towards the field boundary, precisely where cell 9 terminates causing a net influx of soil.

To examine performance of the models a least squared error analysis was carried out and is summarised in Table 4.24.

Cell	$^{137}\text{Cs}$ derived ( $\text{kg m}^{-2} \text{ yr}^{-1}$ )	Optimised net model 1 ( $\text{kg m}^{-2} \text{ yr}^{-1}$ )	Error <sup>2</sup>	Optimised model 2 ( $\text{kg m}^{-2} \text{ yr}^{-1}$ )	Error <sup>2</sup>	Optimised model 3 ( $\text{kg m}^{-2} \text{ yr}^{-1}$ )	Error <sup>2</sup>	Optimised model 4 ( $\text{kg m}^{-2} \text{ yr}^{-1}$ )	Error <sup>2</sup>
b1	+6.35	+5.17	1.41	+1.99	18.99	+3.34	9.10	+3.17	10.13
2	-0.89	-4.16	19.81	-0.46	0.19	-1.00	0.01	-0.91	0.00
3	-1.34	-1.37	0.23	-0.11	1.51	-0.31	1.06	-0.40	0.89
4	+1.13	-0.51	0.69	-0.13	1.59	-0.38	2.30	-0.33	2.13
5	-0.06	-0.46	2.53	-0.09	0.00	-0.35	0.08	+0.80	0.73
6	-1.29	+0.71	0.59	-0.56	0.53	-1.44	0.02	+0.08	1.89
7	+0.13	-0.48	0.66	-0.37	0.25	-0.98	1.22	+0.04	0.01
8	0.41	-0.33	0.21	-0.49	0.79	-1.26	2.77	-0.50	0.82
9	+1.44	-0.98	1.93	-0.29	3.01	-0.65	4.38	-0.84	5.20
		RMSE	1.29	RMSE	1.73	RMSE	1.53	RMSE	1.56

Table 4.24. Performance of the various erosion models at Loanleven (excluding cell 1).

Model 1 = net optimised model  
 Model 2 = water portion of net model  
 Model 3 = Optimised water only model  
 Model 4 = Optimised tillage only model

Regression analysis was not carried out on the data set due to the poor spread of data values in the distribution. Referring to Figure 4.24, the three outliers in the top right corner of the plot had considerable influence on the results of the regression analysis. The application of such a test could not therefore be justified.

Finally, the water erosion model (model 3) *alone* was optimised against the  $^{137}\text{Cs}$  derived observed erosion/deposition budget. Tillage translocation was not simulated here in an attempt to ascertain whether its exclusion results in a deterioration of the model's predictive ability. The results proved surprising. When allowing the water model to optimise itself to the  $^{137}\text{Cs}$  derived erosion/deposition budget without modelling tillage translocation the best-fit parameter set was as follows:

Slope m =	1.4
Scal n =	0.9
$k_2$ =	20
<b>Rmse =</b>	<b>1.526</b>

The only change is the decreased slope exponent. Figure 4.26 plots a direct comparison of the optimised net model (inclusive of tillage) and the optimised water model (exclusive of tillage). The results are remarkably similar. Although the rmse is higher (Figure 4.23) for the optimised water model parameter set than for the optimised net model, there are subtle differences.

Both models predict very similar trends throughout the transect yet at the base cell (50m) tillage translocation has provided more net deposition required to match the observed values. Further differential occurred at cell 7 (225m). The optimised water model does, however predict a better trend at cells 8 and 9. The optimised net model predictions in these loci actually begin to diverge away from the  $^{137}\text{Cs}$  data.

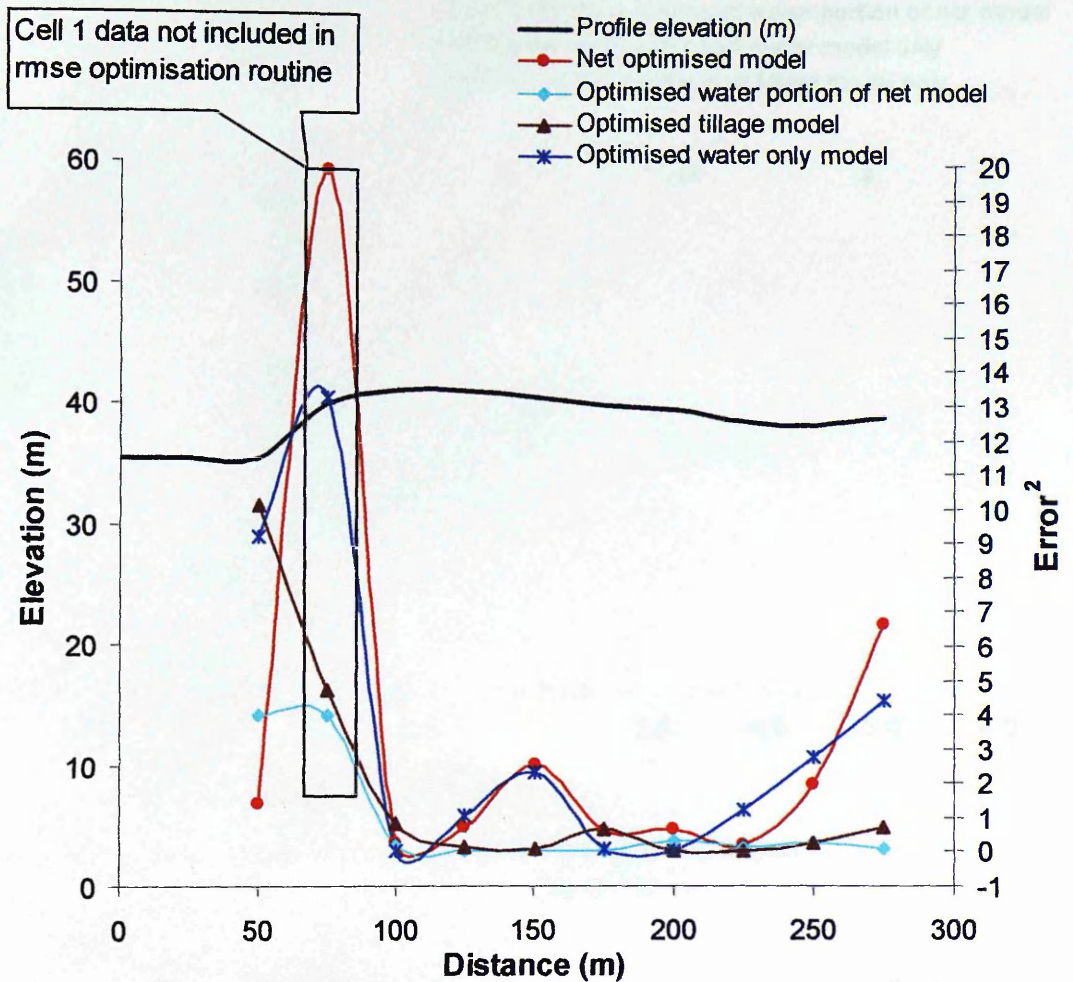


Figure 4.23. Distribution of errors across the Loanleven transect from the optimised models. Comparison of the net erosion/deposition model and water only model is made.

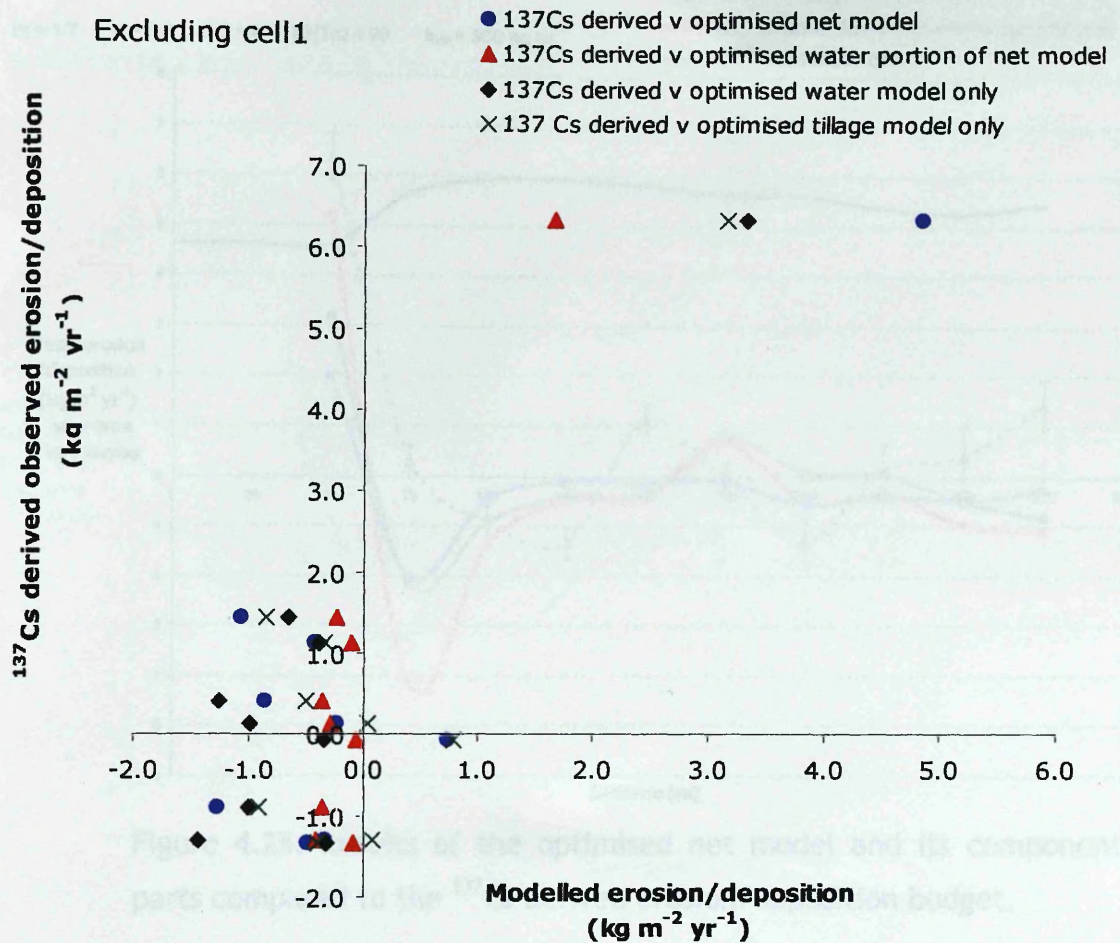


Figure 4.24. Plot of modelled erosion/deposition versus  $^{137}\text{Cs}$  derived erosion/deposition with and without tillage translocation at Loanleven.

Finally evidence provided from a soil augering scheme across the transect has confirmed the validity of the  $^{137}\text{Cs}$  technique in estimating medium-term mean erosion/deposition rates. Topsoil depths were strongly related to  $^{137}\text{Cs}$  derived erosion/deposition rates ( $r^2 = 0.89$ ,  $p = 0.000$ ,  $n = 10$ ) and the affinity is displayed in Figure 4.27. Such a strong mirroring of results is unlikely to be coincidental and must be simply attributed to the accuracy of the  $^{137}\text{Cs}$  in this field. Furthermore, the whole optimisation procedure can be subsequently viewed with considerable merit and reliability.

$m = 1.7$     $n = 0.9$     $k_1 = 4$     $k_2(Tc) = 20$     $k_{till} = 300 \text{ kg m}^{-1}$

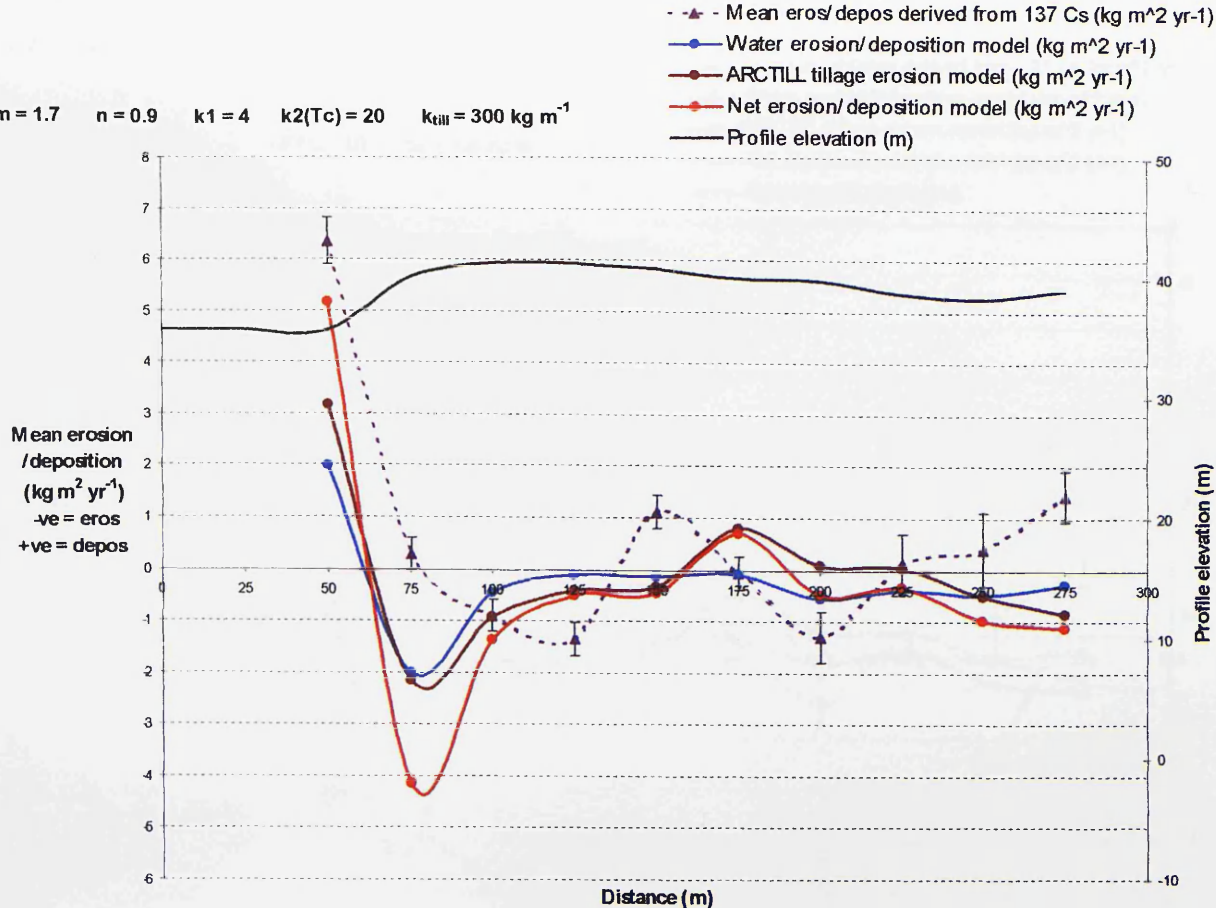


Figure 4.25. Results of the optimised net model and its component parts compared to the  $^{137}\text{Cs}$  derived erosion/deposition budget.

Optimised net model :  $m = 1.8$     $n = 0.9$     $k_1 = 4$     $k_2(Tc) = 20$   
 $k_{till} = 300 \text{ kg m}^{-1}$

Optimised water model (minus tillage) :  $m = 1.4$     $n = 0.9$     $k_1 = 4$   
 $k_2(Tc) = 20$

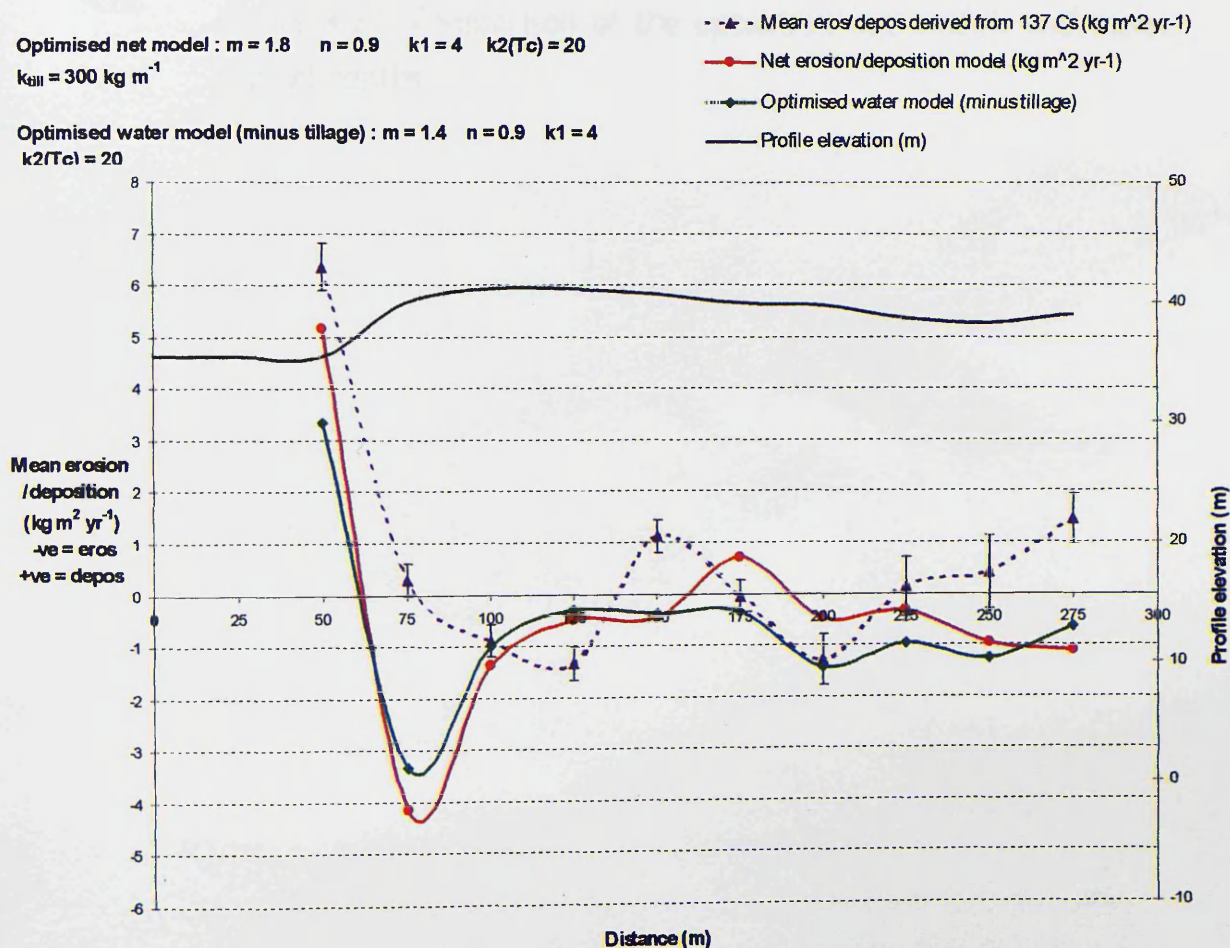


Figure 4.26. Comparison of the optimised net model and optimised water model (minus tillage)

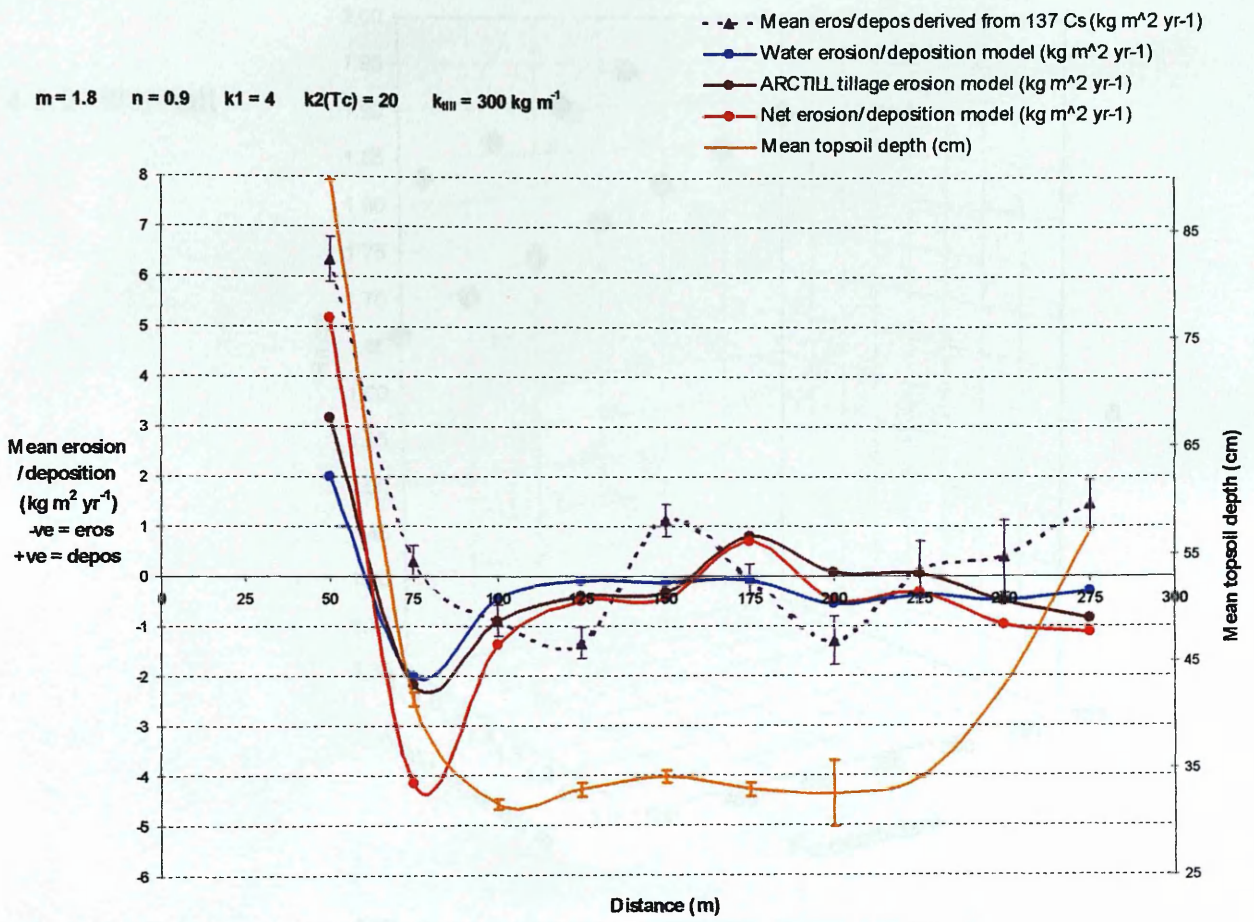
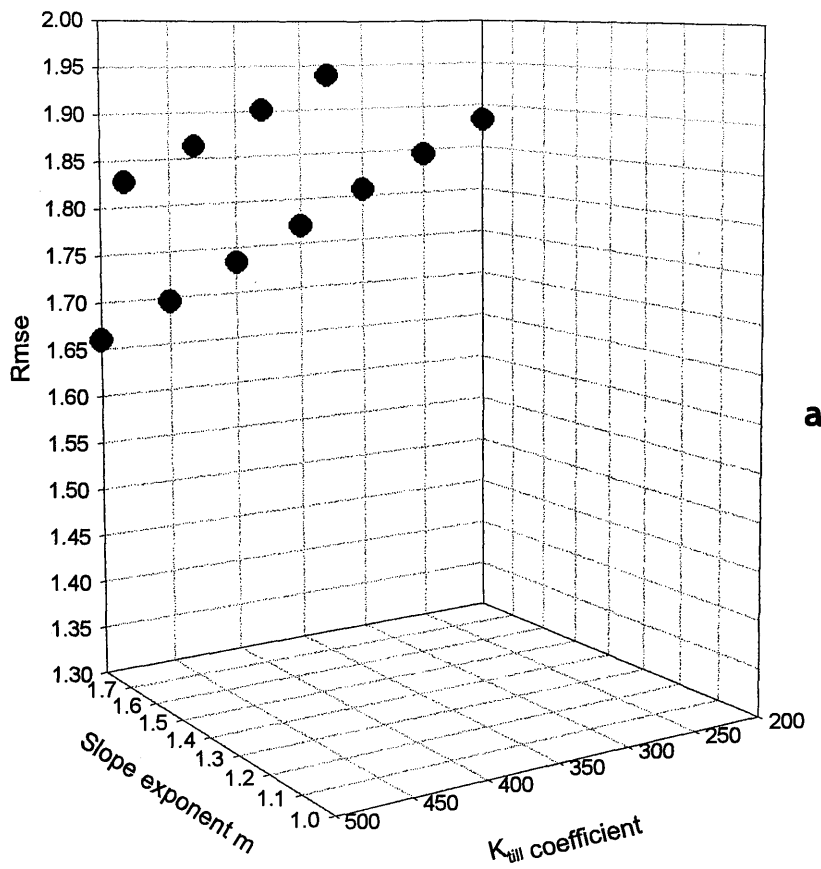
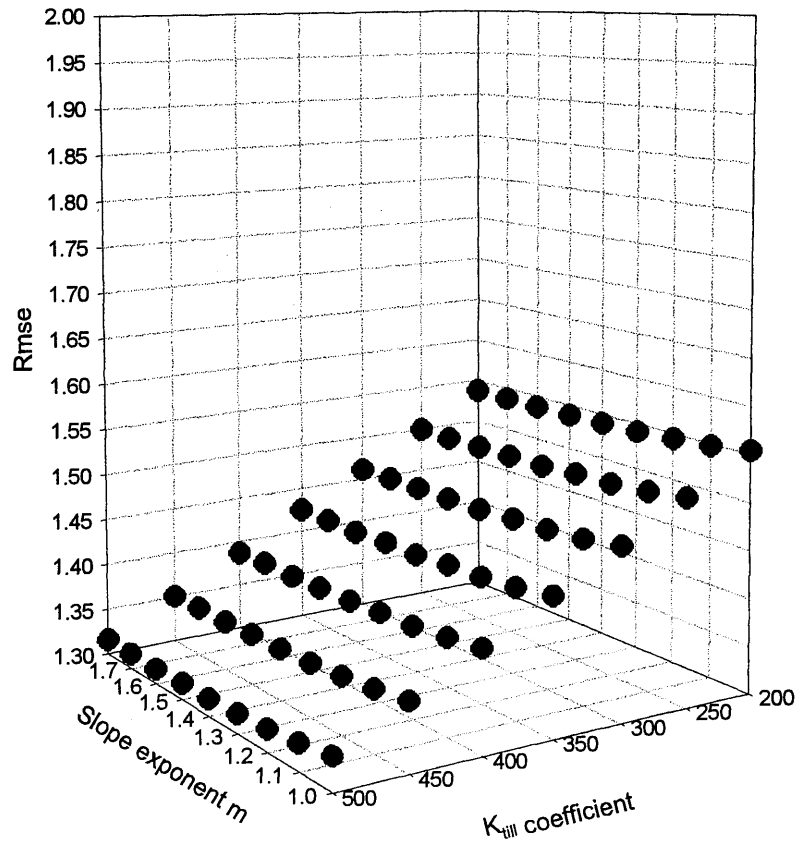


Figure 4.27. Comparison of the optimised net models and mean topsoil depths.

4.6.2 Blairhall



a



b

Figure 4.28. Error response for Blairhall by varying the slope exponent  $m$  and  $K_{till}$  variables, whilst holding the specific catchment area exponent  $n$  and  $k_2$  at (a) minimum and (b) maximum.



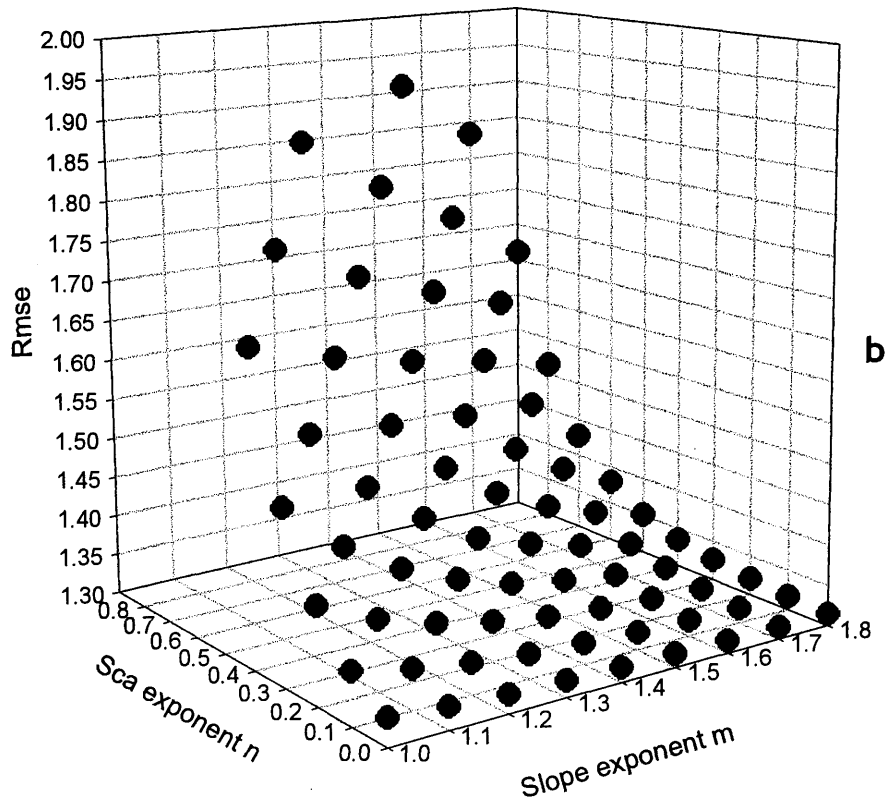
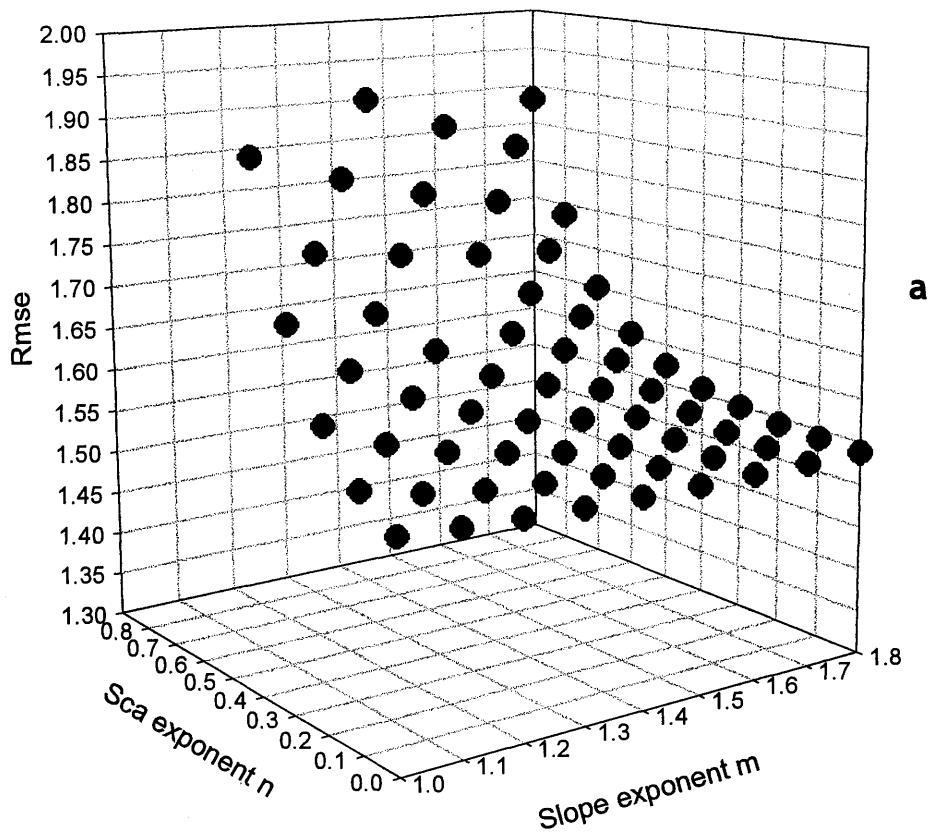


Figure 4.29. Error response for Blairhall by varying the slope exponent  $m$  and the specific catchment area exponent  $n$ , whilst holding variables  $k_{till}$  and  $k_2$  at (a) minimum and (b) maximum.

The optimised parameter set for the Blairhall net erosion/deposition model is:

Slope  $m = 1.8$   
 Sca  $n = 0$   
 $K_2 = 20$   
 $k_{till} = 500$   
**Rmse = 1.3163**

#### 4.6.2.1 Effects of varying $m$ , $n$ , $k_{till}$ and $k_2$

Examining Figure 4.28a and Figure 4.28b it became immediately apparent that the influence of the specific catchment area exponent has been totally reversed when compared to the Loanleven scenario. Firstly, maximising  $n$  as a constant (Figure 4.28b) has restricted the number of model runs that fall within the 10% acceptance threshold, and secondly the few that are within the threshold are all above rmse of 1.65. Tillage translocation in the form of the  $k_{till}$  coefficient, optimised at  $500 \text{ kg m}^{-1}$ , is therefore more dominant across the Blairhall field than was optimised at Loanleven. Once optimised at this high value the rmse values reduced drastically. Table 4.25 presents the 5 lowest error values taken from Figure 4.28a and Table 4.26 the lowest 5 from Figure 4.28b.

$m$	$n$	$K_2$	$k_{till}$	rmse
1.8	0	20	500	1.316
1.7	0	20	500	1.316
1.6	0	20	500	1.317
1.5	0	20	500	1.318
1.4	0	20	500	1.319

Table 4.25. The lowest 5 rmse values taken from Figure 4.28a when sca  $n$  and  $k_2$  are minimised.

$m$	$n$	$K_2$	$k_{till}$	rmse
1.7	0.9	160	350	1.943
1.7	0.9	160	400	1.906
1.7	0.9	160	450	1.870
1.7	0.9	160	500	1.834
1.8	0.9	160	200	1.883

Table 4.26. The lowest 5 rmse values taken from Figure 4.28b when sca  $n$  and  $k_2$  are maximised.

Minimising  $n$  (Figure 4.28a) generated a substantial fall in rmse values confirming the need for  $n$  to be set low. The slope  $m$  exponent demonstrates almost identical behaviour noted in the equivalent Table 4.20 and Table 4.21 at the Loanleven field site. Although the rmse was strictly at its lowest with slope  $m$  set at 1.8 the rmse values increased only very marginally as slope  $m$  incremented through to 1.4. In fact the rmse varied only 0.1% as a result of slope  $m$  changing to 1.4. This reaffirmed that the model was particularly insensitive to the slope  $m$  parameter.

A similar effect was evident in Figure 4.29a and Figure 4.29b when plotting slope  $m$  versus  $sca\ n$ . Holding the  $k_{till}$  and  $k_2$  parameter at minimum allowed error values to bottom out only at 1.53. The error surface strongly reflected the influence of slope  $m$  and  $sca\ n$ , dipped towards high slope  $m$  and low  $sca\ n$  values, yet the low  $k_{till}$  of  $200\text{ kg m}^{-1}$  was preventing error values close to the optimised from being obtained. After maximising  $k_{till}$ , rmse values reduced in a similar fashion but in reverse to those in Figure 4.18 at Loanleven suggesting  $k_{till}$  be set to  $500\text{ kg m}^{-1}$ .

$k_{till}$	rmse
200	1.554
250	1.517
300	1.479
350	1.442
400	1.406
450	1.370
500	1.335

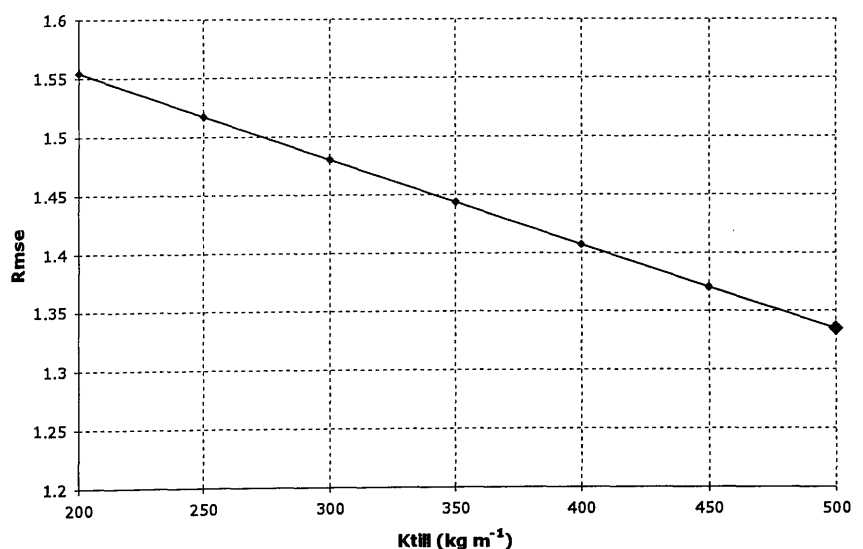


Figure 4.30 and Table 4.27. Best fit  $k_{till}$  coefficient for the Blairhall site and error sensitivity either side of it.

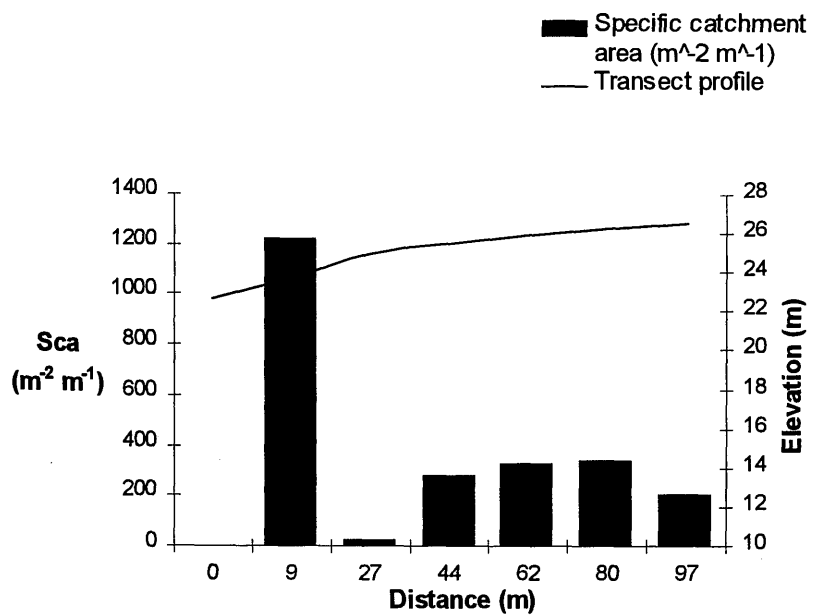


Figure 4.31. Variation in specific catchment area across the Blairhall transect.

Table 4.28 presents 50 of the lowest generated rmse values along with the corresponding parameters. The rmse values increased only slightly (0.23%) through 50 model runs, yet the high variability in possible slope  $m$  values capable of contributing to such low error values is quite noticeable. There are however no slope  $m$  values below 1.4 present in the table. The situation with  $sca_n$  and  $k_{till}$  is strikingly different. Low  $sca_n$  values have consistently worked towards the lowest rmse values.  $k_{till}$  has been set to its maximum value in all cases of the 50 lowest rmse values produced at Blairhall.  $k_2$  is further highlighted here as being the least influential.

#### 4.6.2.2 Sensitivity analysis

From a magnitude standpoint, varying the four parameters produced virtually the same change in erosion/deposition rates. Topography provided very little driving force for transport processes, therefore it has been difficult to make any conclusions as to the dominance of any one parameter. The results are shown in Figure 4.32 and Figure 4.33.

a

m	n	k <sub>2</sub>	k <sub>till</sub>	rmse
1.8	0	20	500	1.316
1.8	0	40	500	1.316
1.8	0	60	500	1.316
1.8	0	80	500	1.316
1.8	0	100	500	1.316
1.8	0	120	500	1.316
1.8	0	140	500	1.316
1.8	0	160	500	1.316
1.7	0	20	500	1.317
1.7	0	40	500	1.317
1.7	0	60	500	1.317
1.7	0	80	500	1.317
1.7	0	100	500	1.317
1.7	0	120	500	1.317
1.7	0	140	500	1.317
1.7	0	160	500	1.317
1.6	0	20	500	1.317
1.6	0	40	500	1.317
1.6	0	60	500	1.317
1.6	0	80	500	1.317
1.6	0	100	500	1.317
1.6	0	120	500	1.317
1.6	0	140	500	1.317
1.6	0	160	500	1.317
1.8	0.1	20	500	1.318
1.8	0.1	40	500	1.318
1.8	0.1	60	500	1.318
1.8	0.1	80	500	1.318
1.8	0.1	100	500	1.318
1.8	0.1	120	500	1.318
1.8	0.1	140	500	1.318
1.8	0.1	160	500	1.318
1.5	0	20	500	1.318
1.5	0	40	500	1.318
1.5	0	60	500	1.318
1.5	0	80	500	1.318
1.5	0	100	500	1.318
1.5	0	120	500	1.318
1.5	0	140	500	1.318
1.5	0	160	500	1.318
1.4	0	40	500	1.319
1.4	0	60	500	1.319
1.4	0	80	500	1.319
1.4	0	100	500	1.319
1.4	0	120	500	1.319
1.4	0	140	500	1.319
1.4	0	160	500	1.319
1.7	0.1	20	500	1.319
1.7	0.1	40	500	1.319
1.7	0.1	60	500	1.319

b

m	n	k <sub>2</sub>	k <sub>till</sub>	rmse
1.6	0.8	140	250	1.921
1.6	0.8	160	250	1.921
1.3	0.6	20	200	1.931
1.3	0.6	40	200	1.931
1.3	0.6	60	200	1.931
1.3	0.6	80	200	1.931
1.3	0.6	100	200	1.931
1.3	0.6	120	200	1.931
1.3	0.6	140	200	1.931
1.3	0.6	160	200	1.931
1.7	0.9	20	350	1.943
1.7	0.9	40	350	1.943
1.7	0.9	60	350	1.943
1.7	0.9	80	350	1.943
1.7	0.9	100	350	1.943
1.7	0.9	120	350	1.943
1.7	0.9	140	350	1.943
1.7	0.9	160	350	1.943
1.4	0.7	20	300	1.950
1.4	0.7	40	300	1.950
1.4	0.7	60	300	1.950
1.4	0.7	80	300	1.950
1.4	0.7	100	300	1.950
1.4	0.7	120	300	1.950
1.4	0.7	140	300	1.950
1.4	0.7	160	300	1.950
1.5	0.8	20	450	1.954
1.5	0.8	40	450	1.954
1.5	0.8	60	450	1.954
1.5	0.8	80	450	1.954
1.5	0.8	100	450	1.954
1.5	0.8	120	450	1.954
1.5	0.8	140	450	1.954
1.5	0.8	160	450	1.954
1.1	0.5	20	250	1.955
1.1	0.5	40	250	1.955
1.1	0.5	60	250	1.955
1.1	0.5	80	250	1.955
1.1	0.5	100	250	1.955
1.1	0.5	120	250	1.955
1.1	0.5	140	250	1.955
1.1	0.5	160	250	1.955
1.2	0.6	20	400	1.955
1.2	0.6	40	400	1.955
1.2	0.6	60	400	1.955
1.2	0.6	80	400	1.955
1.2	0.6	100	400	1.955
1.2	0.6	120	400	1.955
1.2	0.6	140	400	1.955
1.2	0.6	160	400	1.955

Table 4.28. The 50 lowest (a) and highest (b) rmse values at Blairhall with associated parameters taken from within the 10% threshold set of model runs.

#### 4.6.2.3 Model performance at Blairhall

	kg m <sup>-2</sup> yr <sup>-1</sup>	mm yr <sup>-1</sup>
Mean water erosion	-0.005	0.003
Max water erosion	-0.01	-0.006
Max water deposition	0.00	0
Mean tillage erosion	-0.27	-0.17
Max tillage erosion	-0.75	-0.47
Max tillage deposition	0.75	+0.47
Mean net erosion	-0.27	-0.17
Max net erosion	-0.76	-0.48
Max net deposition	0.74	+0.46

Table 4.29. Summary of modelled erosion/deposition rates across the Blairhall transect.

Blairhall transect is by far less active in terms of erosion and deposition (Figure 4.34 and Table 4.29) due to the near-zero topography. Predicted water erosion rates are extremely low (mean  $-0.001 \text{ kg m}^{-2} \text{ yr}^{-1}$ ) and can be effectively described as negligible across the whole length of the transect. The water model predicts no areas of deposition along the transect. All slope gradients are  $< 0.03 \text{ m m}^{-1}$  ( $< 3\%$ ) and specific catchment areas are similar to those at Loanleven. The flow pathway actually diverts to the northeast around cell 2 (27m) and returns to flow through cell 1, hence there being an sca of  $1222 \text{ m}^2 \text{ m}^{-1}$  (Figure 4.31). The net model has produced quite respectable results along the backslope of the transect (cell 2 to 6), however, the errors begin to rise considerably as the convex shoulder section is approached. The model has also encountered problems when predicting deposition at the footslope (cell1). The  $^{137}\text{Cs}$  derived observed value at this position is  $+3.3 \text{ kg m}^{-2} \text{ yr}^{-1}$  ( $+2.1 \text{ mm yr}^{-1}$ ) yet the net model in its optimised form has been capable only of  $+0.74 \text{ kg m}^{-2} \text{ yr}^{-1}$  ( $+0.5 \text{ mm yr}^{-1}$ ). Almost the whole of the modelled erosion/deposition has been made up of that predicted by the ARCTILL tillage model as tillage erosion and deposition. The graph in Figure 4.34 shows this. The mean modelled erosion rate due to tillage was  $-0.27 \text{ kg m}^{-2} \text{ yr}^{-1}$  ( $-0.17 \text{ mm yr}^{-1}$ ), which is effectively 100% of the mean erosion rate predicted by the net model. The maximum soil loss rate occurred on

the slope shoulder ( $-0.76 \text{ kg m}^{-2} \text{ yr}^{-1}$  or  $-0.5 \text{ mm yr}^{-1}$ ). Note there that the ARCTILL model prediction curve was tightly behind the net model curve. More importantly, predictions from the net erosion/deposition model fall within the uncertainty margins of each cell. No error is calculated for the base cell since only one sample was used as input to the  $^{137}\text{Cs}$  technique. Three replicates were taken within the base cell but the two at the northeast and central positions were deemed too close to the fence line to be representative of the whole cell.  $^{137}\text{Cs}$  activity at these two loci ( $1567 \text{ Bq m}^{-2}$  and  $1511 \text{ Bq m}^{-2}$ ) strongly point towards a large net loss of soil. In fact both cores reflect a mean net loss of  $-2.15 \text{ kg m}^{-2} \text{ yr}^{-1}$  or  $-1.35 \text{ mm yr}^{-1}$  (similar to that derived by  $^{137}\text{Cs}$  at the convex shoulder of the transect). Given that such a mean net loss is large for such a flat locus (slope =  $0.035 \text{ m m}^{-1}$ ), tillage once again must be a prime candidate as explanation. A zone the width of a plough set will be ploughed as a headland and will more than likely be turned inwards away from the fence. This could have accounted for the losses being resolved by  $^{137}\text{Cs}$ . Furthermore, if ploughing the headland in this way is practised then the flux of soil may be contributing to the high rates of deposition derived at the northeast and central loci of the base cell. Flow direction derived from the DTM confirmed that material from cell 1 does move due to tillage to the base cell. So considering the  $^{137}\text{Cs}$  derived erosion rate of  $-2.14 \text{ kg m}^{-2} \text{ yr}^{-1}$  at cell 1 it is expected that this material be subsequently deposited in the base cell. There was, however, a disparity of some  $1.2 \text{ kg m}^{-2} \text{ yr}^{-1}$  between the erosion rate in cell 1 and the deposition rate in the base cell. The flow direction algorithm in the water erosion model could have routed sediment detached in cell 1 to other neighbouring cells since it always spreads flow to two downslope neighbouring cells. This could be causing a very small amount of soil to avoid the base cell but even this tiny  $-0.01 \text{ kg m}^{-2} \text{ yr}^{-1}$  failed to account for the deficit. Alternatively the high sca value of this base cell could have caused some soil loss through accumulated flow detachment although realistically rather doubtful since there was no evidence of flow channels or wash.

Least squared error analysis was carried out on the Blairhall data and is presented alongside regression tests. The net erosion/deposition model statistically predicted well ( $r^2 = 0.786$ ,  $p = 0.019$ ,  $n = 6$ ) as displayed in Figure 4.36. The net model also generated a low rmse value (Table 4.30). Tillage translocation was then subtracted from the optimised net model to test the impact on predictive ability. The  $r^2$  value decreased to 0.001 ( $p = 0.961$ ,  $n = 6$ ), suggesting the importance of tillage processes at least at this site. Stepwise regression was applied to the variables and found that using tillage translocation alone to predict the derived values is 78.8% effective ( $p = 0.018$ ,  $n = 6$ ). When tillage was combined with the water portion of the optimised net model in a regression model, the  $r^2$  value rose slightly to 0.804 ( $p = 0.087$ ,  $n = 6$ ). In addition to the relationship being not significant the estimated error squared value was higher (1.045) than for the optimised net model alone (0.949), so the optimised net model still provided the best agreement. When ARCTILL was used as a standalone model the rmse was less than that produced by the net model (model 4 in Table 4.30). This suggests that water erosion at Blairhall is negligible. A persistent problem with the model has been with deposition. Error values are extremely low along the transect until reaching the shoulder and footslope cells.



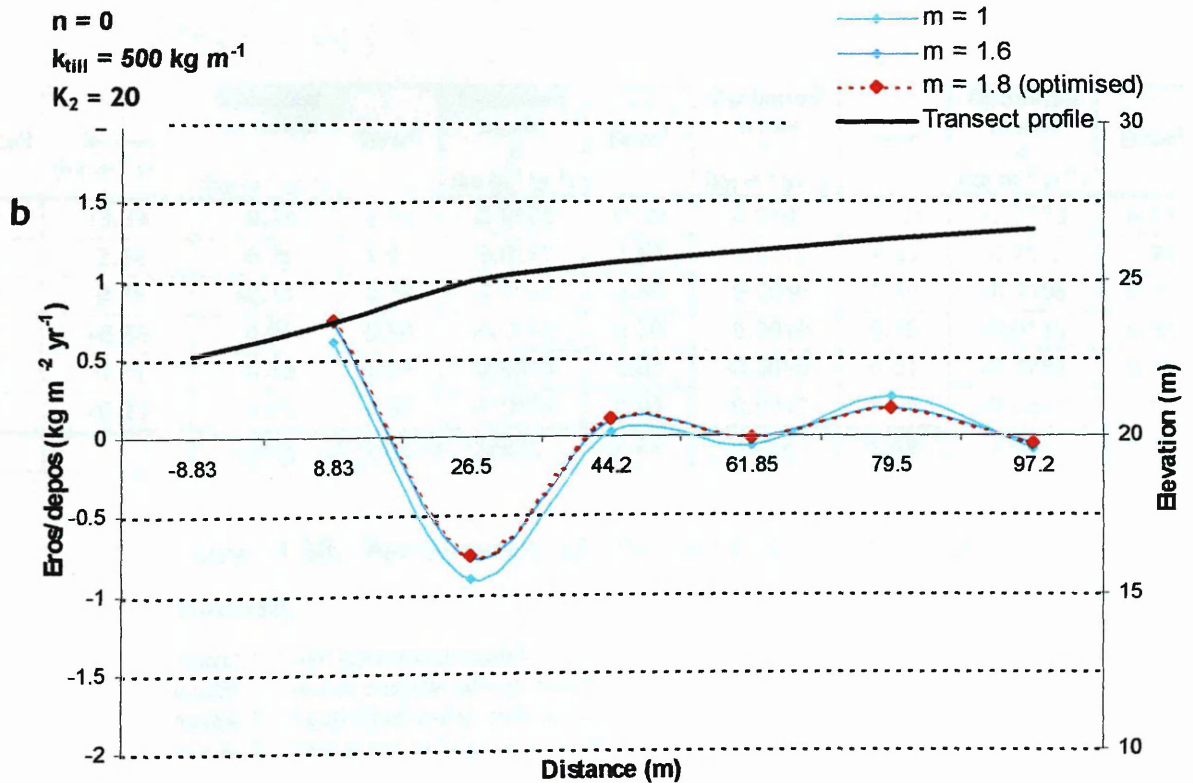
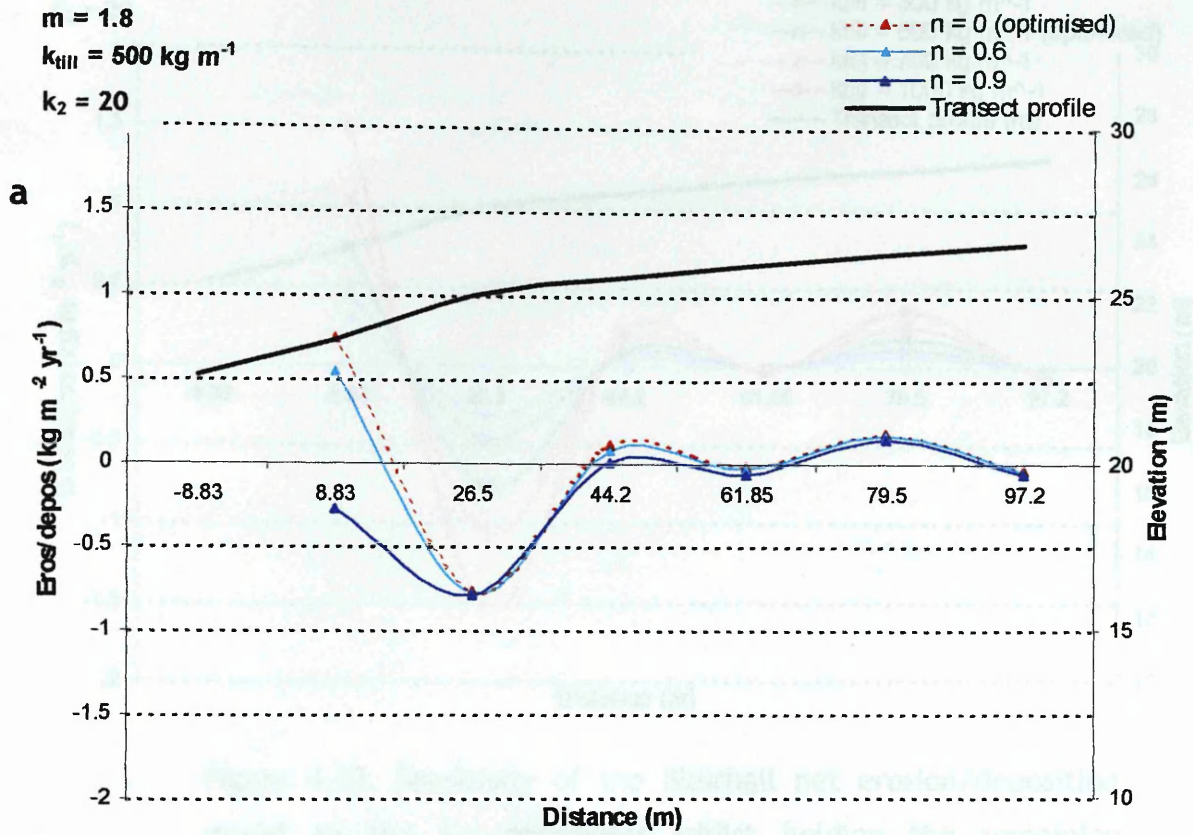


Figure 4.32. Sensitivity of the Blairhall net erosion/deposition model to the scale  $n$  (a) and slope  $m$  (b) parameters whilst holding the remaining parameters at optimised values.

$m = 1.8$   
 $n = 0$   
 $K_2 = 20$

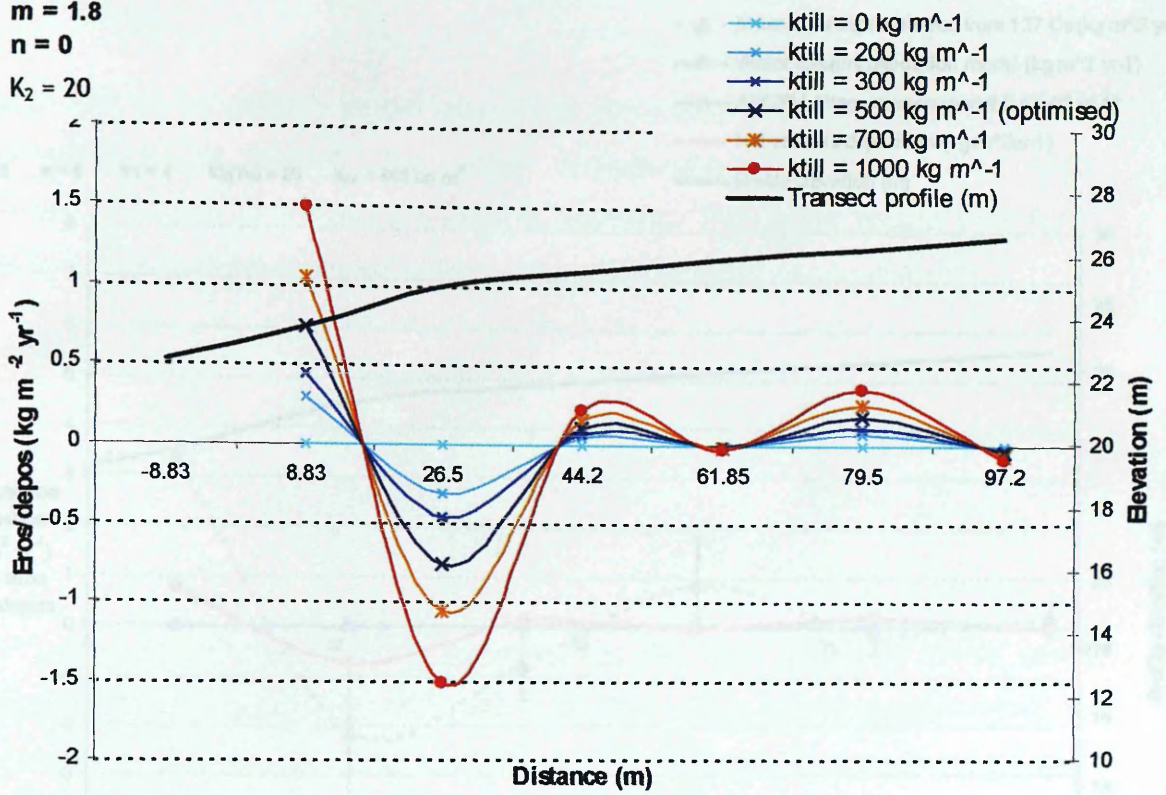


Figure 4.33. Sensitivity of the Blairhall net erosion/deposition model to the  $k_{till}$  parameter whilst holding the remaining parameters at optimised values.

Figure 4.34. Predictions of the optimized models across the Blairhall site.

Cell	$^{137}\text{Cs}$ derived ( $\text{kg m}^{-2} \text{yr}^{-1}$ )	Optimised net model 1 ( $\text{kg m}^{-2} \text{yr}^{-1}$ )	Error <sup>2</sup>	Optimised model 2 ( $\text{kg m}^{-2} \text{yr}^{-1}$ )	Error <sup>2</sup>	Optimised model 3 ( $\text{kg m}^{-2} \text{yr}^{-1}$ )	Error <sup>2</sup>	Optimised model 4 ( $\text{kg m}^{-2} \text{yr}^{-1}$ )	Error <sup>2</sup>
1	+3.34	+0.74	6.74	-0.0100	11.21	-0.0100	11.21	+0.7523	6.69
2	-2.14	-0.76	1.91	-0.0110	4.55	-0.0110	4.55	-0.7523	1.94
3	-0.78	+0.11	0.78	-0.0040	0.60	-0.0040	0.60	+0.1106	0.79
4	+0.88	-0.01	0.80	-0.0010	0.78	-0.0010	0.78	-0.0136	0.80
5	-0.12	+0.18	0.09	-0.0010	0.01	-0.0010	0.01	+0.1782	0.09
6	+0.23	-0.05	0.07	-0.0010	0.05	-0.0010	0.05	-0.0447	0.07
		RMSE	1.32	RMSE	1.69	RMSE	1.69	RMSE	1.31

Table 4.30. Performance of the various erosion models at Blairhall.

Model 1 = net optimised model  
 Model 2 = water portion of net model  
 Model 3 = Optimised water only model  
 Model 4 = Optimised tillage only model

Figure 4.35. Comparison of the predicted erosion/deposition rates across the Blairhall site.

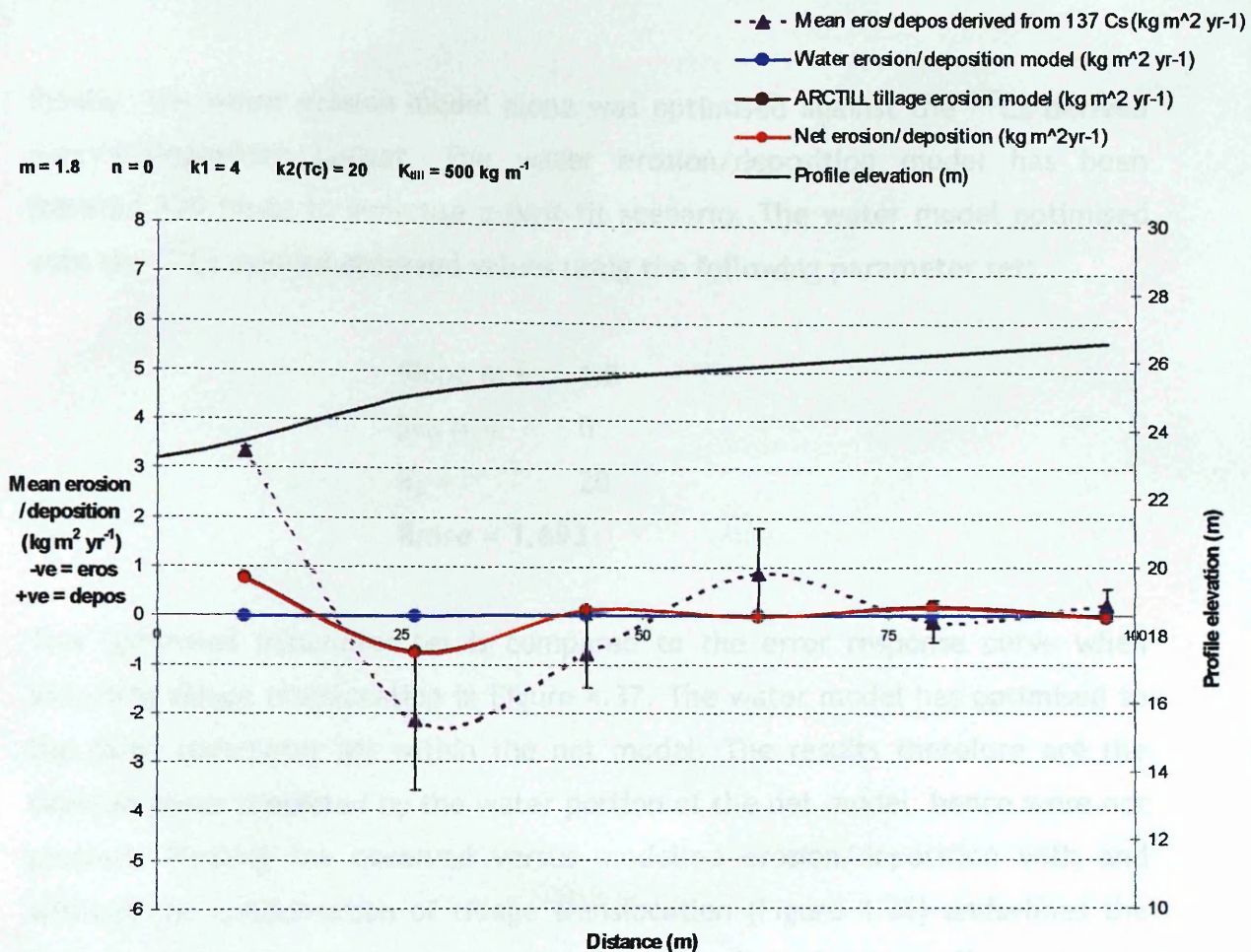


Figure 4.34. Predictions of the optimised models across the Blairhall site.

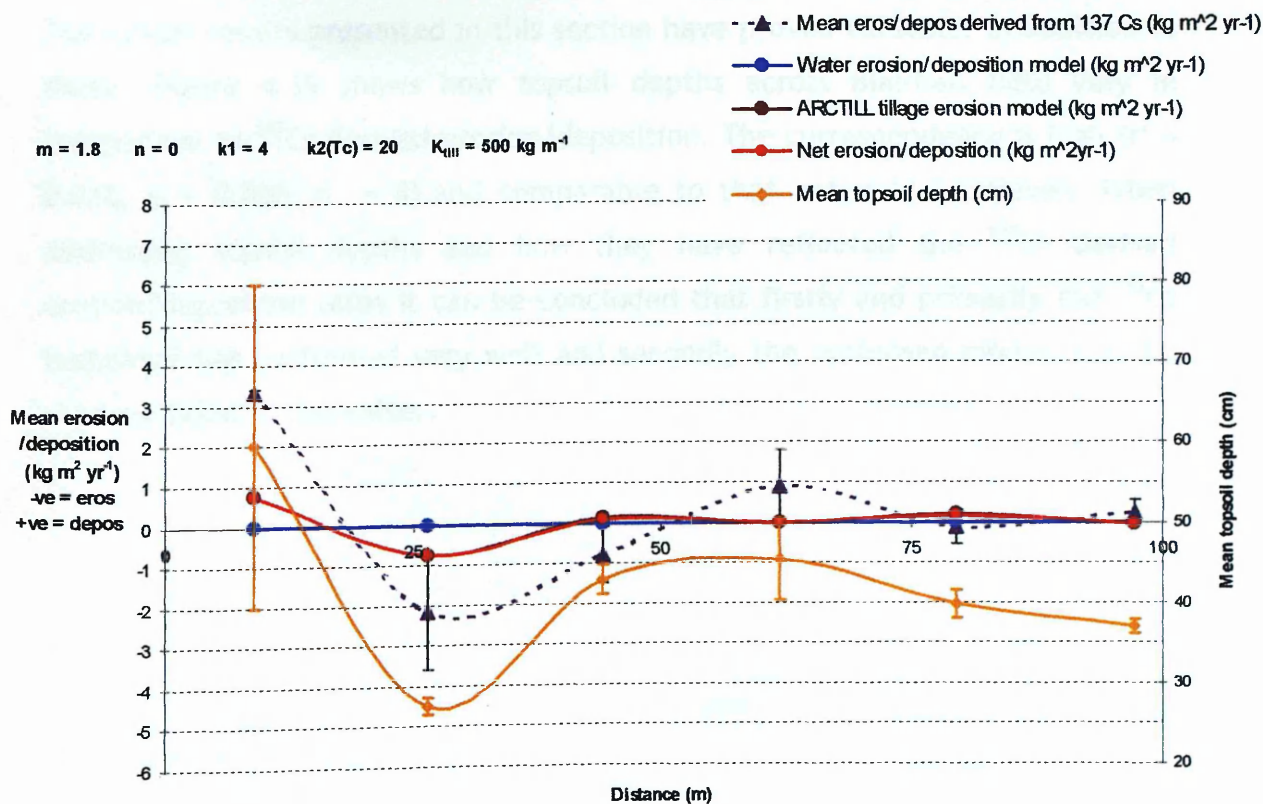


Figure 4.35. Comparison of the optimised net models and mean topsoil depths across the Blairhall site.

Finally, the water erosion model alone was optimised against the  $^{137}\text{Cs}$  derived erosion/deposition budget. The water erosion/deposition model has been iterated 720 times to generate a best-fit scenario. The water model optimised with the  $^{137}\text{Cs}$  derived observed values using the following parameter set:

Slope m = 1.8  
Scan = 0  
 $K_2$  = 20  
**Rmse = 1.693**

This optimised parameter set is compared to the error response curve when including tillage translocation in Figure 4.37. The water model has optimised to the same parameter set within the net model. The results therefore are the same as those predicted by the water portion of the net model, hence were not plotted. Plotting the observed versus modelled erosion/deposition with and without the consideration of tillage translocation (Figure 4.36) underlines the fact that tillage must be included. Not doing so will evidently lead to such poor ability to explain soil erosion/deposition patterns.

The model results presented in this section have proved valuable. In addition to these, Figure 4.35 shows how topsoil depths across Blairhall field vary in comparison to  $^{137}\text{Cs}$  derived erosion/deposition. The correspondence is high ( $r^2 = 0.878$ ,  $p = 0.006$ ,  $n = 6$ ) and comparable to that noted at Loanleven. When addressing topsoil depths and how they have reflected the  $^{137}\text{Cs}$  derived erosion/deposition rates it can be concluded that firstly and primarily the  $^{137}\text{Cs}$  technique has performed very well and secondly the optimised models may be used confidently thereafter.

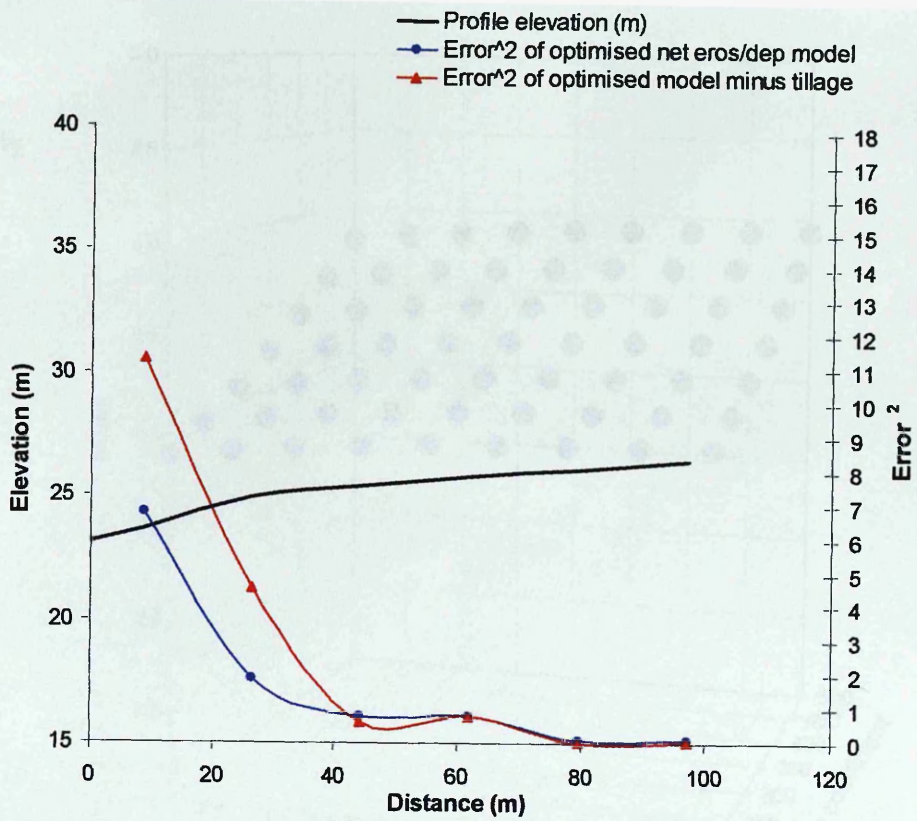


Figure 4.36. Plot of modelled erosion/deposition versus <sup>137</sup>Cs derived erosion/deposition with and without tillage translocation at Blairhall.

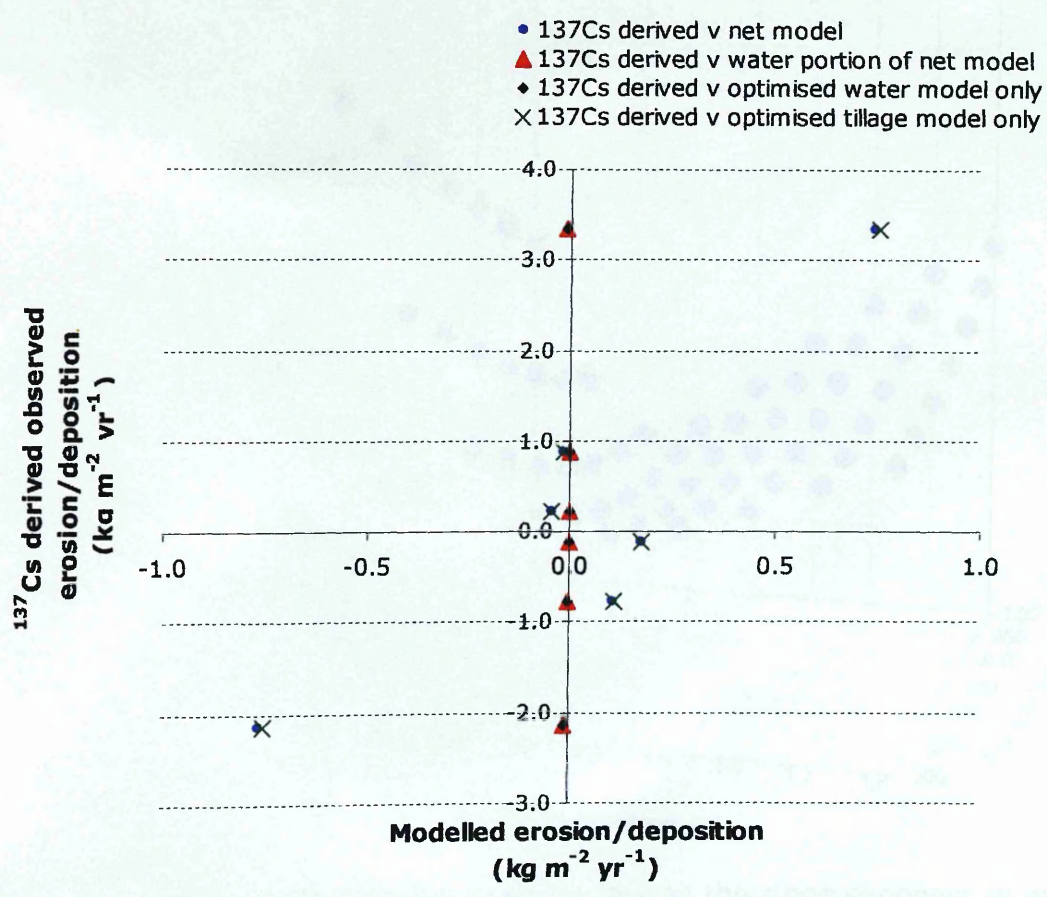


Figure 4.37. Distribution of errors across the Blairhall transect from the optimised models. Comparison of the net eros/dep model and water model minus tillage translocation is made.

### 4.6.3 Leadketty

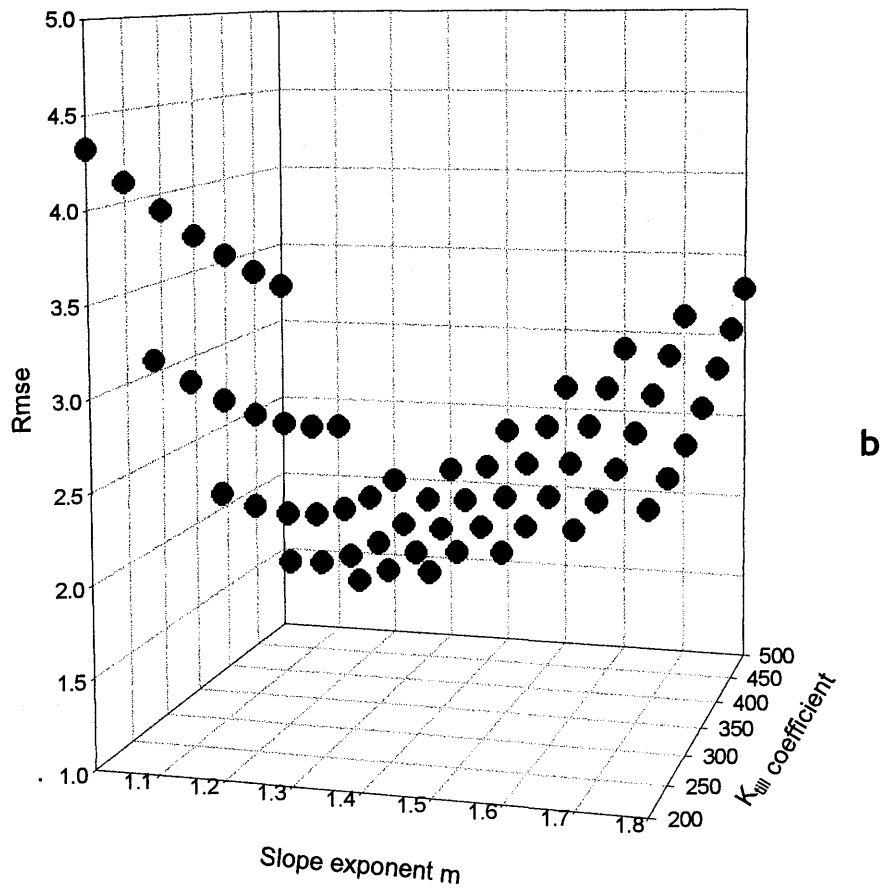
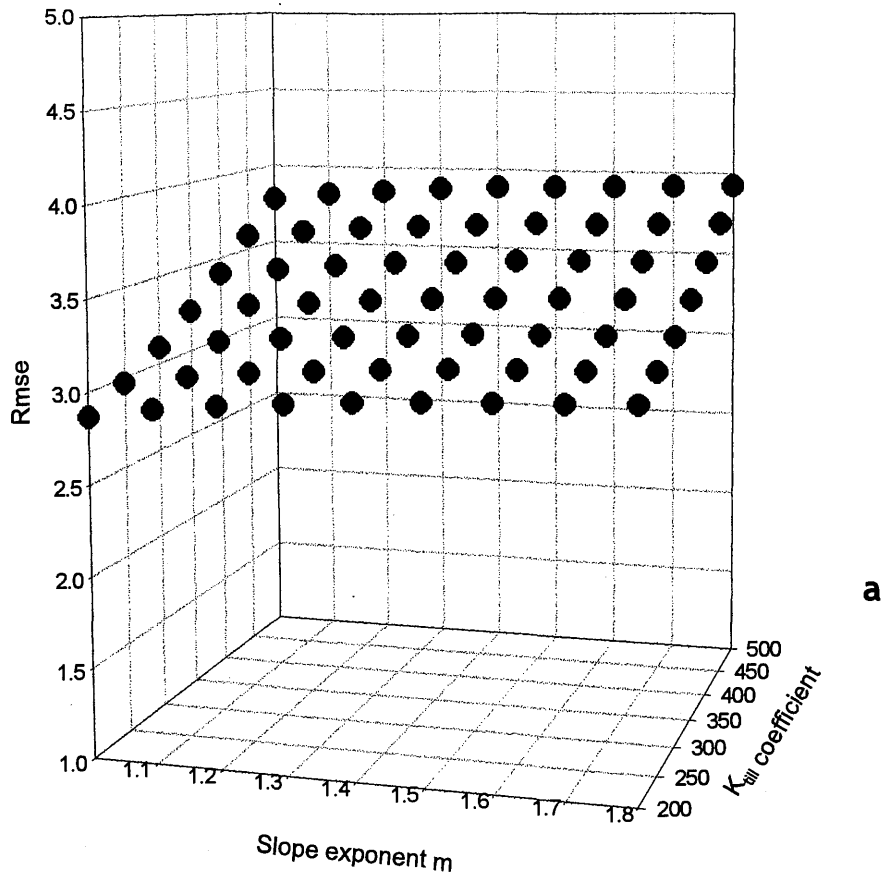


Figure 4.38. Error response by varying the slope exponent  $m$  and  $K_{till}$  variables, whilst holding the specific catchment area exponent  $n$  and  $k_2$  at (a) minimum and (b) maximum.

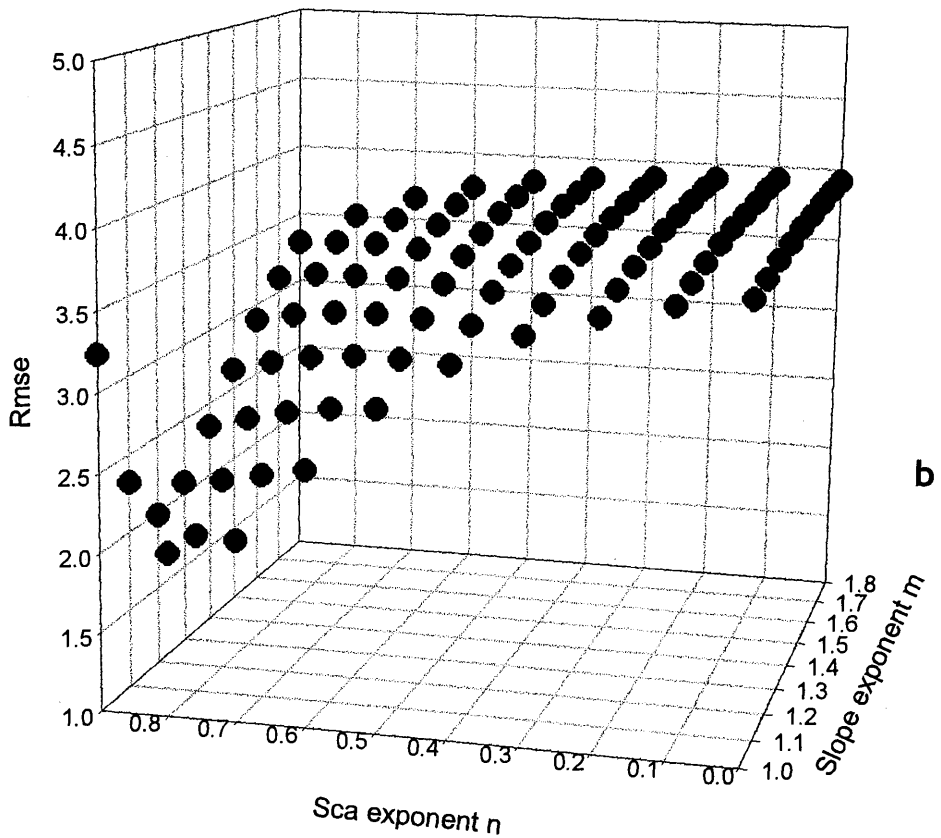
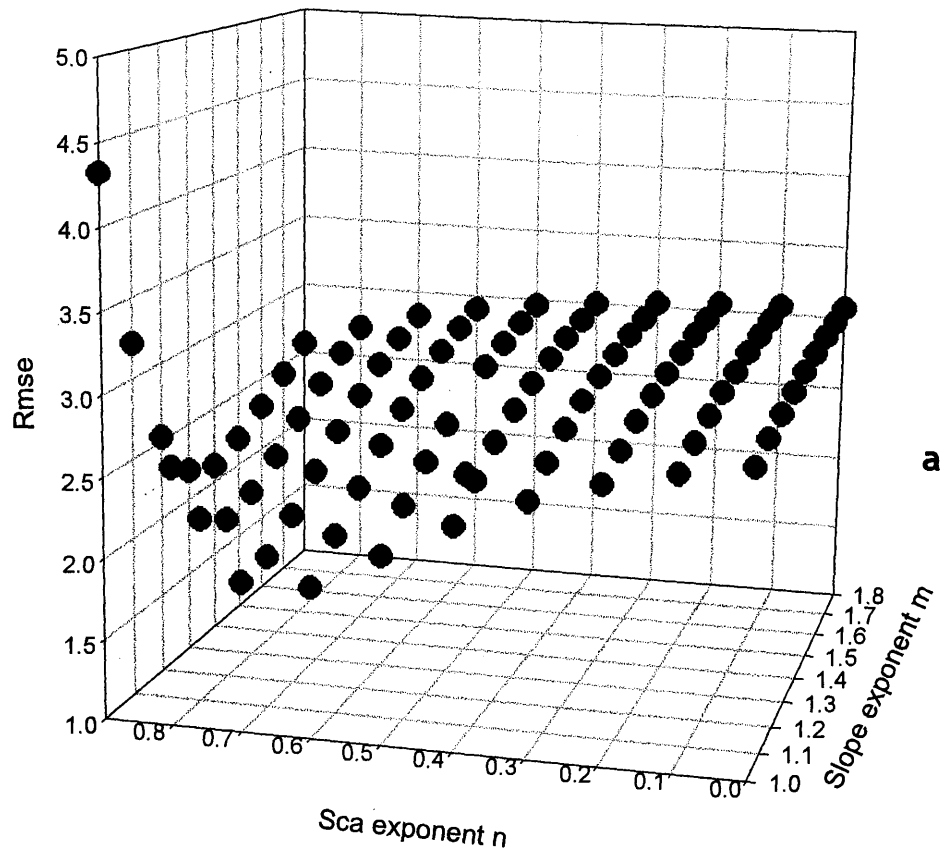


Figure 4.39. Error response by varying the slope exponent  $m$  and the specific catchment area exponent  $n$ , whilst holding variables  $k_{till}$  and  $k_2$  at (a) minimum and (b) maximum.

The optimised parameter set for the Leadketty net erosion/deposition model is:

Slope  $m = 1.7$   
Sca  $n = 0.9$   
 $K_2 = 20$   
 $k_{till} = 300$   
**Rmse = 1.829**

The error response surfaces in Figure 4.38 and Figure 4.39 have been taken from the full set of model runs as opposed to from within the 10% threshold. This was done to aid display purposes because the 10% threshold in combination with the minimum and maximum constant criteria proved so restrictive. In line with Loanleven and Blairhall, sca  $n$  has displayed strong influence on the generation of rmse values. Bearing in mind the optimum rmse value of 1.829 and the cut-off of 2.079 it was clear that only do the model predictions come close to the observed once sca  $n$  has been maximised. Nested within this trend are those of  $k_{till}$  and slope  $m$ . The model approaches optimisation when driven by low  $k_{till}$  values and mid-level slope  $m$  values (Figure 4.38a and b). Further decrease in  $m$  towards 1 after the 1.3 mark has provoked a rapid rise in error due to the maximised influence of sca  $n$  held constant. Table 4.31 and Table 4.32 display the data.

Varying slope  $m$  and sca  $n$  whilst holding  $k_2$  and  $k_{till}$  constant identified a pronounced dip in errors towards mid-high sca  $n$  and low slope  $m$  values. A subtle difference is noticeable in the rmse levels where the surfaces plateau out both in the minimum and maximum  $k_{till}$  scenarios (Figure 4.39a and b). When  $k_{till}$  is maximised the mean error is much larger (3.427) than when  $k_{till}$  is minimised (2.709) hinting that  $k_{till}$  be set to a low value in preference to high. The lowest and highest 50 rmse outputs are shown in Table 4.33. In contrast to the previous fields the range of rmse within the lowest 50 run excerpt is much larger and the dip to the optimised set is quite 'sharp'. The model has behaved in a very sensitive manner at Leadketty and only very small fluctuations in either of the 3 parameters forces the rmse to change rapidly. Examining the first 24 model runs in Table 4.33a reveals that the variation in rmse has been explained solely by the change in  $k_{till}$  from 250 to 350. To reach optimisation the model calibrated to



mid-high  $sca$   $n$  values and low slope  $m$  values (Figure 4.39a and b). High  $k_{till}$  values alongside slightly higher slope  $m$  and maximised  $sca$   $n$  values resulted in less favourable scenarios.

Similarly with the Loanleven and Blairhall field sites the optimisation routine has failed to register any influence due to the  $k_2$  or transport capacity parameter. Reasons for this have been discussed in the Loanleven data section. This field (21 ha) is however considerably larger than Loanleven (6.5 ha) and even though smaller than Blairhall (24 ha) has a far more complex topography increasing the likelihood of concentrated overland flow (figure 4). Therefore transport capacity will almost certainly play a significant role and possibly more so here at Leadketty.

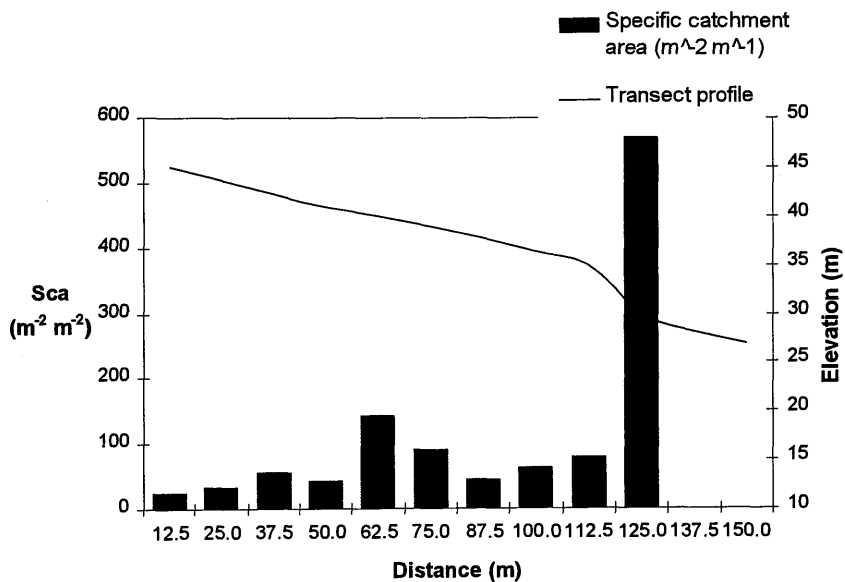


Figure 4.40. Variation in specific catchment area across the Leadketty transect

$m$	$n$	$k_2$	$k_{till}$	rmse
1.3	0.9	160	350	1.951
1.3	0.9	160	400	1.952
1.2	0.9	160	450	1.988
1.3	0.9	160	300	1.994
1.2	0.9	160	500	1.994

Table 4.31. The lowest 5 rmse values taken from Figure 4.38b when  $sca$  and  $k_2$  are maximised.

<b>m</b>	<b>n</b>	<b>k<sub>2</sub></b>	<b>k<sub>till</sub></b>	<b>rmse</b>
1	0	20	200	2.875
1.1	0	20	200	2.928
1.2	0	20	200	2.968
1	0	20	250	2.975
1.3	0	20	200	3.000

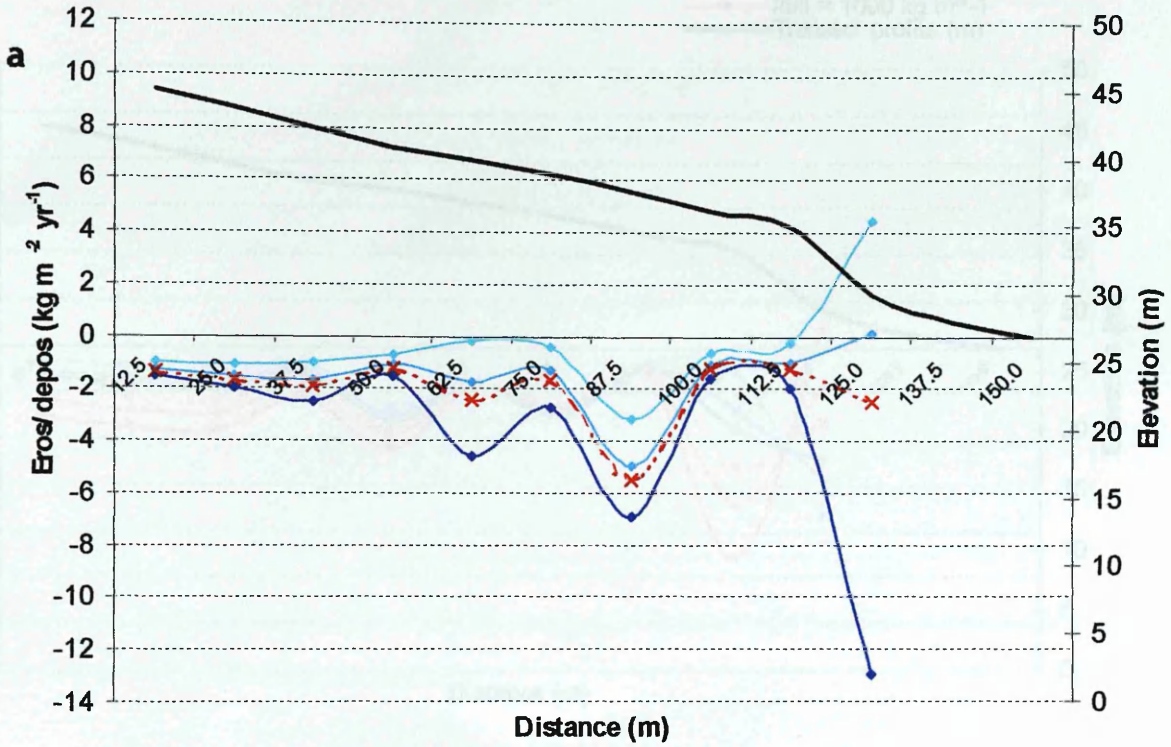
Table 4.32. The lowest 5 rmse values taken from Figure 4.38a when sca and k<sub>2</sub> are minimised.

a					b				
m	n	Tc	k <sub>fill</sub>	rmse	m	n	Tc	k <sub>fill</sub>	rmse
1	0.7	20	300	1.829	1.1	0.8	140	250	2.037
1	0.7	40	300	1.829	1.1	0.8	160	250	2.037
1	0.7	60	300	1.829	1	0.8	20	500	2.038
1	0.7	80	300	1.829	1	0.8	40	500	2.038
1	0.7	100	300	1.829	1	0.8	60	500	2.038
1	0.7	120	300	1.829	1	0.8	80	500	2.038
1	0.7	140	300	1.829	1	0.8	100	500	2.038
1	0.7	160	300	1.829	1	0.8	120	500	2.038
1	0.7	20	350	1.845	1	0.8	140	500	2.038
1	0.7	40	350	1.845	1	0.8	160	500	2.038
1	0.7	60	350	1.845	1	0.8	20	450	2.040
1	0.7	80	350	1.845	1	0.8	40	450	2.040
1	0.7	100	350	1.845	1	0.8	60	450	2.040
1	0.7	120	350	1.845	1	0.8	80	450	2.040
1	0.7	140	350	1.845	1	0.8	100	450	2.040
1	0.7	160	350	1.845	1	0.8	120	450	2.040
1	0.7	20	250	1.860	1	0.8	140	450	2.040
1	0.7	40	250	1.860	1	0.8	160	450	2.040
1	0.7	60	250	1.860	1.4	0.9	20	350	2.055
1	0.7	80	250	1.860	1.4	0.9	40	350	2.055
1	0.7	100	250	1.860	1.4	0.9	60	350	2.055
1	0.7	120	250	1.860	1.4	0.9	80	350	2.055
1	0.7	140	250	1.860	1.4	0.9	100	350	2.055
1	0.7	160	250	1.860	1.4	0.9	120	350	2.055
1.1	0.8	20	400	1.890	1.4	0.9	140	350	2.055
1.1	0.8	40	400	1.890	1.4	0.9	160	350	2.055
1.1	0.8	60	400	1.890	1.4	0.9	20	250	2.058
1.1	0.8	80	400	1.890	1.4	0.9	40	250	2.058
1.1	0.8	100	400	1.890	1.4	0.9	60	250	2.058
1.1	0.8	120	400	1.890	1.4	0.9	80	250	2.058
1.1	0.8	140	400	1.890	1.4	0.9	100	250	2.058
1.1	0.8	160	400	1.890	1.4	0.9	120	250	2.058
1.1	0.8	20	350	1.895	1.4	0.9	140	250	2.058
1.1	0.8	40	350	1.895	1.4	0.9	160	250	2.058
1.1	0.8	60	350	1.895	1.3	0.8	20	250	2.066
1.1	0.8	80	350	1.895	1.3	0.8	40	250	2.066
1.1	0.8	100	350	1.895	1.3	0.8	60	250	2.066
1.1	0.8	120	350	1.895	1.3	0.8	80	250	2.066
1.1	0.8	140	350	1.895	1.3	0.8	100	250	2.066
1.1	0.8	160	350	1.895	1.3	0.8	120	250	2.066
1	0.7	20	400	1.906	1.3	0.8	140	250	2.066
1	0.7	40	400	1.906	1.3	0.8	160	250	2.066
1	0.7	60	400	1.906	1.3	0.9	20	250	2.078
1	0.7	80	400	1.906	1.3	0.9	40	250	2.078
1	0.7	100	400	1.906	1.3	0.9	60	250	2.078
1	0.7	120	400	1.906	1.3	0.9	80	250	2.078
1	0.7	140	400	1.906	1.3	0.9	100	250	2.078
1	0.7	160	400	1.906	1.3	0.9	120	250	2.078
1.1	0.8	20	450	1.930	1.3	0.9	140	250	2.078
1.1	0.8	40	450	1.930	1.3	0.9	160	250	2.078

Table 4.33. The 50 lowest (a) and highest (b) rmse values at Leadketty with associated parameters.

$m = 1$   
 $k_{\text{till}} = 300 \text{ kg m}^{-1}$   
 $k_2 = 20$

$n = 0$   
 $n = 0.6$   
 $n = 0.9$   
 $n = 0.7$  (optimised)  
 Transect profile



$n = 0.7$   
 $k_{\text{till}} = 300 \text{ kg m}^{-1}$   
 $k_2 = 20$

$m = 1$  (optimised)  
 $m = 1.6$   
 $m = 1.9$   
 Transect profile

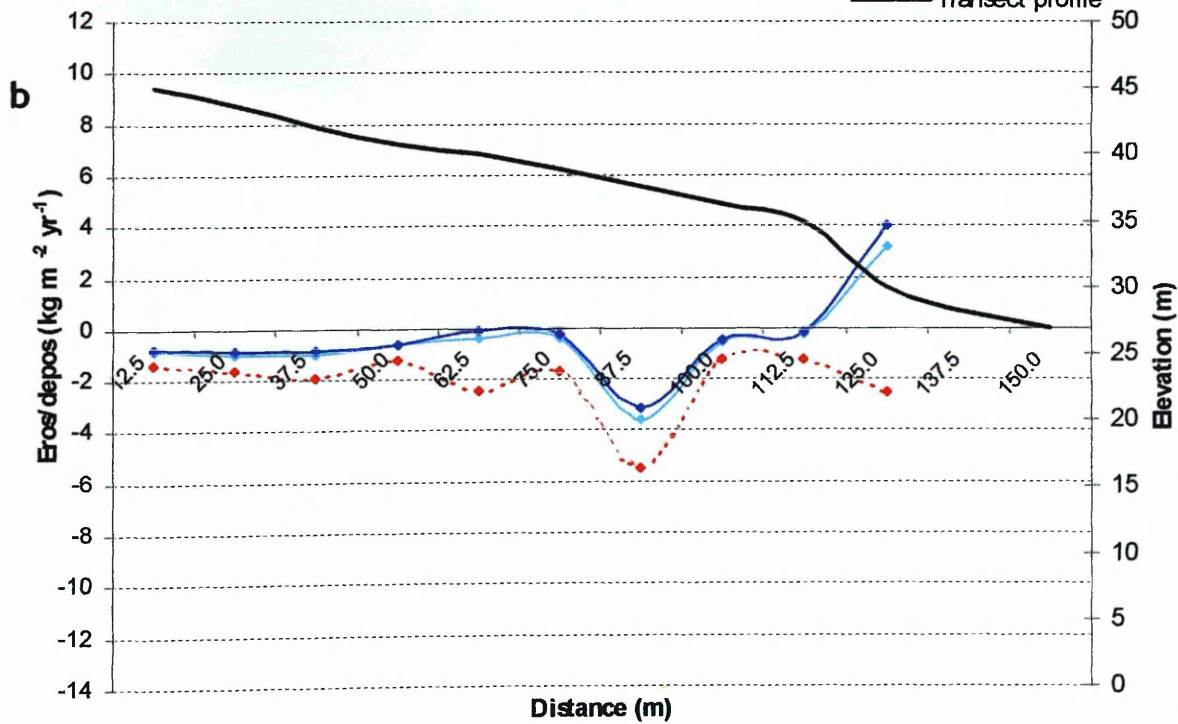


Figure 4.41. Sensitivity of the net erosion/deposition model to the scale  $n$  (a) and slope  $m$  (b) parameters whilst holding the remaining parameters at optimised values.

$m = 1$   
 $n = 0.7$   
 $k_2 = 20$

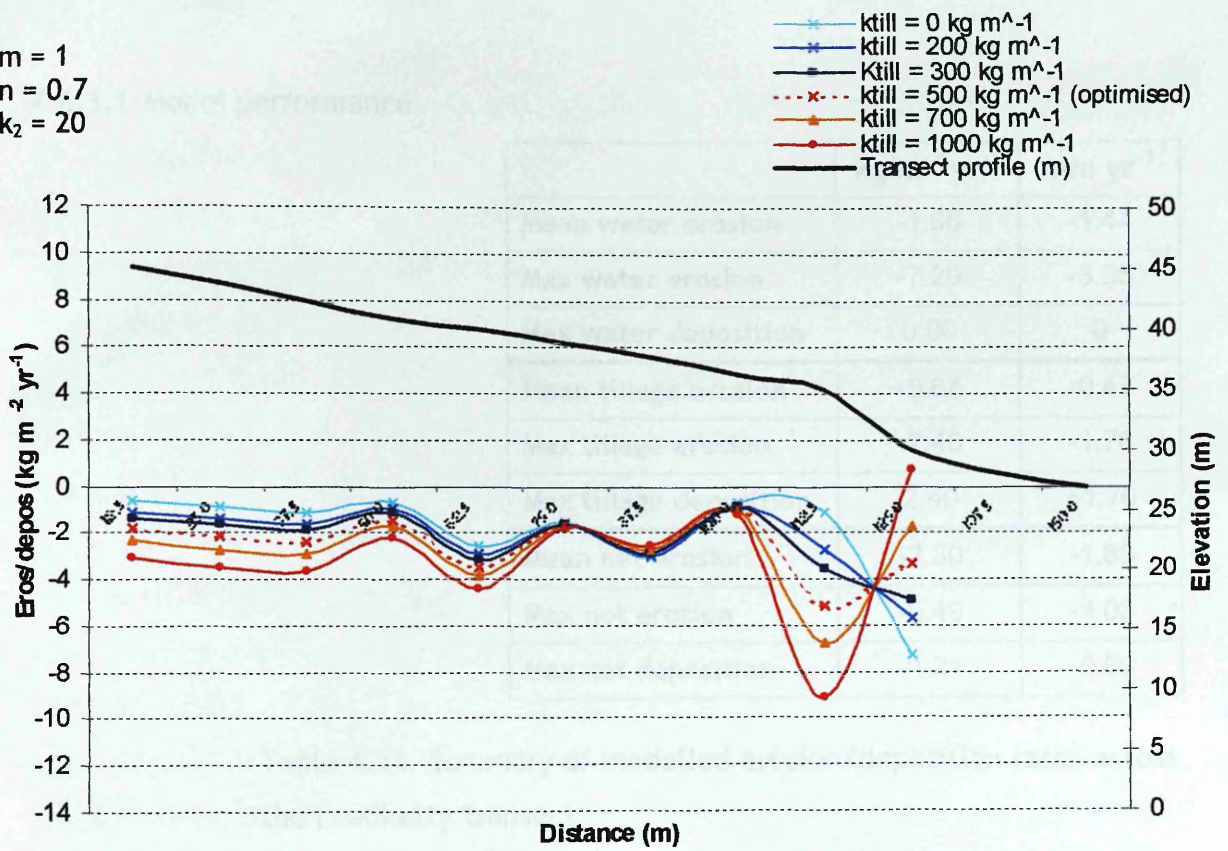


Figure 4.42. Sensitivity of the net erosion/deposition model to the  $k_{till}$  parameter whilst holding the remaining parameters at optimised values.

$^{137}Cs$ derived erosion rate (mm yr <sup>-1</sup> )	Profile curvature (m m <sup>-2</sup> )
0.00	0.174
0.10	0.130
0.20	0.093
0.30	0.062
0.40	0.037
0.50	0.016
0.60	0.000
0.70	-0.130

Table 4.35. Comparison of  $^{137}Cs$  derived erosion rates with profile curvature values.

Table 4.35 offers poor agreement of the rates, in particular the first two, which are located very close to the knoll peak in the field exactly where I made a few minor adjustments to the profile. The two values which are

#### 4.6.3.1 Model performance

	kg m <sup>-2</sup> yr <sup>-1</sup>	mm yr <sup>-1</sup>
Mean water erosion	-1.96	-1.44
Max water erosion	-7.29	-5.35
Max water deposition	0.00	0
Mean tillage erosion	-0.64	-0.47
Max tillage erosion	-2.40	-1.76
Max tillage deposition	2.40	+1.76
Mean net erosion	-2.30	-1.69
Max net erosion	-5.49	-4.03
Max net deposition	-1.21	-0.89

Table 4.34. Summary of modelled erosion/deposition rates across the Leadketty transect.

The most noteworthy point here is that the <sup>137</sup>Cs derived observed results are showing no areas of deposition along the transect. This was surprising given the variety in topography. Erosion rates oscillated widely throughout the slope length and based on topography (Figure 4.45) they are rather difficult to explain.

<sup>137</sup> Cs derived erosion (kg m <sup>-2</sup> yr <sup>-1</sup> )	Profile Curvature +ve = convex -ve = concave
-4.33	0.344
-3.58	0.136
-1.96	0.033
-4.89	-0.031
-1.10	0.132
-2.41	0.015
-1.66	0.012
-1.18	0.080
-3.46	0.739
-2.48	-0.658

Table 4.35. Comparison of <sup>137</sup>Cs derived erosion rates with profile curvature values.

Table 4.35 offers part explanation of the rates. In particular the first two cells, which are located very close to the knoll peak in the field exactly where the main archaeological enclosure is positioned, are rapidly eroding (between -2.7

and  $-2.2 \text{ mm yr}^{-1}$ ) and are both strongly convex. Tillage translocation could only be responsible for this since hydrologically there is negligible accumulation of overland flow ( $25 \text{ m}^{-2} \text{ m}^{-1}$ ). This trend weakens somewhat further down the transect and at point 7 there is a sharp sub-peak in erosion both quarter way down and at the transect's terminus. The increase in specific catchment area (Figure 4.40) could account for the peak at the end of the transect in the form of concentrated flow detachment. The large peak in erosion rates at the 50m mark ( $-4.89 \text{ kg m}^{-2} \text{ yr}^{-1}$  or  $-3\text{mm yr}^{-1}$ ) estimated by  $^{137}\text{Cs}$  is poorly simulated by both the water and tillage models. There is a 192% increase in concavity (profile curvature) here yet the tillage model predicted erosion of  $-0.47 \text{ kg m}^{-2} \text{ yr}^{-1}$  and the water model  $-0.75 \text{ kg m}^{-2} \text{ yr}^{-1}$ . Given the slope position, erosion due to concentrated flow would be unlikely due to the low levels of flow accumulation (sca of only  $43 \text{ m}^{-2} \text{ m}^{-1}$ ). Such a large rise in erosion rates could only be generated by strong tillage translocation on convex terrain or by concentrated flow erosion in concave swale-like terrain. Neither of these were present at this point in the transect. It is likely that the shape of the slope has been inaccurately detected by the DTM. The final cell is shallowing out ( $-0.657 =$  concave) where a flow accumulation of  $570 \text{ m}^{-2} \text{ yr}^{-1}$  would be expected. The optimised water portion of the net model has in fact simulated this well (Figure 4.45).

The optimised net erosion/deposition model has predicted all cells to be experiencing net erosion. However, there are cells (3, 5, 8, 9, 10) with very close agreements with the observed values. Unfortunately predictions for the remainder of cells are poor and at times predicting inversely (cells 1, 2, 4, 7). A least square error analysis was carried out on the modelling and the results are shown in Table 4.36. Overall the net optimised model performed the best although the rmse value is considerably larger than for Blairhall and Loanleven. The tillage erosion model alone performed the worst of all suggesting that water erosion is responsible in part for the whole budget.

Tillage translocation was removed totally from the optimisation routine leaving only the water erosion/deposition model as a prediction tool. 720 runs of the model in all combinations of parameters resulted in the following best-fit set:

$$\begin{aligned}\text{Slope } m &= 1 \\ \text{Scan} &= 0.6 \\ k_2 &= 20 \\ \text{Rmse} &= 2.285\end{aligned}$$

Figure 4.46 displays the predicted budget compared to the optimised net erosion/deposition model predictions and the  $^{137}\text{Cs}$  derived budget. Although there are positions in the transect where better predictions have been made there are in turn worse fits, for example at cell 10. Model 4 (Table 4.36) representing tillage erosion only predicted erosion/deposition very poorly. The poor ability of the models at predicting the  $^{137}\text{Cs}$  derived values has raised suspicion as to whether the baseline  $^{137}\text{Cs}$  activity at the reference site has caused the strange results.

Of particular concern is the lack of depositional areas given the topography. Even despite the longer slope length involved, a certain level of accumulation or near stability conditions was expected at the footslope mid-backslope section. By overlaying the mean topsoil depths onto the model predictions (Figure 4.47) the erosion rate observed at the end of the transect at the convex shoulder would appear to be in good agreement with the sharp decrease in topsoil depth. Besides this, a slight shallowing trend in topsoil depths up-transect run contrary to the deepening trend suggested by the  $^{137}\text{Cs}$  derived values.

The cause for the suspicion is the lack of confidence in the  $^{137}\text{Cs}$  derived budget. Great difficulties were encountered finding an undisturbed reference site. The site used was found very late in the study and displayed all the signs of non-cultivation. The activity used for the reference site was  $2043 \text{ Bq m}^{-2}$ , which is slightly higher than at Loanleven  $1746 \text{ Bq m}^{-2}$  (10km further north at the same elevation) and  $1879 \text{ Bq m}^{-2}$  at Blairhall. Given more time a further two replicate cores for use as baseline activity need to be taken to increase confidence.



Cell	<sup>137</sup> Cs derived (kg m <sup>-2</sup> yr <sup>-1</sup> )	Optimised net model 1 (kg m <sup>-2</sup> yr <sup>-1</sup> )	Error <sup>2</sup>	Optimised model 2 (kg m <sup>-2</sup> yr <sup>-1</sup> )	Error <sup>2</sup>	Optimised model 3 (kg m <sup>-2</sup> yr <sup>-1</sup> )	Error <sup>2</sup>	Optimised model 4 (kg m <sup>-2</sup> yr <sup>-1</sup> )	Error <sup>2</sup>
1	-4.33	-1.35	8.86	-0.62	13.77	-0.54	14.34	-0.73	12.91
2	-3.58	-1.64	3.77	-0.83	7.54	-0.71	8.24	-0.80	7.70
3	-1.96	-1.89	0.00	-1.13	0.68	-0.92	1.09	-0.76	1.43
4	-4.89	-1.21	13.56	-0.75	17.20	-0.60	18.47	-0.47	19.61
5	-1.10	-1.21	0.01	-0.67	0.19	-0.55	0.30	-0.54	0.31
6	-2.42	-1.24	1.40	-1.16	1.58	-0.91	2.28	-0.07	5.50
7	-1.66	-2.41	0.56	-2.56	0.82	-1.88	0.05	0.15	3.29
8	-1.18	-1.68	0.25	-1.54	0.13	-1.19	0.00	-0.13	1.10
9	-3.46	-5.49	4.11	-3.09	0.14	-2.54	0.83	-2.40	1.12
10	-2.48	-4.89	5.83	-7.29	23.17	-4.67	4.82	+2.40	23.79
		RMSE	1.96	RMSE	2.55	RMSE	2.245	RMSE	2.770

Table 4.36. Performance of the various erosion models at Leadketty.

Model 1 = net optimised model  
 Model 2 = water portion of net model  
 Model 3 = optimised water only  
 Model 4 = optimised tillage only

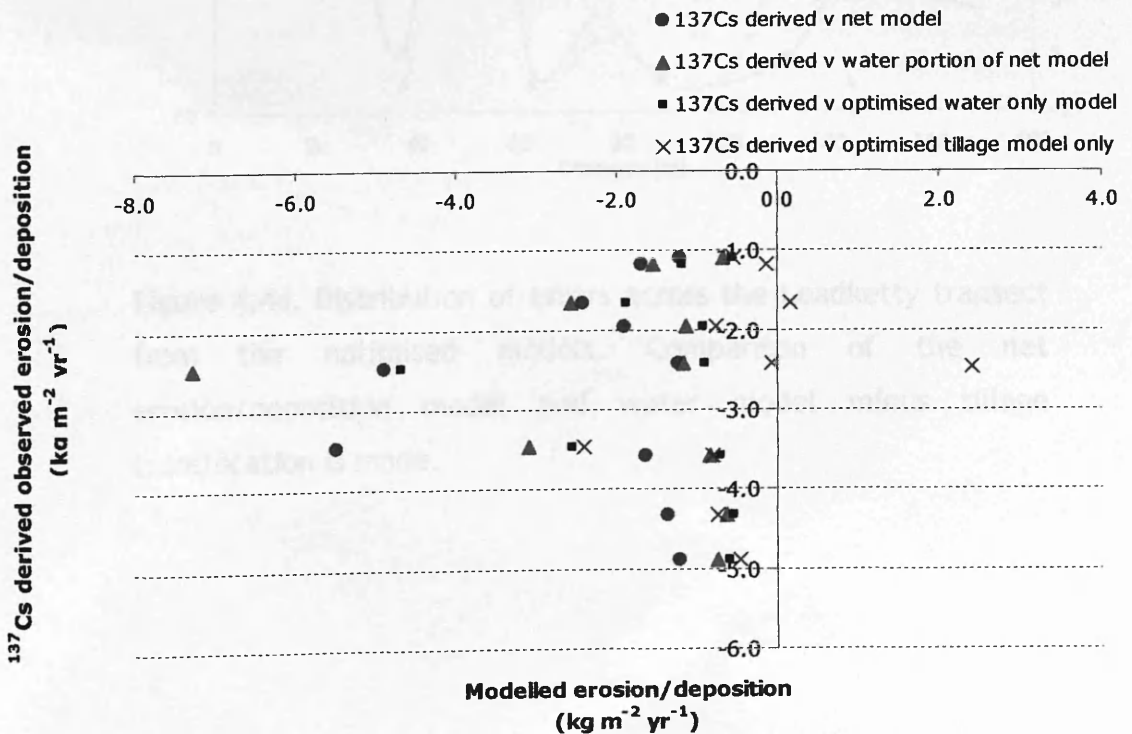


Figure 4.43. Plot of modelled erosion/deposition versus <sup>137</sup>Cs derived erosion/deposition with and without tillage translocation at Leadketty.

Adding to the suspicion surrounding  $^{137}\text{Cs}$  derived observed erosion data is the fact that mean topsoil depth correlated very poorly with  $^{137}\text{Cs}$  derived erosion/deposition budget ( $r^2 = 0.19$ ,  $p = 0.207$ ,  $n = 10$ ). Further work would be needed to rectify the issue of reference site  $^{137}\text{Cs}$  activity at Leadketty.

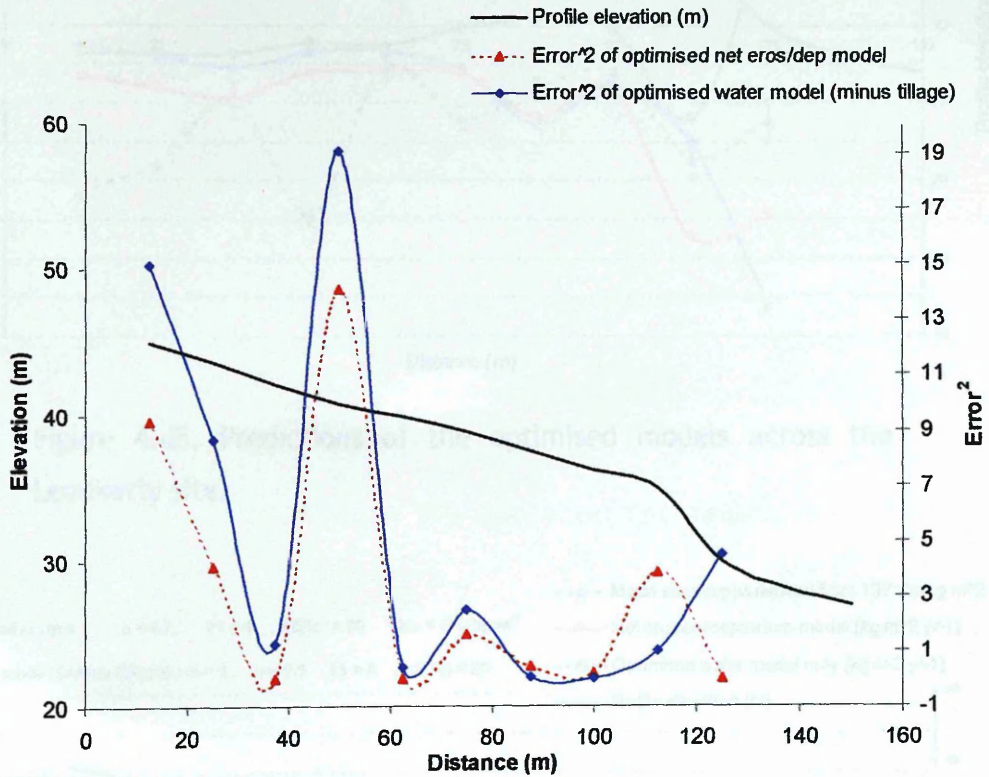


Figure 4.44. Distribution of errors across the Leadketty transect from the optimised models. Comparison of the net erosion/deposition model and water model minus tillage translocation is made.

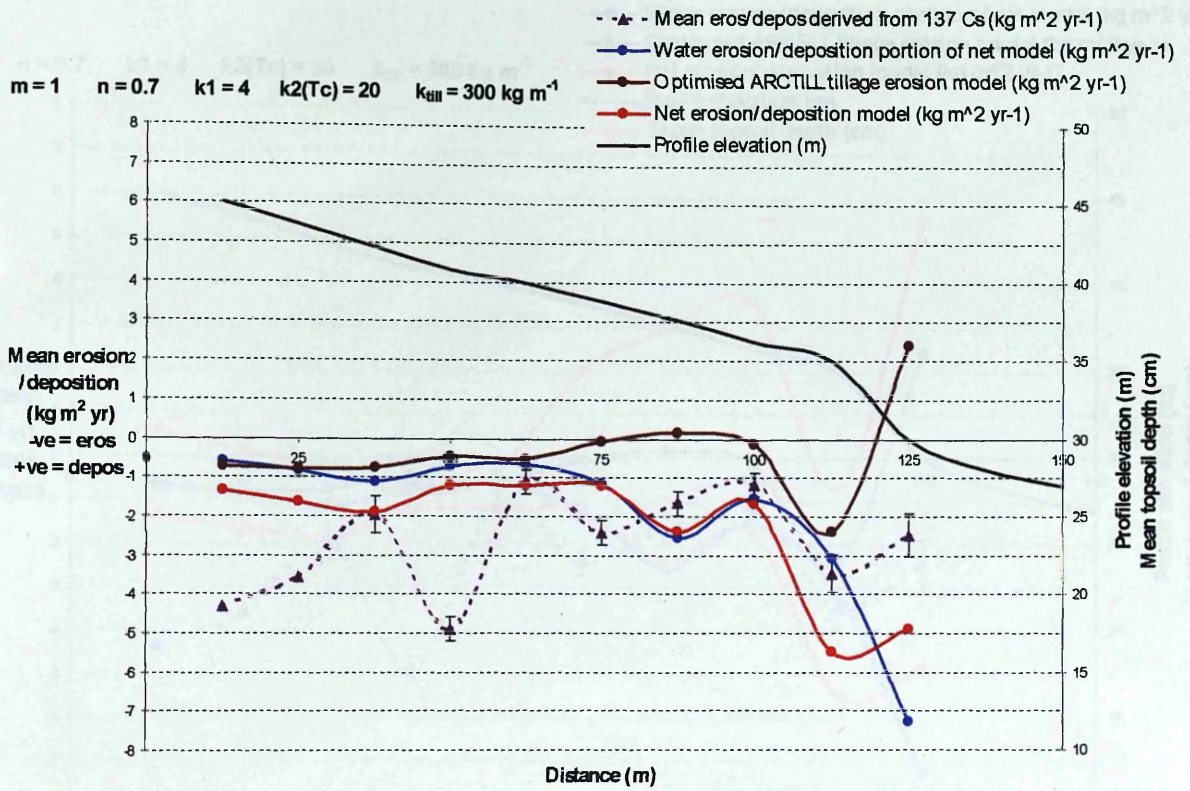


Figure 4.45. Predictions of the optimised models across the Leadketty site.

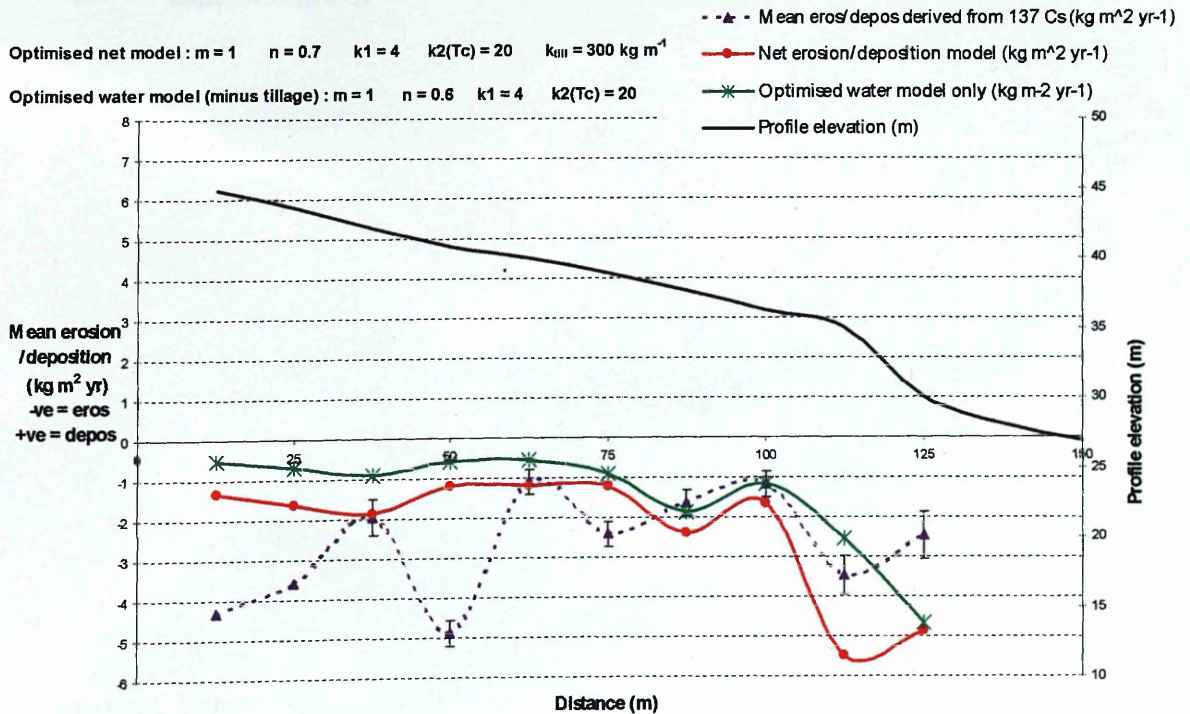


Figure 4.46. Comparison of the optimised net model and optimised water model (minus tillage)

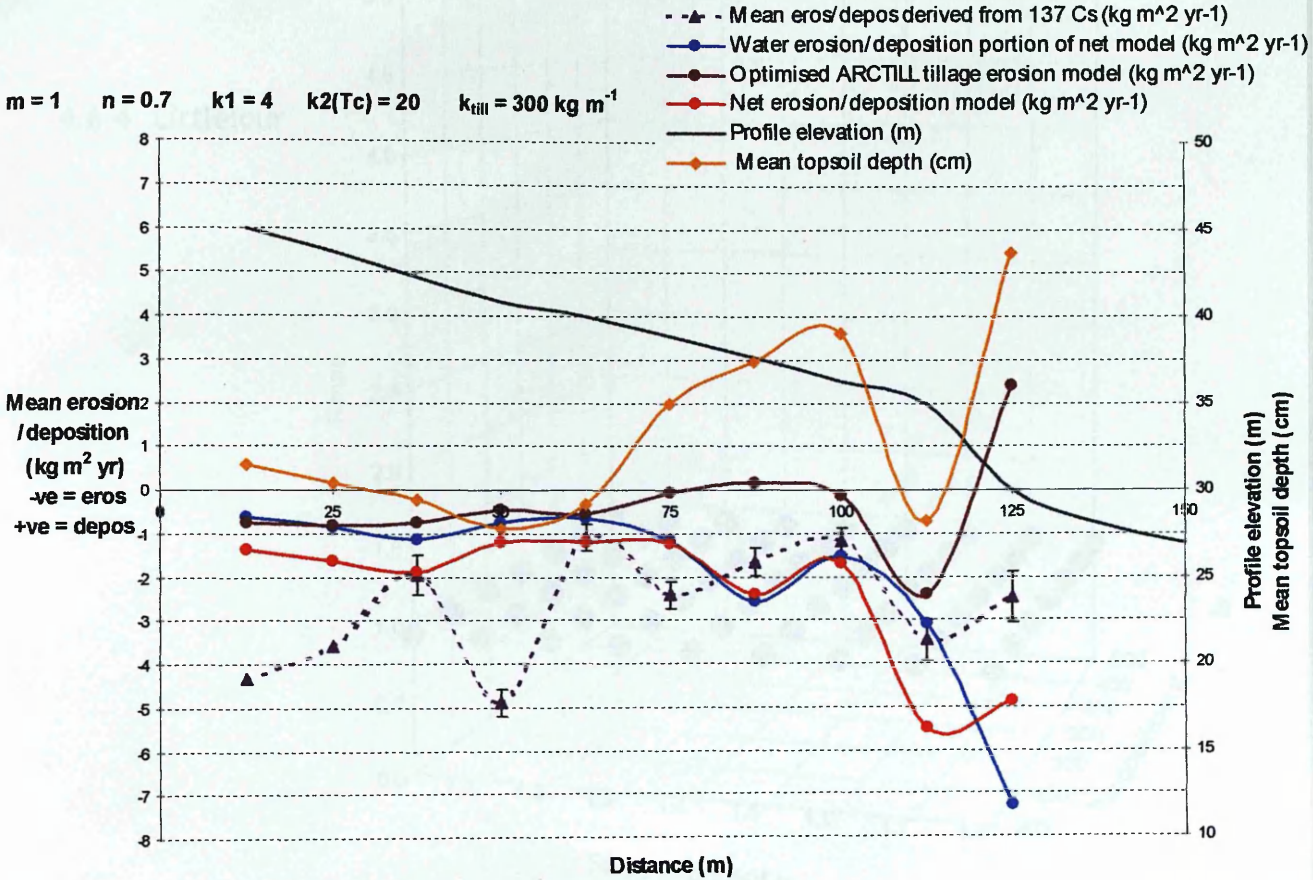


Figure 4.47. Comparison of the optimised net models and mean topsoil depths.

4.6.4 Littlelour

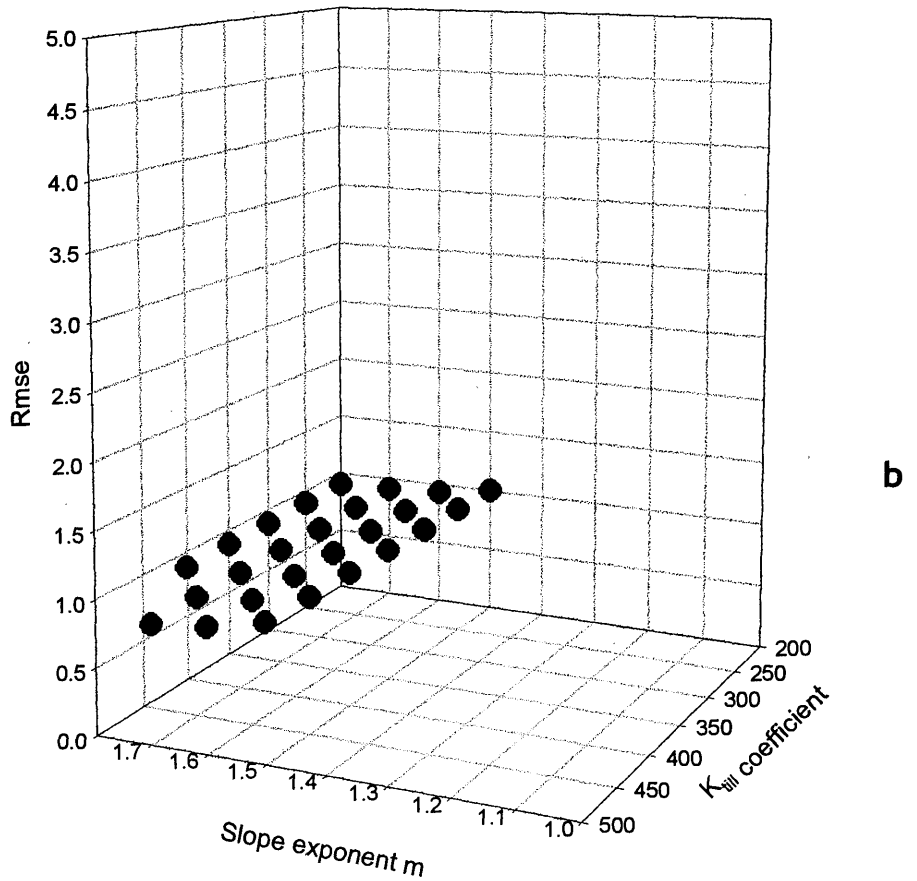
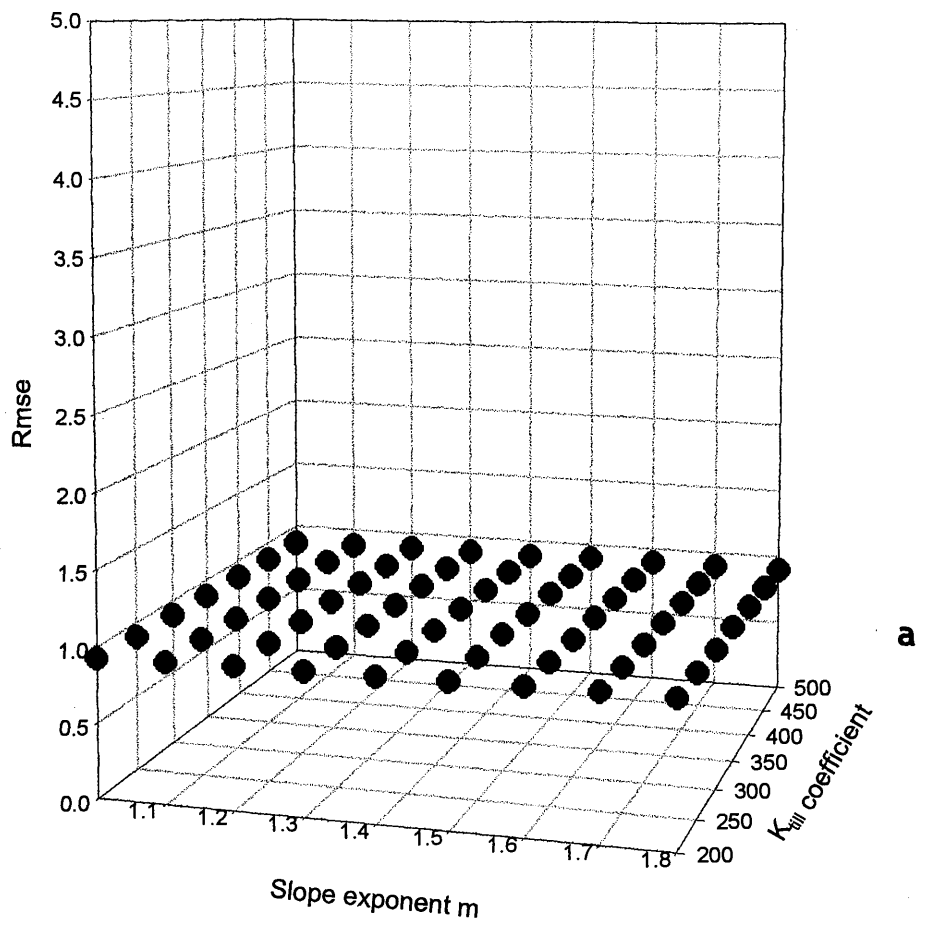


Figure 4.48. Error response by varying the slope exponent  $m$  and  $k_{till}$  variables, whilst holding the specific catchment area exponent  $n$  and  $k_2$  at (a) minimum and (b) maximum.

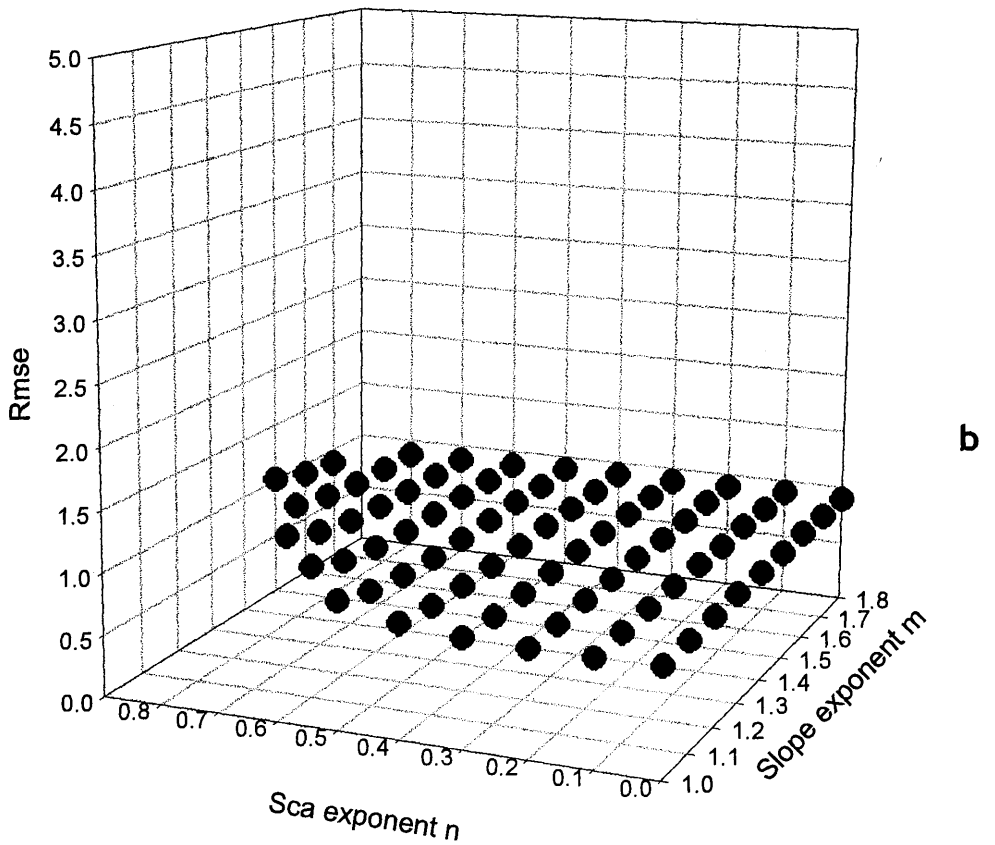
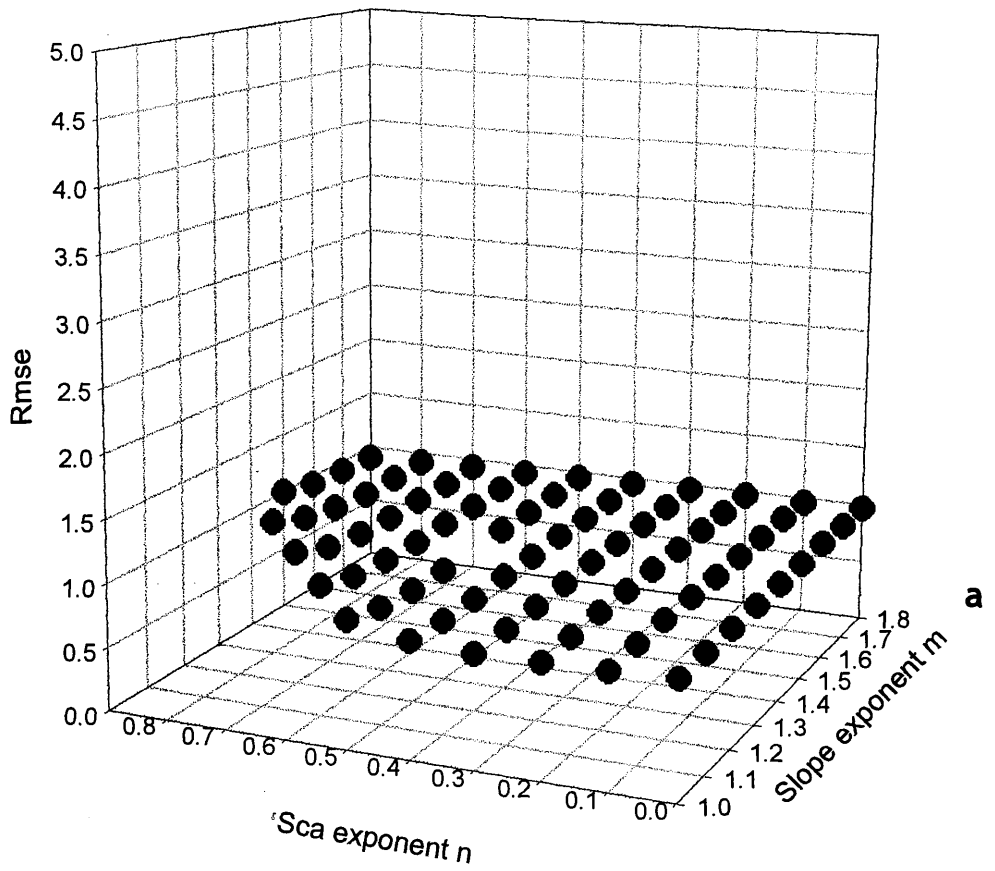


Figure 4.49. Error response by varying the slope exponent  $m$  and sca  $n$  variables, whilst holding  $k_{till}$  and  $k_2$  at (a) minimum and (b) maximum.

The optimised set of parameters for net erosion/deposition model at the Littlelour site is:

Slope  $m = 1$   
Sca  $n = 0.2$   
 $k_2 = 20$   
 $k_{till} = 500$   
**Rmse = 0.79**

The specific catchment area parameter has behaved most influentially throughout the analysis of this optimisation data. Although in general the error response surfaces are very much more homogenous, the impact of the sca  $n$  exponent is detectable. It is most noticeable in Figure 4.48 when set to maximum as one of the constants. At maximum the rmse values have struggled to encroach below the 10% threshold level. Minimising  $n$  (Figure 4.48a) releases the tight restriction yet little is conclusive in terms of trends in slope and  $k_{till}$ . The surfaces in Figure 4.49 do however reveal a little more on the tendency for rising sca  $n$  to push up rmse values. Not so clear from the both parts of Figure 4.49 is the slight downwards tilt in the surface from high to low slope  $m$  values. This becomes visible when changing the azimuth and angle of view to the graph.

Focussing on the data, (Table 4.37) the combinations required to meet quality best-fit scenarios are very obvious.

Slope and sca exponent variable behaviour was examined when combined with the minima and maxima of the remaining parameters (Figure 4.48 and Figure 4.49). Both slope  $m$  and sca  $n$  behaved in an almost identical manner noted at the Loanleven, and Blairhall field sites. High values of sca had to be present in one way or other for the model to be pushed into non-behavioural rmse values. It may appear in Figure 4.48b as though lower values of slope  $m$  are causing the rmse value to rise (and be restricted by threshold). In fact it must be remembered that sca  $n$  is held at maximum as a constant therefore slope is more likely to be masking the real cause, sca. During this analysis at no point do either  $k_{till}$  or  $k_2$  (not graphed) have sufficient influence to increase rmse values. Variation in  $k_{till}$  in both parts of Table 4.37 resulted in extremely little rise in rmse.

a

m	n	k <sub>2</sub>	k <sub>till</sub>	rmse
1	0.2	20	500	0.858
1	0.2	40	500	0.858
1	0.2	60	500	0.858
1	0.2	80	500	0.858
1	0.2	100	500	0.858
1	0.2	120	500	0.858
1	0.2	140	500	0.858
1	0.2	160	500	0.858
1	0.1	20	500	0.862
1	0.1	40	500	0.862
1	0.1	60	500	0.862
1	0.1	80	500	0.862
1	0.1	100	500	0.862
1	0.1	120	500	0.862
1	0.1	140	500	0.862
1	0.1	160	500	0.862
1.1	0.3	20	500	0.863
1.1	0.3	40	500	0.863
1.1	0.3	60	500	0.863
1.1	0.3	80	500	0.863
1.1	0.3	100	500	0.863
1.1	0.3	120	500	0.863
1.1	0.3	140	500	0.863
1.1	0.3	160	500	0.863
1	0.2	20	450	0.863
1	0.2	40	450	0.863
1	0.2	60	450	0.863
1	0.2	80	450	0.863
1	0.2	100	450	0.863
1	0.2	120	450	0.863
1	0.2	140	450	0.863
1	0.2	160	450	0.863
1.1	0.2	20	500	0.864
1.1	0.2	40	500	0.864
1.1	0.2	60	500	0.864
1.1	0.2	80	500	0.864
1.1	0.2	100	500	0.864
1.1	0.2	120	500	0.864
1.1	0.2	140	500	0.864
1.1	0.2	160	500	0.864
1.2	0.3	20	500	0.866
1.2	0.3	40	500	0.866
1.2	0.3	60	500	0.866
1.2	0.3	80	500	0.866
1.2	0.3	100	500	0.866
1.2	0.3	120	500	0.866
1.2	0.3	140	500	0.866
1.2	0.3	160	500	0.866
1.2	0.4	20	500	0.867
1.2	0.4	40	500	0.867

b

m	n	k <sub>2</sub>	k <sub>till</sub>	rmse
1.2	0.7	140	250	1.073
1.2	0.7	160	250	1.073
1.2	0.7	20	300	1.077
1.2	0.7	40	300	1.077
1.2	0.7	60	300	1.077
1.2	0.7	80	300	1.077
1.2	0.7	100	300	1.077
1.2	0.7	120	300	1.077
1.2	0.7	140	300	1.077
1.2	0.7	160	300	1.077
1.2	0.7	20	350	1.082
1.2	0.7	40	350	1.082
1.2	0.7	60	350	1.082
1.2	0.7	80	350	1.082
1.2	0.7	100	350	1.082
1.2	0.7	120	350	1.082
1.2	0.7	140	350	1.082
1.2	0.7	160	350	1.082
1.2	0.7	20	400	1.087
1.2	0.7	40	400	1.087
1.2	0.7	60	400	1.087
1.2	0.7	80	400	1.087
1.2	0.7	100	400	1.087
1.2	0.7	120	400	1.087
1.2	0.7	140	400	1.087
1.2	0.7	160	400	1.087
1.2	0.7	20	450	1.093
1.2	0.7	40	450	1.093
1.2	0.7	60	450	1.093
1.2	0.7	80	450	1.093
1.2	0.7	100	450	1.093
1.2	0.7	120	450	1.093
1.2	0.7	140	450	1.093
1.2	0.7	160	450	1.093
1.2	0.7	20	500	1.099
1.2	0.7	40	500	1.099
1.2	0.7	60	500	1.099
1.2	0.7	80	500	1.099
1.2	0.7	100	500	1.099
1.2	0.7	120	500	1.099
1.2	0.7	140	500	1.099
1.2	0.7	160	500	1.099
1.3	0.8	20	200	1.108
1.3	0.8	40	200	1.108
1.3	0.8	60	200	1.108
1.3	0.8	80	200	1.108
1.3	0.8	100	200	1.108
1.3	0.8	120	200	1.108
1.3	0.8	140	200	1.108
1.3	0.8	160	200	1.108

Table 4.37. The 50 lowest (a) and highest (b) rmse values at Littlelour with associated parameters taken from the whole set of model runs.



Figure 4.50 and Figure 4.51 put this into a spatial context across the field. There is no doubt that the net model is most sensitive to the  $sca\ n$  parameter. Raising  $n$  from 0 to 0.6 and then to 0.9 increases the erosion rate by 116% and 111% respectively.

#### 4.6.4.1 Sensitivity analysis

The net model was examined for sensitivity to the parameters and Figure 4.50 and Figure 4.51 display the results graphically. Optimised values were held constant whilst varying one of the three used. As with the other fields is it worth noting the dominance of  $sca\ n$  when in the right slope  $m$  combination (low). Topography is such at Littlelour that even implementing tillage translocation with a  $1000\text{ kg m}^{-1}$  coefficient has failed to produce anywhere near 50% of the effect  $sca\ n$  has. The net model here has again been very insensitive to changes in slope.

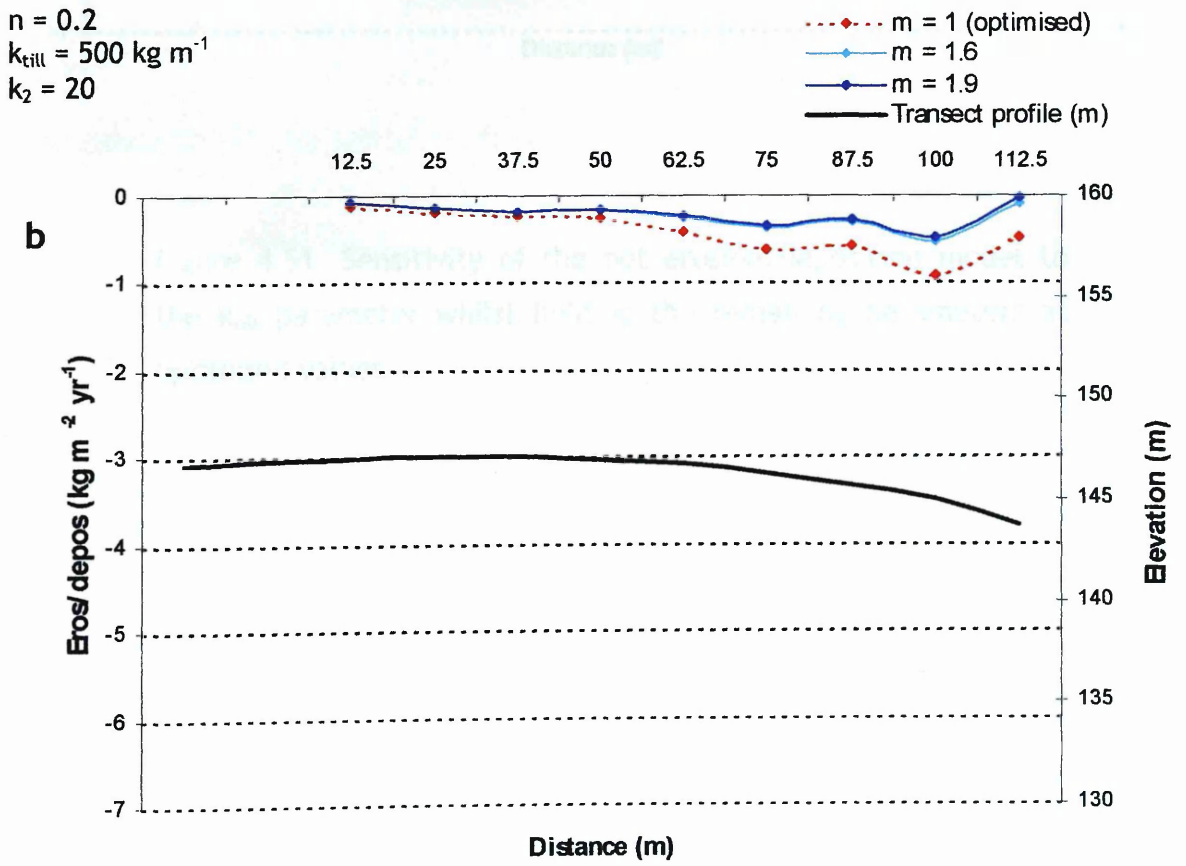
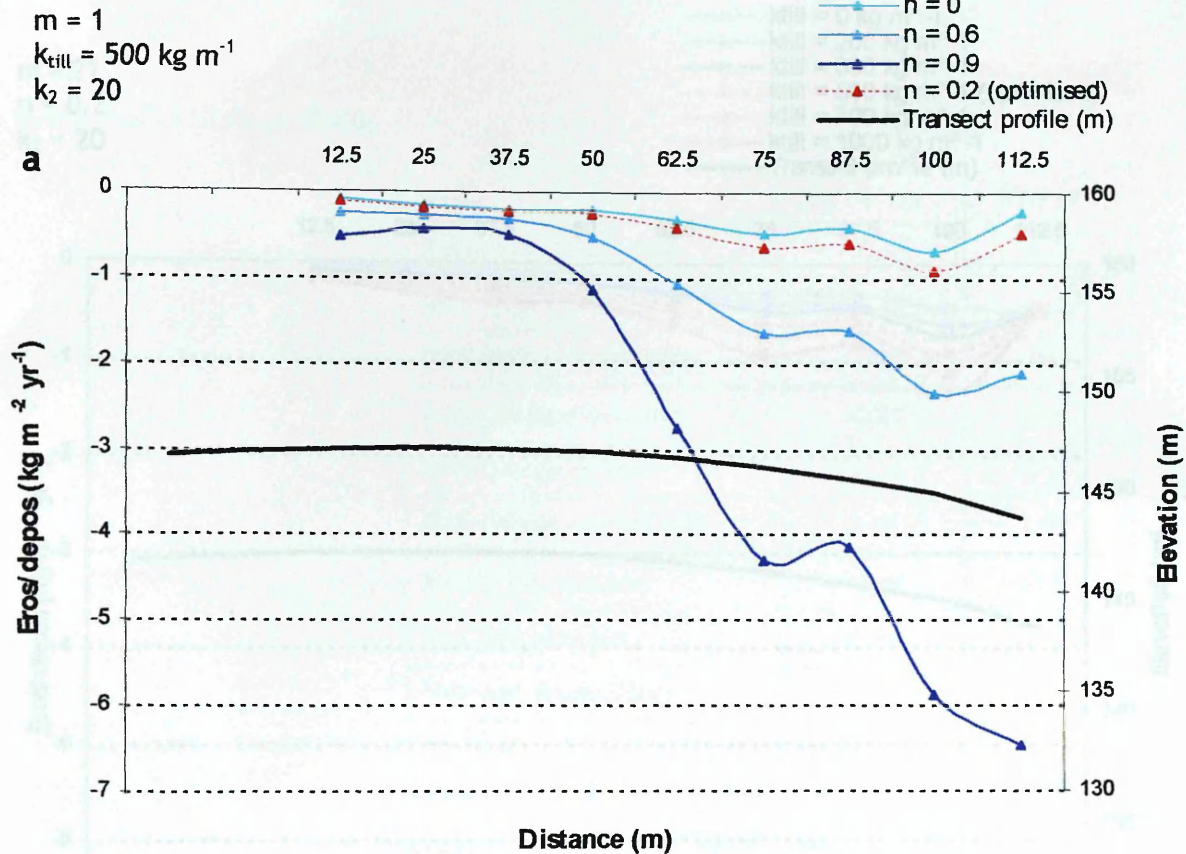


Figure 4.50. Sensitivity of the net erosion/deposition model to the slope  $n$  (a) and slope  $m$  (b) parameters whilst holding the remaining parameters at optimised values.

$m = 0.1$   
 $n = 0.2$   
 $k_2 = 20$

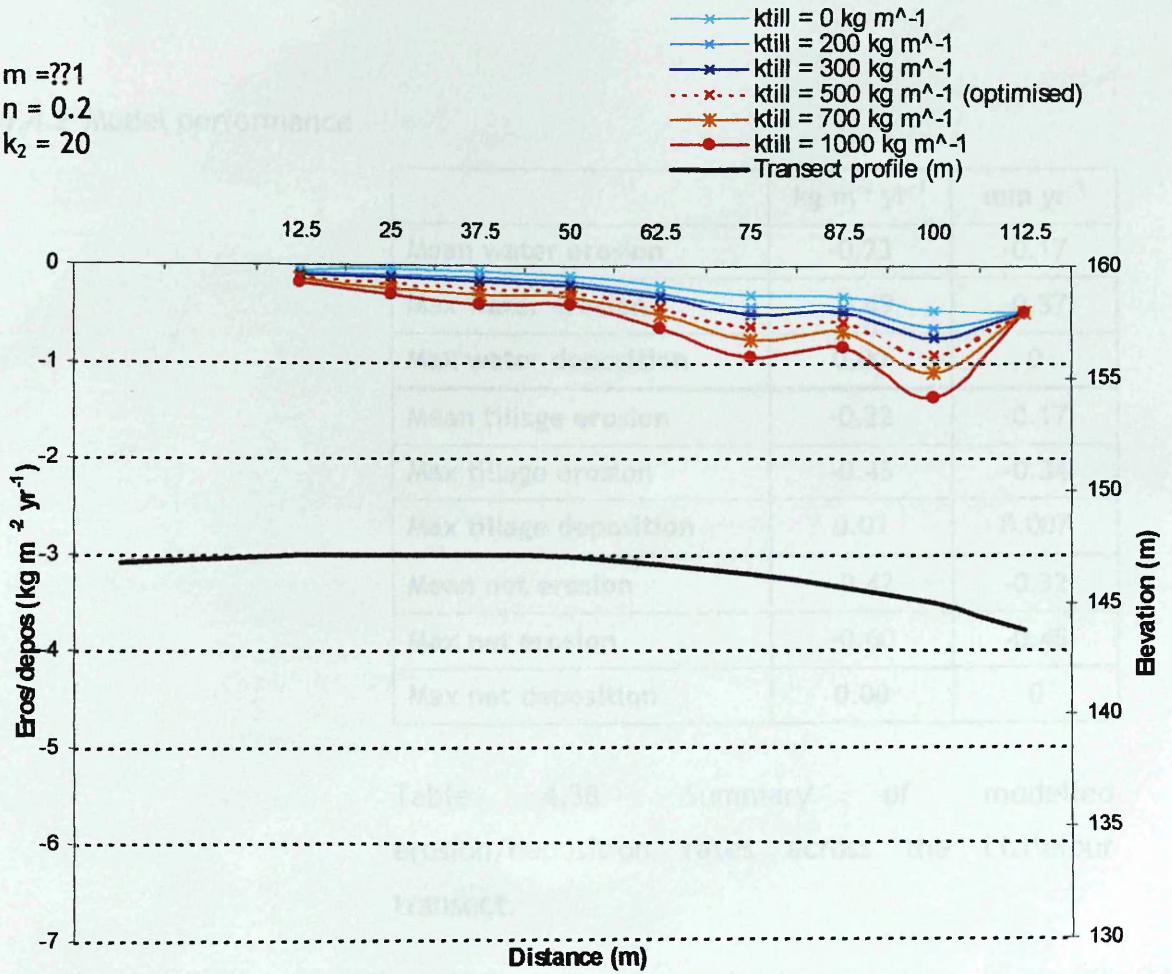


Figure 4.51. Sensitivity of the net erosion/deposition model to the  $k_{till}$  parameter whilst holding the remaining parameters at optimised values.

#### 4.6.4.2 Model performance

	kg m <sup>-2</sup> yr <sup>-1</sup>	mm yr <sup>-1</sup>
<b>Mean water erosion</b>	-0.23	-0.17
<b>Max water erosion</b>	-0.49	-0.37
<b>Max water deposition</b>	0.00	0
<b>Mean tillage erosion</b>	-0.22	-0.17
<b>Max tillage erosion</b>	-0.45	-0.34
<b>Max tillage deposition</b>	0.01	0.007
<b>Mean net erosion</b>	-0.42	-0.32
<b>Max net erosion</b>	-0.60	-0.45
<b>Max net deposition</b>	0.00	0

Table 4.38. Summary of modelled erosion/deposition rates across the Littlelour transect.

The topography of the Littlelour field is far less complex than Leadketty or Loanleven. Table 4.38 shows summary data on erosion and deposition across the transect. There are no sudden changes from convexities to concavities and vice versa and in effect it is a slightly convex surface increasing so towards the end of the transect. Given this the models were expected to perform better. As with the other field sites <sup>137</sup>Cs derived erosion/deposition budgets were compared with the optimised net erosion/deposition model, the water portion of the optimised net model, the tillage translocation model and the optimised water model. A summary of the results from a least squares analysis is presented and shown in Table 4.39.

Compared with the models at the other field sites the Littlelour models have produced the lowest error values. Studying Figure 4.52 to Figure 4.54 highlights cells 3 and 8 as being responsible for raising the rmse values in all models. Here quite large differentials have developed between modelled and observed yet offering an explanation as to why is not straight forward. Errors

Cell	<sup>137</sup> Cs derived (kg m <sup>-2</sup> yr <sup>-1</sup> )	Optimised net model 1 (kg m <sup>-2</sup> yr <sup>-1</sup> )	Error <sup>2</sup>	Optimised model 2 (kg m <sup>-2</sup> yr <sup>-1</sup> )	Error <sup>2</sup>	Optimised model 3 (kg m <sup>-2</sup> yr <sup>-1</sup> )	Error <sup>2</sup>	Optimised model 4 (kg m <sup>-2</sup> yr <sup>-1</sup> )	Error <sup>2</sup>
1	-0.54	-0.55	0.00	-0.49	0.00	-0.70	0.03	-0.06	0.23
2	-0.52	-0.60	0.01	-0.47	0.00	-0.66	0.02	-0.13	0.15
3	-2.53	-0.50	4.12	-0.33	4.85	-0.47	4.26	-0.17	5.57
4	-0.50	-0.45	0.00	-0.30	0.04	-0.43	0.00	-0.15	0.12
5	+0.20	-0.42	0.39	-0.20	0.16	-0.28	0.23	-0.23	0.18
6	+0.04	-0.44	0.23	-0.11	0.02	-0.15	0.04	-0.33	0.14
7	-0.76	-0.31	0.20	-0.06	0.50	-0.07	0.48	-0.26	0.26
8	-1.26	-0.50	0.58	-0.05	1.48	-0.06	1.45	-0.45	0.65
9	-0.40	-0.05	0.13	-0.05	0.12	-0.07	0.11	+0.01	0.17
		<b>RMSE</b>	<b>0.79</b>	<b>RMSE</b>	<b>0.89</b>	<b>RMSE</b>	<b>0.86</b>	<b>RMSE</b>	<b>0.91</b>

Model 1 = net optimised model

Model 2 = water portion of net model

Model 3 = optimised water only

Model 4 = optimised tillage only

Table 4.39. Performance of the various erosion models at Leadketty.

inherent in the <sup>137</sup>Cs technique are normal and in line with the other sites and topography at these cells is uniform and simple. The centre of cell 3 (37.5m) is effectively the centre of the sub-surface barrow feature. The site has a pronounced rise with the highest point in the field immediately prior to the slightly convex main backslope. The elevation spot data for each cell has been derived from the DTM not from an EDM survey and according to this data cell 2 is the highest point albeit only by some 2cm. The differential in reality is more like 30-50cm so the shape of the transect's topography has therefore been poorly modelled and it must have an underlying effect. The inability of the 25m cell to resolve the realistic shape of the terrain once more could be manifesting itself on the performance of the models. In defence of the TOPOGRID algorithms used in ARC/INFO, the contour data taken from the 1:50 000 OS map also badly represents the rise. A more detailed EDM topographic survey would identify the rise of the barrow feature and erosion due to tillage translocation would certainly increase at cell 3. In turn the level of accumulation would also increase just downslope of the convex rise. This would produce closer agreement between modelled erosion/deposition and <sup>137</sup>Cs derived budgets at cells 3 (37.5m) and 8 (100m). This would partly improve the statistical performance of

the net model. Removing the tillage translocation portion of the optimised net model increased the rmse value, hinting that tillage is playing an important role.

The water erosion/deposition model alone was iterated 720 times to reach a best-fit scenario. Optimisation was reached via the following:

Slope m = 1  
Sca n = 0.3  
k<sub>2</sub> = 20  
Rmse = 0.9177

The results of this model are shown in Figure 4.53 and the deterioration in fit is evident particularly from 75m onwards. Results in Table 4.39 detail the increase in rmse value after removing tillage translocation from the net model. Surface wash processes alone have been unable to detach sufficient soil to model those required as defined by the <sup>137</sup>Cs technique.

There has been some further reassuring support for the <sup>137</sup>Cs technique in general. Figure 4.54 outlines the model and <sup>137</sup>Cs predictions with regard to mean topsoil depth. The affinity between the <sup>137</sup>Cs derived observations and topsoil depth is high ( $r^2 = 0.63$ ,  $p = 0.011$ ,  $n = 9$ ) and this should certainly be viewed as a substantial confidence boost in the technique as a whole.

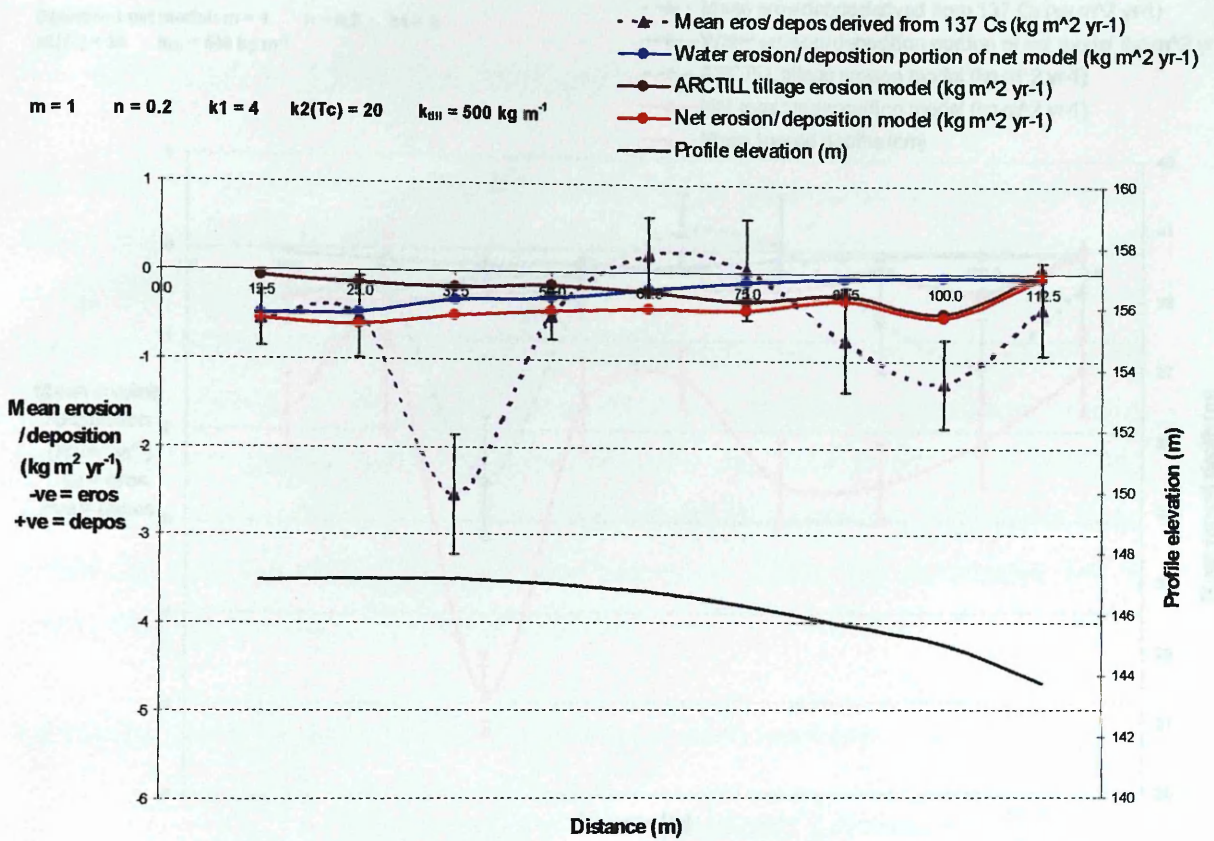


Figure 4.52. Predictions of the optimised models across the Littlelour site.

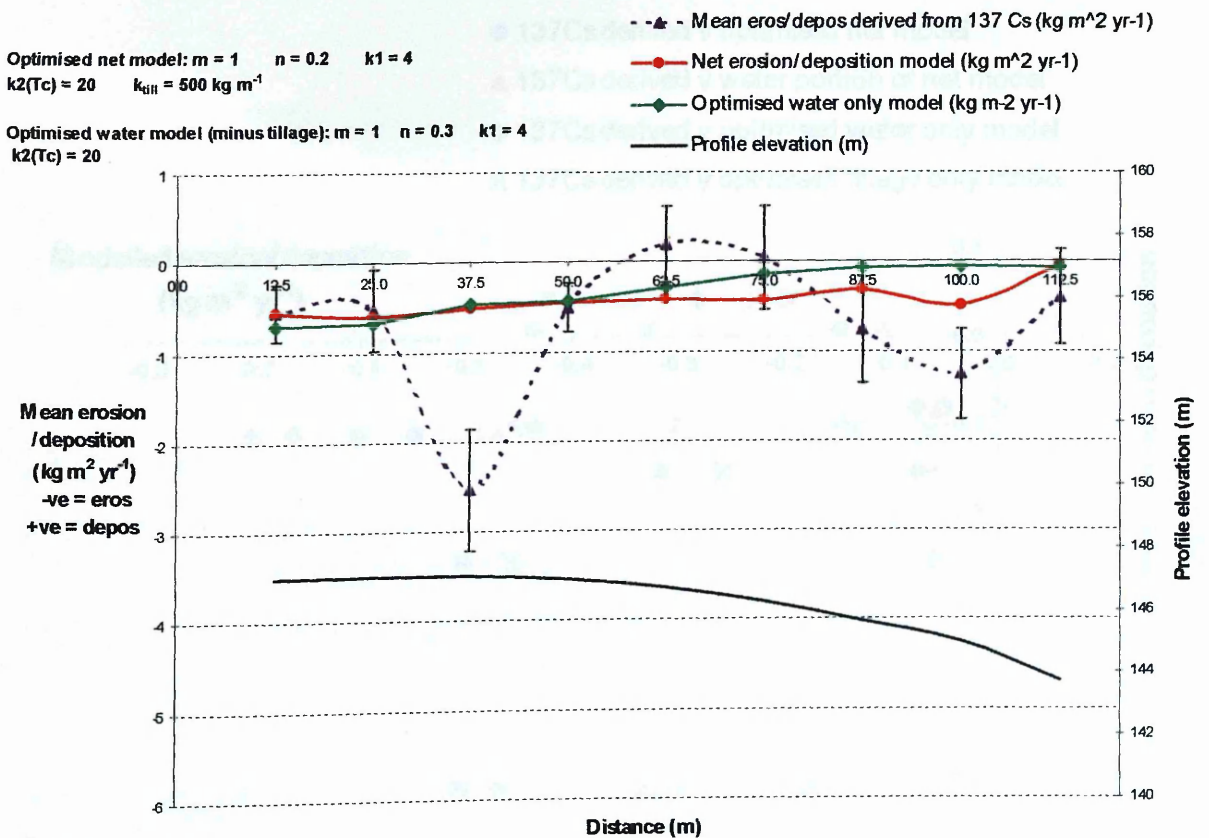


Figure 4.53. Comparison of the optimised net model and optimised water model (minus tillage) at Littlelour.

Optimised net model:  $m = 1$   $n = 0.2$   $k1 = 4$   
 $k2(Tc) = 20$   $k_{till} = 500 \text{ kg m}^{-1}$

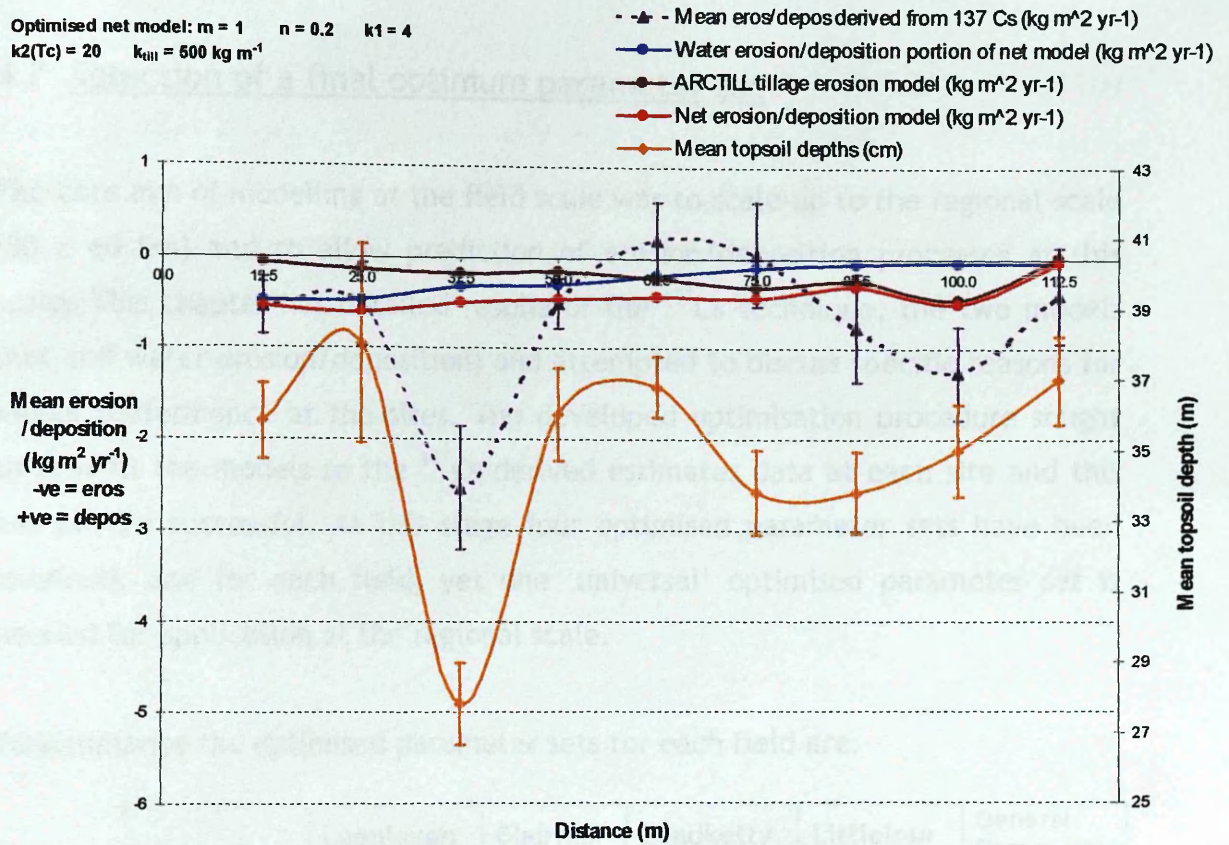


Figure 4.54. Comparison of the optimised net models and mean topsoil depths at the Littlelour site.

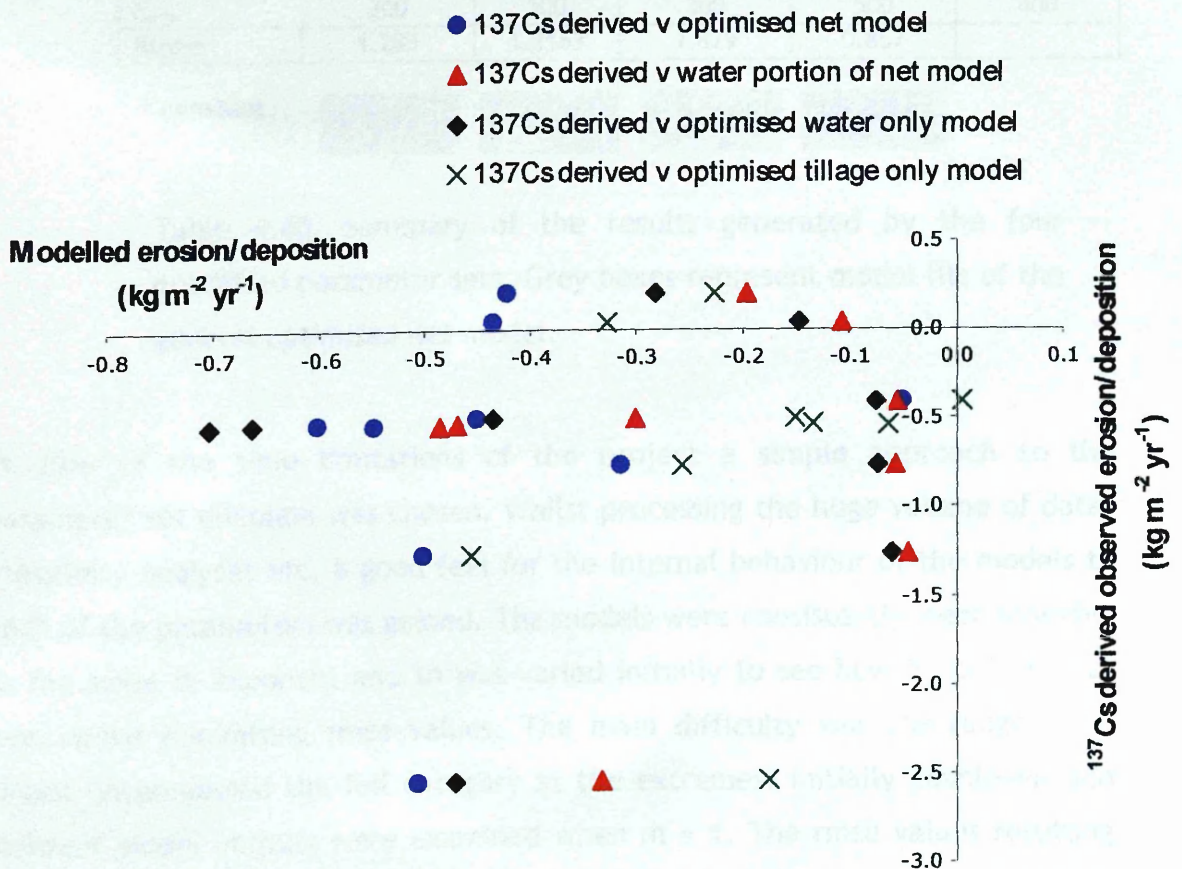


Figure 4.55. Plot of modelled erosion/deposition versus  $^{137}\text{Cs}$  derived erosion/deposition with and without tillage translocation at Littlelour.



#### 4.7 Selection of a final optimum parameter set

The core aim of modelling at the field scale was to scale-up to the regional scale (80 x 60 km) and to allow prediction of erosion/deposition processes at this scale. This chapter has detailed results of the  $^{137}\text{Cs}$  technique, the two models (net and water erosion/deposition) and attempted to discuss specific reasons for model performance at the sites. The developed optimisation procedure sought to best-fit the models to the  $^{137}\text{Cs}$  derived estimates data at each site and this has proved successful. At this stage four optimised parameter sets have been obtained, one for each field, yet one 'universal' optimised parameter set is needed for application at the regional scale.

To summarise the optimised parameter sets for each field are:

	Loanleven	Blairhall	Leadketty	Littlelour	General Param. set
Slope m	1.7	1.8	1	1	1.8
Sca n	0.9	0	0.7	0.2	0.5
$K_1$	4	4	4	4	4
$K_2$	20	20	20	20	20
$K_{\text{till}}$	300	500	300	500	400
Rmse	1.285	1.3163	1.829	0.857	

\* constant

1.37

1.42

3.46

0.901

Table 4.40. Summary of the results generated by the four optimised parameter sets. Grey boxes represent model fits of the general optimised net model.

In view of the time limitations of the project a simple approach to the parameter set dilemma was chosen. Whilst processing the huge volume of data, sensitivity analyses etc, a good feel for the internal behaviour of the models to each of the parameters was gained. The models were consistently least sensitive to the slope m exponent and so was varied initially to see how it could be set best whilst minimising rmse values. The main difficulty was the range of m values encompassed the full category at the extremes. Initially Loanleven and Blairhall model outputs were examined when  $m = 1$ . The rmse values resulting from this increase are highlighted in grey in Table 4.40. No clear trend is in

evidence. Slope  $m$  at the Leadketty and Littlelour sites was raised to 1.8 and the model outputs marked similarly. Given that confidence levels in the results at Leadketty were lower than with the other sites, it is proposed that the large rmse increase encountered here through raising  $m$  to 1.8 be overlooked and be accepted as the final value. The range of the sca n exponent was also large yet more uniform. Here an arithmetic mean was taken as with the  $k_{till}$  parameter. The general optimised parameter set for the net model is:

$$\text{Slope } m = 1.8$$

$$\text{Sca n} = 0.5$$

$$K_1 = 4$$

$$K_2 = 20$$

$$K_{till} = 400 \text{ kg m}^{-1}$$

Running the general optimised net model across the four fields produced new predictions and these are shown in contrast to the field specific optimised net model predictions in Figure 4.57 and Figure 4.58. Changes in model performance associated with the new general optimised net model parameter set are shown in Table 4.41.

Model	RMSE*	RMSE**
Loanleven	1.29	1.37
Blairhall	1.32	1.42
Leadketty	1.96	3.46
Littlelour	0.79	0.91

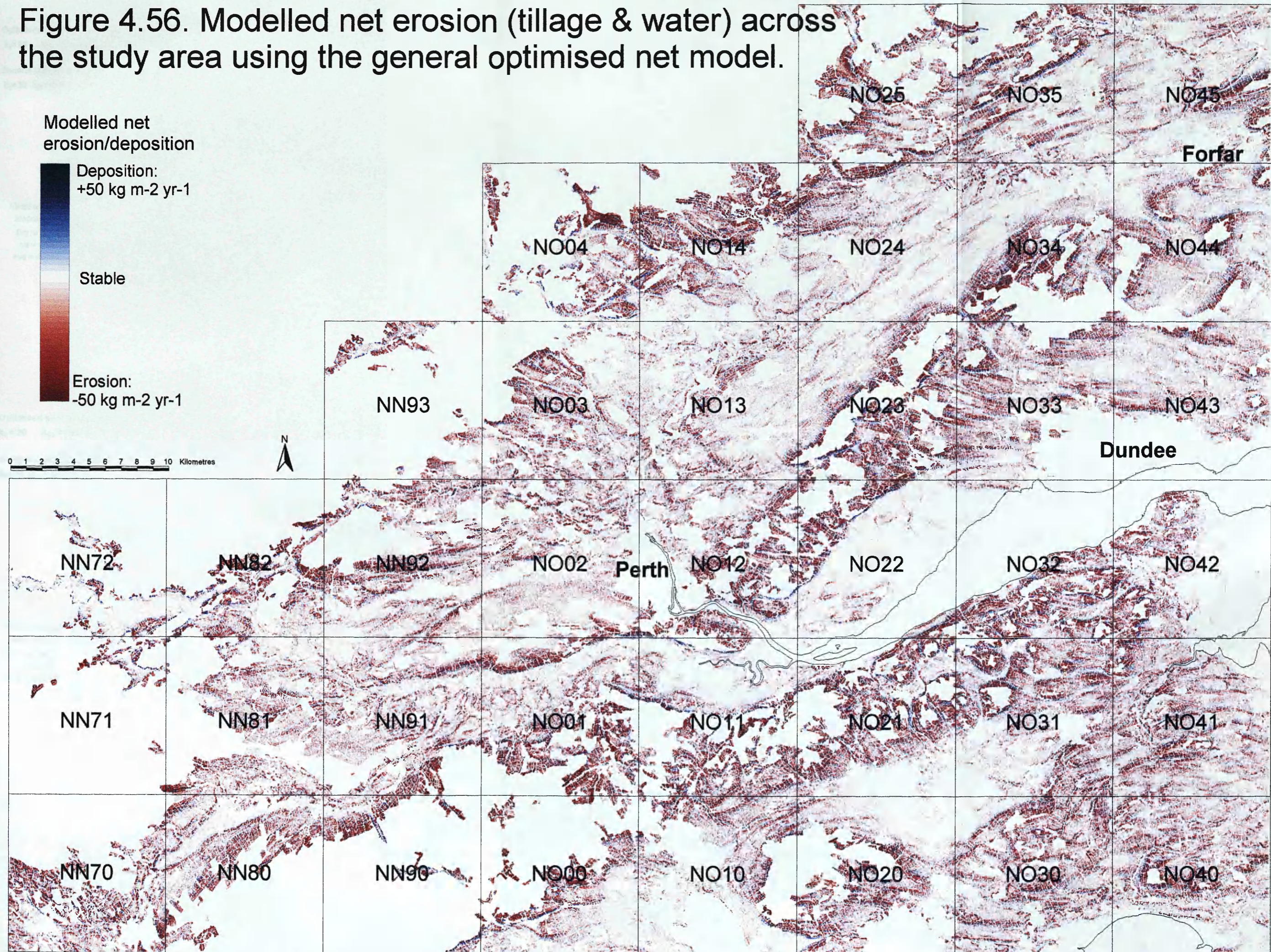
\* = optimised net model for field

\*\* = general optimised net model

Table 4.41. Comparison of the performance of the field specific optimised net models and the general optimised net models.

The general optimised net model was run for the whole study area and is presented in Figure 4.56.

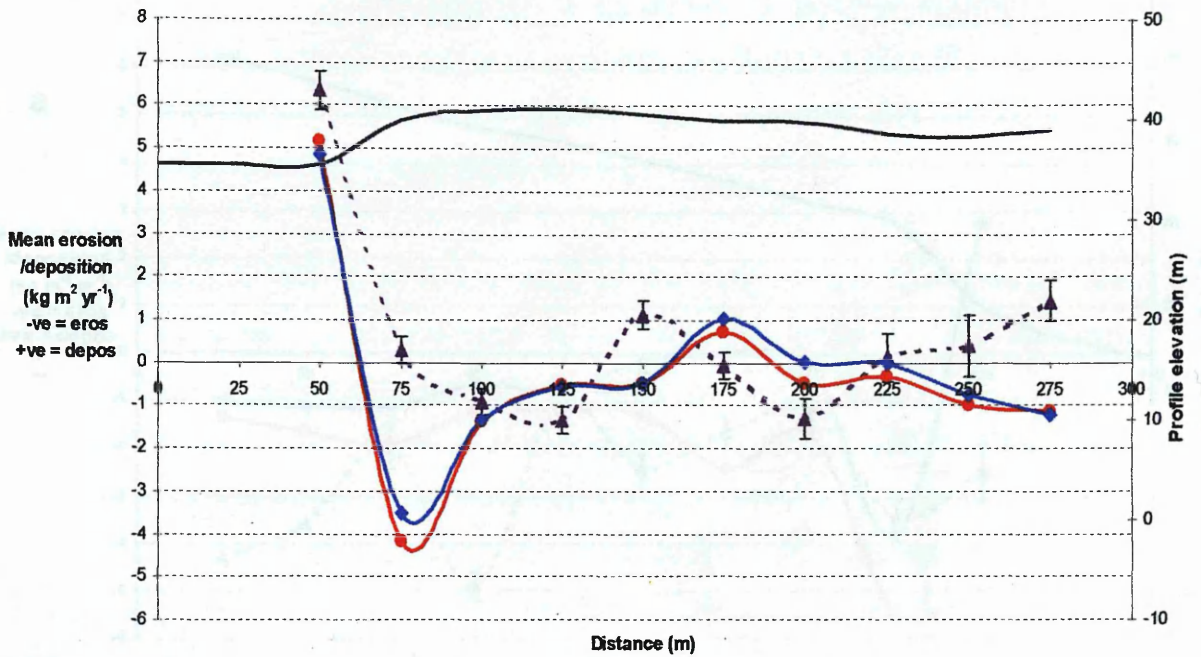
Figure 4.56. Modelled net erosion (tillage & water) across the study area using the general optimised net model.



Optimised net model :  $m = 1.7$   $n = 0.9$   $k_1 = 4$   
 $k_2 = 20$   $k_{till} = 300 \text{ kg m}^{-1}$

General optimised net model :  $m = 1.4$   $n = 0.5$   $k_1 = 4$   
 $k_2 = 20$   $k_{till} = 400 \text{ kg m}^{-1}$

-▲- Mean eros/depos derived from 137 Cs ( $\text{kg m}^2 \text{ yr}^{-1}$ )  
 -●- Net erosion/deposition model ( $\text{kg m}^2 \text{ yr}^{-1}$ )  
 -◆- General optimised net model ( $\text{kg m}^2 \text{ yr}^{-1}$ )  
 — Profile elevation (m)



Optimised net model:  $m = 1.8$   $n = 0$   $k_1 = 4$   
 $k_2 = 20$   $k_{till} = 500 \text{ kg m}^{-1}$

General optimised net model:  $m = 1.4$   $n = 0.5$   $k_1 = 4$   
 $k_2 = 20$   $k_{till} = 400 \text{ kg m}^{-1}$

-▲- Mean eros/depos derived from 137 Cs ( $\text{kg m}^2 \text{ yr}^{-1}$ )  
 -●- Net erosion/deposition ( $\text{kg m}^2 \text{ yr}^{-1}$ )  
 -◆- General optimised net model ( $\text{kg m}^2 \text{ yr}^{-1}$ )  
 — Profile elevation (m)

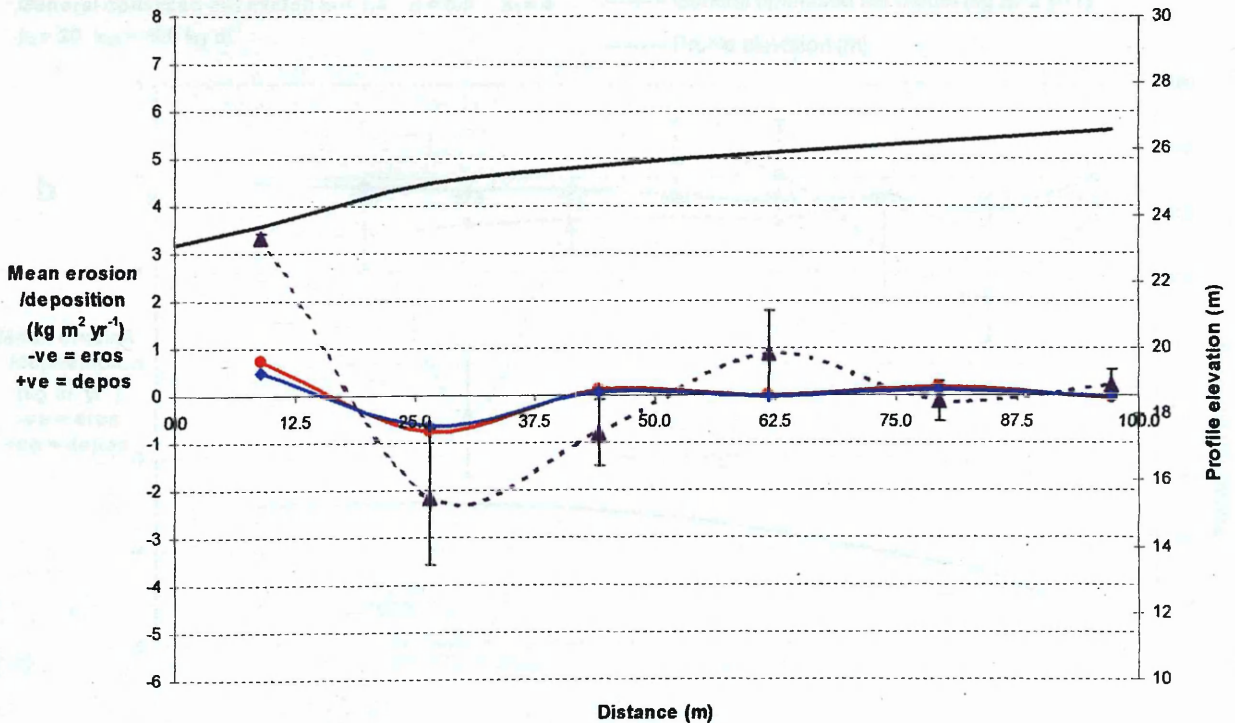
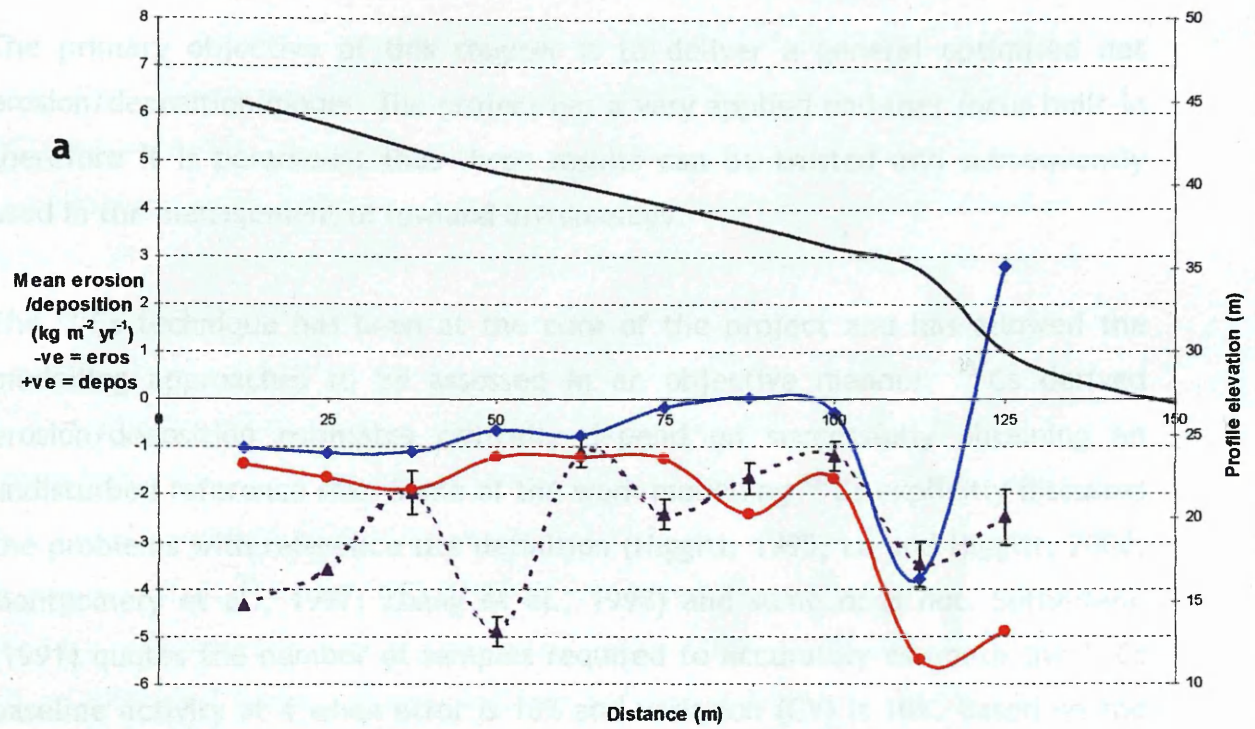


Figure 4.57. Comparison of the final general net erosion/deposition model with the field specific net model at Loanleven (a) and Blairhall (b).

Optimised net model :  $m = 1$   $n = 0.7$   $k_1 = 4$   
 $k_2 = 20$   $k_{III} = 300 \text{ kg m}^{-1}$

General optimised net model :  $m = 1.4$   $n = 0.5$   $k_1 = 4$   
 $k_2 = 20$   $k_{III} = 400 \text{ kg m}^{-1}$

-▲- Mean eros/depos derived from 137 Cs ( $\text{kg m}^2 \text{ yr}^{-1}$ )  
 ● Net erosion/deposition model ( $\text{kg m}^2 \text{ yr}^{-1}$ )  
 ◆ General optimised net model ( $\text{kg m}^2 \text{ yr}^{-1}$ )  
 — Profile elevation (m)



Optimised net model:  $m = 1$   $n = 0.2$   $k_1 = 4$   
 $k_2 = 20$   $k_{III} = 500 \text{ kg m}^{-1}$

General optimised net model:  $m = 1.4$   $n = 0.5$   $k_1 = 4$   
 $k_2 = 20$   $k_{III} = 400 \text{ kg m}^{-1}$

-▲- Mean eros/depos derived from 137 Cs ( $\text{kg m}^2 \text{ yr}^{-1}$ )  
 ● Net erosion/deposition model ( $\text{kg m}^2 \text{ yr}^{-1}$ )  
 ◆ General optimised net model ( $\text{kg m}^2 \text{ yr}^{-1}$ )  
 — Profile elevation (m)

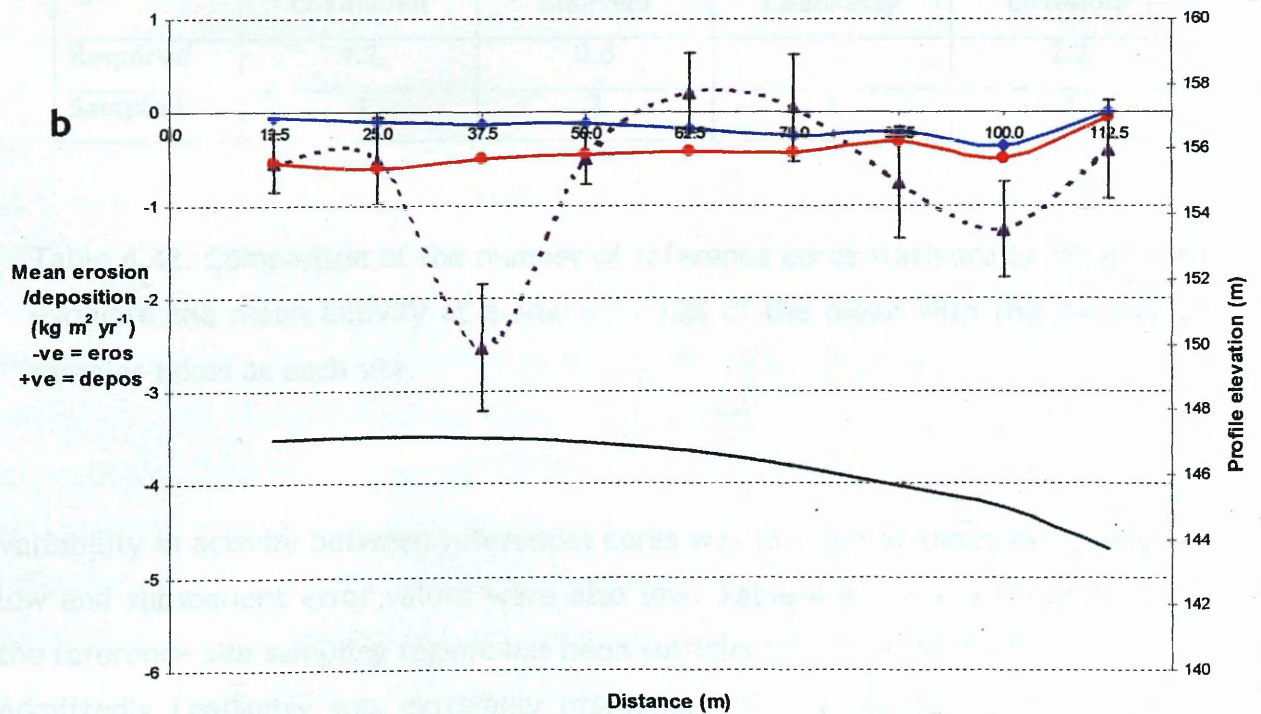


Figure 4.58. Comparison of the final general net erosion/deposition model with the field specific net model at Leadketty (a) and Littlelour (b).

## 4.8 Modelling discussion

The primary objective of this chapter is to deliver a general optimised net erosion/deposition model. The project has a very applied end-user focus built-in therefore it is paramount that these results can be trusted and subsequently used in the management of lowland archaeology.

The  $^{137}\text{Cs}$  technique has been at the core of the project and has allowed the modelling approaches to be assessed in an objective manner.  $^{137}\text{Cs}$  derived erosion/deposition estimates critically depend on successfully obtaining an undisturbed reference site. Some of the work modelling  $^{137}\text{Cs}$  explicitly discusses the problems with reference site definition (Higgitt, 1995; Lu and Higgitt, 2000; Montgomery et al., 1997; Zhang et al., 1998) and some does not. Sutherland (1991) quotes the number of samples required to accurately estimate the  $^{137}\text{Cs}$  baseline activity at 4 when error is 10% and variation (CV) is 10%. Based on the standard deviations of reference cores taken at each site the number of reference samples per site required to estimate the mean reference  $^{137}\text{Cs}$  activity within 10% are shown in Table 4.42.

	Loanleven	Blairhall	Leadketty	Littlelour
Required	4.2	0.6	-	2.2
Sampled	4	3	1	3

Table 4.42. Comparison of the number of reference cores statistically required to estimate the mean activity at a site with 10% of the mean with the number of samples taken at each site.

Variability in activity between reference cores was low and at times extremely low and subsequent error values were also low. Table 4.42 clearly shows that the reference site sampling regime has been sufficient at three of the four sites. Admittedly Leadketty was extremely problematical and resulted in only one reference sample being taken due to time and foot and mouth restrictions.

Model performance at the Leadketty site was poor in comparison to the other 3 sites and requires further reference cores to be taken. In conclusion, baseline  $^{137}\text{Cs}$  activity, possibly the most important step in the technique, at the other three sites has been confidently estimated. In hindsight strict attention needs to be paid from the very start of such a project to locating and appropriately sampling potential reference sites. Such intensive soil coring schemes also require the support of automatic coring machinery rather than the use of the Tacit manual golf-hole corer.

$^{137}\text{Cs}$  activity across the fields has demonstrated poor correlation with topography. Raw  $^{137}\text{Cs}$  activity ( $\text{Bq m}^{-2}$ ) with all transect data lumped together ( $n = 35$ ) was correlated (Spearman rank) with slope (-0.447) and profile curvature (-0.440). After calibration into erosion/deposition rates, curvature displayed a stronger relationship still (-0.562) and with slope at -0.465. These results correspond well with data published by Kosmas et al. (2001) after correlating profile curvature (reversed signs) with  $^{137}\text{Cs}$  inventories ( $r = 0.45$ ). Such trends are not new but they serve an important purpose in confirming what is expected theoretically and being confident in what is then being applied.

The optimisation technique has been outlined in terms of its mechanics earlier in this chapter. It is essentially an orthodox optimisation technique that addresses both the issues of water and tillage erosion and at the same time that of untangling the two and defining proportionality. Key work by Quine (1999a;1999b), Quine et al., (1999a), Quine et al., (1997) and Govers (1996; 1993; 1994; 1999b) has set about attempting to deconvolute the processes of water borne and tillage erosion from the net budget. In this project it may have possibly been more suitable to use upslope boundary zones (close to fencelines, walls, etc.) for sample taking. Here water erosion is negligible and upslope influx of soil via tillage is near-zero so that the tillage transport coefficient ( $k_{\text{till}}$ ) will provide 100% of the erosion observed at this point. This method is an effective way of ascertaining the proportionality of tillage erosion within the whole erosion/deposition budget at other points in the field. Zhang et al. (1998) used the same approach as that used in this project to deliver what they termed a 'corrected' water erosion estimate, equivalent to the 'goal' value here. The procedure implemented to optimise modelled with observed values does appear

to have delivered a basic attempt at addressing the issues relating to tillage and water erosion. There is however the possibility that equifinality within the models is masking the correct optimised results. With the exception of Leadketty, Table 4.22, Table 4.28, Table 4.37 (50 lowest and highest rmse) indicate definite trends in the tillage transport coefficient  $k_{till}$  in relation to decreasing error values. In essence equifinality has occurred in all 4 of the model optimisations since there has been small ranges in parameters producing clustered low rmse values. Does it bear any significance? If the model is to be applied once to a specific site then the best-fit result is of primary interest and equifinality is unimportant. However, when the model is applied at a different location it will in theory behave differently depending on local topography but should not need any re-parameterisation, as the modelled processes are in effect the same. Reality is different, as the tests here have demonstrated. This could be due to the cumulative effects of internal experimental error or associated with the variation in tillage operations at each site.

Assumptions have been made as to the definition of a standard annual set of tillage operations (chapter 3). There will be variations on this definition such as plough depth, ploughing speed, implement design, type, tractor size, tractor power, single or multi-pass system. Attempting to set a constant tillage transport coefficient ( $k_{till}$ ) for the whole area is rather unrealistic. Early research by Govers et al. (1993) found the best correspondence was produced by a  $k_{till}$  of  $325 \text{ kg m}^{-1}$  in southern England. They also discovered that modelled water erosion alone (no tillage simulation) explained 82% of the observed patterns, therefore questioning the relevance of tillage processes. Govers et al. (1996) found variation in the best-fit  $k_{till}$  coefficients between two UK arable fields. They quote values of 348 and  $397 \text{ kg m}^{-1}$ . Annual values for central Belgium of  $400\text{-}600 \text{ kg m}^{-1}$  (Govers et al., 1994) have been proposed based on a compound of tillage operations. More recent work in Belgium by Quine et al. (1997) defined the annual  $k_{till}$  as being  $550 \text{ kg m}^{-1}$  again comprising of multiple treatments. The authors quote a single mouldboard pass as being in the range of  $250\text{-}350 \text{ kg m}^{-1}$  and that their data suggest a value lower than  $400 \text{ kg m}^{-1}$  is inappropriate to mouldboard ploughing combined with other tillage treatments. If this data is correct then the limits set for  $k_{till}$  here could be slightly low. Optimised  $k_{till}$  values set here of  $300\text{-}500 \text{ kg m}^{-1}$  are satisfactorily in agreement with the



consistent literature data on this topic. The effects of widening the  $k_{\text{till}}$  category limits on the optimisation would be interesting. This would test whether the limits were over restrictive of the optimisation procedure.

Based on the  $^{137}\text{Cs}$  derived erosion/deposition estimates how well have the models performed? Table 4.43 summarises.

Model	RMSE*	RMSE**
Loanleven	1.29	1.37
Blairhall	1.32	1.73
Leadketty	1.96	2.90
Littlelour	0.79	1.00

\* = optimised net model for field

\*\* = general optimised net model

Table 4.43. Summary of model performance at each field site.

There has been a clear split in the model's goodness of fit. Applied at Loanleven, Blairhall and Littlelour the models have performed very well. At Leadketty the models have performed very poorly from a statistical standpoint. At Loanleven both the water and tillage models have demonstrated good predictive capabilities (Table 4.43) and the data implies that water erosion processes alone have been more efficient at modelling the whole erosion/deposition budget. Erosion through tillage processes also has had a very strong presence so topographic form at Loanleven has been diverse enough to provide areas conducive to both water and tillage borne erosion. Under the optimised net erosion/deposition model tillage has on average contributed to 75% of the erosion/deposition estimate and when used standalone to model the whole erosion/deposition budget explained 64% of variation.

The Blairhall application of the models has created a much simpler picture of erosion and deposition. The optimised net erosion/deposition model predicts the best-fit and unequivocally dominated by tillage erosion. Predicted

erosion/deposition via the water model had no resemblance with  $^{137}\text{Cs}$  derived estimates. From numerous field visits it is hard to imagine how water erosion could play a significant role. Besides the sharp convex ridge in the northeast corner there was almost no topography in the field and  $^{137}\text{Cs}$  inventories in this almost flat area hovered close to the reference activity level. Blairhall has been a particularly suitable site for resolving the tillage erosion signal. Tillage translocation at Blairhall has on average contributed some 69% towards erosion and it is suspected that the combination of edge and intra-field ploughing patterns at certain points in the field may be having an effect of  $^{137}\text{Cs}$  derived estimates.

Littlelour site conditions are relatively similar to those at Blairhall and the model produced the closest-fit out of all fields. The site appears susceptible to water erosion particularly from the middle of the transect onwards where slope increases and slope length becomes significant. It has transpired that poor agreement between the models and the  $^{137}\text{Cs}$  derived estimates was likely caused by problems with digital terrain modelling techniques and its questionable representation of the real terrain. An immediate proposal would therefore be a reduction in cell size assuming the appropriate processing power.

The final model has been by default a compromise in performance to enable the quantitative modelling of erosion and deposition to be achieved at the regional scale. Regardless of this the general net model has produced quality predictions at both Loanleven, Blairhall, and Littlelour.

# Chapter 5

## 5. Evaluating the erosion threat in an archaeological context.

The net erosion budget has been divided into water and tillage erosion components and examined in chapters two and three respectively. Historic Scotland is interested in determining the overall threat of erosion as a whole to the archaeology of the four specific field sites as well as to the whole study area. Secondly and possibly of greater significance is the attempt at apportioning the relative importance of each erosion component. This section collates the results of 2D model predictions from chapter two and three, transect based  $^{137}\text{Cs}$  derived erosion estimates from chapter five and attempts to evaluate the threat from an archaeological standpoint.

It is necessary to compare any erosion estimates to some appropriate benchmark of loss tolerance. Qualitative evaluations may then be made. A commonly quoted soil loss tolerance for UK conditions is  $0.1 \text{ mm yr}^{-1}$  (Kirkby and Morgan, 1980). This will be used as the benchmark for all erosion evaluations.

### 5.1 Loanleven

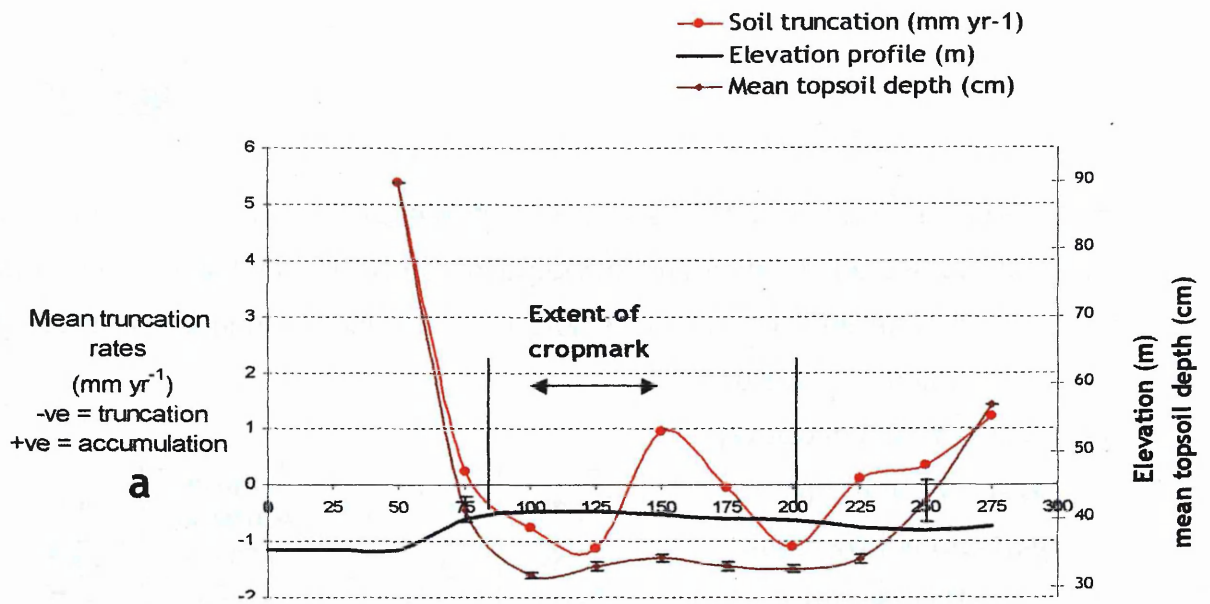
The 4 sites have been described in detail in chapter one. Figure 5.1 presents the rates of soil truncation along the transect derived from the  $^{137}\text{Cs}$  technique and spatial estimations of truncation from the field specific optimised net erosion model. The approximate extents of the enclosure are clearly within the zone of maximum soil erosion. The dark ditch feature seen in the aerial photograph (Figure 1.17, chapter 1) coincides very closely with the break of slope at approximately 75m and 200m. At 75m, according to the  $^{137}\text{Cs}$  estimates there is a net accumulation of soil. This point has been discussed in chapter five as to its validity and it is likely to be experiencing net erosion. A higher rate of soil loss at this point would in fact corroborate the large rate of accumulation found at the slope base.

m	Profile curvature*	kg m <sup>-2</sup> yr <sup>-1</sup>	mm yr <sup>-1</sup>
50	-0.8993	+6.35	+5.38
75	0.8061	+0.29	+0.25
100	0.3264	-0.89	-0.76
125	0.1247	-1.34	-1.14
150	-0.0228	+1.13	+0.96
175	-0.2117	-0.06	-0.05
200	0.0494	-1.29	-1.10
225	-0.0269	+0.13	+0.11
250	-0.0398	+0.41	+0.34
275	0.0642	+1.44	+1.22

\* +ve = convex

Table 5.1. <sup>137</sup>Cs derived soil truncation rates along the Loanleven transect.

At 200m (-1.10 mm yr<sup>-1</sup>) and 125m (-1.14 mm yr<sup>-1</sup>) the estimated rates are a scale of magnitude greater than 0.1 mm yr<sup>-1</sup>, which over the medium-term represents serious threat. Within the optimised net erosion model specific to Loanleven, tillage erosion contributed 83% at 125m and 72% at 100m towards the net erosion budget. When using the general net erosion model, tillage contribution at the two loci increased to 90% and 95% respectively. The modelling exercise has highlighted the importance and dominance of tillage translocation on topographically complex fields. Loanleven is a complex of short convex-concave slopes in a north to south direction and patterns of modelled sediment movement (Figure 5.1b) mirror this strongly. As distance from the central zone of the plateau-type feature (centre approx. 150m) increases to the north and south, there is a steady increase in rates of soil erosion to the convex shoulders where they peak. The shallowest topsoil depths are also found here, therefore ploughing can only be responsible for such gradual truncation of the edges of the plateau.



### Optimised net erosion

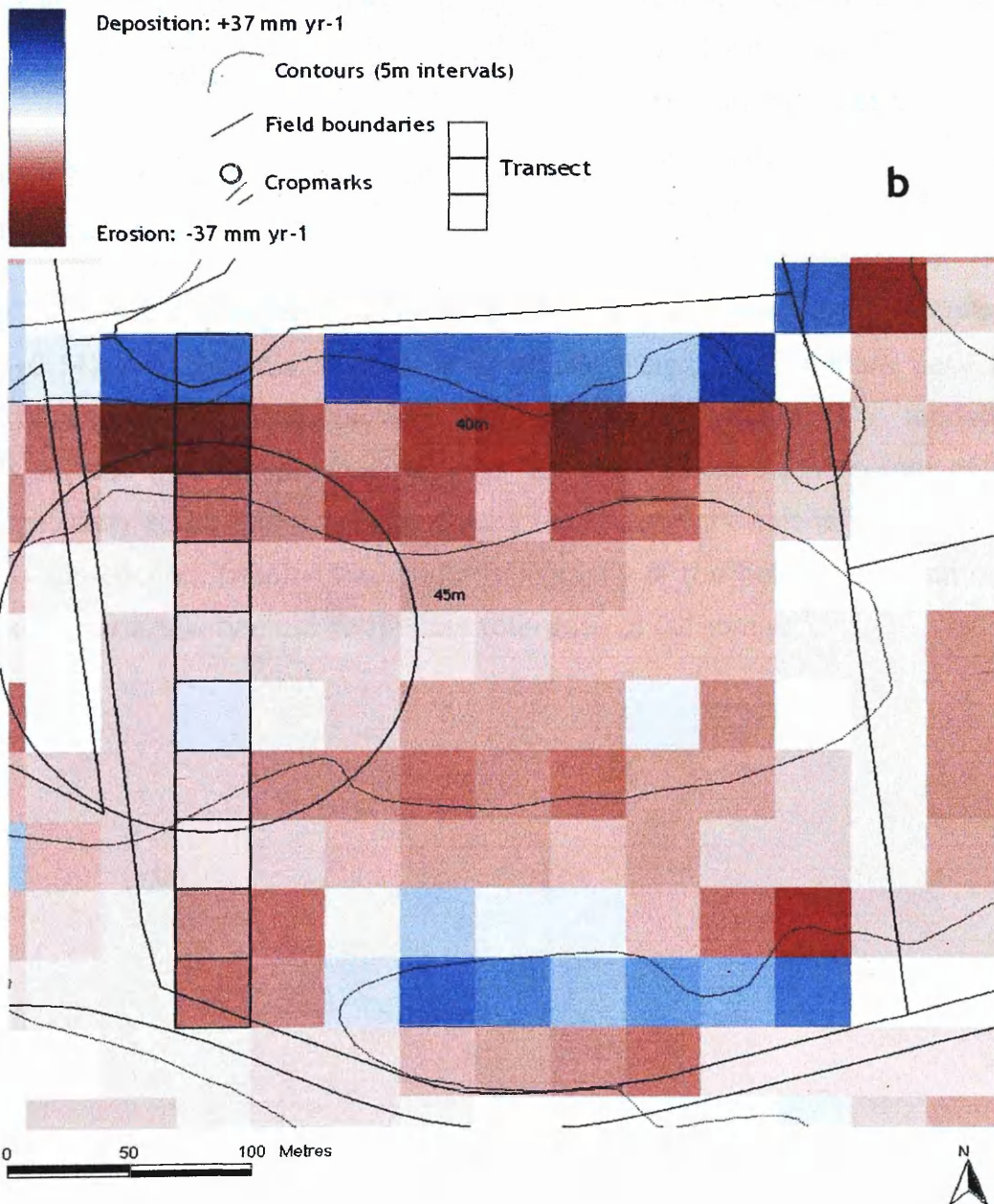


Figure 5.1. Rates of soil truncation based on the <sup>137</sup>Cs transect data (a) and optimised net erosion model predictions (b) across Loanleven.

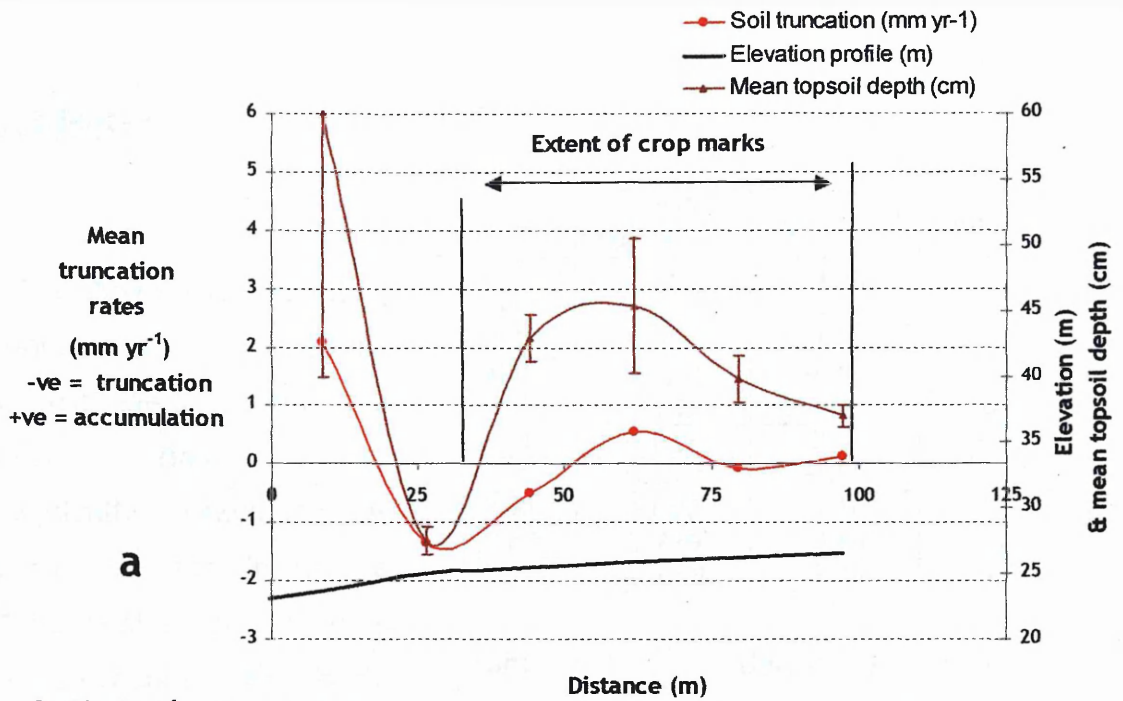
## 5.2 Blairhall

The cropmark features across Blairhall field are varied in type and are widely distributed. The selected transect incorporates the edge of the cursus feature, a ring-ditch, small linear cropmarks and pits (Figure 5.2b). The main body of the

m	Profile curvature*	kg m <sup>-2</sup> yr <sup>-1</sup>	mm yr <sup>-1</sup>
8.83	0.0072	+3.34	+2.09
26.5	0.1412	-2.14	-1.34
44.2	0.0171	-0.78	-0.49
61.85	-0.004	+0.88	+0.55
79.5	-0.018	-0.12	-0.08
97.2	-0.008	+0.23	+0.14

Table 5.2. <sup>137</sup>Cs derived soil truncation rates along the Blairhall transect.

cursus monument is positioned on flat land but is experiencing rates of tillage erosion less than -0.15 mm yr<sup>-1</sup>. The trend in topsoil depth corresponds well with the <sup>137</sup>Cs derived truncation rates which oscillate from net accumulation to a maximum net loss of -1.34 mm yr<sup>-1</sup> (Table 5.2). This peak loss is located on a sharp convex shoulder (profile curv: +0.14) although according to the available digitised cropmark data this locus does appear to contain fewer archaeological features. The modelling results suggest that the linear cropmarks towards the northeast corner of the field are likely to be under greater threat (-0.72 to -0.11 mm yr<sup>-1</sup>) as break of slope is approached. Despite the simple topography of the field, truncation rates still exceed or are very close to the loss tolerance of 0.1 mm yr<sup>-1</sup>.



Optimised net erosion

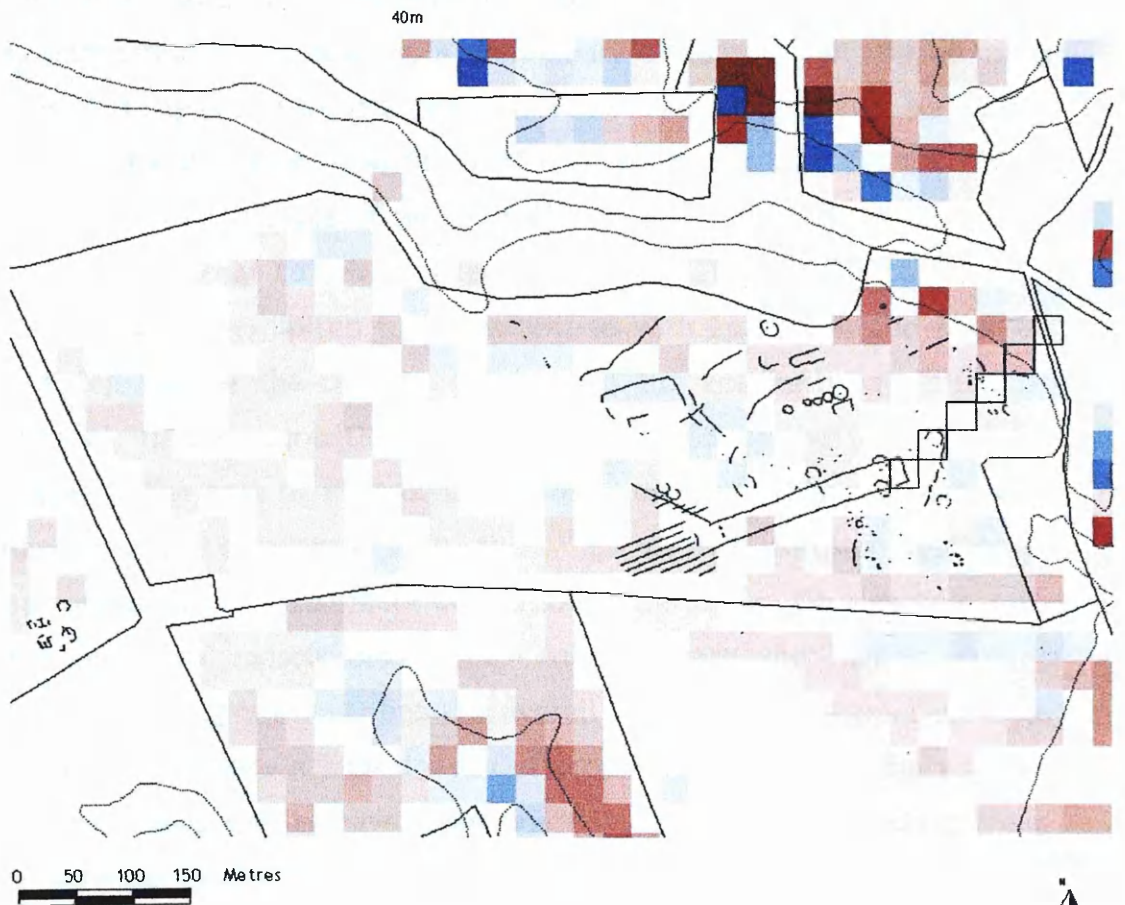
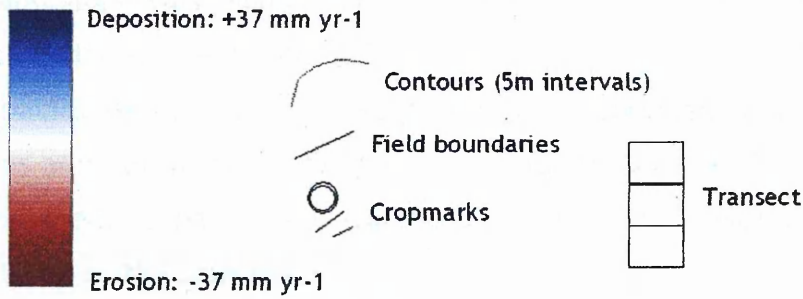


Figure 5.2. Rates of soil truncation based on the  $^{137}\text{Cs}$  transect data (a) and optimised net erosion model predictions (b) across Blairhall.

### 5.3 Leadketty

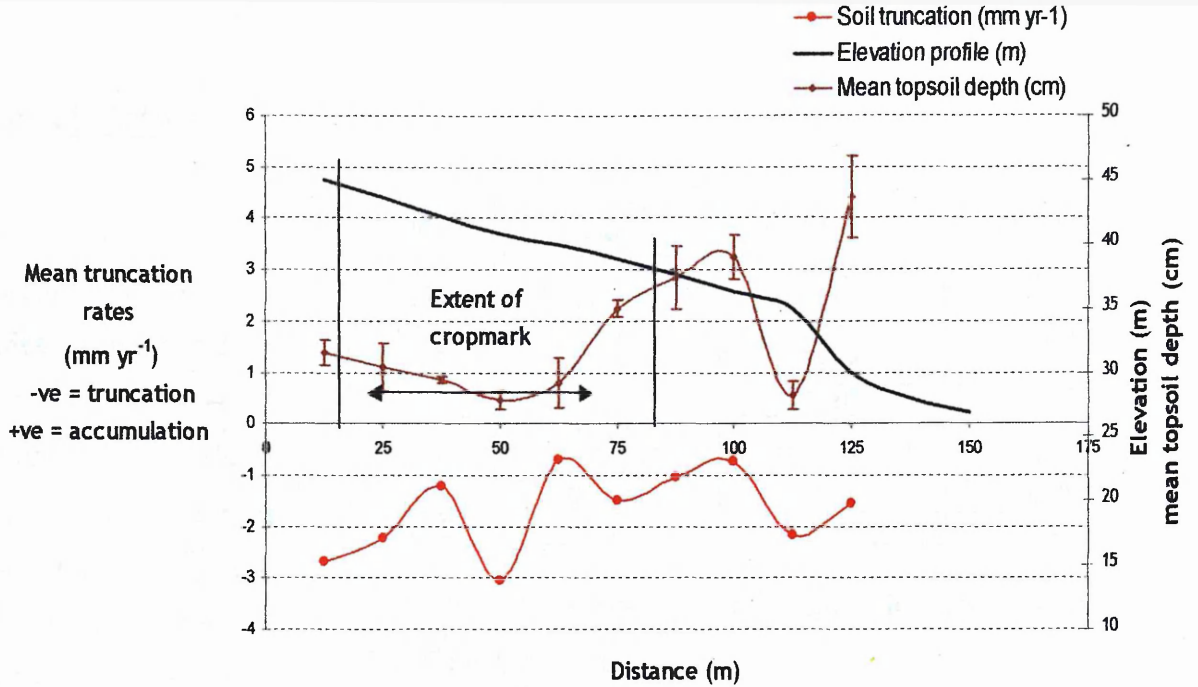
Figure 5.3 shows the modelling predictions and  $^{137}\text{Cs}$  derived erosion estimates across the Leadketty field site. Topographically Leadketty is similar to Loanleven in that a prominent central rise/knoll is present. Surrounding the knoll, aspect and slope vary widely and the enclosure feature is located

on the backslope of this knoll. Suspicion has surrounded both the  $^{137}\text{Cs}$  derived estimates and optimised model predictions for reasons outlined in chapter four. Problems seem to have been caused by insufficiently estimating the baseline  $^{137}\text{Cs}$  activity of the reference site. Because of this, the rates appear too high. By rectifying the reference site problem, the erosion/deposition pattern as a whole will only shift either up or down so a preliminary evaluation can still be made. From Figure 5.3 the enclosure is located on a stretch of slope that is susceptible to water and tillage erosion. The first half of the transect contains the highest  $^{137}\text{Cs}$  derived truncation rates of up to  $-3.05 \text{ mm yr}^{-1}$ . Rates of this magnitude pose very serious threat to sub-surface archaeology. The dominance of tillage erosion has not been exhibited to the extent as with Loanleven and Blairhall. Across the top half of the transect when using the Leadketty optimised net erosion model, tillage accounted on average for 45.5% of the total modelled erosion budget. The best-fit models did, however display rather poor predictive performance when compared with the  $^{137}\text{Cs}$  derived erosion estimates, therefore, preventing any confident conclusion to be drawn. On a more general level, the minimum topsoil depth does coincide with the highest rate of truncation (50m along transect) but the overall trend along the transect is not clear. Leadketty contains a high density of cropmark sites as do the adjacent fields. Unfortunately results have been unsatisfactory and interpreting trends and untangling the erosion budget has been difficult.

m	Profile curvature	kg m <sup>-2</sup> yr <sup>-1</sup>	mm yr <sup>-1</sup>
12.5	0.344	-4.33	-2.70
25.0	0.136	-3.58	-2.23
37.5	0.033	-1.96	-1.22
50.0	-0.031	-4.89	-3.05
62.5	0.132	-1.10	-0.68
75.0	0.015	-2.42	-1.51
87.5	0.012	-1.66	-1.03
100.0	0.080	-1.18	-0.74
112.5	0.739	-3.46	-2.16
125.0	-0.658	-2.48	-1.54

Table 5.3.  $^{137}\text{Cs}$  derived soil truncation rates along the Leadketty transect.





**Optimised net erosion**

Deposition: +37  $\text{mm yr}^{-1}$



Erosion: -37  $\text{mm yr}^{-1}$

- Contours (5m intervals)
- Field boundaries
- Cropmarks
- Transect

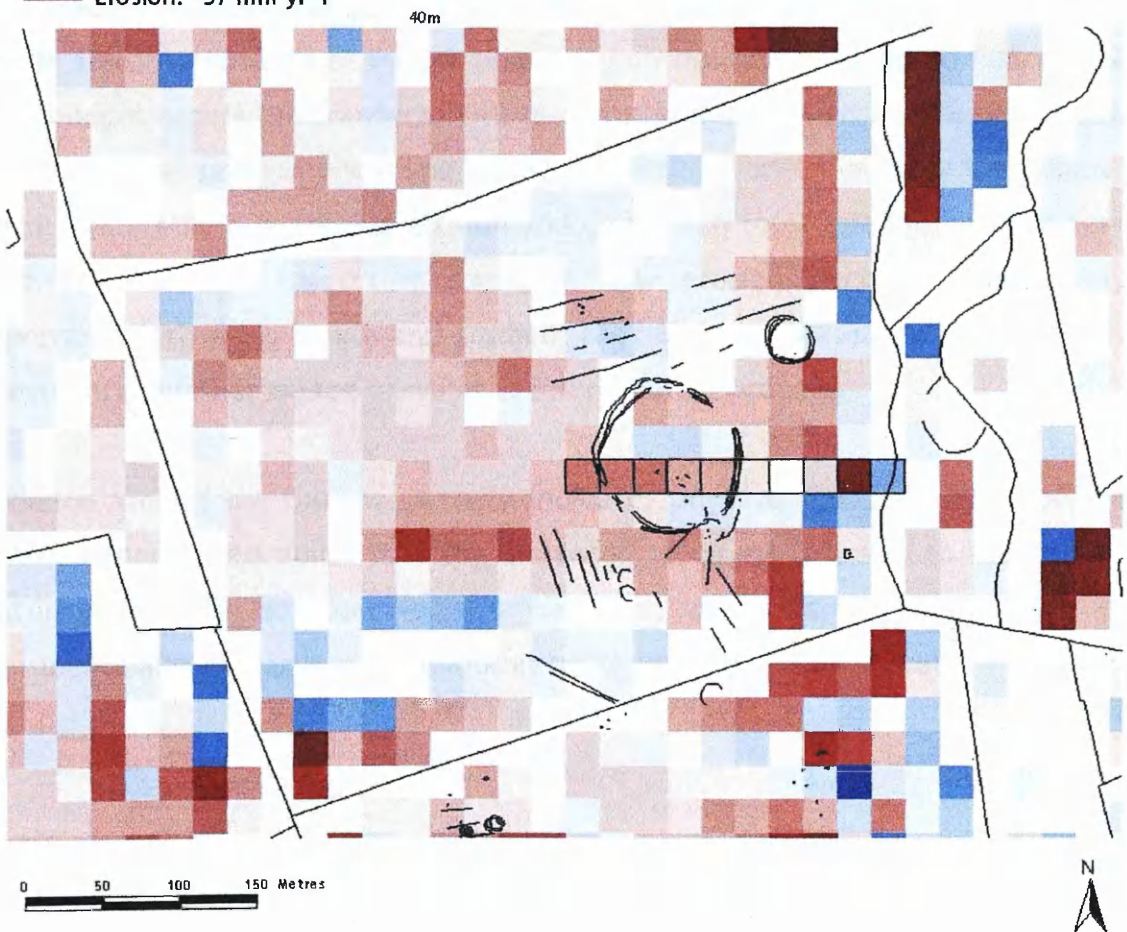


Figure 5.3. Rates of soil truncation based on the  $^{137}\text{Cs}$  transect data (a) and optimised net erosion model predictions (b) across Leadketty.

## 5.4 Littlelour

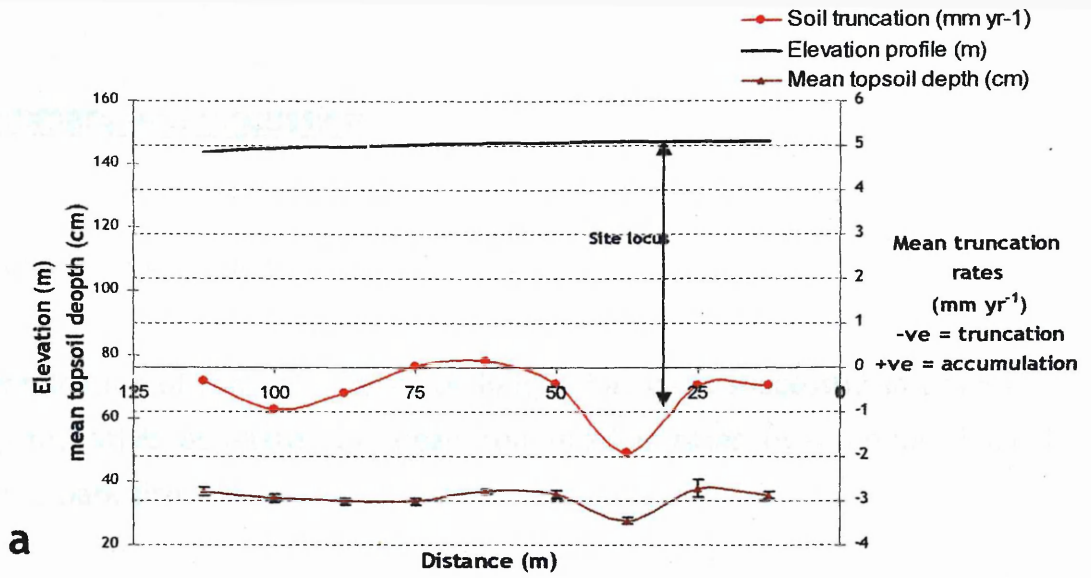
The single barrow feature present is quite pronounced on the field's topography. Upon inspection during the last 3 years, there has been a consistent increase in surface stoniness

within a 4-5m radius of the mound centre. The data from the  $^{137}\text{Cs}$  technique are supporting this visible evidence of plough damage (Table 5.4). The  $^{137}\text{Cs}$  technique has estimated the highest truncation rate ( $-1.91 \text{ mm yr}^{-1}$ ) directly over the barrow (37.5m) and all but one of the transect positions are above the  $0.1 \text{ mm yr}^{-1}$  tolerance threshold. Either side of the barrow truncation rates decrease as curvature reduces. Ploughing is the cause of such rates of soil loss and based on the field optimised net model tillage is contributing on average 50% of the total budget across the transect. Tillage contributions as high as 90% and as low as 11% are also present according to the optimised model. Spatially the general net model predicts increasing erosion and deposition towards the lower western edge of the field suggesting overland flow erosion becomes increasingly important. Both slope length and gradient are higher in this area so it is difficult to estimate whether tillage or water is the dominant process.

Evidence around the barrow strongly indicates physical plough damage of the feature. There is no doubt that the increased stoniness is linked to the barrow feature. This, in addition to the continued net loss of topsoil due to translocation must result in Littlelour as being under extreme threat.

m	Profile curvature	$\text{kg m}^{-2} \text{ yr}^{-1}$	$\text{mm yr}^{-1}$
12.5	0.0246	-0.54	-0.41
25	0.0237	-0.52	-0.39
*37.5	0.0264	-2.53	-1.91
50	0.0283	-0.50	-0.38
62.5	0.0275	0.20	0.15
75	0.0224	0.04	0.03
87.5	0.0174	-0.76	-0.58
100	0.0981	-1.26	-0.95
112.5	-0.09	-0.40	-0.30

Table 5.4.  $^{137}\text{Cs}$  derived soil truncation rates along the Littlelour transect.



### Optimised net erosion

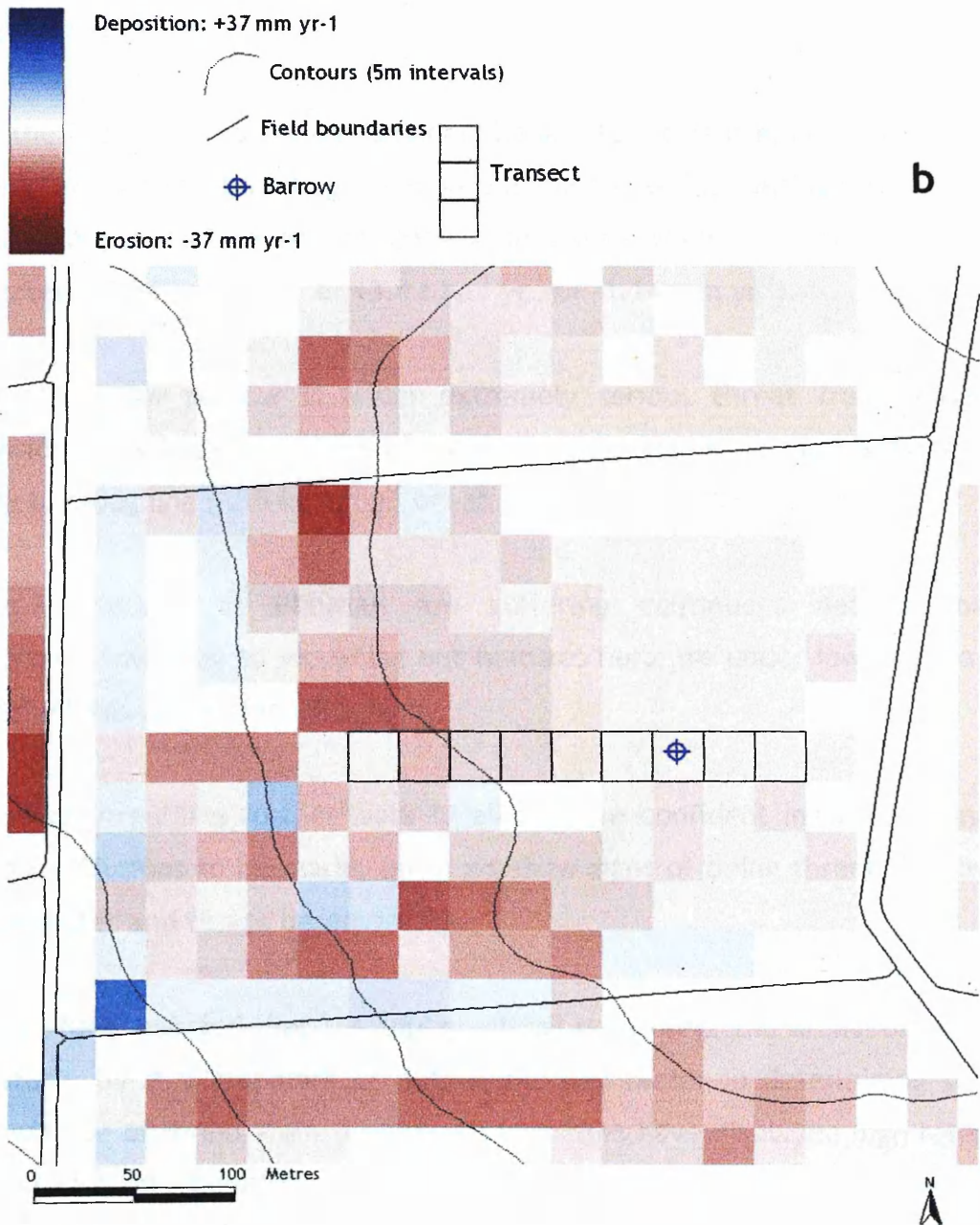


Figure 5.4. Rates of soil truncation based on the <sup>137</sup>Cs transect data (a) and optimised net erosion model predictions (b) across Littlelour.

## 5.5 Summary and discussion

### 5.5.1 Field site evaluation

1. Application of the  $^{137}\text{Cs}$  tracer technique has been successful in providing quantitative estimates of mean soil erosion rates over archaeological cropmark sites.
2. If the assumption that  $0.1 \text{ mm yr}^{-1}$  as a soil loss tolerance is appropriate, then much of the archaeology in the four fields should be viewed as under significant threat.
3. Of the four sites, Loanleven is under the greatest threat mainly due to its complex topography. Tillage erosion is dominant and is causing potentially damaging truncation of the convex shoulders where the enclosure is located ( $-1.34 \text{ kg m}^{-2} \text{ yr}^{-1}$  or  $13.4 \text{ t ha}^{-1} \text{ yr}^{-1}$  or  $-1.14 \text{ mm yr}^{-1}$ ).
4. The Littlelour barrow is under extremely serious threat from tillage erosion. This is the only site where convincing visible damage is evident due to ploughing ( $-2.5 \text{ kg m}^{-2} \text{ yr}^{-1}$  or  $-25 \text{ t ha}^{-1} \text{ yr}^{-1}$  or  $-1.91 \text{ mm yr}^{-1}$ ).
5. The cropmarks at Blairhall are suffering continuous net erosion predominantly due to ploughing but features here are under lower threat on the basis of the flat topography.
6. Leadketty requires further work to allow more confident interpretations and conclusions to be made, but does show signs of being threatened by both water and tillage based erosion.
7. It can be concluded that the topographical position of the archaeological feature, be it a cropmark or not, is the key factor in determining the magnitude of threat from erosion. All four sites have displayed high rates of erosion at shoulder convexities. Estimates of soil accumulation in concavities have also been made by the  $^{137}\text{Cs}$  technique. Correspondence

of estimated soil erosion rate ( $^{137}\text{Cs}$  based) and slope profile curvature was poor at all sites (chapter four). Small sample sizes and use of non-parametric tests have masked the relationship with topography. The results clearly demonstrate that topographic shape determines whether the archaeological features will be losing topsoil cover and therefore threatened or subsequently protected further by accumulating soil.

### 5.5.2 Regional evaluation

1. Across the whole study area, some 942 or 55% of the 1707 sites defined as cropmarks are located on convex land (profile curvature  $> 0$ ). 728 or 25% of cropmark features are positioned on concave land (profile curvature  $< 0$ ). This research suggests that since convex landscape positions are susceptible to high erosion rates, half of the cropmark sites in the study area could be highly vulnerable to agricultural plough damage.

#### 5.5.2.1 Discussion

Using a 5 x 5 cell kernel (50m buffer), the mean erosion rate for all sites was calculated to give a more spatially representative value. The generalised net erosion model predicted some 65% of all archaeological sites to be experiencing net erosion. The model predicted 63% of cropmark sites located in arable land to be experiencing net soil loss, 84% of these and 79% of all archaeological sites were predicted to be eroding up to  $-0.5 \text{ kg m}^{-2} \text{ yr}^{-1}$  ( $-5 \text{ t ha}^{-1} \text{ yr}^{-1}$ ). Table 5.5 shows the distribution in the range of predicted erosion rates for all archaeological sites and cropmark sites after classification.

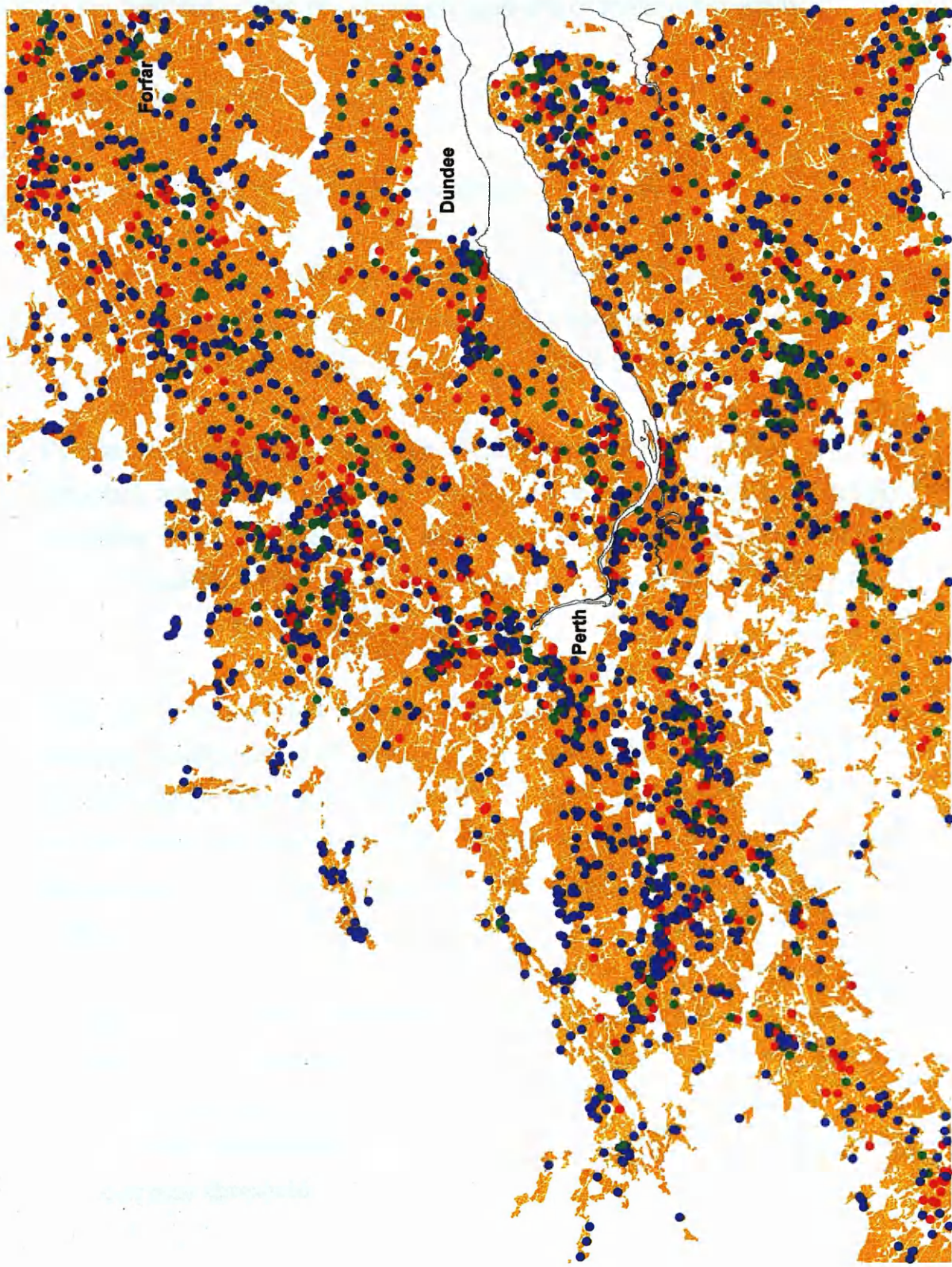
Frequency of all archaeological sites	Erosion rate class ( $\text{kg m}^{-2} \text{ yr}^{-1}$ )	Frequency of cropmark sites
1457	0 to -0.499	903
252	-5 to -0.999	125
102	-1 to -1.999	36
24	-2 to -4.999	5
2	-5 to -9.999	0
1	-10 to -29.999	1
<b>1838</b>		<b>1070</b>

Table 5.5. Predicted erosion rates of all archaeological sites and cropmarks within the whole study area.

The threat posed can be evaluated by applying the Kirkby (1980) soil loss tolerance value ( $0.1\text{mm yr}^{-1}$ ). Assuming a bulk density of  $1300\text{ kg m}^{-3}$ , an erosion rate of  $0.13\text{ kg m}^{-2}\text{ yr}^{-1}$  was used as a threshold value. Based on this, 547 cropmark sites exceed the tolerance threshold, some 32% of all cropmarks. Out of all archaeological sites present, 1053 (37%) exceed the soil loss tolerance limit. Potentially more important are the higher rates of erosion predicted for other types of archaeological site. 129 sites or 5% of all archaeological sites and 42 or 4% of cropmark sites in the study area according to the predictions are eroding more than  $-1\text{ kg m}^{-2}\text{ yr}^{-1}$  ( $-10\text{ t ha}^{-1}\text{ yr}^{-1}$ ). These sites should be viewed as being under very serious threat from soil loss.

The evaluation of erosion threat to archaeological sites has been based on the coordinate data from the NMRS database. There is an obvious problem when using a point x,y co-ordinate to represent a cropmark site that may be spatially large in reality. Topography and erosion/deposition rates vary widely in space, therefore use of a mean erosion value based on surrounding cells rather than a point specific erosion rate aimed to make the value more representative.

Finally, evaluation of the erosion threat would be refined by knowing the depth of the cropmark features. This is at present unknown and ascertaining such data would involve invasive excavation. However, combining depth to feature with truncation rates will enable a more useful estimation of time to exposure or destruction.



- Within SLT or no erosion
- Eroding but within SLT
- Exceeding SLT
- Arable land classes (LCS, 1988)

SLT = Soil Loss Tolerance (0.13kg m<sup>-2</sup> yr<sup>-1</sup>)



Figure 5.5. Distribution of the predicted erosion threat to cropland sites

# Chapter 6

## 6. Summary of main results and conclusions.

The key findings and issues from the previous six chapters are summarised here. This is followed by a wider discussion on each one of these conclusions.

### 6.1 Principal results

The primary aim of the study was defined as follows:

To assess the threat of erosion posed to archaeological cropmarks sites by quantitatively modelling soil erosion rates across arable lands of lowland mid-Scotland.

1. The research has ascertained that within the study area, 63% of some 1707 cropmark features are predicted as being on land experiencing net erosion. According to the generalised net model, 65% of all archaeological sites (2849 in total) located within the study area are also predicted as being on land experiencing net erosion.
2. Using the Kirkby (1980) soil loss tolerance threshold of  $0.1\text{mm yr}^{-1}$  and assuming a bulk density of  $1300\text{ kg m}^{-3}$ , up to  $-0.13\text{ kg m}^{-2}\text{ yr}^{-1}$  of soil loss can be tolerated. It is assumed that within the soil loss threshold the soil incurs no long-term net degradation and is able to offset impacts through the development of new soil. Using this, the following conclusions have been made:
  - a. 547 cropmark sites exceeded the tolerance threshold. This corresponds to 32% of all cropmarks or 19% of all archaeological sites present within the study area.
  - b. Out of all archaeological sites present, 1053 (37%) exceeded the soil loss tolerance threshold.



3. Of the four field sites investigated, the archaeological features at Loanleven and Littlelour are under serious threat from erosion caused by ploughing practices of up to  $-1.34 \text{ kg m}^{-2} \text{ yr}^{-1}$  ( $-1.14 \text{ mm yr}^{-1}$ ) and  $-2.14 \text{ kg m}^{-2} \text{ yr}^{-1}$  ( $-1.34 \text{ mm yr}^{-1}$ ) respectively. The Blairhall archaeology sites are also at risk but to a much lesser extent. The threat at Blairhall is dominated by tillage erosion but is overall very low in magnitude. The Leadketty sites have been rather inconclusive due to problematic results due to the insufficiently defining the baseline  $^{137}\text{Cs}$  activity. The pattern of  $^{137}\text{Cs}$  derived erosion/deposition does, however indicate that the sites will be experiencing high soil loss rates though further work is required.

In summary, this research proposes that sub-surface archaeological features within arable mid-Scotland are under sufficient threat from erosion caused primarily by cultivation to justify concern. Over half of all archaeological sites and cropmark sites are predicted as eroding with approximately one third of both exceeding the soil loss tolerance threshold. Figure 5.5 illustrates the distribution of the predicted soil erosion threat in relation to cropmark sites.

## 6.2 Other results

1. Application of the  $^{137}\text{Cs}$  tracer technique has proved to be a valuable tool and successful at estimating medium-term mean net rates of soil erosion. Spatial analysis of  $^{137}\text{Cs}$  derived erosion estimates has detected that:
  - a. Topographic shape (curvature) is the fundamental factor controlling the magnitude of soil loss within the cultivated field so that:
    - i. the highest net erosion rates are largely located on convex slope positions and
    - ii. the highest deposition rates are located on concave slope positions.

The data imply that only the process of tillage translocation at such convex positions could be responsible for the high rates of soil loss. The

plough is therefore posing the most erosive threat to the investigated archaeological sites.

- b. Spatial variability of  $^{137}\text{Cs}$  can be extremely high within small areas and must be addressed carefully if deriving mean estimates from samples. Percentage error on mean estimates of  $^{137}\text{Cs}$  activity per 25m cell ranged from 2 to 34 %. Analysis of spatial variability must play an important role in defining the grid cell and sampling grid size when validating GIS models.
2. The simple mass-balance sediment transport model has demonstrated the ability to simulate patterns of water erosion and deposition in a spatial framework. The model is very robust and handled large datasets with ease.
  3. The topographically based tillage erosion model ARCTILL developed in chapter 3 performed extremely well when compared with the established TEP model (Lindstrom, 2000). ARCTILL subsequently delivered confident 2D predictions of net soil loss and gain due to ploughing.
  4. Field boundaries play a vital and significant role in shaping the patterns and changing the magnitudes of water based erosion and deposition. Erosion rates are attenuated and sediment is less likely to be lost from fields, instead being contained within in the field unit. Field boundaries thus act as an effective soil conservation tool.
  5.  $^{137}\text{Cs}$  has proved to be an effective calibration tool for optimising water, tillage and net erosion models. The following conclusions can be drawn:
    - a. According to the optimisation results, tillage translocation must be incorporated into landscape evolution models for predictions to be realistic. The net optimised models (water + tillage) at Loanleven and Blairhall performed better than as individual component models.
    - b. Optimised parameters of the water erosion model are similar to those previously published.

- c. Optimised tillage transport coefficients ( $k_{\text{till}}$ ) at the four field sites were not consistent and agreement with published values was varied.
- d. The optimisation procedure failed to detect the influence of the transport capacity parameter ( $k_2$ ) within the erosion model. This needs to be addressed in further work since from chapter 2 there has been a clear impact.
- e. Equifinality in model results was noted although it is unlikely to have been important. Chapter 5 outlined how the observed flexibility of the slope and sca exponent combinations produced only extremely small increases in rmse value. The  $k_{\text{till}}$  parameter exhibited little variability in the lowest 50 rmse value.

### 6.3 Concluding discussion.

#### 1. The $^{137}\text{Cs}$ tracer technique

- a. Measurements of soil resident  $^{137}\text{Cs}$  have provided mean soil erosion/deposition rates for the last 36 years through a successful calibration process. Erosion/deposition estimates were produced quicker than via monitoring schemes, usually limited to a 3 year period.
- b.  $^{137}\text{Cs}$  derived estimates of erosion/deposition reflected well the spatial variation within the processes influencing sediment transport. Statistically  $^{137}\text{Cs}$  erosion/deposition estimates were very poorly related to topographic form but visually the role of topography is quite clear.
- c. From analysis of variability of  $^{137}\text{Cs}$  activity it can be concluded that:
  - i. Intracell variability along the transects was at times very high (Loanleven, 1 - 8.5%; Blairhall, 2.4 - 34%; Leadketty, 6.5 - 22%; Littlelour, 6.7 - 17%). A mean approach to estimating

- erosion/deposition per cell based on such variability could therefore be questioned. Reducing the grid cell resolution will help but at what resolution does variability significantly reduce? At 10m resolution, the absolute highest useable at the scale used here, similar variability within cells is likely to persist (Tyler, 1994). It would be difficult therefore to justify increasing resolution solely with a view to addressing variability. Therefore, optimising such medium-resolution models using such locally sensitive and variable data will result in only approximate predictions.
- ii. Confidence was high in the final results at three sites due to low variability in inter-reference site cores; 10% at Loanleven, 4% at Blairhall and 7.5% at Littlelour.
  - iii. The soil homogenisation process used on the cores prior to sub-sampling was successful at producing results with consistently low variability (< 7%; chapter 5).
- d. High priority must be given to satisfactorily defining the  $^{137}\text{Cs}$  inventory at the reference site. This must be the first task when embarking on such project work since considerable extra time was spent finding undisturbed sites at the unfortunate expense of desk-based modelling and lab work. Very little undisturbed land existed adjacent to the four field sites.

## 2. Cell size

- a. 25m grid cells may have been too large for the modelling approach. Use of a 25x25m grid cell for the modelling has caused problems, mainly relating to landscape representation. The DTM at 25m resolution assumed the  $625\text{m}^2$  area within each cell to be a uniform planar surface. This may not have reflected the actual variation in terrain within the corresponding area. This has been noted along the field transects and in one example in particular at Loanleven. Cell 1 is strongly convex (+0.48) and has a slope gradient of 18% ( $10^\circ$ ), yet the calculation of the erosion/deposition rates using the calibration technique developed by Zhang et al.,

(1990) resulted in a high level of intracell variability. As a result the mean soil erosion/deposition rate calculated from the five samples in the cell was  $+0.293 \text{ kg m}^{-2} \text{ yr}^{-1}$ . This rate of deposition is unlikely at such a location. Examining the distribution of variability in intracell erosion rates based on  $^{137}\text{Cs}$ , a smaller grid cell may have been capable of more accurately representing the change in topography within the cell rather than assuming uniformity. In doing so, the finer resolution of landscape change would hopefully reflect the very local  $^{137}\text{Cs}$  derived erosion/deposition rates. Tyler (1994) found that similar variability in  $^{137}\text{Cs}$  activity was still present even within a 2 m x 2 m cell so the decision to reduce cell size is clear-cut at least from a variability standpoint.

- b. Grid cell size has other implications when spatially modelling catchment-scale hydrological attributes (Quinn et al., 1995). Larger cell sizes were reported to exhibit bias towards sharper frequency distributions with overall higher drainage area value in the distribution peak. Quinn et al., (1995) recommended a maximum cell size of 50m for catchment modelling but strongly advised finer resolutions. 10m has been suggested as a optimal size for modelling hydrologic and geomorphic processes (Zhang and Montgomery, 1994). Grid cell size also has been reported to affect modelled erosion/deposition magnitude (Schoorl et al., 2000). Increasing cell size from 1m to 81m led to the overestimation of erosion and underestimation of deposition. They proposed that use of a multi-direction flow algorithm and finer grid scales will produce more plausible rates of erosion and deposition.
- c. Cell size is always a compromise between computing power and modelling requirements. The study area at 25m resolution produced some 6,080,000 cells for processing. Scaling-down to a 15m resolution would have increased the cell count to 16,444,444, a rise of over 170% in demands on processing power and time. Further reduction to 10m corresponds to 38,000,000 cells and over a 500% rise in PC and time demands.

2. Choice of cell size must also be made with consideration for the resolution of the source data. The Landform Profile® data set supplied by the Ordnance Survey is primarily a 5m interval contour dataset.

a. Overall the 25m grid cell has proved a reasonable choice in terms of ability to model catchment-scale properties against the trade-off with available PC power. 25m was possibly too large for the field-scale validation of the models using  $^{137}\text{Cs}$ , and on the basis of this alone the cell size should have been reduced to approximately 15m.

### 3. The water erosion model

a. The hillslope storage model (Kirkby, 1971) modified by Desmet (1995) has demonstrated good ability to spatially predict erosion and deposition patterns across the study area. Integration of the  $D_{\infty}$  (Tarboton, 1997) flow algorithm has generated more credible patterns than those expected from simpler single-direction flow routines (Desmet and Govers, 1996).

b. When optimizing at individual sites the two variables displayed some disparity. Sensitivity analysis concluded that the specific catchment area exponent  $n$  was the most influential and requires careful attention when optimising.

c. The switch mechanism controlling the transition from erosion to deposition is governed by transport capacity ( $T_c$ ) as defined by  $k_2$ . The unfortunate topographical circumstances at each field site prevented the optimisation routine from detecting any  $T_c$  influence upon the erosion/deposition patterns. This is contrary to results presented by Desmet (1995) where the frequency occurrence of deposition increased with decreasing  $k_2$ . Results presented in chapter two support this.

- d. The model was most sensitive to the specific catchment (sca) area variable. This work has concluded that the assertion of field boundary influence on catchment drainage and erosion/deposition is relevant. Use of similar models demands focus on accurately representing the linear structure of the landscape in terms of type, shape, and porosity.
- e. A simple topographically driven model, easily parameterized, has performed in a very robust manner at a technologically challenging scale. It proves that there may be no need to tackle the problems of parameterization associated with more complex models when simpler ones perform as well (Kirkby, 1988).

#### 4. Field boundaries

- a. The presence of modelled field boundaries on the DTM landscape had very significant effects on both catchment hydrology and erosion/deposition patterns and magnitudes. Reductions of up to 25% in mean erosion rate and 53% in median erosion rate in the four clip areas were noted. At the field sites, reductions of 16% at Loanleven, 20% at Leadketty, and 33% at Littlelour in median erosion rates were observed. Mean erosion rates at the field sites were also significantly reduced.
- b. The effectiveness of field boundaries at attenuating erosion should be evaluated at the local scale and not statistically using large spatial data sets such as used in this work. The model has predicted that the most beneficial reductions occur only locally and not consistently across the landscape. Although statistical tests have proved their significance, the interpretation questions their effectiveness from a practical standpoint. Put another way, the statistical differences in erosion rate with and without field boundaries would be practically insignificant or unnoticeable to the farmer or conservationist. Resource managers and farmers are interested in measurable benefits that justify the financial outlay and effort in managing parcel boundaries. The statistical tests in chapter two do not clearly convey that proper maintenance and conservation of field boundaries can be highly effective in reducing

water induced soil loss. Examining their influence locally will however be more effective.

- c. The boundary 'burst' effect described in chapter 2, relating to the way in which flow appears to transit parcel boundaries, needs to be addressed further but is simple and relatively quick to solve.
- d. Albeit a simple approach, the field boundary model has proved valuable in presenting preliminary data on a relatively new research topic area. Further work needs to be done on implementing an element of porosity to the boundaries since not all are impermeable.

## 5. Tillage translocation

- a. ARCTILL was developed and performed extremely well alongside TEP (Lindstrom, 2000). It is a topographically driven model, based on one-dimensional flux of soil (in accordance with aspect) and that is sensitive to field boundary pattern. It has delivered intuitively good spatial predictions. ARCTILL predicts soil truncation at convex positions and infilling of hollows or concavities. No account of tillage direction was taken which has been recently reported as being a further significant factor in the magnitude and direction of soil flux (de Alba, 2001).
- b. Optimized results from two out of the three sites suggest tillage translocation as being the major component of soil erosion as reported by an increasing body of literature (Gerontidis et al., 2001; Govers et al., 1996; Govers et al., 1994; Kosmas, 2001; Lindstrom et al., 1990; Lindstrom et al., 1992; Lobb, 1999a; Quine, 1999; Quine et al., 1997; Tsara et al., 2001; Van Muysen et al., 2000). Tillage erosion on average has contributed 75% and 69% at Loanleven and Blairhall respectively clearly demonstrating the significance of the process. Tillage transport coefficients ( $k_{\text{till}}$ ) after optimization were set at  $300 \text{ kg m}^{-1}$  for half and  $500 \text{ kg m}^{-1}$  for the other half of field sites. The  $k_{\text{till}}$  parameter in the final general optimized model applied at the whole study area scale was set to  $400 \text{ kg m}^{-1}$ . These values are in agreement with optimized  $k_{\text{till}}$  values



published from work in Western Europe (348 and 397 kg m<sup>-1</sup>, UK (Govers et al., 1996), 400-600 kg m<sup>-1</sup>, Belgium (Govers et al., 1994), 133 - 360 kg m<sup>-1</sup> (Gerontidis et al., 2001)). However, there is some considerable variability in quoted  $k_{\text{till}}$  values. Quine, (1997) used a  $k_{\text{till}}$  value of 550 kg m<sup>-1</sup> representing a single mouldboard, disc and harrow operation. Quine, (1997) claimed that more ploughing will subsequently increase the  $k_{\text{till}}$  value. Van Oost (2000) reported  $k_{\text{till}}$  for Belgium as being ca. 800 kg m<sup>-1</sup>. Govers et al., (1994) suggested also that a compound annual plough operation may be represented by a  $k_{\text{till}}$  of 400-600 kg m<sup>-1</sup>. In view of such data it may have been more appropriate to widen the optimization limits from 200-500 kg m<sup>-1</sup> to 200-900 kg m<sup>-1</sup>.

- c. Field boundaries have been modelled in ARCTILL. They act as zones of zero flux, therefore halting the loss of soil to adjacent field units or streams.

This study aimed to benefit two audiences, primarily archaeologists and soil scientists. This work has highlighted the dominance of intensive agricultural practices in threatening Scotland's archaeological resource. Although not a new finding in itself, the results act as strong corroboration for what was already well known as the major agent of damage to archaeological sites. The proposed quantitative predictions of erosion and deposition have filled the gap in knowledge and now offer the opportunity to contribute towards Historic Scotland's monument protection strategy. Secondly, soil scientists, resource managers and policy planners can evaluate the status of erosion in lowland arable mid-Scotland. Finally, these validated erosion data sets and spatial predictions will further contribute to the discussion around and development of the Soil Protection Strategy for Scotland (Adderley et al., 2001).

# Appendix A.

## AML code for the ARCTILL routine.

For a pseudo code description see section 3.2.2, page 151.

```
/* tillage erosion aml based on the slope of terrain slope using a tillage
/*diffusion constant. Each cell is generating a flux of soil in response to
/*tillage which is fundamentally driven by the slope. Material (sediment) is
/*passed to the steepest downslope neighbour in accordance with D8 flow direction
/*principles so that each cell has an inflow value (accumulated sediment) and an
/*outflow value (tillage flux). To derive erosion/deposition rates a mass balance
/*calculation is carried out : INPUTS - OUTPUTS.
```

```
/* first step is to generate D8 flow directions from DTM using GRID's
/*flowdirection command.
```

```
/*grid
```

```
&sys cls
```

```
&TYPE #####
```

```
&TYPE ### ALGORITHM FOR MODELLING TILLAGE TRANSLOCATION ###
```

```
&TYPE #####
```

```
&type
```

```
&type This code initially calculates tillage flux at each cell using local slope
&type and a tillage diffusion parameter (Ktil). It models the field as a closed
&type system by preventing cells neighbouring field boundaries from outputting
&type soil material. By doing this the model attempts to simulate the build-up
&type of material against a hedge/wall. The algorithm roams a 3x3 cell window
&type across each cell identifying to which neighbouring cells it is
&type contributing. It then takes a tillage flux value (Kg m) from each
&type corresponding contributing cell and adds it to the cell being processed.
&type This repeats for all 8 neighbouring cells. See notes in code for details
```

```
&type WRITTEN BY: Jonathan Bowes, 2001.
```

```
&type
```

```
&type Data requirements:
```

```
&type
```

- ```
&type 1) DTM minus field boundaries for derivation of flow directions
&type 2) Slope grid (m m) for calculation of tillage flux
&type 3) Grid of field boundaries (0's) and fields with the appropriate
&type Ktil parameter
```

```
&type
```

```
&type
```

```
&type
```

```

&type
&type
&type

/*Setting mask so as to ignore non-arable land and other nodata areas
/*&sv mask = [getgrid * 'Select GRID to de used as mask']
/*&sv dtm = [getgrid * 'Select DTM for procedure']
/*setmask %mask%
/*prevents focalflow a neighbourhood notation processing
/*from 'seeing' NODATA values in non-arable/fieldboundary areas.
/*fflow = focalflow(%dtm%)      /* calculates which neighbouring cells are
/*inflowing
&type
&type
&type
&type

&sv flow = dtmclean /*[getgrid * 'Define grid to be used in flowdirection']
&sv flowdir = flowdirec /*[response 'Name resultant flowdirection grid']
&sv inflow = influx /*[response 'Name resultant 'inflow' grid']
&type
&type          ##### Calculating flow direction #####
&type
flowd = flowdirection(%flow%)

/* first of all change all NODATA values to ZERO's to prevent the neighbourhood
notation
/* from 'spreading' NODATA values during iterative process.

flowd2 = con(isnull(flowd), 0, flowd)

rename flowd2 %flowdir%

/*setmask off

/*Initiate procedure to calculate the flux of soil from each cell based on local
/*slope angle (m m). This cell-by-cell procedure will assign a flux value of ZERO
/*to cells that 'would' flow across a fieldboundary in an attempt to model the
/*build-up of soil against a wall/hedge at the base of a slope.

&type
&type          #####
&type          ##### Initiating calculation of #####
&type          ##### soil flux due to tillage #####
&type          #####

```

```

&type
&type
&type

&sv slope = slope /*[getgrid * 'Select slope grid']
&sv tillflux = tflux /*[response 'Name the tillage flux grid to be generated']
&sv mask2 = mask400 /*[getgrid * 'Select grid to be used as mask for fields']

docell

if(%flowdir% && 1 & %mask2%(1, 0) == 0)
    %tillflux% = 0

else if (%flowdir% && 2 & %mask2%(1, 1) == 0)
    %tillflux% = 0

else if (%flowdir% && 4 & %mask2%(0, 1) == 0)
    %tillflux% = 0

else if (%flowdir% && 8 & %mask2%(-1, 1) == 0)
    %tillflux% = 0

else if (%flowdir% && 16 & %mask2%(-1, 0) == 0)
    %tillflux% = 0

else if (%flowdir% && 32 & %mask2%(-1, -1) == 0)
    %tillflux% = 0

else if (%flowdir% && 64 & %mask2%(0, -1) == 0)
    %tillflux% = 0

else if (%flowdir% && 128 & %mask2%(1, -1) == 0)
    %tillflux% = 0

else %tillflux% = (%slope% * %mask2%) * 25

end

&type
&type #####
&type ##### Tillage flux (kg per cell) grid generated #####
&type #####
&type #####
&type ##### Calculating inflow of soil to each cell based #####
&type ##### on local slope gradient and flowdirection (D8)#####
&type #####

```

```

&type

&sv e = %tillflux%(1, 0)
&sv se = %tillflux%(1, 1)
&sv s = %tillflux%(0, 1)
&sv sw = %tillflux%(-1, 1)
&sv w = %tillflux%(-1, 0)
&sv nw = %tillflux%(-1, -1)
&sv n = %tillflux%(0, -1)
&sv ne = %tillflux%(1, -1)
&type
&type
&sv tillerodep = teros400 /* [response 'Name of resultant erosion/deposition
grid']
&type
&type
&type
&type
&type          *****
&type          **** Beginning iterative procedure ****
&type          *****
&type

docell

if (%flowdir%(1, 0) && 16)
  e := %e%
else
  e := 0

if (%flowdir%(1, 1) && 32)
  se := %se%
else
  se := 0

  if (%flowdir%(0, 1) && 64)
    s := %s%
  else
    s := 0

if (%flowdir%(-1, 1) && 128)
  sw := %sw%
else
  sw := 0

if (%flowdir%(-1, 0) && 1)
  w := %w%
else

```

```

w := 0

if (%flowdir%(-1, -1) && 2)
  nw := %nw%
else
  nw := 0

if (%flowdir%(0, -1) && 4)
  n := %n%
  else
  n := 0

if (%flowdir%(1, -1) && 8)
  nea := %nea%
  else
  nea := 0

%inflow% = n + s + e + w + nea + nw + se + sw

end /*DOCELL procedure finishes

/* final procedure for calculating the net deposition/erosion at each cell
/* essentially is: INPUTS - OUTPUTS

%tillerodep% = (%inflow% - %tillflux%) / 625

&type #####
&type #### NOTE - THE UNITS HAVE BEEN CONVERTED TO KG PER M2 ####
&type #####
&type
&type
&type #####
&type ##### Your erosion/deposition grid is now complete #####
&type #####

&return

```

## Appendix B.

### AML code for the optimisation routine.

For a pseudo code description see section 4.5.1, page 202.

```
/*Calib.aml
/*
/* This code basically runs through the whole procedure of modelling soil
/*erosion/deposition. It calculates Ep and Tc by varying the slope m exponent,
/*sca n exponent, whilst keeping k1 constant. These parameters are varied by
/*reading in parameter triplets (all combinations) from a text file previously
/*created. The triplets are formed by: taking 3 columns of data - one for each
/*parameter m, n, k. Each column is a range incremented by some value. All
/*combinations of triplets are then calculated. These then form the basis to Ep
/*and Tc. TARDEM (Tarboton /*1997), generates the sca and slope grids.
/*Sedinfav.exe is called and run from within the aml and is supplied with Ep and
/*Tc so as to calculate erosion/deposition. A con statement generates the final
/*eros/depos grid which is then compared to a 137Cs grid (observed). Error values
/*are generated and output to a text file using the sample command. This text
/*file is then read and records written to a master error.txt file. This above is
/*then iterated x times depending on how many times required (or number of
/*combinations). Details in code should provide orientation to what the code is
/*doing.

&terminal 9999
&messages &off &all
&sys cls
&TYPE
&TYPE
&TYPE
&TYPE *****
&TYPE ***** LOOP PROCEDURE FOR RUNNING EROSION/DEPOSITION MODEL *****
&TYPE ***** x NUMBER OF TIMES AS CALIBRATION *****
&TYPE *****
&TYPE Written by
&TYPE Jonathan Bowes
&type Dept. of Env. Science
&type Uni. of Stirling
/*Data requirements:
/*1. DTM
/*2. Slope (m m-1)
/*3. Sca (m2 m-1)or runoff (from SPR)
/*4. Mask (for output to txt)
/*5. 'Goal' grid to calibrate eros/depos grid to (usually 137Cs - Tillage /*eros)
&type
&type
&type

&type Looping.....

&sv dir = f:\phdproject\gis\modelling\optim\loanleven /*[response 'Browse to
required directory']
&sv slope = dtmslp /*[getgrid * 'Select Slope grid']
&sv sca = runoff /*[getgrid * 'Select Specific catchment area grid']
&sv grid = dtmfld /*[getgrid * 'Select DTM required for procedure']
&sv mask = mask /*[getgrid * 'Select grid to used as transect mask']
&sv 137cs = cs137 /*[getgrid * 'Select grid to be used as observed
/*eros/depos values']
&sv x = 5400 /*[response 'Input number of param. combinations
/*(iterations)']

&sv combin = [open missedcombs1.txt openstat -read]
&if %openstat% <> 0 &then
&return &warning Error opening file.
/* Read from file
&sv combrec = [unquote[read %combin% readstat]]
```

```

&if %readstat% <> 0 &then
&return &warning Could not read file.

/* Establish the loop
&do counter = 1 &to %x% &while %readstat% = 0
/*&type Run # = %counter%

    &sv m = [extract 1 %combrec%] /* pulls out first m value in col 1
    &sv n = [extract 2 %combrec%] /* pulls out first n value in col 2
    &sv k = 4 /*[extract 3 %combrec%] /* k1 is constant
    &sv k2 = [extract 4 %combrec%] /* pulls out first n value in col 4
    &sv ktil = [extract 5 %combrec%] /* pulls out first n value in col 5

&sv variables = %m%,%n%,%k%,%k2%,%ktil%

/* calculation of Ep and Tc commence as first
/*quad of m, n, k, t combinations have been extracted

ep = %k% * pow(%slope%, %m%) * pow(%sca%, %n%) /* Ep now calculated

    &sv ep = ep

tc = %ep% * %k2% /* Tc now calculated
&sv tc = tc

/* We now set the correct path within DOS so
/*TARDEM's sedinf moduel knows where to operate.

    &sys cd %dir%

/* Now pass the command-line syntax to TARDEM's
/*sedinf module to run the erosion/deposition model

&data sedinfav %grid% -wg %ep% %tc% -nc
&end

/*&type
/*&type
/*&type **** Sediment routing and mass balance calculations complete *****
/*&type
/*&type ***** Outputting results *****
/*&type
/*&type

/* Final con statement in GRID to amalgamate eroding and depositing cells /*in to
one
/* grid

setmask %mask%

erosdep = con(%grid%wsca < %tc%, - %ep%, %tc%dep)

&sv erosdep = erosdep

/* The transect of interest is masked out and the cell
/*LINE 100
/* values are dumped to an ascii file using the sample
/* command. This file will then be opened, it's values
/* read which are then appended to the results.txt file
/*&messages &off &all

/* we compare the predicted model ouputs with
/* observed (137 Cs) to derive an error value at each cell

goal = %137cs% - %ktil%teros /* subtracts tillage erosion from /*137cs
budget to gain a 'required' water erosion level
&sv goal = goal
error = sqr(%goal% - %erosdep%)
transect.txt = sample(%mask%, %erosdep%, error)

```



```

Kill (!%ep% %tc% %grid%wsca tcdep erosdep error goal!) all /*clean up
/*LINE 120
&sv transect = [open transect.txt openstatus -read]
/*open transect.txt to read the data
    &sv combin2 = [open new3.txt openstat -a]
/*opens the newerror1.txt file to which the data will be appended
&sv vars = [write %combin2% %variables%]
&sv record = [unquote[read %transect% readstat]]
&do &while %readstat% = 0 /* reads the rest of the data to the bottom
    &sv w = [write %combin2% [quote %record%]] /* writes the error data /*to
    error.txt
    &sv record := [unquote[read %transect% readstat]]

/*LINE 150
&end /* ENDS THE LOOP USED TO READ AND WRITE THE RECORDS TO ERROR.TXT

&sv run = [write %combin2% 'NEW RUN']

setmask off

&if [close %combin2% -all] > 0 &then
    &type correll.txt NOT closed

&if [close %transect% -all] > 0 &then
    &type Transect.txt NOT closed

    &sv counter = [calc %counter% + 1]
    &if %counter% = 50 or %counter% = 150 or %counter% = 250 or %counter% = 340 &then
        &type Procedure just starting %counter%th iteration out of %x%

    &sys del transect.txt
    &sv combrec = [unquote[read %combin% readstat]]

&delvar correl .correlation_out vars corrvar
&end /* ENDS THE MASTER LOOP AND RETURNS TO THE TOP FOR RUN #2

&do
&messages &on
&sv time = [date -full]
&type PROCEDURE LOOPED [calc %counter% - 1] TIMES
&type and finished at time %time%
&sv finclos = [close %combin2% -all]
&end
&return

```

## 7. References

Adderley, P.W., Davidson, D.A., Grieve, I.C., Hopkins, D.W., Salt, C.A., 2001. Issues associated with the development of a Soil Protection Strategy for Scotland. A report to the Scottish Executive Environmental Rural Affairs Department. Department of Environmental Science. 81.

Agassi, M. and Ben-Hur, M. 1991. Effect of Slope Length, Aspect, and Phosphogypsum on Runoff and Erosion from Steep Slopes. *Australian Journal of Soil Resources*, 29, 197-207.

Agassi, M., Morin, J., Shainberg, I., Warrington, D. 1989. Slope and Phosphogypsum's Effects on Runoff and Erosion. *Soil Science Society American Journal*, 53, 1201-1205.

Arnoldus, H.M.J. 1980. An approximation of the rainfall factor in the universal soil loss equation. in: *Assessment of Soil Erosion*. (eds. DeBoodt, M. & Gabriels, D.) John Wiley & Sons. 127-132.

Barclay, G.J. and Maxwell, G.S., 1998. The Cleaven Dyke. A Perthshire Cursus Monument in its Context. *Historic Scotland*. 119

Batjes, N.H., 1996. Global Assessment of Land Vulnerability to Water Erosion on a 0.5 degree by 0.5 degree Grid. International Soil Reference and Information Centre, National Institute of Public Health and Environment, United Nations Environment Programme

Bernard, C. and Laverdiere, M.R. 1993. Assessment of Soil Erosion in Quebec (Canada) with Cs-137. in: *Farm Land Erosion - In Temperate Plains Environment and Hills*. (ed. Wicherek, S.) Elsevier. 253-259.

Beven, K. and Freer, J. 2001. Equifinality, data assimilation, and uncertainty estimation in mechanistic modelling of complex environmental systems using the GLUE methodology. *Journal of Hydrology*, 249, 11-29.

Beven, K.J. and Binley, A.M. 1992. The future of distributed models: model calibration and uncertainty prediction. *Hydrological processes*, 6, 279-298.

Boardman, J. 1990. Soil erosion on the South Downs: a review. in: *Soil Erosion on Agricultural Land*. (eds. Boardman, J., *et al.*) Wiley. 87-105.

Boardman, J. and Favis-Mortlock, D.T. 1993. Simple methods of characterizing erosive rainfall with reference to the Southern Downs, Southern England. in: *Farmland Erosion: In Temperate Plains Environment and Hills*. (ed. Wicherek, S.) Elsevier. 17-29.

- Bolline, A., Laurante, A., Rosseau, P., Pauwells, J.M., Gabriels, D., Aelterman, J. 1980. Provisional rain erosivity map of Belgium. in: Assessment of Erosion. (eds. DeBoodt, M. & Gabriels, D.) Wiley & Sons. 111-120.
- Boorman, D.B., Hollis, J.M., Lilly, A., 1995. Hydrology of soil types: a hydrologically based classification of the soils of the United Kingdom. Institute of Hydrology. 137.
- Bridges, E.M. and Harding, D.M. 1971. Micro-erosion processes and factors affecting slope development in the Lower Swansea Valley. in: Slopes: form and process. (ed. Brunson, D.) Institute of British Geographers. 65-79.
- Bryan, R.B. and Poesen, J.W. 1989. Laboratory experiments on the influences of slope length on runoff, percolation and rill development. *Earth Surface Processes and Landforms*, 14, 211-231.
- Burt, T.P. and Butcher, D.P. 1985. Topographic controls of soil moisture distribution. *Journal of Soil Science*, 36, 469 - 489.
- Busacca, A.J., Cook, C.A., Mulla, D.J. 1993. Comparing landscape-scale estimation of soil erosion in the Palouse using Cs-137 and RUSLE. *Journal of Soil and Water Conservation*, 48, 361-367.
- Carter, M.W. and Moghissi, A.A. 1977. Three decades of nuclear testing. *Health Physics*, 33, 55-71.
- Castillo, V.M., Martinez-Mena, M., Albaladejo, J. 1997. Runoff and soil loss response to vegetation removal in a semi-arid environment. *Soil Sci. Soc. Am. J.*, 61, 1116-1121.
- Cerda, A. 1998. The influence of aspect and vegetation on seasonal changes in erosion under rainfall simulation on a clay soil in Spain. *Canadian Journal of Soil Science*, 78, 321-330.
- Cerda, A. and Garcia-Fayos, P. 1997. The influence of slope angle on sediment, water and seed losses on badland landscapes. *Geomorphology*, 18, 77-90.
- Chambers, B.J., Davies, D.B., Holmes, S. 1992. Monitoring of soil erosion on arable farms in England and Wales, 1989-1990. *Soil Use and Management*, 8, 163-169.
- Chambers, B.J. and Garwood, T.W.D. 2000. Monitoring of soil erosion on arable farms in England and Wales, 1990-1994. *Soil Use and Management*, 16, 93-99.
- Chaplot, V. and LeBissonnais, Y. 2000. Field measurements of interrill erosion under different slopes and plot sizes. *Earth Surface Processes and Landforms*, 25, 145-153.

- Coleman, N.T. and Le Roux, F.H. 1965. Ion-exchange displacement of Cs from soil vermiculite. *Soil Science*, 99
- Royal Commission, 1996. Sustainable Use of Soil, Royal Commission on Environmental Pollution Nineteenth Report. Royal Commission
- Costa-Cabral, M. and Burges, S.J. 1994. Digital Elevation Model Networks (DEMON): A model of flow over hillslopes for computation of contributing and dispersal areas. *Water Resources Research*, 30, 1681 - 1692.
- Darvill, T. and Fulton, A., 1998. The Monuments at Risk Survey of England. English Heritage. 328.
- Davidson, D.A., Grieve, I.C., Tyler, A.N., Barclay, G., Maxwell, G.S. 1998. Archaeological Sites: Assessment of Erosion Risk. *Journal of Archaeological Sites*, 25, 857-860.
- Davidson, D.A. and Harrison, D.J. 1995. The Nature, causes and implications of water erosion on arable land in Scotland. *Soil Use and Management*, 11, 63-68.
- de Alba, S. 2001. Modelling the effects of complex topography and patterns of tillage on soil translocation by tillage with a mouldboard plough. *Journal of Soil and Water Conservation*, 56, 335-345.
- de Jong, E.; Begg, C.B.M., Kachanoski, R.G. 1983. Estimates of soil erosion and deposition for some Saskatchewan soils. *Canadian Journal of Soil Science*, 63, 607-617.
- de Jong, E., Villar, H., Bettany, J.R. 1982. Preliminary investigations on the use of <sup>137</sup>Cs to estimate erosion in Saskatchewan. *Canadian Journal of Soil Science*, 62, 673-683.
- De Roo, A.P.J. 1998. Modelling runoff and sediment transport in catchments using GIS. *Hydrological Processes*, 12, 905-922.
- DePloey, J., Kirkby, M.J., Ahnert, F. 1991. Hillslope erosion by rainstorms - A magnitude frequency analysis. *Earth Surface Processes and Landforms*, 16, 399-409.
- De Roo, A.P.J., Wesseling, C.G., Ritsema, C.J. 1995. LISEM: a single event physically based hydrological and soil erosion model for drainage basins: theory, input and output. *Hydrological Processes*, 10, 1107-1117.
- Desmet, P.J.J. 1997. Effects of interpolation errors on the analysis of DEMs. *Earth Surface Processes and Landforms*, 22, 563-580.

- Desmet, P.J.J. and Govers, G. 1995. GIS-based simulation of erosion and deposition patterns in an agricultural landscape: a comparison of model results with soil map information. *Catena*, 25, 389-401.
- Desmet, P.J.J. and Govers, G. 1996. Comparison of routing algorithms for digital elevation models and their implications for predicting ephemeral gullies. *International Journal of Geographic Information Systems*, 10, 311-331.
- Desmet, P.J.J. and Govers, G. 1996. A GIS procedure for automatically calculating the USLE LS factor on topographically complex landscape units. *Journal of Soil and Water Conservation*, 51, 27-433.
- Desmet, P.J.J. and Govers, G. 1997. Two-dimensional modelling of the within-field variation in rill and gully geometry and location related to topography. *Catena*, 29, 283-306.
- Djorovic, M. 1980. Slope effect on run-off and erosion. in: *Assessment of Soil Erosion*. (eds. DeBoodt, M. & Gabriels, D.) Wiley. 215-226.
- Douglas, I. 1976. Erosion Rates and Climate: Geomorphological Implications. in: *Geomorphology and Climate*. (ed. Derbyshire, E.) Wiley. 269-87.
- Duck, W. and McManus, J. 1987. Soil erosion near Barry, Angus. *Scottish Geographical Magazine*, 103, 44-46.
- Evans, R. 1980. Mechanics of water erosion and their spatial and temporal controls: an empirical viewpoint. in: *Soil Erosion*. (eds. Kirkby, M. J. & Morgan, R. P. C.) Wiley. 109-128.
- Evans, R. 1990a. Soils at risk of accelerated erosion in England and Wales. *Soil Use Management*, 6, 125-131.
- Evans, R. 1990b. Water erosion in British Farmers' fields - causes, impacts, predictions. *Progress in Physical Geography*, 14, 199-219.
- Fournier, F. 1972. *Soil Conservation*. Council of Europe. 194
- Fox, D.M. and Bryan, R.B. 1999. The relationship of soil loss by interrill erosion to slope gradient. *Catena*, 38, 211-222.
- Freeman, T.G. 1991. Calculating catchment area with divergent flow based on a regular grid. *Computers and Geosciences*, 17, 413-422.

- Froehlich, W., Higgitt, D.L., Walling, D.E. 1993. The use of caesium-137 to investigate the soil erosion and sediment delivery from cultivated slopes in the Polish Carpathians. in: *Farm Land Erosion: In Temperate Plains Environment and Hills*. (ed. Wicherek, S.) Elsevier. 271-283.
- Frost, C.A. and Speirs, R.B. 1984. Water erosion of soils in south-east Scotland - a case study. *Research and Development in Agriculture*, 1, 145-152.
- Frost, C.A. and Speirs, R.B. 1987. Review: Soil water erosion on arable land in the United Kingdom. *Research and Development in Agriculture*, 4, 1-11.
- Fullen, M.A. 1991. A comparison of runoff and erosion rates on bare and grassed loamy sand soils. *Soil Use and Management*, 7, 136-139.
- Fullen, M.A. and Reed, A.H. 1986. Rainfall, runoff and erosion on bare arable soils in East Shropshire, England. *Earth Surface Processes and Landforms*, 11, 413-425.
- Gerontidis, D.V.S., Kosmas, C., Detsis, B., Maranthianou, M., Zafirious, T., Tsara, M. 2001. The Effect of mouldboard plow on tillage erosion along a hillslope. *Journal of Soil and water Conservation*, 56, 147 - 152.
- Gilley, J.E., Eghball, B., Kramer, L.A., Moorman, T.B. 2000. Narrow grass hedge effects on runoff and soil loss. *Journal of Soil and Water Conservation*, 55, 190-196.
- Govers, G., Quine, T.A., Desmet, P.J.J., Walling, D.E. 1996. The relative contribution of soil tillage and overland flow erosion to soil distribution on agricultural land. *Earth Surface Processes and Landforms*, 21, 929-946.
- Govers, G., Quine, T.A., Walling, W.A. 1993. The effect of water erosion and tillage movement on hillslope profile development: a comparison of field observations and model results. in: *Farm Land Erosion: In Temperate Plains Environment and Hills*. (ed. Wicherek, S.) Elsevier Science. 285-300.
- Govers, G., Vandaele, K., Desmet, P., Poeson, J., Bunte, K. 1994. The role of tillage in soil redistribution on hillslopes. *European Journal of Soil Science*, 45, 469-478.
- Gregory, K.J. and Walling, D.E. 1973. Drainage basin form and process. Arnold Ltd. 458
- Harrison, S.J. 1993. Recent changes in the weather in central Scotland. *Forth Naturalist and Historian*, 16, 11-24.
- Higgitt, D.L. 1990. The use of caesium-137 measurements in erosion investigations. PhD, University of Exeter, Exeter.

- Higgitt, D.L. 1995. The Development and Application of Caesium-137 Measurements in Erosion Investigations. in: *Sediment and Water Quality in River Catchments*. (eds. Foster, I. D. L., *et al.*) John Wiley and Sons Ltd. 287-305.
- Hinchliffe, J. and Schadler-Hall, R.T., 1980. *The Past Under the Plough*. Directorate of Ancient Monuments and Historic Buildings. Occasional paper. 151.
- Holmgren, P. 1994. Multiple flow direction algorithms for runoff modelling in grid based elevation models: an empirical evaluation. *Hydrological Processes*, 8, 327-334.
- Hutchinson, M.F. Year. Calculation of hydrologically sound digital elevation models. in: *Third International Symposium on Spatial Data Handling*, Sydney. 1988.
- Hutchinson, M.F. 1989. A new procedure for gridding elevation and stream line data with automatic removal of spurious pits. *Journal of Hydrology*, 106, 211-232.
- Ingamells, C.O. 1974. Control of geochemical error through sampling and sub-sampling diagrams. *Geochemica et Cosmoch. Acta.*, 38, 1225-1237.
- Jenson, S.K. and Domingue, J.O. 1988. Extracting topographic structure from digital elevation model data for geographic information systems analysis. *Photogrammetric Engineering and Remote Sensing*, 54, 1593-1600.
- Kachanoski, R.G. and De Jong, E. 1984. Predicting the temporal relationship between soil caesium-137 and erosion rate. *Journal of Environmental Quality*, 13, 301-304.
- King, D., Le Bissonnais, Y., Hardy, R. 1993. Regional assessment of runoff and erosion risk. Example of the Nord/Pas-de-Calais region, France. in: *Farmland erosion: In Temperate Plains Environment and Hills*. (ed. Wicherek, S.) Elsevier Science. 191-205.
- Kirkbridge, M.P. and Reeves, A.D. 1993. Soil erosion caused by low intensity rainfall in Angus, Scotland. *Applied Geography*, 13, 299-311.
- Kirkby, M.J. 1971. Hillslope process models based on the continuity equation. *Institute of British Geographers Special Publication*, 3, 331-344.
- Kirkby, M.J. 1988. Hillslope runoff processes and models. *Journal of hydrology*, 100, 315-339.
- Kirkby, M.J. and Chorley, R.J. 1967. Throughflow, overland flow and erosion. *Bull. Int. Assoc. Hydrol. Sci.*, 12, 5-21.

Kirkby, M.J. and Cox, N.J. 1995. A climatic index for soil erosion potential (CSEP) including seasonal and vegetation factors. *Catena*, 25, 333-352.

Kirkby, M.J. and Morgan, R.P.C. 1980. *Soil Erosion*. John Wiley & Sons. 312

Kosmas, C., Gerontidis, S., Marathianou, M., Detsis, B., Zafiriou, T., Muysen, W. N., Govers, G., Quine, T., Vanoost, K., 2001. The effects of tillage displaced soil on soil properties and wheat biomass. *Soil and Tillage Research*, 58, 31-44.

Laflen, J.M., Lane, L.J., Foster, G.R. 1991. WEPP: a new generation of erosion prediction technology. *Journal of Soil and Water Conservation*, 46, 34-38.

Laing, D., Robertson, J.S., Birse, E.L. 1974. *The Soils of the Country round Perth, Arbroath, and Dundee*. Her Majesty's Stationary Office. 328

Lal, R. 1976. Soil erosion on Alfisols in western Nigeria III. Effect of rainfall characteristics. *Geoderma*, 16, 389-401.

Lambrick, G., 1977. *Archaeology and Agriculture: a survey of modern cultivation equipment and the problems of assessing plough damage to Archaeological sites*. Council of British Archaeology and Oxfordshire Archaeological Unit.

Lambrick, G: 1980. Effects of modern cultivation equipment on archaeological sites. in: *The Past under the Plough*. (eds. Hinchliffe, J. & Schadler-Hall, R. T.) Directorate of Ancient Monuments and Historic Buildings. 18-21.

Lea, N.L. 1992. An aspect driven kinematic routing algorithm. in: *Overland Flow: Hydraulics and Erosion Mechanics*. (eds. Parsons, A. J. & Abrahams, A. D.) Chapman and Hall. 393-407.

LeBissonnais, Y., Singer, M.J., Bradford, J.M. 1993. Assessment of soil erodability: the relationship between soil properties, erosion processes and susceptibility to erosion. in: *Farm Land Erosion: In Temperate Plains Environment and Hills*. (ed. Wicherek, S.) Elsevier. 87-92.

Lilly, A., Hudson, G., Birnie, R.V., Horne, P.L., 2002. The inherent geomorphological risk of soil erosion by overland flow in Scotland. *Scottish Natural Heritage*

Lindstrom, M.J., Schumacher, J.A., Schumacher, T.E. 2000. TEP: A Tillage Erosion Prediction model to calculate soil translocation rates from tillage. *Journal of Soil and Water Conservation*, 55, 105-108.

Lindstrom, M.J., Nelson, W.W., Schumacher, T.E., Lemme, G.D. 1990. Soil movement by tillage as affected by slope. *Soil and Tillage Research*, 17, 255-264.



- Lindstrom, M.J., Nelson, W.W., Schumacher, T.E., Lemme, G.D. 1992. Quantifying tillage erosion rates due to moldboard ploughing. *Soil and Tillage Research*, 24, 243-255.
- Lobb, D.A., Kachanoski, G. R. 1999a. Modelling tillage erosion in the topographically complex landscapes of southwestern Ontario, Canada. *Soil & Tillage Research*, 51, 261-277.
- Lobb, D.A., Kachanoski, R.G., Miller, M.H. 1999b. Tillage translocation and tillage erosion in the complex upland landscapes of southwestern Ontario, Canada. *Soil & Tillage Research*, 51, 189-209.
- Lobb, D.A., Kachanoski, R.G., Miller, M.H. 1995. Tillage Translocation and Tillage Erosion On Shoulder Slope Landscape Positions Measured Using Cs-137 As a Tracer. *Canadian Journal of Soil Science*, 75, 211-218.
- Lobb, D.A. and Kachanoski, R.G. 1996. The impact of tillage translocation and tillage erosion on the estimation of soil loss using <sup>137</sup>Cs. *Can. J. Soil Sci.*, 76, 241.
- Longmore, M.E., O'Leary, B.W., Rose, C.W., Chindica, A.L. 1983. Mapping soil erosion and accumulation with the fallout isotope caesium-137. *Aust. J. Soil. Res.*, 21, 373-385.
- Lu, X.X. and Higgitt, D.L. 2000. Estimating erosion rates on sloping agricultural land in the Yangtze Three Gorges, China, from caesium-137 measurements. *Catena*, 39, 33-51.
- Ludwig, B., Boiffin, J., Chadoeuf, J., Auzet, A.V. 1995. Hydrological Structure and Erosion Damage Caused by Concentrated Flow in Cultivated Catchments. *Catena*, 25, 227-252.
- MAFF, 1998. Code of Good Agricultural Practice for the Protection of Soil. 66.
- Martz, L. and De Jong, E. 1988. Catch: a fortran program for measuring catchment area from digital elevation models. *Computers and Geosciences*, 14, 627-640.
- McHarg, I.L. 1969. *Design with Nature*. Garden City: Doubleday / Natural History Press.
- McHenry, J.R. and Ritchie, J.C., 1977a. Estimating field erosion losses from fallout cesium-137 measurements. *IAHS-AISH*. 26-33.
- Mech, S.J. and Free, G.A. 1942. Movement of soil during tillage operations. *Agricultural Engineering*, 23, 379-382.
- Menzel, R.G. 1960. Transport of strontium-90 in runoff. *Science*, 131, 499-500.

- Mitchell, J.K., Bubbenzer, G.D., McHenry, J.R., Ritchie, J.C. 1980. Soil loss estimation from fallout caesium-137 measurements. in: Assessment of soil erosion. (eds. Deboodt, M. & Gabriels, D.) John Wiley & Sons. 393-401.
- Montgomery, J.A., McCool, D.K., Busacca, A.J., Frazier, B.E. 1999. Quantifying tillage translocation and deposition rates due to moldboard ploughing in the Palouse region of the Pacific Northwest. *Soil & Tillage Research*, 51, 175-187.
- Montgomery, J.A., Busacca, A.J., Frazier, B.E., D.K., M. 1997. Estimating Soil Movement Using Caesium-137 and the revised Universal Soil Loss Equation. *Soil. Sci. Soc. Am. J.*, 61, 571-579.
- Moore, I.D., Grayson, R.B., Ladson, A.R. 1991. Digital Terrain Modelling. *Hydrological Processes*, 5, 3-30.
- Moore, I.D., Turner, A.K., Wilson, J.P., Jenson, S.K., Band, L.E. 1993. GIS and land surface-subsurface modeling. in: *Environmental Modeling with GIS*. (eds. Goodchild, M. F., *et al.*) Oxford University Press. 196-230.
- Moore, I.D. and Wilson, J.P. 1992. Length-slope factors for the Revised Universal Soil Loss Equation: Simplified method of estimation. *Journal of Soil and Water Conservation*, 47, 423-428.
- Morgan, R.P.C. 1980. Mapping soil erosion risk in England and Wales. in: *Assessment of Soil Erosion*. (eds. DeBoodt, M. & Gabriels, D.) Wiley & Sons. 89-95.
- Morgan, R.P.C. 1980. Soil erosion and conservation in Britain. *Progress in Physical Geography*, 4, 25-47.
- Morgan, R.P.C. 1985. Assessment of soil erosion risk in England and Wales. *Soil Use and Management*, 1, 127-131.
- Morgan, R.P.C. 1990. Soils at risk of accelerated erosion in England and Wales. *Soil Use and Management*, 6, 125-131.
- Morgan, R.P.C. 1993. *Soil Erosion and Conservation*. Longman Group UK Ltd.
- Morgan, R.P.C. 1995. *Soil erosion and conservation*. Longman.
- Morgan, R.P.C., Quinton, J.N., Smith, R.E., Govers, G., Poeson, J.W.A., Auerswald, K., Chisci, G., Torri, D., Styczen, M.E. 1998. The European Soil Erosion Model (EUROSEM): a dynamic approach for predicting sediment transport from fields and small catchments. *Earth Surface Processes and Landforms*, 23, 527-544.

Nachtergaele, J., Poesen, J., Steegen, A., Takken, I., Beuselinck, L., Govers, G. Year. Ephemeral gully erosion in the Belgian loess belt. in: Verstraeten, G., Ed. International Symposium on Gully Erosion under Global Change, Leuven. Laboratory of Experimental Geomorphology, K.U. Leuven, 2000.

Nearing, M.A. 1997. A single, continuous function for slope steepness influence on soil loss. Soil Science Soc. Am. J., 61, 917-919.

Nicholson, R.J. 1980. Modern ploughing techniques. in: The Past under the Plough. (eds. Hinchliffe, J. & Schadler-Hall, R. T.) Directorate of Ancient Monuments and Historic Buildings. 22-25.

O'Callaghan, J.F. and Mark, D.M. 1984. The extraction of drainage networks from digital elevation data. Computer Vision, Graphics and Image Processing, 28, 328-344.

Panuska, J.C., Moore, I.D., Kramer, L.A. 1991. Terrain analysis: integration into the Agricultural Non-point Source (AGNPS) pollution model. Journal of Soil and Water Conservation, 46, 59 - 64.

Papendick, R.I. and Miller, D.E. 1977. Conservation tillage in the pacific Northwest. Journal of Soil Water Conservation, 32, 49-56.

Parsons, A.J. and Abrahams, A.D. 1992. Overland Flow - Hydraulics and Erosion Mechanics. UCL Press. 438

Poesen, J.W., Vandaele, K., Van Wesemael, B. Year. Contribution of gully erosion to sediment production on cultivated lands and rangelands. in: Walling, D. E. & Webb, W., Eds. Erosion and Sediment Yield: Global and Regional Perspectives, Exeter, UK. IAHS, 1996.

Poeson, J.W.A. 1992. Mechanisms of overland-flow generation and sediment production on loamy and sandy soils with and without rock fragments. in: Overland Flow - Hydraulics and Erosion Mechanics. (eds. Parsons, A. J. & Abrahams, A. D.) UCL Press. 275-305.

Quansah, C. 1981. The effects of soil type, slope, rain intensity and their interactions on splash detachment and transport. Journal of Soil Science, 32, 215-224.

Quine, T. 1995. Estimation of erosion rates from caesium-137 data: The calibration problem. in: Sediment and Water Quality in River Catchments. (eds. Foster, I. D. L., *et al.*) John Wiley & Sons Ltd. 307-329.

Quine, T.A. 1999a. Use of caesium-137 data for validation of spatially distributed erosion models: the implications of tillage erosion. Catena, 37, 415-430.

- Quine, T.A., Govers, G., Walling, D.E., Zhang, X.B., Desmet, P.J.J., Zhang, Y.S., Vandaele, K. 1997. Erosion processes and landform evolution on agricultural land - New perspectives from caesium-137 measurements and topographic- based erosion modelling. *Earth Surface Processes and Landforms*, 22, 799-816.
- Quine, T.A. and Walling, D.E. 1991. Rates of soil erosion on arable fields in Britain: quantitative data from caesium-137 measurements. *Soil Use Management*, 7, 169-176.
- Quine, T.A. and Walling, D.E. 1993. Assessing recent rates of soil loss from areas of arable cultivation in the UK. in: *Farm Land Erosion - In Temperate Plains Environment and Hills*. (ed. Wicherek, S.) Elsevier. 357-371.
- Quine, T.A., Walling, D.E., Chakela, Q.K., Mandiringana, O.T., Zhang, X. 1999a. Rates and patterns of tillage and water erosion on terraces and contour strips: evidence from caesium-137 measurements. *Catena*, 36, 115-142.
- Quine, T.A., Walling, D.E., Zhang, X. 1999b. Tillage erosion, water erosion and soil quality on cultivated terraces near Xifeng in the Loess Plateau, China. *Land Degradation & Development*, 10, 251-274.
- Quine, T.A. and Zhang, Y. 2002. An investigation of spatial variation in soil erosion, soil properties, and crop production within an agricultural field in Devon, United Kingdom. *Journal of Soil and Water Conservation*, 57, 55-65.
- Quinn, P., Beven, K., Chevallier, P., Planchon, O. 1991. The prediction of hillslope flow paths for distributed hydrological modelling using digital terrain models. *Hydrological Processes*, 5, 59-79.
- Quinn, P.F., Beven, K.J., Lamb, R. 1995. The  $\ln(a/\tan B)$  index: How to calculate it and how to use it within the TOPMODEL framework. *Hydrological Processes*, 9, 161-182.
- Quinton, J.N., Edwards, G.M., Morgan, R.P.C. 1997. The influence of vegetation species and plant properties on runoff and soil erosion: results from a rainfall simulation study in south east Spain. *Soil Use and Management*, 13, 143-148.
- Reed, A.H. 1983. The erosion risk of compaction. *Soil and Water*, 11, 29-33.
- Reed, A.H. 1986. Soil loss from tractor wheelings. *Soil and Water*, 14, 12-14.
- Renard, K.G., Foster, G.R., Weesies, G.A., Porter, J.P. 1991. Revised Universal Soil Loss Equation. *J. Soil and Water Cons.*, 46, 30-34.

Renard, K.G. and Freimund, J.R. 1994. Using monthly precipitation data to estimate the R-factor in the RUSLE. *Journal of Hydrology*, 157, 287-306.

Ritchie, J.C. and McHenry, J.R. 1975. Fallout Cs-137: a tool in conservation research. *Journal of Soil and Water Conservation*, , 283-286.

Ritchie, J.C. and McHenry, J.R. 1990. Application of radioactive fallout caesium-137 for measuring soil erosion and sediment accumulation rates and patterns: A review. *Journal of Environmental Quality*, 19, 215-233.

Ritchie, J.C., Spraberry, J.A., McHenry, J.R. 1974. Estimating soil erosion from the redistribution of fallout 137Cs. *Soil Sci. Soc. Am. Proc.*, 38, 137-139.

Robbins, J.A. 1978. Geochemical and geophysical applications of radioactive lead. in: *The Biochemistry of lead in the environment.* (ed. Nriagu, J. O.) Elsevier. 285-393.

Rogers, R.D. and Schumm, S.A. 1991. The effect of sparse vegetative cover on erosion and sediment yield. *Journal of Hydrology*, 123, 19-24.

Rogowski, A.S. and Tamura, T. 1965. Movement of 137Cs by runoff, erosion and infiltration on the alluvial Captina silt loam. *Health Phys.*, 11.

Rogowski, A.S. and Tamura, T. 1970a. Environmental mobility of cesium-137. *Radiat. Bot.*, 10, 35-45.

Rogowski, A.S. and Tamura, T. 1970b. Erosional behaviour of caesium-137. *Health Phys.*, 18, 467-477.

Rustomji, P. and Prosser, I. 2001. Spatial patterns of sediment delivery to valley floors: sensitivity to sediment transport capacity and hillslope hydrology relations. *Hydrological Processes*, 15, 1003 - 1018.

Sawney, B.L. 1972. Selective sorption and fixation of cations by clay minerals: A review. *Clays and Clay Minerals*, 20, 93-100.

Schoorl, J.M., Sonneveld, M.P.W., Veldkamp, A. 2000. Three-dimensional landscape process modelling: the effect of DEM resolution. *Earth Surface Processes and Landforms*, 25, 1025-1034.

Scottish Executive. 1998. Agricultural and Horticultural Census. Scottish Executive Environment and Rural Affairs Department

Scottish Executive. 1999. Agricultural and Horticultural Census. Scottish Executive Environment and Rural Affairs Department

Select Committee on Environment, 1998. The Protection of Field Boundaries - Thirteenth report. Houses of Parliament

Sinzot, A., Bolline, A., Laurant, A., Erpicum, M., Pissart, A. 1989. A Contribution to the Development of an Erosivity Index Adapted to the Prediction of Erosion in Belgium. *Earth Surface Processes and Landforms*, 14, 509-515.

Skinner, R.J. and Chambers, B.J. 1996. A survey to assess the extent of soil water erosion in lowland England and Wales. *Soil Use and Management*, 12, 214-220.

Souchere, V., King, D., Daroussin, J., Papy, F., Capillon, A. 1998. Effects of tillage on runoff directions: consequences on runoff contributing area within agricultural catchments. *Journal of Hydrology*, 206, 256-267.

Speirs, R.B.F., C.A. 1987. Soil water erosion on arable land in the United Kingdom. *Research and Development in Agriculture*, 4, 1-11.

Spoor, G. 1980. Agronomic justification and technique for subsoil disturbance. in: *The Past under the Plough*. (eds. Hinchliffe, J. & Schalder-Hall, R. T.) Directorate of Ancient Monuments and Historic Buildings. 26-31.

Stocking, M., 1987. A Methodology for Soil Erosion Hazard Mapping of the SADCC Region. Overseas Development Group. 31.

Sutherland, R.A. 1991. Examination of caesium-137 aerial activities in control (uneroded) locations. *Soil Technology*, 4, 33-50.

Takken, I., Jetten, V., Govers, G., Nachtergaele, J., Steegen, A. 2001. The effect of tillage-induced roughness on runoff and erosion patterns. *Geomorphology*, 37, 1-14.

Tarboton, D.G. 1997. A new method for the determination of flow directions and upslope areas in grid digital elevation models. *Water Resources Research*, 33, 309-319.

Trott, K.E. and Singer, M.J. 1983. Relative erodibility of 20 Californian range and forest soils. *Soil Science Society American Journal*, 47, 753-749.

Tsara, M., Gerontidis, S., Marathianou, M., Kosmas, C. 2001. The long-term effect of tillage on soil displacement of hilly areas used for growing wheat in Greece. *Soil Use and Management*, 17, 113-120.

- Tyler, A.N. 1994. Environmental influences on gamma ray spectrometry. PhD, Glasgow, Glasgow.
- Tyler, A.N. 1999. In situ monitoring of anthropogenic radioactivity in salt marsh environments. *Journal of Environmental Radioactivity*, 45, 235-252.
- Tyler, A.N., Carter, S., Davidson, D.A., Long, D.J., Tipping, R. 2001. The extent and significance of bioturbation on <sup>137</sup>Cs distributions in upland soils. *Catena*, 43, 81-99.
- Tyler, A.N., Davidson, D.A., Bradley, S., 1995. Preliminary investigation of soil erosion rates from <sup>137</sup>Cs activity distribution on a tilled site at Meikleour, Perthshire. *Historic Scotland*
- Tyler, A.N., Davidson, D.A., Grieve, I.C. 1998. Estimating Soil Loss at littleour, Perthshire: Using the <sup>137</sup> Cs methodology. in: *The Cleaven Dyke: a Perthshire cursus monument in its context.* (eds. Barclay, G. J. & Maxwell, G. S.) *Historic Scotland*. 83-91.
- Tyler, A.N., Davidson, D.A., Grieve, I.C. 2001b. In situ radiometric mapping of soil erosion and field-moist bulk density on cultivated fields. *Soil Use and Management*, 17, 88-96.
- Tyler, A.N. and Heal, K.V. 2000. Predicting areas of <sup>137</sup>-Cs loss and accumulation in upland catchments. *Water and Soil Pollution*, 121, 271-288.
- Tyler, A.N., Sanderson, D.C.W., Scott, E.M. 1996b. Estimating and Accounting for <sup>137</sup>Cs Source Burial through In-situ Gamma Spectrometry in Salt Marsh Environments. *Journal of Environmental Radioactivity*, 33, 195-212.
- Tyler, A.N., Sanderson, D.C.W., Scott, E.M., Allyson, J.D. 1996. Accounting for Spatial Variability and Fields of View in Environmental Gamma Ray Spectrometry. *Journal of Environmental Radioactivity*, 33, 213-235.
- Van Muysen, W., Govers, G., Van Oost, K., Van Rompaey, A. 2000. The effect of tillage depth, tillage speed, and soil condition on chisel tillage erosivity. *Journal of Soil and Water Conservation*, 55, 355-364.
- Van Oost, K., Govers, G., Desmet, P. 2000. Evaluating the effects of changes in landscape structure on soil erosion by water and tillage. *Landscape Ecology*, 15, 577-589.
- Voroney, R.P., van Veen, J.A., Paul, E.A. 1981. Organic carbon dynamics in grassland soils. II. Model validation and simulation of the long-term effects on cultivation and rainfall erosion. *Canadian Journal of Soil Science*, 61

- Walling, D.E. 1974. Suspended sediment and solute yields from a small catchment prior to urbanisation. in: *Fluvial processes in instrumented watersheds*. (eds. Gregory, K. J. & Walling, D. E.) Institute of British Geographers. 169-192.
- Walling, D.E. 1982. Physical hydrology. *Progress in Physical Geography*, 6, 122-133.
- Walling, D.E. and Quine, T.A. 1990. Calibration of caesium-137 measurements to provide quantitative erosion rate data. *Land Degradation and Rehabilitation*, 2, 161-175.
- Walling, D.E. and Quine, T.A. 1991. Potential limitations of the <sup>137</sup>Cs technique of soil erosion assessment. *Journal of Soil Science*, 7, 169-176.
- Walling, D.E. and Woodward, J.C. Year. Use of radiometric fingerprints to derive information on suspended sediment sources. in: Bogen, J., *et al.*, Eds. *Erosion and Sediment Transport Monitoring Programmes in River Basins*, Oslo. IAHS, 1992.
- Warrington, D., Shainberg, I., Agassi, M., Morin, J. 1989. Slope and phosphogypsum's effects on runoff and erosion. *Soil Science Society American Journal*, 53, 1201-1205.
- Webster. 1998. *The New International Webster's Comprehensive Dictionary of the English Language*. Trident Press International.
- Wicherek, S. and Bernard, C. 1995. Assessment of soil movements in a watershed from Cs-137 data and conventional measurements (example: the Parisian Basin). *Catena*, 25, 141-151.
- Wiersum, K.F. 1985. Effects of various vegetation layers in an *Acacia auriculiformis* forest plantation on surface erosion in Java, Indonesia. in: *Soil Erosion and Conservation*. (eds. El-Swaify, S. A., *et al.*) Soil Conservation Society of America. 793.
- Wilson, D.R. 1982. *Aerial photography for archaeologists*. B T Batsford Ltd. 212
- Wischmeier, W.H. and Smith, D.D. 1958. Rainfall energy and its relationship to soil loss. *Trans. Am. geophys. Un.*, 39, 285-91.
- Wischmeier, W.H. and Smith, D.D. 1978. *Predicting rainfall erosion losses, a guide to conservation planning*. USDA Agr. Res. Serv. Handbook 537.
- Wise, S.M. 1980. Caesium-137 and Lead-210: A review of techniques and some applications in geomorphology. in: *Timescales in Geomorphology*. (ed. Cullingford, R. A. e. a.) Wiley & Sons. 109-127.



- Wolock, D.M., Hornberger, G.M., Musgrove, T.J. 1990. Topographic effects on flow path and surface water chemistry of the LlynBrianne catchment in Wales. *Journal of Hydrology*, 115, 243 - 259.
- Woo, M., Fang, G., diCenzo, P.D. 1997. The role of vegetation in the retardation of rill erosion. *Catena*, 29, 145-159.
- Wright, S.M., Howard, B.J., Strand, P., Nylén, T., Sickel, M.A.K. 1999. Prediction of Cs-137 deposition from atmospheric nuclear weapons tests within the Arctic. *Environmental Pollution*, 104, 131-143.
- Young, R.A. and Mutchler, C.K. 1977. Erodibility of some Minnesota soils. *Journal of Soil and Water Conservation*, 32, 180-182.
- Zevenbergen, L.W. and Thorne, C.R. 1987. Quantitative analysis of land surface topography. *Earth Surface Processes and Landforms*, 12, 47-56.
- Zhang, W. and Montgomery, D.R. 1994. Digital elevation model grid size, landscape representation and hydrologic simulations. *Water Resources Research*, 30, 1019-1028.
- Zhang, X., Higgitt, D.L., Walling, D.E. 1990. A preliminary assessment of the potential for using caesium-137 to estimate erosion of soil in the loess plateau of China. *Hydrological Science*, 35, 243-252.
- Zhang, X., Quine, T.A., Walling, D.E. 1998. Soil erosion rates on sloping cultivated land on the Loess Plateau near Ansai, Shaanxi Province, China: An investigation using Cs-137 and rill measurements. *Hydrological Processes*, 12, 171-189.